Enhancing clinical care and investigating a novel therapeutic approach for multiple paragangliomas

Thesis presented by:

Nicola Kerry Tufton, MBBS, Bsc

Thesis submitted in partial fulfillment of the requirements of the Degree of:

Doctor of Philosophy (PhD)

Under the supervision of:

Dr Scott A Akker

Prof. Márta Korbonits

Centre for Endocrinology,

William Harvey Research Institute,

Barts and the London School of Medicine and Dentistry,

Queen Mary University of London

July 2023

Statement of originality

I, Nicola Kerry Tufton, confirm that the research included within this thesis is my own work or that where it has been carried out in collaboration with, or supported by others, that this is duly acknowledged below and my contribution indicated. Previously published material is also acknowledged below.

I attest that I have exercised reasonable care to ensure that the work is original, and does not to the best of my knowledge break any UK law, infringe any third party's copyright or other Intellectual Property Right, or contain any confidential material.

I accept that the College has the right to use plagiarism detection software to check the electronic version of the thesis.

I confirm that this thesis has not been previously submitted for the award of a degree by this or any other university.

The copyright of this thesis rests with the author and no quotation from it or information derived from it may be published without the prior written consent of the author.

Signature:

Date: 31st July 2023

Published articles based on work from this thesis

Tufton N, Hearnden RJ, Berney DM, Drake WM, Parvanta L, Chapple JP, Akker SA. The immune cell infiltrate in the tumour microenvironment of phaeochromocytomas and paragangliomas. Endocr Relat Cancer. 2022.

Williams ST, Chatzikyriakou P, Carroll PV, McGowan BM, Velusamy A, White G, Obholzer R, Akker S, Tufton N, Casey RT, Maher ER, Park SM, Porteous M, Dyer R, Tan T, Wernig F, Brady AF, Kosicka-Slawinska M, Whitelaw BC, Dorkins H, Lalloo F, Brennan P, Carlow J, Martin R, Mitchell AL, Harrison R, Hawkes L, Newell-Price J, Kelsall A, Igbokwe R, Adlard J, Schirwani S, Davidson R, Morrison PJ, Chung TT, Bowles C, Izatt L. *SDHC* phaeochromocytoma and paraganglioma: A UK-wide case series. Clin Endocrinol (Oxf). 2022;96(4):499-512.

Winzeler B, Tufton N, E SL, Challis BG, Park SM, Izatt L, Carroll PV, Velusamy A, Hulse T, Whitelaw BC, Martin E, Rodger F, Maranian M, Clark GR, S AA, Maher ER, Casey RT. Investigating the role of somatic sequencing platforms for phaeochromocytoma and paraganglioma in a large UK cohort. Clin Endocrinol (Oxf). 2021.

Amar L, Pacak K, Steichen O, Akker SA, Aylwin SJB, Baudin E, Buffet A, Burnichon N, Clifton-Bligh RJ, Dahia PLM, Fassnacht M, Grossman AB, Herman P, Hicks RJ, Januszewicz A, Jimenez C, Kunst HPM, Lewis D, Mannelli M, Naruse M, Robledo M, Taieb D, Taylor DR, Timmers H, Treglia G, Tufton N, Young WF, Lenders JWM, Gimenez-Roqueplo AP, Lussey-Lepoutre C. International consensus on initial screening and follow-up of asymptomatic *SDH* mutation carriers. Nat Rev Endocrinol. 2021;17(7):435-44.

White G, Tufton N, Akker SA. First-positive surveillance screening in an asymptomatic *SDHA* germline mutation carrier. Endocrinol Diabetes Metab Case Rep. 2019;2019(1).

Tufton N, White G, Drake WM, Sahdev A, Akker SA. Diffusion-weighted imaging (DWI) highlights *SDHB*-related tumours: A pilot study. Clin Endocrinol (Oxf). 2019;91(1):104-9.

Tufton N, Shapiro L, Sahdev A, Kumar AV, Martin L, Drake WM, Akker SA, Storr HL. An analysis of surveillance screening for *SDHB*-related disease in childhood and adolescence. Endocr Connect. 2019;8(3):162-72.

Tufton N, Sahdev A, Drake WM, Akker SA. Can subunit-specific phenotypes guide surveillance imaging decisions in asymptomatic *SDH* mutation carriers? Clin Endocrinol (Oxf). 2019;90(1):31-46.

Maher M, Roncaroli F, Mendoza N, Meeran K, Canham N, Kosicka-Slawinska M, Bernhard B, Collier D, Drummond J, Skordilis K, Tufton N, Gontsarova A, Martin N, Korbonits M, Wernig F. A patient with a germline *SDHB* mutation presenting with an isolated pituitary macroprolactinoma. Endocrinol Diabetes Metab Case Rep. 2018;2018.

Tufton N SA, Akker SA. Radiological Surveillance Screening in Asymptomatic Succinate Dehydrogenase Mutation Carriers. Journal of the Endocrine Society. 2017;1(7):897-907.

Tufton N, Shapiro L, Srirangalingam U, Richards P, Sahdev A, Kumar AV, McAndrew L, Martin L, Berney D, Monson J, Chew SL, Waterhouse M, Druce M, Korbonits M, Metcalfe K, Drake WM, Storr HL, Akker SA. Outcomes of annual surveillance imaging in an adult and paediatric cohort of succinate dehydrogenase B mutation carriers. Clin Endocrinol (Oxf). 2017;86(2):286-96.

Tufton N, Roncaroli F, Hadjidemetriou I, Dang MN, Denes J, Guasti L, Thom M, Powell M, Baldeweg SE, Fersht N, Korbonits M. Pituitary Carcinoma in a Patient with an *SDHB* Mutation. Endocr Pathol. 2017.

Tufton N, Ghelani R, Srirangalingam U, Kumar VKA, Drake W, Iacovazzo D, Skordilis K, Berney DM, Al-Mrayat M, Khoo B, Akker S. *SDHA* mutated paragangliomas may be at high risk of metastasis. Endocr Relat Cancer. 2017.

Tufton N, Akker SA. Excluding the pheochromocytoma. Int J Cardiol. 2017;249:326-7.

Srirangalingam U, LeCain M, Tufton N, Akker SA, Drake WM, Metcalfe K. Four generations of *SDHB*-related disease: complexities in management. Fam Cancer. 2017;16(2):279-82.

Tufton N, Gunganah K, Hussain S, Druce M, Carpenter R, Ashby M, Drake WM, Akker SA. Alpha blockade-not to be underdone. Clin Endocrinol (Oxf). 2016.

Other published work completed during this time but not directly related to thesis:

Langton K, <u>Tufton N</u>, Akker S, Deinum J, Eisenhofer G, Timmers H, Spaanderman M, Lenders J. Pregnancy and phaeochromocytoma/paraganglioma: clinical clues affecting diagnosis and outcome - a systematic review. BJOG. 2021;128(8):1264-72.

Bancos I, Atkinson E, Eng C, Young WF, Jr., Neumann HPH, International P, Pregnancy Study G. Maternal and fetal outcomes in phaeochromocytoma and pregnancy: a multicentre retrospective cohort study and systematic review of literature. Lancet Diabetes Endocrinol. 2021;9(1):13-21.

Marques P, <u>Tufton N</u>, Bhattacharya S, Caulfield M, Akker SA. Hypertension due to a deoxycorticosterone-secreting adrenal tumour diagnosed during pregnancy. Endocrinol Diabetes Metab Case Rep. 2019;2019.

Abstract

Paragangliomas (PGLs) are rare tumours of the autonomic nervous system that cause high morbidity and mortality. Diagnosis and management can be challenging and no consensus on pre-operative management exists. PGLs arise in sporadic and familial forms and have the potential for malignant transformation. Despite significant advances in identification of genetic causes there is still a lack of understanding in the pathogenesis of the different clinical phenotypes. Surgical resection is the only cure, but once metastases have occurred treatment options are limited.

This thesis aims to address some of these issues with the overall objective of improving clinical care for affected patients and their relatives.

The first part of this research focuses on pre-operative management. Using home blood pressure monitoring and personalised titration of medications, the presented data show improved compliance with alpha-blockade medication. Duration of treatment appears to be an important factor in intra- and post-operative haemodynamic instability. Analysis of bioimpedance and serum inflammatory markers demonstrated that medical therapy is potentially able to reverse the inflammatory and catabolic effects of catecholamine excess.

Part two focuses on mutations within the Succinate Dehydrogenase (*SDH*) genes. Mutations in any of these can cause disruption in SDH enzymatic function, but penetrance, clinical presentation and tumour aggressiveness differ between subunits. A model for surveillance monitoring is proposed based on collated data.

The final part investigates the immune cell composition of the tumour microenvironment (TME). Emerging evidence suggests that the TME correlates with clinical outcome, however, little is known about the TME of PGLs. Immune cells in the TME were assessed using immunohistochemistry. There was a higher proportion of immune cells in tumour tissue compared to non-pathological medulla, with a predominance of macrophages. Differences in the TME were observed between aggressive and benign tumours. These observations could potentially be exploited as an aid in predicting tumour behaviour.

Acknowledgements

Details of collaborations

Table of contents

List of figures

List of tables

List of abbreviations

3MT — 3-methoxy-tyramine
4E-BP1 — Eukaryotic initiation factor 4E-binding protein 1
5mC — 5-methlycytosine hydroxylases
ABPM — ambulatory blood pressure monitor
ACC — adrenal cell carcinoma
AKT — protein kinase B
AIK — Akaike information criterion
AMEND — The Association for Multiple Endocrine neoplasia disorders
ATP — adenosine triphosphate
AUC — area under the curve
BD — bis in die (twice daily)
BL PCC — bilateral phaeochromocytoma
BM — bone marrow
BMI — body mass index
BMR — basal metabolic rate
BNP — beta natriuretic peptide
BP — blood pressure
CAFs — cancer associated fibroblasts
CD — cluster of differentiation
cDNA — complementary DNA
CM — complete media
COMT — catechol-O-methyltransferase
COPPs — composite pheochromocytoma /paraganglioma prognostic score
CP — craniopharyngioma
CPS — clinical prediction score
CRH — cortisol releasing hormone
CRP — c-reactive protein
CT — computed tomography
CTLA4 — cytotoxic T lymphocyte antigen 4
DAB — 3.3′-diaminobenzidine tetrahydrochloride
DAPI — 4',6-diamidino-2-phenylindole
DC — dendritic cells
DHPG — 3,4-dihydroxyphenylglycol
DMEM — Dulbecco´s modified eagle´s medium
DOTATATE — Dodecanetetraacetic acid-Octreotate
DWI — diffusion-weighted imaging
EC — epithelial cells
ECM — extra cellular matrix
ECW — extra-cellular water
EGF — endothelial growth factor
EGLN — Egl 9 homolog (PHD2)
ELISA — enzyme-linked immunosorbent assay
EMT — epithelial-mesenchymal transition

EPAS1 — endothelial PAS domain-containing protein 1 (HIF2α)
EPO — erythropoietin
ERK — extracellular signal-regulated kinase
FACS — fluorescence activated cell sorting
FAD — flavin adenine dinucleotide
FADH — flavin adenine dinucleotide hydroquinone
FBC — full blood count
FBS — foetal bovine serum
FDG — 18 F-fluorodeoxyglucose
FGF — Fibroblast growth factor
FH — fumarate hydratase
FOXP3 — forkhead box P3
GAPP — Grading system for phaeochromocytoma and paraganglioma
GIST — gastrointestinal stromal tumour
G-CSF — Granulocyte stimulating factor
GPS — Glasgow prognostic score
HDI — haemodynamic instability
H&E — haemoxylin and eosin
HIF — hypoxia inducible factor
HIF2A — hypoxia inducible factor 2A (EPAS1)
HNPGL — head & neck paraganglioma
HR — heart rate
ICB — immune checkpoint blockade
ICW — intra-cellular water
Ig — immunoglobulin
IHC — immunohistochemistry
IL — Interleukin
IFN-γ — Interferon gamma
JUMD — Jumonji histone demethylase family
KIF1β — kinesin family member 1B
LFT — liver function tests
LIF — leukaemia inhibitory factor
LMR — lymphocyte-monocyte ratio
LoH — loss of heterozygosity
mPPGL — metastatic PPGL
M1 — classically activated macrophages
M2 — tumour associated macrophages
MAO — monoamine oxidase
MAP — mean arterial pressure
MAX — myc-associated factor X
MCP1 — monocyte chemoattractant protein 1
MDH — malate dehydrogenase
MEN2 — multiple endocrine neoplasia type2

MERTK	cMER proto-oncogene tyrosine kinase receptor	RET	rearranged during transfection proto-oncogene
MHC	major histocompatibility complex	ROC	receiver operating characteristics curve
MHPG	3-methoxy-4-hydroxyphenylglycol		
MIBG	metaiodobenzylguanidine	ROS	reactive oxidative reactive species
MIP	macrophage inflammatory protein	SII	systemic inflammatory index
MN	metanephrine	SC	stem cells
MRI	magnetic resonance imaging	SD	standard deviation
mRNA	messenger RNA	SDH	succinate dehydrogenase
MTC	medullary thyroid carcinoma	SDHA	succinate dehydrogenase subunit A
mTOR	mammalian target of rapamycin	SDHAF2	succinate dehydrogenase subunit AF2
NE	neutrophils	SDHB	succinate dehydrogenase subunit B
NET	neuro-endocrine tumour	SDHC	succinate dehydrogenase subunit C
NF1	neurofibromatosis 1	SDHD	succinate dehydrogenase subunit D
NK	natural killer cells	*SDH*	succinate dehydrogenase subunit (x=all/any of the subunits)
NLR	neutrophil-platelet ratio		
NM	non-pathological adrenal medulla	SEM	standard error of the mean
NMN	normetanephrine	SP	substance P
NPS	neutrophil-platelet score	SSA	somatostatin analogue
NR	normal reference range	SST	somatostatin
NT	not tested	SSTR	somatostatin receptor
OD	omnie die (once daily)	STAT	signal transducer and activator of transcription
P13K	phosphoinositide-3-kinase		
PA	pituitary adenoma	SULT1A3	sulfotransferase type 1A3
PASS	phaeochromocytoma of the adrenal gland scoring system	Sv	Sievert
		TAM	tumour associated macrophage
PBS	phosphate buffered saline	TAPGL	thoracic and abdominal PGL
PCAP	pituitary adenylate cyclase-activating polypeptide	TBW	total body water
		Tc	cytotoxic T lymphocytes (CD8+)
PCC	phaeochromocytoma	TCA	tricarboxylic acid cycle
PD-L	programmed cell death protein 1	TDS	ter die sumendum (thrice daily)
PDL1	programmed cell death ligand 1	TET	ten-eleven translocation
PET	position emission tomography	TGF	transforming growth factor
PGL	paraganglioma	Th	T helper lymphocyte (CD4+)
PHD	prolyl hydroxylase (EGLN)	TH	tyrosine hydroxylase
PHTP	primary hyperparathyroidism	TIL	tumour infiltrating lymphocytes
PKC	protein kinase C	TME	tissue microenvironnement
PLR	platelet-lymphocyte ratio	TMEM127	transmembrane protein 127
pNET	pancreatic neuroendocrine tumour	TNF	tumour necrosis factor
PNI	prognostic nutrition score	TP53	tumour protein p53
PNMT	phenylethanolamine N-methyltransferase	Tregs	T regulatory cells
		UE	urea and electrolytes
PPGL	phaeochromocytoma and paraganglioma	ULN	upper limit of normal range
		VEGF	vascular endothelial growth factor
PRRT	peptide receptor radionuclide therapy	VHL	von Hippel Lindau
PTEN	phosphate and tensin homolog protein	VMA	vanillylmandelic acid
		VIP	vasoactive peptide
QDS	quarter in die (four times a day)	VUS	variant of unknown significance
RANTES	regulated on activation, normal T cell expressed and secreted		
RCC	renal cell carcinoma		

Chapter 1. Introduction

1.1   General introduction

Paragangliomas are rare vascular tumours of the autonomic nervous system that originate from paraganglia. Paraganglia are non-neural, neuroendocrine organs derived from neural crest tissue dispersed from skull base to the pelvic floor that secrete catecholamines and peptides. Paragangliomas cause high morbidity and mortality due to their secretory nature and due to mass effects. They arise as both sporadic and familial forms. There have been significant advances in the understanding of the underlying genetic causes of these tumours and the mechanisms of tumourigenesis in the last 20 years; however, the clinical management of these patients has not progressed at the same rate. There is a lag in the translation of these scientific advances to the clinical arena and many of the potential clinical benefits have yet to be realised. The overarching aim of this research is to identify the clinical implications of these scientific advances in order to directly translate them to the benefit of patients.

1.1.1   Background to phaeochromocytoma and paraganglioma

Paraganglia are comprised of chromaffin cells, and lie in close proximity to the sympathetic ganglia, with which they communicate. A description of the sympathetic nervous system was introduced by Langley at the turn of the 20th century[1,2]. The term 'chromaffin' refers to the distinct colour reaction of adrenal medulla tissue when exposed to chromium salts. These cells selectively take up chromium salts to give the chromaffin reaction (staining yellow colour with dichromate salts and green with ferric chloride), as first described by Werner (1857) and further explored by Henle (1865) and Carmichael (1857) and Kohn (1903). To activate chromaffin cells the splanchnic nerves of the sympathetic nervous system release acetylcholine, which binds to nicotinic acetylcholine receptors on the adrenal medulla, causing the release of catecholamines (80% epinephrine, 20% norepinephrine). Chromaffin cells are concentrated within the adrenal medulla and in clusters along the sympathetic ganglia, such as the organ of Zuckerkandl (paired organ prominent in foetuses and newborn infants, found in the abdomen at the root of the inferior mesenteric artery[2]) and in clusters along the paravertebral chain, mediastinum, kidney, liver hila, aortic bifurcation and bladder[3].

Paraganglia differentiate into either sympathetic or parasympathetic cell lines during embryological development. The term paraganglioma (PGL) is used to describe any tumour arising from the paraganglia, whether of sympathetic origin (e.g. chromaffin cells) or of parasympathetic (e.g. glomus

cells). PGLs can therefore occur anywhere from the skull base to the pelvis. The term phaeochromocytoma (PCC) specifically describes a PGL arising in the adrenal medulla[4] and was first described in 1886[5] in an 18 year old girl with a one year history of episodic symptoms of palpitations, vomiting, headaches, dizziness and anxiety with long standing hypertension. She subsequently died of a presumed hypertensive crisis, and on post-mortem Fraenkel identified bilateral adrenal tumours that originated from the adrenal medulla[2,6]. Paraganglia of sympathetic origin have endocrine functions (production of catecholamines) and those of parasympathetic origin function as chemoreceptors. Paraganglia are involved in the homeostasis of hypoxia, bleeding, cold and hypoglycaemia[3]. They act directly as chemical sensors or by producing catecholamines in response to stress[7]. The major metabolic function of catecholamines is to increase glycogenolysis for oxidation metabolism and chemoreceptors sense changes in oxygen and carbon dioxide levels and regulate the volume and rate of breathing.

PCCs are the more common tumour with a reported incidence of 2-8 per million person-years[8-10]. Extra-adrenal PGL are rarer with an incidence of 0.5 per million person-years[7]. The reported combined prevalence of phaeochromocytoma and paraganglioma (PPGL) is 1 in 2500-6500 individuals[11]. Prevalence within the hypertensive population is only 0.2-0.6%[12] and only 5% of incidentally found adrenal lesions are PCCs[12], although up to 25% of PPGLs are discovered incidentally on imaging for unrelated disorders[13]. The incidence is higher in autopsy series (1:2000), implying many tumours remain undetected and may be responsible for early demise[14-16].

Catecholamines are produced from tyrosine in a multi-step pathway (Figure 1.1), culminating in the conversion of dopamine to norepinephrine by the action of dopamine β-hydroxylase, and norepinephrine to epinephrine by the enzyme phenylethanolamine *N*-methyltransferase (PNMT)[17]. The rate limiting step, the conversion of tyrosine to 3,4-dihydroxyphenlalanine by the enzyme tyrosine hydroxylase (TH), is the first step in the pathway. The conversion of dopamine to norepinephrine occurs within storage vesicles present in noradrenergic neurons and adrenal chromaffin cells. The enzyme PNMT is only present in the cytoplasm of adrenal medullary chromaffin cells and therefore norepinephrine can only be converted to epinephrine when norepinephrine leaks from the storage vesicles into the cytoplasm within these cells[18]. After epinephrine is synthesised it is then taken up by storage vesicles within the chromaffin cell. The activity of PNMT is upregulated by high levels of cortisol.

Catecholamines are episodically secreted from granules within chromaffin cells into the circulation and it is these catecholamines that cause the symptoms, such as episodic headache, palpitations and diaphoresis. Within neuronal cells norepinephrine is metabolised to 3,4-dihydroxyphenylglycol

(DHPG) by mono-amine oxidase (MAO), but within extra-neuronal cells, including those of the adrenal medulla and tumour cells, catecholamines leak from the granules into the cell cytoplasm where they undergo either reuptake into the granules or are metabolised by catechol-O-methyl transferases (COMT)[19] to their O-methylated metabolites, known as metanephrines (metanephrine/metadrenaline (MN), normetanephrine/normetadrenaline (NMN) and 3-methoxytyramine (3MT))[20,21]. Less differentiated tumours tend to produce intermediate metabolites, as they lack the final enzymes, thus metanephrine profiles can be used to indicate possible underlying genetic causes[22]. Increased levels of 3MT, the breakdown product of dopamine, has been suggested as a marker of more aggressive disease in sympathetic PGL[23].

Catecholamines are rapidly cleared by specific neuronal and extra-neuronal reuptake mechanisms; however, their metabolites, the metanephrines, continuously diffuse from the cell into the circulation. In addition to the metanephrines there are several other pathways for the metabolism of catecholamines; 3-methoxy-4-hydroxyphenylglycol (MHPG) is formed by the O-methylation of DHPG by COMT (within sympathetic neurones) and MAO deaminates metanephrines in extra-neuronal tissue, including adrenal chromaffin cells. MHPG is then taken up by the liver and converted to vanillylmandelic acid (VMA) or by the gastrointestinal system to form sulphate conjugates[19]. These metabolites are then cleared by the kidneys and excreted in the urine (Figure 1.1).
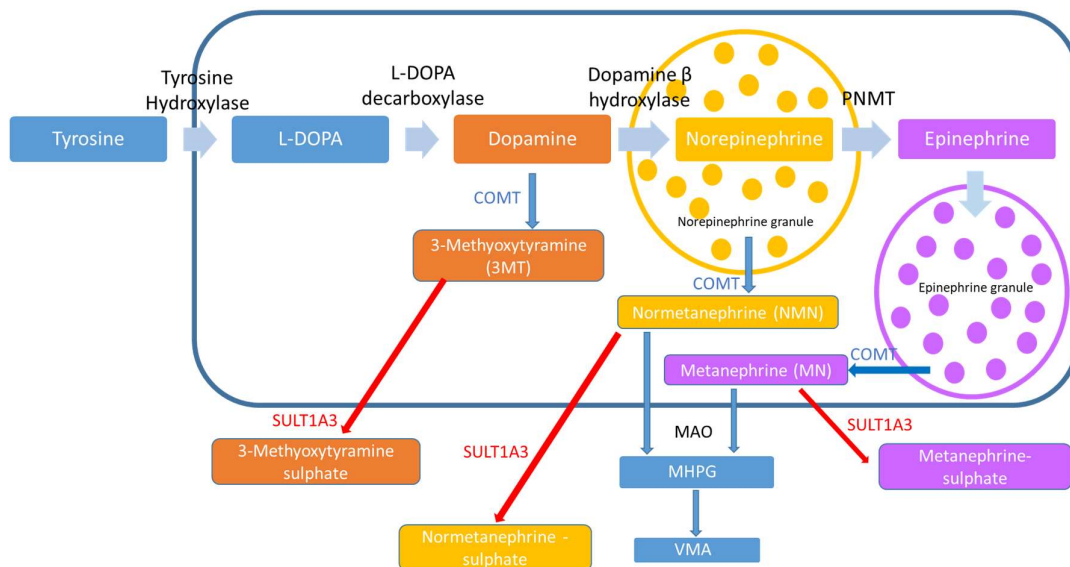
Figure 1.1: Catecholamine biosynthesis and metabolism. *Diagrammatic representation of catecholamine biosynthesis pathway within a chromaffin cell and different routes of metabolism. NMN, MN, DHPG, MHPG are converted to VMA in the liver. The sulphate conjugates and VMA are excreted via the kidneys. MN metanephrine, NMN normetanephrine, PNMT phenylethanolamine N-methyltransferase, MAO monoamine oxidase, COMT catechol-O-methyltransferase, SULT1A3 sulfotransferase type 1A3, MHPG 3-methoxy-4-hydroxyphenylglycol, VMA vanillylmandelic acid. Adapted from Eisenhofer et al[19] and Pacak[17].*

For simplicity the terms 'functional PPGLs' will be used in this thesis to describe hormonally functional PPGLs that produce and secrete catecholamines in excess that results in measured metanephrine levels above the reference ranges, and 'biochemically silent' PPGLs that do not have measured metanephrine levels above the reference ranges[12]. Metanephrine levels are used as a surrogate marker for their corresponding excess catecholamine levels produced by the tumour.

PPGLs can occur in both sporadic and familial forms. Historically it was believed that only 10% of all PPGLs were familial. As more genes are identified however, it is recognised that PPGLs have the highest rate of associated inherited cancer susceptibility syndromes of all tumour types[24]; it is now thought to be as high as 40-50%[24].

1.1.2 Cluster hypothesis

PPGL tumours have been classified into two main clusters based on different signalling pathways causing tumourigenesis, to identify targeted therapeutic options. The different clusters have distinct phenotypes and secretory profiles[25] (Table 1.1).

Cluster 1 is characterised by inappropriate activation of the hypoxia-angiogenesis pathway. The associated genes are tumour suppressor genes and have recently been further sub-classified into 1a and 1b based on the position of the gene mutation and have different clinical features and prognosis[26]. Mutations in cluster 1a include mutations of the genes encoding the enzymes of the TCA (tricarboxylic acid) cycle e.g. subunits of succinate dehydrogenase (*SDHA-D, AF2*), malate dehydrogenase (*MDH2*) and fumarate hydratase (*FH*). Mutated genes in cluster 1b include von Hippel Lindau (*VHL*), endothelial PAS domain-containing protein 1 (*EPAS1*) which encodes for the hypoxia-inducible factor 2α protein, and Egl nine homolog (*EGLN)* 1 and 2 genes (which encode enzymes prolyl hydroxylase (PHD) domain-containing protein 2 and 1 respectively). Mutations in these genes, are thought to cause dysfunction of the TCA cycle and thus pseudohypoxia, with abnormal angiogenesis.

Mutations of genes in cluster 2 affect kinase signalling pathways and include neurofibromatosis 1 (*NF1*), rearranged during transfection proto-oncogene (*RET*), transmembrane protein 127 (*TMEM127*), myc-associated factor X (*MAX*), and kinesin family member 1B (*KIF1B*). Recently further molecular classification has been attempted extending the classification to include a Wnt-altered subtype[27]. The Wnt-altered subtype includes somatic mutations in cold shock domain containing E1 (*CSDE1*) and mastermind like transcriptional coactivator 3 (*MAML3*) fusion genes, and occur only in PCCs[27,28].

This research focuses mainly on mutations in cluster 1 genes.
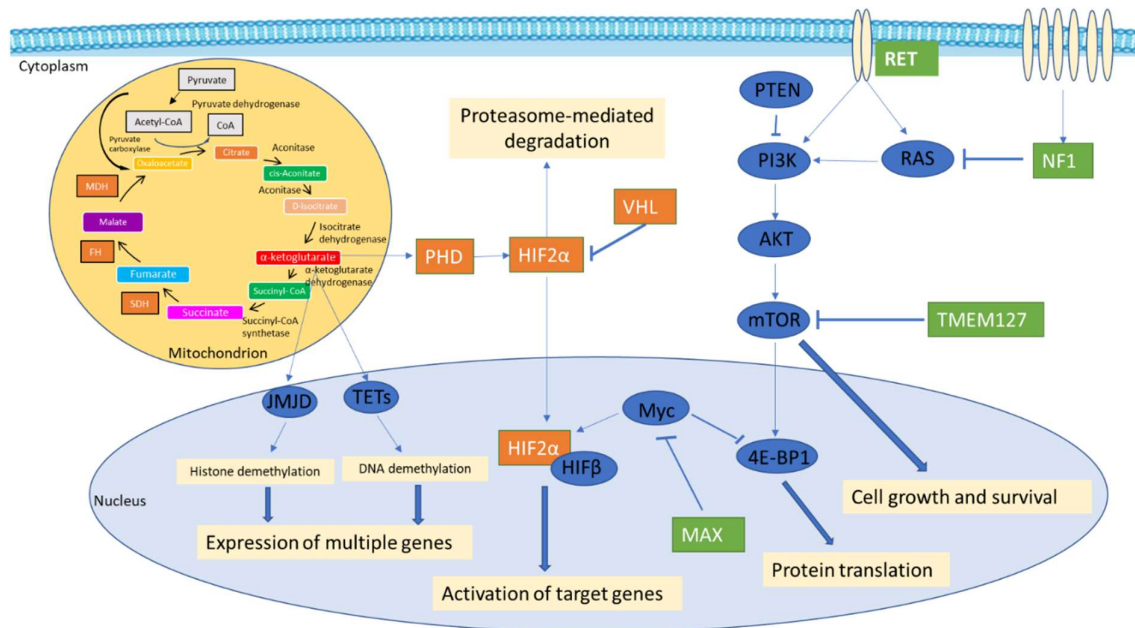
Figure 1.2: Diagrammatic representation of the tumourigenic pathways associated with PPGL formation. *Cluster 1 genes are shown in the orange pathway and cluster 2 genes in the green pathway. Adapted from Dahia et al[24] and Castro-Vega et al[29]. SDH succinate dehydrogenase, MDH malate dehydrogenase, FH fumarate hydratase, PHD prolyl hydroxylase, VHL von hippel Lindau protein, JMJD Jumonji histone demethylase family, TET ten-eleven translocation, HIF hypoxia inducible factor, RET rearranged during transfection protocogene, NF1 neurofibromatosis 1, TMEM127 transmembrane protein 127, MAX myc-associated factor X, mTOR mammalian target of rapamycin, PTEN phosphate and tensin homolog protein, P13K phosphoinositide-3-kinase, 4E-BP1 Eukaryotic initiation factor 4E-binding protein 1, AKT protein kinase B*

Cluster	Genes	Phenotype
1a	*SDH, MDH, FH*	PPGL, mainly NA producing. Predisposed to recurrence and metastatic disease. 100% germline mutations.
1b	*VHL, EPAS, EGLN*	Mainly PCC, NA producing. 20% germline
2	*NF1, RET, MAX, TMEM127, KIF1B, MERTK*	PCC, mainly A producing
3	*CSDE1, MAML3 fusion*	PCC, somatic mutations only

Table 1.1: Summary of PPGL cluster classification. *SDH succinate dehydrogenase, MDH malate dehydrogenase, FH fumarate hydratase, PHD prolyl hydroxylase, VHL von hippel Lindau protein, RET rearranged during transfection protocogene, NF1 neurofibromatosis 1, TMEM127 transmembrane protein 127, MAX myc-associated factor X, mTOR, EPAS endothelial PAS domain-containing protein 1 (HIF2α), EGLN Egl 9 homolog (PHD2), CSDE1 cold shock domain containing E1, MAML3 mastermind like transcriptional coactivator 3, A adrenaline, NA noradrenaline*

1.1.2.1 Cluster 1 (Pseudohypoxia)

The signature of cluster 1 mutations is pseudohypoxia. In normal physiology hypoxia inducible factors (HIFs) are activated in response to low cellular oxygen levels. HIFs are heterodimeric transcription factors, with inducible components (α-subunits), that drive the expression of genes in different pathways. Alpha subunits dimerise with beta subunits to form active units (i.e. HIFα-HIFβ). HIF1α drives the expression of genes for apoptotic and glycolytic pathways (e.g. glucose transporter 1

(GLUT1), hexokinase, glycerophosphate kinase) and leads to an increase in production of adenosine triphosphate (ATP) and lactate. HIF2α activates genes involved in cell proliferation and angiogenesis (e.g. VEGF, PDGF, TGFα). This process is regulated by hydroxylation and proteasomal degradation. At normal oxygen levels, the alpha subunit of HIF is hydroxylated by the enzyme prolyl hydroxylase. This hydroxylated HIF is recognised by VHL, which subsequently targets it for proteasomal degradation, thus preventing the activation of target genes. Prolyl hydroxylase domain proteins (PHDs) are α-ketoglutarate dependant dioxygenases. The TCA cycle substrate α-ketoglutarate-2-oxoglutarate regulates PHD activity and PHD activity is competitively inhibited by succinate and fumarate. Other 2-oxoglutarate-dependant enzymes include the Jumonji histone demethylase family and Ten-eleven translocation family of 5-methylcytosine enzyme hydroxylases, which are involved in histone and DNA demethylation respectively. This process is outlined in Figure 1.2.

Mutations in any of the enzymes of the TCA cycle or VHL interferes with the regulation of HIF, causing unregulated activation of specific pathways. Mutations in enzymes of the TCA cycle result in an accumulation of intracellular oncometabolites such as succinate, which inhibit multiple 2-oxoglutarate-dependant dioxygenases by competitive inhibition (e.g. PHD, histone or DNA demethylases). When succinate inhibits PHD, it cannot hydroxylate HIFα, therefore HIFα is stabilised and is not degraded even in the presence of oxygen. Stabilised HIFα then translocates to the nucleus where it forms a complex with HIFβ, and subsequently activation of the hypoxia signalling pathways in normoxic conditions occurs (pseudohypoxia).

Within the same cluster or pathway it is well recognised that there are distinct differences in the disease phenotypes[30,31], for example site of tumour formation, aggressiveness of tumours and associated other disease, caused by different gene mutations (Table 1.2) despite the same mechanism of tumourigenesis. This is even more intriguing when focusing on one specific defect in the pathway, which can give rise to different disease phenotypes.

1.1.3 Genetic causes of PPGL

Familial paraganglioma syndromes were first described in 1933[32], but only more recently have the culprit genes been identified. Susceptibility to PPGLs was first recognised in three genetic syndromes: neurofibromatosis type 1 (NF1), multiple endocrine neoplasia type 2 (MEN2) and von Hippel-Lindau syndrome (vHL). In the 1990's the culprit genes were identified: *NF1* gene[33], oncogene *RET*[34] and tumour suppressor gene *VHL*[35,36] respectively. Germline mutations in at least 18 genes (*NF1, RET, MEN1, VHL, SDHD, SDHB, SDHC, KIF1ß, SDHAF2, SDHA, TMEM127, PHD2/EGLN1, MAX, EPAS1/HIF2A, FH, MDH2, PHD1/EGLN2, MERTK* – Figure 1.3) have now been implicated in tumourigenesis of familial

PPGL syndromes, with multiple additional mutations occurring at the somatic level. More recently additional genes (*DNMT3A*[37], *SLC25A11*[38], *DLST*[39]) have been suggested as possible PPGL susceptibility genes by genomic sequencing analysis in single or familial cases, although further work is needed to prove causality[40]. At the time this work was undertaken in the UK the standard PPGL 10 gene panel included: *SDHA, SDHB, SDHC, SDHD, SDHAF2, RET, MAX, TMEM127, VHL*, and *FH.*
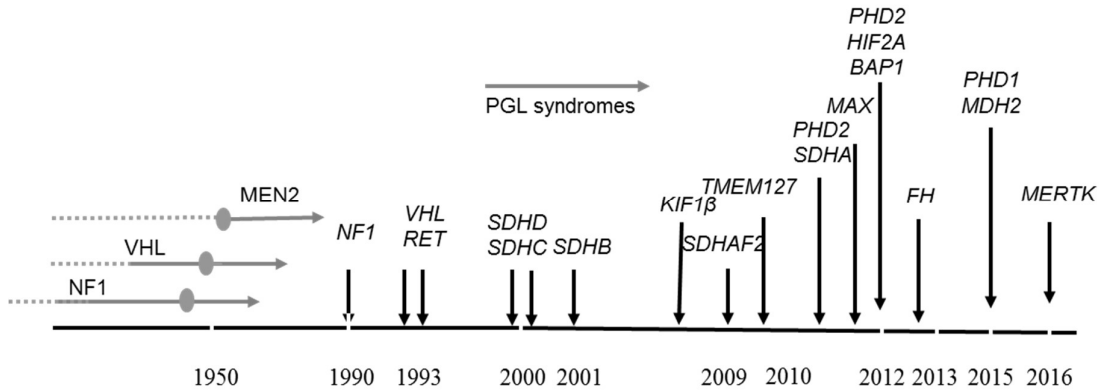
Figure 1.3: Timeline of discovery of germline mutations known to cause familial PGL syndromes *(adapted from Eisenhower & Pacak, with permission). NF1 neurofibromatosis 1, VHL von Hippel Lindau, MEN2 multiple endocrine neoplasia type2, RET rearranged during transfection proto-oncogene, SDHD succinate dehydrogenase subunit D, SDHC succinate dehydrogenase subunit C, SDHB succinate dehydrogenase subunit B, KIF1β kinesin family member 1B, SDHAF2 succinate dehydrogenase subunit AF2, TMEM127 transmembrane protein 127, SDHA succinate dehydrogenase subunit A, PHD prolyl hydroxylase (EGLN), MAX myc-associated factor X, HIF2A hypoxia inducible factor 2A (EPAS1), BAP1 BRCA1-assocaited protein, FH fumarate hydratase, MDH malate dehydrogenase, MERTK cMER proto-oncogene tyrosine kinase receptor*

Gene	Gene Name	Cluster	Year of discovery	Syndrome/disease name	Penetrance of PPGL	Phenotype
NF1	neurofibromatosis 1	2	1990	Neurofibromatosis 1	<6%	café-au-lait spots, neurofibromas, axillary freckling, lisch nodules, ossesous lesions, optic gliomas, PCC
RET*$^\$$	proto-oncogene tyrosine protein kinase receptor Ret (rearranged during transcription)	2	1990	Multiple endocrine neoplasia (MEN) type 2A and 2B	50%	MEN2A - MTC, PHPT, PCC MEN2B MTC, Marfanoid habitus, mucocutaneous neuromas, gastrointestinal ganglioneuromatosis, PCC
MEN1	multiple neuroendocrine neoplasia 1		1997	MEN1 (MENIN protein)	<1%	PHPT (95%), NET (30-80%), PA (15-90%). 20% NFA adenoma
VHL*	von Hippel Lindau	1b	1993	Von Hippel Lindau syndrome	10-20%	CNS haemangioblastomas, renal cysts, RCC, pNETs, endolymphatic sac tumours, broad-ligament cystadenomas, BL PCC
SDHD*	succinate dehydrogenase subunit D	1a	2000	Familial paraganglioma syndrome type 1 (paternal inheritance)	60-85%	PPGL (predominantly HN), RCC, GIST, PA
SDHC*	succinate dehydrogenase subunit C	1a	2000	Familial paraganglioma syndrome type 3	4%	PPGL, RCC, GIST, PA
SDHB*	succinate dehydrogenase subunit B	1a	2001	Familial paraganglioma syndrome type 4	50%	PPGL, RCC, GIST, PA
KIF1β	kinesin family member 1B	2	2008		Rare	PCC, neuroblastoma
SDHAF2*	succinate dehydrogenase subunit AF2	1a	2009	Familial paraganglioma syndrome type 2 (paternal inheritance)	75-100%	HNPGL
SDHA*	succinate dehydrogenase subunit A	1a	2010	Familial paraganglioma syndrome type 5	1%	PPGL, GIST
TMEM127*	transmembrane protein 127	2	2010	Familial phaeochromocytoma	Rare	PPGL, RCC
PHD2 (EGLN1)	prolyl hydoxylase domain containing protein	1b	2011	Polycythaemia paraganglioma syndrome	Rare	Polycythaemia, PPGL
MAX* (paternal inheritance)	myc-associated factor X	2	2011		<10%	Neuroblastoma + PCC
EPAS1 (HIF2A)	hypoxia inducible factor 2	1b	2012	Polycythaemia paraganglioma syndrome	Rare	polycythaemia, somatostatinoma, PPGL
FH*	fumarate hydratase	1a	2013	Reed syndrome	Rare	Skin & uterus Leiomyomatosis and RCC
MDH2	Malate dehydrogenase	1a	2015	Familial PGL syndrome	Rare	TAPGL
PHD1 (EGLN2)	prolyl hydroxylase	1b	2015	Polycythaemia paraganglioma syndrome	Rare	Polycythaemia, PPGL

Gene	Gene Name	Cluster	Year of discovery	Syndrome/disease name	Penetrance of PPGL	Phenotype
MERTK	c-MER proto-oncogene tyrosine kinase receptor	2	2016	Reported case of MEN2 phenotype in RET negative	Rare	PPGL, MTC, RCC

Table 1.2: Mutations associated with PPGL formation. *The table outlines the different mutations associated with PPGL formation and provides a brief clinical description of the associated syndrome and the prevalence of PPGL occurrence in each syndrome. *Tested as part of 10 panel PPGL genetics screen PPGL phaeochromocytoma and paraganglioma, BL PCC bilateral phaeochromocytoma, PGL paraganglioma, HNPGL head & neck paraganglioma, TAPGL thoracic and abdominal PGL, RCC renal cell carcinoma, MTC medullary thyroid carcinoma, GIST gastrointestinal stromal tumour, PA pituitary adenoma, NET neuroendocrine tumour, pNET pancreatic neuroendocrine tumour, PHTP primary hyperparathyroidism, SDH succinate dehydrogenase, MDH2 malate dehydrogenase, FH fumarate hydratase, VHL von Hippel Lindau, EPAS1 Endothelial PAS domain-containing protein 1, HIF2α hypoxia-inducible factor 2α, PHD prolyl hydroxylase, EGLN Egl nine homolog, NF1 neurofibromatosis 1, RET rearranged during transfection proto-oncogene (RET), TMEM127 transmembrane protein 127, MAX myc-associated factor X, KIF1Bkinesin family member 1B.*

1.1.4   Succinate Dehydrogenase

Mutations in the genes that encode the subunits of the SDH enzyme are thought to cause tumourigenesis through a cluster 1a action. SDH is a mitochondrial enzyme that is part of both the tricarboxylic acid (TCA) cycle and the electron transport chain (Figure 1.4). It catalyses the oxidation of succinate to fumarate and transfers electrons to the ubiquinone pool to prevent formation of potentially damaging reactive oxidative species (ROS)[41]. The SDH protein consists of four subunits and a flavination protein. It is comprised of two hydrophobic anchorage proteins (SDHC and SDHD), which anchor the complex to the inner mitochondrial membrane and provide a binding site for ubiquinone and two hydrophilic catalytic proteins (SDHA and SDHB). SDHA provides the substrate binding site and SDHB is an iron-sulphur protein involved in electron transfer[41]. The final component of the complex is a flavination protein (SDHAF2), which acts as an assembly factor and is essential for the complex to form. These five proteins are encoded by five nuclear genes: *SDHA* (15 exons, chromosome 5p15), *SDHB* (eight exons, chromosome 1p36), *SDHC* (six exons, chromosome 1q23), *SDHD* (four exons, on chromosome 11q23), and *SDHAF2* (four exons, chromosome 11q13) (Figure 1.4 and Table 1.3).
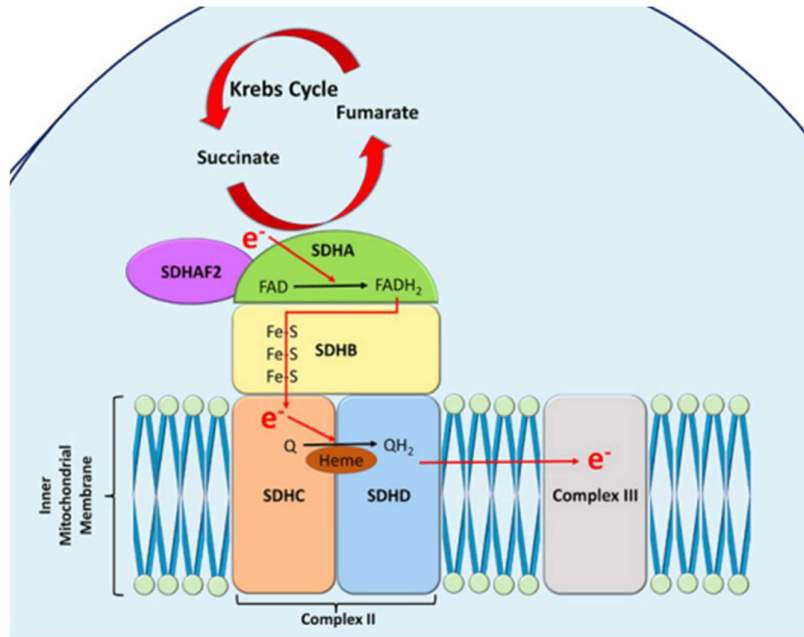
Figure 1.4: Mitochondrial complex II. *Diagrammatic representation of mitochondrial complex II, showing the different subunits that make up the succinate dehydrogenase enzyme. SDHA and SDHB subunits catalyse the oxidation of succinate to fumarate as part of the TCA cycle within the mitochondrial matrix. The electrons generated by this process (e-) reduce FAD to $FADH_2$ within the SDHA subunit and then reduce ubiquinone (Q) to ubiquinol (QH_2) within SDHC and SDHD subunits. Image adapted from P.B.Loughrey with permission[42]. Image generated with Biorender.com.*

SDH subunit	Chromosome	Gene length (kb)	No. of exons	Length of mRNA (bp)	Protein Length (amino acids)	Notes
SDHA	5p15	38.4	15	2405	664	
SDHB	1p36	35.4	8	1161	280	
SDHC	1q23	50.3	6	2858	169	
SDHD	11q23	8.9	4	1313	159	Paternal inheritance*
SDHAF2	11q13	23643	4	1227	166	Paternal inheritance*

Table 1.3: Genes that encode for SDH subunits. *Table summarises the molecular features of the genes that encode the different SDH subunits, outlining the chromosome number, gene length, number of exons of the gene, mRNA length and length of subsequent protein and type of inheritance pattern.**Disease only occurs when gene is inherited from the father, also known as maternal imprinting.*

Mutations in any of the subunits causes disruption in SDH enzyme function, which leads to an accumulation of succinate in the mitochondria. Excess succinate inhibits α-ketoglutarate dependent enzymes; including PHD, therefore resulting in inappropriate HIF activation, together with histone and DNA demethylases resulting in global hypermethylation of target genes and potential epigenetic silencing[43]. An example of these epigenetic modifications is hypermethylation, due to excess succinate, of the promoter gene that encodes PNMT causing downregulation of this enzyme resulting in premature termination of the catecholamine synthesis pathway, such that epinephrine cannot be

formed. Additionally, disruption of the electron transport chain due to dysfunction of the SDH protein results in superoxide generation which further contributes to PHD inhibition[44] and thus HIF stability.

Tumourigenesis is thought to occur in accordance with Knudson's two-hit hypothesis, such that there is a heterozygous germline mutation in one of the tumour suppressor genes (i.e. *SDHB*) and tumour formation occurs due to a second hit in the form of a somatic loss of the nonmutant allele in the tumour i.e. loss of heterozygosity (LoH)[45]. This results in loss of function of the SDH enzyme.

It was not until the year 2000 that the first causal germline mutations were identified in familial PPGL syndromes due to disruption of SDH; the first with *SDHD*[46,47], closely followed by *SDHC*[48], *SDHB* in 2001[49] and then finally *SDHAF2*[50] and *SDHA*[51]. Over 400 different *SDH* mutations have been identified worldwide[52].

A brief description of the disease caused by mutations in each of the subunits follows, in order of the most commonly to least commonly mutated *SDH* subunits.

1.1.4.1 SDHB

Mutations in the *SDHB* gene account for 10% of cases of all PPGLs and approximately one quarter of familial disease[13,31]. A total of 395 unique mutation variants have been reported in the *SDH* database[52]. Early penetrance figures suggested 80-100% of individual carriers were affected by disease[53,54]. Penetrance estimates have fallen over time as more disease-free asymptomatic carriers are identified. More recent studies suggest penetrance figures as low as 22-26% at age 60 years[55,56] and 30-44% at age 80 years[56,57], and some authors suggest as little as 1-3% at <20 years[55,57,58] in the asymptomatic carrier population.

A recent review[30] concluded that, although the most common site of PGL disease in *SDHB* mutation carriers is intra-abdominal/extra-adrenal, it also highlighted that a significant number of patients present with a PCC (20-25%) and/or a head and neck PGL (HNPGL) (20-30%). *SDHB* mutation carriers have the highest rate of malignant transformation at approximately 30%[59,60]. It has been postulated that this may be due to the higher incidence of disease at extra-adrenal sympathetic sites[23,60-62].

Other types of tumours have been associated with *SDHB* mutations. Approximately 50-60 *SDHB*-related renal cell carcinomas (RCC) have been reported[54-56,63-70]. *SDHB*-related RCC appear to have a more aggressive behaviour than their sporadic counterparts and occur at younger ages[66,71], with bilateral disease occurring in 30% of *SDHB*-deficient cases and metastatic disease occurring in 33% of RCC cases[30]. *SDHB*-related RCCs have distinct clear cell pathological features and are now recognized as a unique subtype of RCC[68,72-74]. It has been hypothesised there may be certain mutations that

increase the risk of developing a renal tumour; those with Arginine substitutes appear particularly predisposed[67,75], although other genotype associations have also been reported[70,76]. Gastrointestinal stromal tumours (GIST) are reported to occur in approximately 2% of *SDHB* carriers[30] and are predominantly gastric in origin. A predisposition to developing pituitary adenomas has also been suggested in the presence of *SDHB* mutations and has been shown to have a specific histological phenotype with large vacuoles[77]. Pituitary adenomas have been reported in nine cases of patients carrying *SDHB* mutations, six of which also had PPGL[78]. Only three of these, however, had confirmed *SDHB* mutation involvement with intracytoplasmic granules, abnormal SDHB expression and proven LoH[77].

1.1.4.2 SDHD

Mutations in the *SDHD* gene account for approximately 9% of cases of all PPGLs[31], and are affected by maternal imprinting, so disease is only penetrant if the abnormal gene is inherited from the paternal line. A recent review[79] highlighted that mutations in *SDHD* are currently the leading cause of hereditary HNPGLs (50%) and PGLs in these locations are the predominant clinical feature of *SDHD* mutation carriers with 85% of carriers developing tumours at these sites[30]. PCC and extra-adrenal sympathetic PGLs are reported to occur less frequently in 10-25% and 20-25% of carriers respectively[53]. Multifocal disease is more common in *SDHD* carriers, with estimates that 55-60% of carriers develop multiple tumours[53]. A total of 182 unique mutation variants have been reported in the *SDH* database[52]. It is recognised that PPGLs occurring in *SDHD* carriers run a more benign course[53,80].

RCC, GIST and pituitary adenoma have also been associated with *SDHD* mutations[78,80]. Very few RCC have been reported in patients with *SDHD* mutations and lifetime risk is extremely low (<1%)[56,66,70,76]. Five cases of patients carrying *SDHD* mutations have been reported with pituitary adenomas and PPGL[78]. Only two of these however had proven LoH and negative SDHB immunostaining, and both were macroprolactinomas[81,82].

1.1.4.3 SDHC

Mutations in the *SDHC* gene account for 1% of cases of all PPGLs[31]. A total of 101 unique mutation variants have been reported in the *SDH* database[52]. Andrews *et al*[56] estimated risk of disease at age 60 years at 25% in mutation positive non-probands.

Many fewer cases of patients with *SDHC* mutations have been reported compared to *SDHB* and *SDHD* and therefore a detailed phenotype is not well described. The reports focus mainly on index cases and suggest a predominance of HNPGLs with a few sympathetic PGLs reported[3,7,56,64,83-92].

Two cases of pituitary adenoma occurring in individuals with *SDHC* mutations have been described with macroprolactinoma and HNPGL, but no tissue was available for LoH studies to prove pathogenicity[78]. Eight RCC[66,70,93] and multiple GISTs[94-96] have been reported in patients harbouring *SDHC* mutations.

1.1.4.4 SDHA

Mutations in the *SDHA* gene were first associated with autosomal recessive inheritance of the mitochondrial disease Leigh syndrome (juvenile encephalopathy)[97] and more recently with severe neurological dysfunction and cardiomyopathy[98]. As an autosomal dominant inherited tumour suppressor gene, *SDHA* mutations were only proven to be associated with inherited familial PGL syndromes in 2010[51] and not surprisingly, there is less clinical understanding of the natural history of this subunit, with the gene being tested for less often and with numerous variants of unknown significance (VUS). To our knowledge no PGL familial disease has been reported in *SDHA* carriers and the penetrance therefore remains unknown but is likely to be very low[99]. Mutations in the *SDHA* gene account for <1% of all PPGL cases[31] and only 3% of familial cases. There are now 178 unique mutation variants reported in the *SDH* database[52].

1.1.4.5 SDHAF2

Very few cases of PPGL associated with mutations in *SDHAF2* have been reported[5,50,100,101]. It was first described in 2009[50] and shown to be affected by maternal imprinting, such that only if the mutation is inherited from the father will the disease be penetrant. Mutations in the *SDHAF2* gene account for <0.1% of cases of all PPGLs[31]. Twenty unique mutation variants of *SDHAF2* are reported in the *SDH* database[52].

Chapter 2. Materials and methods

2.1   Formation of the database

A collaboration with endocrine, radiology, surgery, genetics, and histopathology departments identified patients that had been diagnosed or treated for PPGL disease at our centre from 1970 onwards. This list of patients was entered into an excel spreadsheet and further demographic, clinical, genetic, biochemical, pathological and clinical outcomes were collated for each individual.

2.2   Analysis of *SDH* cohorts

From the above database all patients in the department that carried a genetic germline mutation in one of the *SDH* genes were identified. Further clinical details were collated from individual medical records on diagnosis of PPGL or *SDH*-associated disease (e.g. RCC, GIST, pituitary adenoma). All patients that carry an *SDH* mutation are invited to join a specialist surveillance programme at our centre. The current *SDH* surveillance programme was instituted in 2007 and modified from an earlier 'familial PCC and PGL screening protocol'. The current surveillance programme for all *SDH* mutation carriers involves annual clinical review and annual assessment of metanephrine levels (24-hour urine collection or plasma), annual non-contrast magnetic resonance imaging (MRI) of the abdomen and biennial MRI skull base to pelvis. The surveillance regimen is modified to include appropriate follow-up in patients with known or previous tumours. For children, clinical review is offered routinely from the age of five years and surveillance protocols are then tailored to each individual child. For children aged <10 years, screening includes the measurement of urinary metanephrines, abdomen and neck ultrasound scans and from age 10, plasma metanephrines and MRI of thorax, pelvis and neck if tolerated. Clinical outcomes of all patients were analysed.

A primary tumour was defined as a tumour occurring along the parasympathetic or sympathetic chain at a site of neural crest cells. A metastasis was defined as occurrence of tumour at a site where neural crest cells are not usually found. Index patients were defined as any patient that presented with symptoms of catecholamine excess or mass effect of the tumour. Surveillance patients were defined as relatives identified through cascade screening of an index case (index case not necessarily seen at our centre). The patients classified as 'children' were defined as symptomatic index patients diagnosed aged ≤18 years or individuals in whom surveillance was commenced in childhood (≤18 years).

A literature review was performed to identify all published cohorts of clinical outcomes in *SDH* mutation carriers. Where raw data were available these cohorts were assessed for prevalence of disease at specific body sites and malignancy risks. Statistics are presented as median values with ranges indicated, and as percentage risk of total tumours.

As many VUSs are reported in *SDHA* mutations, to predict the pathogenicity of the DNA variants in the cohort, the missense variants were investigated *in silico* using Polyphen2 and SIFT and assigned a classification according to the American College of Medical Genetics and Genomics (ACMG) guidelines[102] and correlated to SDHB and SDHA immunohistochemistry findings.

2.3   Improving pre-operative management

2.3.1   Phaeochromocytoma alert card

A patient information card was designed using the national 'steroid alert card' as a template. Draft versions were reviewed by consultants and specialist nurses of the endocrine department at St. Bartholomew's Hospital and a selection of endocrine patients in an outpatient setting. Adaptations were made to adjust content and design based on this feedback. This phaeochromocytoma alert card was handed to patients on diagnosis of PPGL and a brief education given about the possible interacting medications. Patients were advised to show the card to any health care professional with whom they had contact between the time of their diagnosis and operation.

2.3.2   Patients

PPGL intervention group

All patients that were diagnosed with a functional PCC or sympathetic PGL (plasma metanephrines above the upper reference range plus positive cross-sectional imaging), arising at any body site, from September 2017 until June 2019 were recruited (intervention group). Baseline investigations were performed including blood tests for full blood count (FBC), renal function (UE), liver function (LFTs), ferritin, HbA1c, pro-beta natriuretic peptide (pro-BNP), Troponin T, C-reactive protein (CRP)[103], chromogranin A and B, and urinary and plasma metanephrine levels. Serum inflammation scores were calculated from these baseline investigations: Neutrophil-lymphocyte ratio (NLR) by dividing the absolute neutrophil count by the absolute lymphocyte count; platelet-lymphocyte ratio (PLR) by dividing the absolute platelet count by the absolute lymphocyte count; lymphocyte-monocyte ratio (LMR) by dividing the absolute lymphocyte count by the absolute monocyte count[104]; systemic inflammatory index (SII) by multiplying the absolute platelet count by the NLR[105]; neutrophil-platelet

score (NPS) was awarded based on absolute neutrophil and platelet values (score of 0 if neutrophils $\leq 7.5 \times 10^9$/L and platelets $\leq 400 \times 10^9$/L, a score of 1 if neutrophils $>7.5 \times 10^9$/L or platelets $>400 \times 10^9$/L, or a score of 2 if neutrophils $>7.5 \times 10^9$/L and platelets $>400 \times 10^9$/L)[106]; prognostic nutrition index (PNI) addition of albumin level (g/L) + (5 x total lymphocyte count)[107]. Twenty-four-hour urine collection was obtained for assessment of metanephrine levels and salt status. Spot urine tests were taken for assessment of albumin:creatinine (ACR) and sodium levels. Electrocardiograms (ECG) were performed on every patient, and echocardiogram was arranged in any high-risk patients. Cross sectional imaging with either MRI or computed tomography (CT) had already been undertaken as part of the diagnostic work up. Bioimpedance measurements including weight, body mass index (BMI), basal metabolic rate (BMR), total body water (TBW), extra cellular water content (ECW), intracellular water content (ICW), bone mass, and muscle mass were recorded at diagnosis and each clinic visit, using a Tanita body composition analyser (model MC-180MA III) in accordance with the manufacture's guidance. This measures bioimpedance by sending small electrical signals through the body that passes with different resistance through different tissue types (e.g. muscle vs fat vs water).Twenty-four-hour ambulatory blood pressure (ABPM) was recorded at diagnosis, at admission to hospital pre-operatively (3-5 days before their operation date) and 6-12 months post operatively. ABPM was recorded using an On Trak ABPM (Spacelabs Healthcare 90227-1), set to measure blood pressure (BP) and heart rate (HR) every 30 minutes throughout the day (08:00-21:00) and at one hour intervals overnight, in accordance with National Institute of Clinical Excellence (NICE) hypertension guidelines[108]. As it was considered unsafe to delay starting alpha blockade once diagnosis of PPGL was confirmed, the majority of patients had their first ABPM recorded on a small dose of phenoxybenzamine (10mg twice daily).

Clinical data was collected including regular BP and HR measurements throughout the time from diagnosis to operation using ABPM and home BP monitoring (HBPM) (outlined below), dose of alpha- and beta-blockade medication achieved in an outpatient setting, final dose required pre-operatively, number of inpatient days pre-operatively, total number of inpatient days, and quantity of intravenous fluid (IVF) required pre-operatively. Intra-operative data collected included BP and HR measurements at times of intra-operative stress (intubation, knife-to-skin, tumour handling), maximum and minimum BP/HR and IVF and inotropic requirements intra-operatively. Post-operative data included duration of operation, BP and HR measurements (immediately post operation, maximum and minimum measurements with the first 6 and 12 hours), inotropic and IVF fluid requirements in the high dependency unit (HDU), and duration of stay in HDU. BP and HR measurements and IVF requirements were also recorded for the first 72 hours post discharge from HDU to ward-based care.

Modified Roizen criteria[109], using BP targets only (80/45 mmHg > BP <160/90 mmHg), were used to determine the success of alpha-blockade pre-operatively and as a measure of intra-operative haemodynamic stability.

PPGL retrospective control group

Retrospective audit data was collected from sixteen patients with functional PPGL previously treated in the department during the preceding five years to the start of the prospective study (2010-2015) that had undergone an adrenalectomy by the same surgeon (LP) and anaesthetist (TP) as the intervention group. The same biochemical (where available) and clinical data, as outlined above, were collected.

Hypertensive control group

Sixteen control patients were selected from new referrals to the tertiary hypertension clinic at St. Bartholomew's Hospital between March and June 2021. Patients underwent a biochemical screen for secondary causes of hypertension before they were enrolled in the study including urine metanephrines, serum renin activity levels and aldosterone and were excluded if a secondary cause of their hypertension was identified. Patients were matched based on age (+/- 5 years), gender and diabetes status (if diabetic +/- 8mmol/mol). Patients were excluded if they were already taking an alpha-blocking anti-hypertensive medication. Patients were invited to attend the study via telephone before their first appointment with the hypertension consultant (VK). Bioimpedance measurements, blood and urine tests (as outlined above for intervention group) were taken at the first appointment and at a follow-up appointment 14-18 weeks later. Patients were provided with HBPM machines and advised to record two measurements daily. Treatment was given as per hypertensive consultant advice, in accordance with current NICE guidelines[108], although use of alpha-blockers was avoided.

2.3.3 Blood pressure monitoring and titration regimen

Patients were commenced on alpha-blockade in the form of phenoxybenzamine at a starting dose of 10mg twice daily, which was then up titrated to reach BP targets. Elective protocols advise that a dose of 60-100mg or 1mg/Kg/day is needed to achieve target BP[12,110]. Beta-blockade, Propranolol, was commenced at a dose of 10mg twice daily, at a minimum of 48-72 hours after the commencement of alpha-blockade and up titrated to control HR. If a patient was already taking Bisoprolol for cardiac protection this was continued as the beta blocking agent. All patients were advised to have a liberal salt diet and to aim to consume 3-4 litres of liquid per day[12,111], to allow gradual volume expansion to counteract the effects of postural hypotension. Patients were provided with a brief education about

their diagnosis and medications and provided with a 'phaeochromocytoma alert card' (Figure 3.1). Patients were provided with and trained how to use a Microlife WatchBP home blood pressure monitor (Microlife WBP Home, N101125). Patients were asked to record their BP and HR twice per day, in a seated and then standing position (after 3 minutes) and record these measurements and any symptoms in their patient diary. The Microlife home BP machine was used in usual mode (patients can take measurements at timings of their own choosing) and recorded three readings for each measurement taken and provided an average of these three readings to improve accuracy, as per guidelines[108]. Patients were initially reviewed in clinic weekly and then intervals of clinic reviews were increased as stability in BP and symptoms improved. Morning spot urine sodium levels were recorded at each clinic visit, with bioimpedance measurements and clinic postural BP/HR. Blood tests were taken every 4-6 weeks to check FBC and UE to assess haemodilution status and renal function. In between clinic reviews, telephone consultations took place 1-2 weekly. Medications were titrated (Figure 2.1) to aim to achieve home readings of seated BP <135/85 mmHg and clinic readings of <140/90 mmHg, with a HR <80 bpm and standing systolic BP >90 mmHg, with HR <80 bpm, in accordance with endocrine society guidelines[12], and to minimise postural symptoms. BP targets were adapted to the individual if there was a history of cardiac or renal disease.
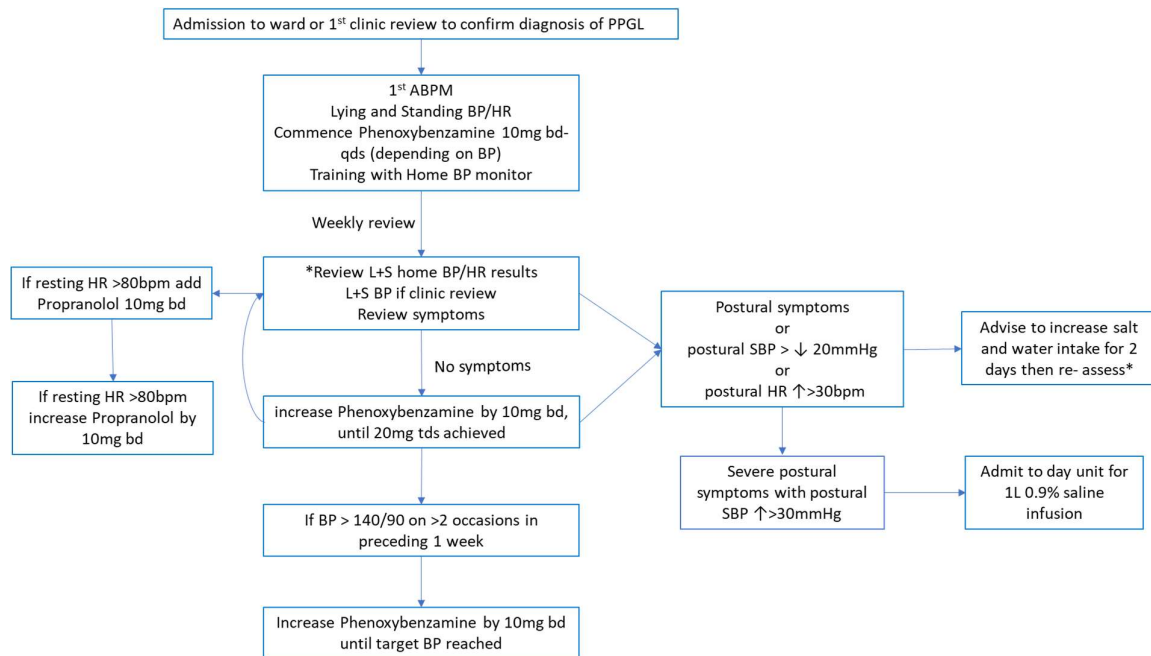
Figure 2.1: Titration of alpha- and beta-blockade pre-operatively *Schematic flowchart showing the initiation and titration of alpha- and beta-blockade pre-operatively to achieve maximal blockade as an outpatient. This was achieved through weekly clinic reviews or telephone clinics (clinic reviews took place 1-2 weekly for first month following diagnosis). ABPM ambulatory blood pressure monitoring, SBP systolic blood pressure, DBP diastolic blood pressure, HR heart rate, bd twice daily, qds four times per day, bpm beats per minute, L+S lying and standing BP.*

Evidence of effective blockade was assessed using modified Roizen criteria by the percentage of BP readings >160/90 mmHg or <80/45 mmHg on both the pre-operative ABPM and the last three full days of HBPM (12 total measurements) and the last week of HBPM (28 total measurements) before admission pre-operatively. Optimum BP/HR control was defined as BP readings <135/85 mmHg and HR <80 bpm. Seated home measurements were used to compare to ABPM measurements.

The HI-score was used to assess HDI as previously described[112]. We applied the same haemodynamic variables and volume criteria, but needed to modify the score to only include the quantity of norepinephrine that was used, as this was the inotrope used by our anaesthetist. Therefore, our modified HI-score was 0-140.

2.4   Symptom questionnaire

A questionnaire was designed to assess symptoms experienced by patients with functional PPGL (Appendix 1). A list of 25 symptoms were derived from a previously published audit[113]. The questionnaire was initially piloted on 10 patients and adapted based on patient feedback. The initial questionnaire was considered too long and cumbersome. The final questionnaire consisted of 22 symptoms requiring a 'yes/no' response: headache, diaphoresis, palpitations, heart racing, heart slowing, anxiety, constipation, diarrhoea, flushing, tremor, chest pain, abdominal pain, back pain, nausea and/or vomiting, weakness, weight loss, dizziness, dyspnoea, visual disturbance, paraesthesia in arms or legs, seizure and an 'impending sense of doom'. The questionnaire was delivered by trained staff to patients in a clinic setting, listing the symptoms one at a time. If patients reported that they experienced any symptom, follow up questions were asked to ascertain character, duration, nature and timing, before proceeding to the next symptom on the list. Patients were also asked the duration of time before they sought medical attention for their symptoms and duration of time before diagnosis. Any patient over the age of 18 years presenting to clinic that had a current or previous diagnosis of functional PPGL was invited to participate. Questionnaires were anonymised, but disease details were recorded; type of PPGL, year of diagnosis, type of catecholamine secreted, metanephrines/catecholamine levels.

A control population was drawn from patients over the age of 18 years with essential hypertension presenting to a tertiary hypertension clinic, who had had a diagnosis of PPGL and adrenal primary aldosteronism biochemically excluded.

From the survey data, a multiple logistic regression equation (Appendix 2) was produced to predict the probability of an individual having a PPGL, using all 22 symptoms as independent predictor

variables. Subsequently to evaluate how well the initial model fit the data, the Akaike Information Criterion (AIC) was calculated (Appendix 2). The AIC is an estimator of the goodness of fit of a particular model (as assessed by the likelihood function) which includes a penalty for increasing model complexity, to avoid overfitting. As such it can be used to compare the quality of different prediction models.

To produce the highest quality logistic regression model, only the symptom variables with predictive power should be included within the model, whilst those without predictive power should be discarded from the model. To identify these variables, a backwards stepwise logistic regression was performed, based on the AIC. In this approach, all 22 individual symptom variables included in the initial logistic regression were evaluated for exclusion (i.e. to be removed from the regression model). The variable that resulted in the greatest decrease in the AIC (analogous with greatest improvement in the model's fit) when excluded was subsequently removed from the model. This was then repeated for all remaining individual symptom variables in the model to re-evaluate the next symptom to exclude to improve the model fit. The entire process was repeated until the exclusion of any individual variable no longer resulted in a decrease in the AIC, thus establishing the final multiple logistic regression model, incorporating only symptoms with predictive power.

To increase the simplicity and thus clinical utility of the predictive model, the final multiple logistic regression equation was converted into a clinical prediction score (CPS). The predictive symptoms included in the final logistic regression were allocated 'scores' derived from their respective regression coefficients (rounded to the nearest integer). These symptom 'scores' were then compiled into a scorecard that allowed individual clinical predictions scores to be calculated for all survey participants, based on the symptoms they reported.

To evaluate the predictive performance of the regression model and CPS an in-sample evaluation of the predictive performance of the final multiple logistic regression model and CPS was conducted by producing receiver operating characteristic (ROC) curves. This estimated the sensitivity and specificity of the regression model and CPS for predicting PPGL at different thresholds. The area under these ROC curves (AUC) was calculated with corresponding 95% confidence intervals. The AUC represents an effective way to summarise the overall statistical accuracy of a model/score (independent of a set threshold).

2.5   Biological materials

Tumour samples were collected from patients with PPGLs that were operated on at St. Bartholomew's Hospital from 1970-2019. Non-pathological medulla was acquired from two separate sources; firstly, adjacent non-pathological medulla was identified from the same specimens containing PPGL tumour and secondly, non-pathological medulla was identified from patients that had undergone an adrenalectomy for removal of an aldosterone producing tumour. For our cohort tumours were defined as malignant if metastases were present or the primary tumour showed evidence of local invasion into surrounding structures. All other tumours were defined as benign, recognising that the benign category will also include those PPGLs that have yet to demonstrate their aggressive potential.

All patients provided written consent for the use of their tissue under the 'Genetics of endocrine tumours' ethics, MREC no. 06/Q0104/133. Blood samples were taken from patients, with consent, who either had a PPGL, were carriers of an *SDH* mutation, or were control patients with essential hypertension.

Tissue Microarray (TMA)

Patients were selected from the PPGL database (see section 2.1). A broad mixture of patients were selected to include both tumour tissue from PCCs and PGLs that occurred at different sites and benign and malignant tumours, as well as a mixture of known underlying genetic mutations (*SDHB, SDHD, VHL, RET*) and sporadic disease (defined as PPGL genetic panel negative). The haematoxylin and eosin (H&E)-stained section from formalin-fixed paraffin-embedded (FFPE) tissue blocks were reviewed by a consultant pathologist (DB). One-millimetre cores were taken from three representative areas of the tumour to construct a tissue microarray. A total of 110 cores were included from 35 patients. Cores from normal post mortem tissue were used for orientation (heart, adrenal cortex, normal pituitary tissue) and as positive and negative controls.

2.6   Immunohistochemistry (IHC)

All immunohistochemistry was performed on 3µm paraffin-embedded tissue sections.

2.6.1   Succinate Dehydrogenase B subunit

Primary antibodies used against SDHB were rabbit polyclonal HPA002868 antibody (Sigma-Aldrich, St Louis, MO, USA) at a dilution of 16:6000 on an automatic Ventana Benchmark Ultra system using

Ultraview DAB detection system. Heat induced epitope retrieval with Ventana cell conditioning 1. The reactions were visualised using Diaminobenzidine (DAB) as a chromogen (Vector laboratories).

A semi-quantitative scoring system was employed as previously described[114] as follows: *Positive* - granular cytoplasmic staining displaying the same intensity as an internal positive control (endothelial cells, sustentacular cells); *Negative* - complete absence of staining in the presence of an internal positive control; *weak diffuse* - a cytoplasmic blush lacking definite granularity compared to an internal positive control. A second form of semi-quantitative scoring was performed for SDHB IHC taking into account intensity of staining (0 - negative, 1 - weak diffuse, 2 - moderate positive staining, 3 - positive staining) and percentage of positive tumour cells in the sample (0-100%). Scoring was performed by a consultant pathologist (DB) experienced in SDH IHC.

2.6.2   Somatostatin receptors

Sections were cut from the designed TMA at a thickness of 3µm and mounted on charged slides.

Primary antibodies (Abcam, Cambridge, UK) were used against SSTR2a (clone UMB-1) at a dilution of 1:500, against SSTR3 (clone UMB-5) and against SSTR5 (clone UMB-4) at a dilution of 1:100 (Table 2.1). The reactions were visualised using DAB as a chromogen (Vector laboratories).

Normal pituitary tissue was used as a positive control and heart muscle tissue was used as negative control.

A semi-quantitative scoring system was employed as previously described[115,116]. This scored both subcellular localisation and the extent of staining. Scoring was as follows: 0 – absence of immunoreactivity, 1 – pure cytoplasmic immunoreactivity (focal or diffuse), 2 – membranous reactivity in less than 50% of tumour cells, 3 – circumferential membranous reactivity in more than 50% of tumour cells (scores 2 and 3 were assigned irrespective of the presence of cytoplasmic staining). Scoring was performed by two observers (NT & DI).

2.6.3   Immune cells

Immunostains for immune cell markers (CD68+, CD3+, neutrophil elastase+, HLADR3+, CD163+, CD4+, CD8+) were performed using the automated Ventana Discovery DAB Map 89 System (Ventana, Illkirch, France). In this system, streptavidin-horseradish peroxidase conjugate (OmniMap HRP) is used to catalyse the DAB/H_2O_2 reaction to produce an insoluble dark brown precipitate that can be visualised targeting the antigen of interest. The slides were deparaffinised and processed for antigen retrieval for 30 minutes with cell conditioning solution CC1 (Ventana), which is a Tris base buffer (pH~9). After

blocking with Blocker D solution (Ventana), slides were incubated with primary antibody for 60 minutes and then with the universal secondary antibody (Ventana) for 20 minutes. Dilution and immunohistochemical experiment conditions were first optimised for each primary antibody, Table 2.1.

Immunostains for the Ki67 marker were performed using the Dako Autostainer Plus (Dako, Glostrup, DeNMNrk). This uses an enhancer polymer detection system - Super SensitiveTM Polymer HRP System (Biogenex, Fremont, CA, USA) to catalyse the DAB/H_2O_2 reaction. In this process the slides were processed for antigen retrieval for 10 minutes with Antigen Unmasking Solution, low pH (Vector Labs, Burlingame, CA USA)) which is a citrate base buffer (pH~6) in a pressure cooker, following deparaffinisation. Slides were incubated with primary antibody for 40 minutes and then with Super-Enhancer for 20 minutes followed by SS-Label for 30 minutes (Biogenex).

Slides were counterstained with haematoxylin. A negative control, where primary antibody was omitted, was included per experiment, to exclude areas of endogenous peroxidase activity and/or non-specific antibody binding, ensuring the specificity of the staining reaction. A positive control, using either tonsil (CD68+, CD3+, HLADR3+, CD163+, CD4+, CD8+, Ki67) or spleen (neutrophil elastase+) tissue, were included per experiment serving as a baseline for evaluating run-to-run and/or day-to-day consistency.

Primary Antibody	Manufacturer	Catalogue Number	Species	Dilution IHC
CD68	DAKO	IR613	Mouse	1:2
CD3	DAKO	A0452	Rabbit	1:300
Neutrophil elastase	Abcam	Ab68672	Rabbit	1:100
CD163	Abcam	Ab74604	Mouse	1:500
HLA-DR (TAL 1B5)	Abcam	Ab20181 M4	Mouse	1:100
CD4	Abcam	Ab133616	Rabbit	1:100
CD8	DAKO	160621	Mouse	1:100
SSTR2	Abcam	Clone UMB-1	Rabbit	1:500
SSTR3	Abcam	Clone UMB-5	Rabbit	1:750
SSTR5	Abcam	Clone UMB-4	Rabbit	1:100
Ki67	DAKO	MIB-1	Mouse	1:500
SDHB	Sigma-Aldrich	HPA002868	Rabbit	16:6000

Table 2.1: Primary antibodies for immunohistochemistry. CD68 macrophages, CD3 lymphocytes, CD163 M" macrophages, HLADR3 M1 macrophages, CD4 T helper lymphocytes, CD8 T cytotoxic lymphocytes, SSTR somatostatin receptor, SDHB succinate dehydrogenase B

A H&E slide was reviewed by a consultant pathologist (DB) for each sample and areas of tumour and/or non-pathological medulla were outlined. Several training hours were spent with the consultant pathologist to be able to correctly identify the positive cells and what was false positive staining (Figure 2.2). Any queries over correct staining were reviewed by the consultant pathologist.
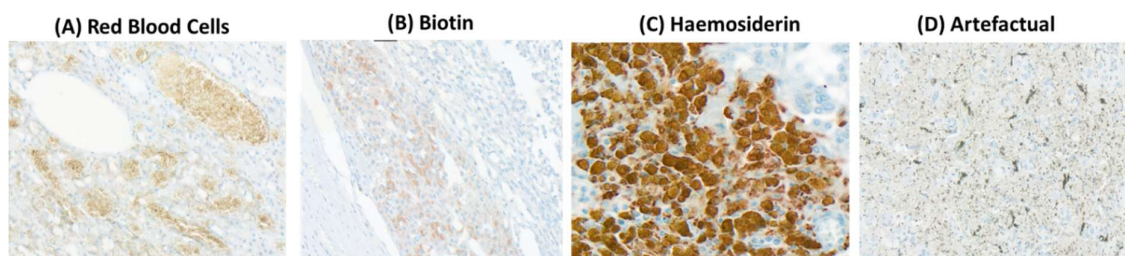
Figure 2.2: Immunohistochemical staining panels showing examples of false positive staining. *(A) Red blood cells stain faintly light brown in clusters inside blood vessels. (B) Biotin cytoplasmic staining faintly orangey-brown in colour. (C) Haemosiderin deposits staining are dark yellow-brown deposits that occur in clusters. (D) Artefactual staining appears as dark spots throughout the tissue.*

The Panoramic Scanner and Viewer Software (3DHISTECH, Budapest, Hungary) was used to scan and analyse stained slides. Immunopositive cells were counted in five different "hot spots" high power fields (HPF) using the software ImageJ (National Institutes of Health, USA). Data were expressed as percentage of immunopositive immune cells relative to the total number of tumour cells per HPF.

2.7   Basic laboratory techniques

2.7.1   DNA extraction

DNA extraction from whole blood samples

Whole blood samples were collected in 7.5mL EDTA tubes. DNA was extracted using a Qiagen DNA blood mini kit (Qiagen 51104) as per the manufacture's protocol (protocol DNA Purification from Blood or Body Fluids (spin protocol)). Briefly, cells were isolated from whole blood by incubating with Protease and buffer AL at 56°C for 10 minutes and then mixing with ethanol and centrifuged for one minute at 8000rpm. DNA was then purified by filtering it with a series of buffers in mini spin columns and centrifugation. DNA was eluted by mixing with buffer AE and incubated at room temperature for five minutes before a further centrifugation at 8000 rpm for one minute. DNA concentrations were calculated using Nanodrop software (ND-1000). Full protocol is available online in manufacture's handbook   (https://www.qiagen.com/us/resources/resourcedetail?id=62a200d6-faf4-469b-b50f-2b59cf738962&lang=en)[117].

DNA extraction from formalin-fixed paraffin-embedded (FFPE) slides

Tumour sections were cut to a thickness of 10μm and placed on uncharged slides. Four to six slides were used per tumour tissue sample. DNA was extracted using a Qiagen QIAamp DNA blood mini kit (Qiagen 51104) as per the manufacture's protocol (spin protocol). Briefly, slides were deparaffinised by heating and then washed with xylene, ethanol and distilled water. Identified tissue sections were removed from the slide and heated in tumour lysis buffer and proteinase K solution at 56°C overnight for 16 hours, followed by one hour at 90°C. DNA was then isolated by mixing the sample with a series of different buffers within spin columns and centrifuging for one minute at 8000rpm before being incubated with buffer TE for five minutes at room temperature. DNA concentrations were calculated using Nanodrop software (ND-1000).

2.7.2 RNA extraction

RNA extraction from whole blood was performed using a PAXgene blood RNA kit (Qiagen 762164) as per the manufacturer's protocol (protocol: Manual Purification of Total RNA from Human Whole Blood Collected into PAXgene Blood RNA Tubes). Full protocol is available online in the manufacture's handbook (https://www.qiagen.com/us/resources/resourcedetail/HB-0181-005_1122167_HB_PAX_Blood_RNA_1220_NA%20(3).pdf)[118]. Reverse transcription was undertaken to synthesise cDNA from extracted RNA working on ice and using the following method.

The volume of solution needed for 1 μg RNA was calculated (1 μg RNA – x μL – add RNase free water (13.75-x)) and 2 μL of random hexamers (NEB 60μM) were added to achieve a final volume of 15.75 μL. This was placed in the thermocycler for five minutes at 65°C and then placed on ice.

The master mix was prepared using the following volumes of reagents. A second master mix was prepared including a negative control with M-MuLV enzyme replaced by RNase free water (negative reverse transcriptase (-RT)).

Master mix	1x (μL)	Product name
M-MuLV RT 10x buffer	2	M-MuLV RT 10x buffer NEB
dNTPs 20 mM	1	dNTPs 100 mM NEB
M-MuLV	1	M-MuLV RT 200 U/μL NEB
RNase inhibitor	0.25	RNase murine inhibitor 40 U/μL NEB
Total	**4.25**	

4.25 μL of the mix was added to each sample to give a final volume of 20 μL. Samples were then incubated in the thermocycler for 10 minutes at 20°C, 60 minutes at 42°C and 10 minutes at 90°C.

cDNA was then stored at -20°C.

2.7.3 Immunocytochemistry

Immunocytochemistry of cells

Cells were plated at a density of 0.5×10^6 on 15 mm coverslips in a 24-well plate in complete medium for 36 hours to allow attachment. Cells were washed thrice in phosphate buffered saline (PBS) and fixed in 4% paraformaldehyde for 20 minutes at room temperature. Following three washes with PBS the cells were permeabilised with 0.2% Triton X-100 for five minutes at room temperature. Following further washes the cells were blocked with 10% goat serum for 45 minutes at room temperature and then incubated with primary antibody (Table 2.2) for two hours at room temperature. The cells were then washed again and incubated with the secondary antibody (Table 2.2) for a further 45 minutes at room temperature. Following further washes, the cells were briefly incubated with 2mg/mL 4,6-diamidino-2-phenylindole dihydrochloride (DAPI) to counterstain the nuclei. Coverslips were then mounted on slides and visualised on a confocal microscope (LSM 880, Zeiss).

Primary antibody	Secondary antibody
Monoclonal rabbit Tyrosine hydroxylase	Alexa 568 (goat anti-mouse) 1:1000
Pre-marked Phalloidin	Alexa 647 (goat anti-mouse) 1:1000
Monoclonal Mouse IgG1 Anti-Human CD3 (clone 4B12) Dako\Code No:M 7254 1:50 pH: 6	Alexa 488 (goat anti-mouse) 1:300
Monoclonal Mouse Anti-Human CD68 (clone F7.2.38) Dako\Code No: 1:50 pH: 6	Alexa 555 1:300
Monoclonal Rabbit Anti-Human CD4 Abcam EPR6855 pH: 6	Alexa 488 (goat anti-rabbit)
Monoclonal Mouse Anti-Human CD8 Thermo Fisher Scientific C8/144B pH: 6	Alexa 568 (goat anti-mouse)
Monoclonal Rabbit Anti-Human CD163 Abcam EPR19519 pH: 6	Alexa 488 (goat anti-mouse)
Actin Molecular Probes R37110 Mouse	2 drops/mL (1:500)

Table 2.2: Antibodies used for immunocytochemistry

Immunocytochemistry of FFPE human tissue

FFPE human tissue blocks (PPGL, non-pathological adrenal) were cut at a thickness of 3 µm and sections placed on charged slides. Sections were pre-heated at 56°C on a hot plate for 20 minutes, and deparaffinisation/rehydration was carried out by washing with xylene twice and then a decreasing concentration gradient of ethanol 100% down to 25%. Heat mediated antigen retrieval in citrate buffer

pH 6 was carried out, sections were then blocked in blocking buffer (PBS pH 7.4, 0.1% Triton, 1% bovine serum albumin, and 10% heat-inactivated goat serum). Sections were then incubated with primary antibodies diluted in blocking buffer (Table 2.2). Sections were then washed and immunolabelled with fluorescent secondary antibodies, and then stained with DAPI. Tonsil tissue sections were used as a positive control. Sections incubated with secondary antibody, but no primary antibody, served as a negative control for non-specific antibody binding. Samples were then mounted in fluorescence mounting medium (DAKO) and analysed on a Hamamatsu S60 slide scanner and by confocal microscopy (LSM 880, Zeiss).

Regions of tissue to be considered for analysis were selected by reviewing, and positively identifying, non-pathological adrenal medulla or tumour tissue on H&E slides. Three regions of each tissue section were randomly selected at 40x magnification and positive cells were identified digitally using QuPath[119]. This allowed the quantification of cells positive for the immune cell markers used. Percentages were then calculated based on the total number of cells present in each region analysed.

2.8   Loss of heterozygosity studies

2.8.1   Primer design

Primers were designed using Primer3Plus software. Gene sequences were obtained from the National centre for Biotechnology Information (NCBI) website. Exon sequences and positions were confirmed using Ensembl. Specific mutation sites were located within the gene sequence and primers designed (18-22 bp) to encompass this region of the gene for polymerase chain reaction (PCR). Primer blast website (http://blast.ncib.nlm.nih.gov/Blast.cgi) was used to test the designed primers to check for genomic similarities. Primers were ordered from Sigma Aldrich (www.sigmaaldrich.com/united-kingdon.html).

2.8.2   Polymerase chain reaction (PCR)

A master mix solution to the volume of 24 µL was made with the following reagents (Table 2.3). 1 µL of DNA was used per experiment unless otherwise stated. Reagents were kept in an ice box throughout, until use, to allow slow thaw. All reagents were vortexed and briefly centrifuged before use.

Master mix	Volume (µL)
primer F (10 µM)	0.5
primer R (10 µM)	0.5
dNTP 10mM	0.5
10x Taq buffer	2.5
Taq Pol	0.125
DEPC water	19.875
Total Vol.	**24.00**

Table 2.3: Components of master mix solution used for PCR experiments

A G-storm or Veriti thermal cycler was used for all experiments and parameters were optimised for each set of primers.

PCR solution was loaded in wells in 2% agarose gel using 5 µL DNA PCR product and 1 µL loading dye (ThermoFisher Scientific R0611). 7 µL of a 100-10000 bp DNA ladder was used for all experiments (GeneRule TM 11873963). Gels were viewed on LiCor Odyssey scanner using Image studio version 5.2 software.

Conditions were optimised for each set of primers for each gene mutation, as described in the results section under each specific mutation investigated.

2.8.3   Sanger sequencing

DNA was purified from PCR product using a QIAquick PCR purification kit (28106) or from agarose gel using a QIAquick Gel purification kit (28706) as per the manufacturer's instructions (https://www.qiagen.com/us/resources/resourcedetail?id=95f10677-aa29-453d-a222-0e19f01ebe17&lang=en).

20 µL of DNA was sent with 20 µL of each primer to GATC Biotech for Sanger sequencing. Sequencing chromatograms were reviewed and analysed using Finch TV Geospiza version 4.2 software.

2.9   Primary PPGL cell culture

Tumour tissue was collected at the time of adrenalectomy from patients operated on at St. Bartholomew's Hospital from October 2016 - April 2019. Tumour tissue was collected into Dulbecco´s modified eagle´s complete medium (DMEM F12 Ham, 10% fetal bovine solution (FBS), 1% insulin-transferrin-sodium selenite (ITS) and 1% Penicillin-Streptomycin antibiotics). Tissue samples were removed from the media and washed with PBS on a sterile petri dish. Fat and fibrous tissue was cut away and discarded. The tumour tissue was transferred to a fresh petri dish, washed with PBS and cut up into 1-2 mm pieces using a scalpel. The tumour tissue was transferred to a falcon tube containing collagenase 50 mg (Sigma C9697) diluted in 15 mL media. This was placed in a water bath heated to 37°C for one hour and the tube was agitated every 15 minutes to aid dispersion. The cell suspension was placed at room temperature for 10 minutes to allow the large debris to settle at the bottom. The cell suspension was then aspirated carefully so as to not disturb the remaining debris and placed in a clean falcon tube. The cell suspension was centrifuged for 10 minutes at 1200 rpm. The cell pellet was washed twice with PBS and the final cell pellet was re-suspended in complete medium.

The above process was repeated for the non-pathological adrenal tissue. After the fat and fibrous tissue had been cut away the adrenal tissue was sliced down the central black line representing the adrenal medulla. The medulla cells were gently scraped off the tissue into media solution and the solution aspirated and transferred to collagenase solution and placed in the water bath for 30 minutes. The remaining normal adrenal cortex was discarded.

Attempts were made to further optimise and purify these cultures using a red blood cell (RBC) lysis solution, however as this involved the culture being chilled for a period of time the cells did not survive, thus this step had to be abandoned.

Alternative methods were initially undertaken to optimise the conditions to perform primary culture of phaeochromocytoma tissue using a vibrotome machine. A vibrotome machine allows thin sections of tissue to be cut (minimum 100 μm) from the tumour due to a vibration of the blade limiting damage to the tissue. These tumour sections can then be cultured intact, maintaining the integrity of the tumour, which would be the ideal method for analysis of the true microenvironment without the effects of traditional single cell culture and damage to and loss of cells during the primary culture process. This method has been optimised by another group investigating Conn's tumours (Professor Brown, QMUL). However, using these same conditions: 200 μm thickness sections, speed 1.5 mm/s, amplitude 3 mm; resulted in the PCC tumour tissue dissolving due to it being a softer tumour than one originating from the adrenal cortex. Multiple other conditions were trialled (section thickness 200-500

µm, speed 0.5-1.5 mm, amplitude 0.1-3 mm) on several different PPGL specimens without success, as the PPGL tumour tissue did not hold its structure. Therefore, all experiments were subsequently undertaken using the single cell primary culture outlined above.

2.9.1 Cytokine analysis

Immediately after dispersing the cells and re-suspending the cell pellet in complete media, 10 µL was mixed with 10 µL of Trypan blue to count the viable cells using a hemocytometer.

Two million cells were plated per well in a six-well plate (in duplicates if there were enough viable cells) in 2 mL of complete media and placed in an incubator at 37°C for 36 hours. After 36 hours complete media was removed and the cells washed twice with PBS. 1 mL of 1% serum media was added and the cells were incubated for a further 24 hours. After 24 hours the supernatant was collected in a cold Eppendorf tube and centrifuged at 10,000 rpm for 10 minutes in a cold room. The supernatant was carefully aspirated and transferred to a fresh Eppendorf tube and stored in -80°C. Millipore MILLIPLEX Discovery assays were performed by Eve technologies Corp, Calgary, AB, Canada. The multiplex assay is performed at Eve Technologies according to their own protocol by using the Bio-Plex™ 200 system (Bio-Rad Laboratories, Inc., Hercules, CA, USA), and a Milliplex cytokine kit (Millipore, St. Charles, MO, USA).

2.9.2 Crystal violet assay

Cell viability and density was assessed using a crystal violet assay kit (Abcam 232855) according to the manufacture's protocol (https://www.abcam.com/ps/products/232/ab232855/documents/Crystal-violet-Assay-Kit-protocol-book-v1d-ab232855%20(website).pdf). Three wells within a 96-well-plate of primary PPGL and non-pathological normal medulla cells were cultured for 36 hours at a density of $0.1\text{x}10^6$. Fresh media was replaced every 24 hours. Absorbance was quantitively read on a microplate reader at an optical density of 570 nm every 24 hours after the cells were washed and stained with crystal violet solution for nine consecutive days.

2.9.3 Metanephrine assay

Samples of supernatant from the cultured primary PPGL cells and non-pathological medulla cells were sent to the Wythenshawe Hospital, Manchester University NHS Foundation Trust for metanephrine analysis.

Plasma metanephrines were analysed by LC-MS/MS using a Waters TQ-XS mass spectrometer coupled to a Waters Acquity UPLC system. Briefly, after addition of an internal standard, samples were extracted by solid phase extraction using a Biotage Evolute Express WCX 10 mg 96-well plate to remove interfering substances. The plate was conditioned with methanol, equilibrated with water and the samples loaded onto the plate. After washing with water and methanol to remove interferences, the metanephrines were eluted off the plate using 1% formic acid in acetonitrile. Samples were injected onto a Waters Atlantis HILIC 3 μm, 2.1 x50 mm column, and chromatography was performed with 100 mmol/L ammonium formate pH 3.2 as the aqueous mobile phase and acetonitrile as the organic mobile phase. Run time for each sample was six minutes 42 seconds.

The lower limit of quantification for the assay was 37.5 pmol/L for metanephrine and 75 pmol/L for normetanephrine and 3-methoxytyramine. Within and between batch variation was <4.7% for all analytes and recovery for all analytes at low, medium and high concentrations was 83-115%.

2.10   Statistical analysis

GraphPad Prism version 9.0 was used for statistical analysis and designing the graphs. Quantitative variables are represented as mean and standard error of mean (SEM) or standard deviation (SD). Gaussian distribution was tested for using the Kolmogorov-Smirnov test and equality of variances was tested using Brown-Forsythe test. For parametric data with equal variances Student independent t test and one-way ANOVA tests (with Tukey's multiple comparisons test) were used for data analysis. For parametric data with unequal variance Welch's unequal variances t tests and Welch's one-way ANOVA (with Dunnett's T3 multiple comparisons test) were used. For non-parametric data Chi squared, Mann Whitney U, Wilcoxon matched rank test and Kruskal-Wallis tests (with Dunn's multiple comparisons test) were used for data analysis. Pearson correlation coefficient r was used to determine correlation between continuous variables. Where analysis of multiple comparisons was undertaken simultaneously data was bootstrapped by applying Benjamini, Krieger and Yekutieli two-stage setup with a false discovery rate of 1%. A p value cut off of <0.05 was used for assessing statistical significance. RStudio (version 2022.02.3+492) was used for performing multiple logistic regression and modelling. This analysis was performed by Colin Munro, as part of his foundation year two academic medical project.

2.11 Ethics

For involvement in the home BP monitoring, medication titration and symptom questionnaire ethics approval was sought from members of the ethics board at Barts Health Trust (Dr Manish Saxena and Professor Johnston). These elements of the study were approved as a quality improvement project.

All patients gave verbal and written consent for the use of their blood and tumour samples under the ethics for '*The genetics of endocrine tumours*' (MREC 06/Q0104/133).

Chapter 3. Clinical aspects of phaeochromocytoma and paraganglioma disease

3.1 Background

3.1.1 Clinical presentation

Paraganglia are neuroendocrine organs derived from neural crest tissue. They are involved in the homeostasis of hypoxia, bleeding, cold and hypoglycaemia[3]. They act directly as chemical sensors or by producing catecholamines in response to stress[7]. PPGLs arise from chromaffin cells of the adrenal medulla and extra adrenal paraganglia respectively. Clinical presentation of these PPGL tumours is due to production of excess catecholamines (epinephrine, norepinephrine and dopamine) or mass effect. PGLs can also arise from the parasympathetic paraganglia of the head and neck (HNPGL). The majority of PGLs arising at these sites do not produce catecholamines[120], and these tumours cause morbidity through mass effect on local neurovascular structures, although a proportion produce dopamine[79]. Catecholamines exert an effect on alpha- and beta-receptors, which are present in a variety of tissues. The dominant beta-receptor in the heart is beta$_1$ with beta$_2$-receptor occurring in smooth muscle. Beta$_1$-receptor activation leads to an increase in cardiac muscle contractile force and heart rate, thus excess stimulation of these receptors results in tachycardia and arrhythmias. Activation of beta$_2$-receptors leads to relaxation of smooth muscle. In vascular smooth muscle the dominant receptor is the alpha$_1$-receptor. Alpha$_1$-receptor activation results in vasoconstriction and thus excess activation causes increased peripheral resistance and systemic hypertension. Epinephrine predominantly activates both subtypes of beta-receptors (and alpha-receptors to a lesser degree) and norepinephrine activates both alpha-receptors, but only beta$_1$-receptors. Therefore, the phenotypic profile of catecholamine production by the tumour will dictate the symptoms the patient experiences. Epinephrine also has metabolic effects, mainly through its action on beta$_2$-receptors, causing increased glycogenolysis, lipolysis, insulin and glucagon secretion. Norepinephrine predominant alpha-receptor activation increases gluconeogenesis and decreases insulin secretion, creating a diabetic metabolic profile[20].

PPGLs are often referred to as the great mimic, as clinical presentation can vary greatly, with a large overlap with many other conditions[120], thus making them particularly difficult to diagnose. Signs and symptoms are usually due to direct effects of excess catecholamines, as outlined above. The classic symptom triad is palpitations, diaphoresis and headaches, but it has been reported that only 4% of

patients actually present with the complete triad[121]. Other symptoms include anxiety, pallor, flushing, tremors, abdominal or chest pain, nausea, fatigue, weight loss, heat intolerance, visual disturbance, postural dizziness, change in bowel habit, neurological symptoms and an "impending sense of doom"[61,113]. Metabolic effects include hyperglycaemia, lactic acidosis and weight loss[120]. Hypertension is common, occurring in 50-60%[120] and can be paroxysmal (30%) or sustained, with or without orthostatic hypotension (10-50%) (more common in patients with excess dopamine producing tumours[120]); however, normotension can occur.

Exocytic secretion of catecholamines by PPGLs (epinephrine and norepinephrine) is unregulated and often paroxysmal, resulting in many patients reporting intermittent symptomatic episodes related to surges in BP with intervening episodes of symptomatic postural hypotension. Long-term risks of excess catecholamines include sustained hypertension, diabetes or impaired glucose tolerance, cardiomyopathy, systolic and diastolic dysfunction, myocardial infarction and stroke[113,120,122].

3.1.2   Management

Morbidity and mortality remain very high, with figures reported at 50-80% in emergency situations[123,124], mainly due to the effects of unregulated catecholamine excess. More recent mortality estimates of patients that present in crisis demonstrate an overall mortality of 28%[110]. High prevalence of phaeochromocytoma in mortality studies (0.05%)[14], implies that tumours are sometimes missed and result in premature death. Due to the difficulty in diagnosis, patients can experience prolonged exposure to excess catecholamines, which can lead to severe and sometimes fatal complications[125]. Thus, a low threshold for investigation and prompt diagnosis is required to avoid morbidity and mortality. A "phaeochromocytoma or hypertensive crisis" has been defined as the acute severe presentation of catecholamine induced haemodynamic instability causing end-organ damage or dysfunction, due to a sudden increase in catecholamine release[110]. Such crises are unpredictable but can be precipitated by several recognised events including anaesthesia and tumour handling, some foods high in tyramine (e.g. cheeses, smoked meats, bananas, avocado etc), micturition, physical activity and a variety of drugs[12,110] (Figure 3.1). The clinical spectrum of organ dysfunction due to a "phaeo crisis" can be wide and often devasting. These include cardiomyopathy, myocardial infarction, arrhythmia and cardiogenic shock, respiratory dysfunction (pulmonary oedema, acute respiratory distress syndrome, massive haemoptysis), neurological sequalae of encephalopathy, stroke and vertebral artery dissection, acute kidney and liver injury and bowel ischaemia, rhabdomyolysis, adrenal haemorrhage, thrombosis and metabolic consequences of lactic or ketoacidosis, and hypo- and hyperglycaemia[110]. Long-term exposure to high catecholamine excess can cause a milder

dysfunction of all of these systems, with the associated long-term consequences and morbidity. Therefore prevention of these hypertensive crises and avoidance of long-term exposure to excess catecholamines is imperative.

Surgical intervention is the only cure for these tumours, although radiotherapy is increasingly used as first line treatment of HNPGLs[126,127], but any intervention itself can result in morbidity and mortality through precipitation of a hypertensive crisis. Thus, before patients can undergo curative surgical resection, medical management is usually commenced in the form of alpha +/- beta adrenergic blockade to provide cardiovascular stability before surgery is attempted; however, no consensus exists as to the correct medical management. Protocols differ across countries and from centre to centre, with regards to the type of medications used for adrenergic blockade, the duration that they are required and whether patients are managed in hospitals or as outpatients. Guidelines recommend a minimum of 14 days of medical blockade before surgical intervention[12], to allow for normotension and euvolaemia to be achieved; but this assumes immediate access to operating lists. Pre-surgical treatment with medical blockade has been shown to reduce perioperative mortality to <1%[128].

Medications that block alpha- and beta-receptors have different effects. It is thus imperative that alpha-blockade is commenced before beta-blockade. When alpha-blockade is commenced it results in vasodilation and therefore a drop in peripheral vascular resistance. Therefore ongoing beta adrenergic stimulation is required to compensate for this with increase in heart rate and contractility to avoid cardiovascular collapse until euvolaemia has been established. This is a recognised cause of a hypertensive crisis. The different functions of the alpha- and beta-receptors also explain the side effect profiles of the medications used to block their effects. Blocking alpha-receptor function will result in vasodilation, and thus decreased peripheral resistance. If this occurs too rapidly, blood pressure will drop dramatically, due to volume depletion and inability to mount further counter measures such as increasing heart rate. This can result in patients experiencing severe side effects of postural hypotension and reflex tachycardia, resulting in discontinuation of these medications.

Phenoxybenzamine is a non-selective irreversible α-adrenergic antagonist, and therefore will cause a reflex tachycardia. Some authors believe that the additional α_2-receptor blockade is beneficial as these receptors contribute to a minor degree of the vasoconstriction[123]. Its long half-life of 24 hours has been hypothesised to contribute to post-operative hypotension in some patients[129,130]. Alternative alpha-blockers include doxazosin, prazosin and terazosin which are competitive selective $alpha_1$-receptor antagonists, and therefore not associated with the same level of tachyarrhythmias. These are not as effective during surgery due to large concentrations of catecholamines competitively displacing the antagonist[123].

Catecholamine excess creates a severe vasoconstricted and volume depleted state. Side effects of the medication could potentially be reduced if blockade of these receptors could be achieved in a more gradual and individualised fashion, allowing time for the body to equilibrate. Delaying the commencement or up-titration of beta-blockade allows for normal compensatory mechanisms (e.g. increasing heart rate). Increasing salt and fluid intake will also improve volume status. Theoretically this will also decrease the risk of post-operative severe hypotension due to the sudden removal of the source of the excess catecholamines[125].

Pre-operative medical management of functional PPGLs is recommended with the use of alpha- and beta-blockade as the anaesthesia and tumour handling during surgery can cause uncontrolled catecholamine release from the tumour which may prove fatal if unopposed. However, no standard protocols on pre-operative medical management of patients exists.

Roizen criteria[131,132] were designed to objectively assess the efficacy of pre-operative alpha-blockade and includes four criteria: 1) No in-hospital BP >160/90 mmHg for 24 hours prior to surgery; 2) No orthostatic hypotension with BP <80/45 mmHg; 3) No ST or T wave changes on ECG for one week prior to surgery; 4) No more than five premature ventricular contractions per minute. The BP criteria have also subsequently been applied in some studies to assess intra-operative haemodynamic instability (HDI)[133].

More recent definitions of successful blockade include normalising BP, with mild orthosis[134] and the presence of nasal stuffiness with evidence of postural hypotension[12]. These are very non-specific guidance, however, and not easily applied to individual patient clinical management.

3.1.3 Gaps in current knowledge to be addressed by this thesis

I.   No clinical trials have been undertaken to investigate the best regimen to use for pre-operative medical management in patients with functional PPGLs and the best method of assessing BP control in this population. No patient information card exists to educate patients and health workers about the risks of their diagnosis and factors that may precipitate a crisis.

II. Symptoms and signs of PPGLs are widely recognised to be non-specific, making diagnosis in the community difficult. No tools exist to identify high risk individuals within the hypertensive population that would benefit from further investigation to rule out PPGL.

III. Any additional benefits of alpha-adrenergic blockade are unknown.

3.2   Aims

I.   **Pre-operative medical preparation**

The aim is to improve the quality of pre-operative medical care provided to patients with functional PPGLs, using home BP monitoring to personalise medication titration to improve patient compliance with medical therapy.

Question: Can the use of home BP monitoring and personalized titration of medication improve patient tolerance, and therefore compliance, with alpha-blockade and achieve blood pressure (BP) and heart rate (HR) targets of SBP <135 mmHg, DBP <80 mmHg and HR <80 bpm in an outpatient setting, thus reducing the need for inpatient pre-operative medical management?

II.   **Effects on body composition**

The aim is to use bioimpedance analysis to investigate whether pre-operative alpha-blockade therapy can reverse the catabolic effects of catecholamine excess.

III.   **Effects on serum inflammatory markers**

The aim is to investigate whether PPGL have evidence of systemic inflammation and whether this can be reversed with alpha-blockade therapy.

IV.   **Earlier diagnosis of patients with PPGLs - screening patients with hypertension**

The aim is to be able to identify patients in the general population earlier that are likely to have an underlying PPGL.

Question: What combination of symptoms or signs that patients with secretory PPGL experience are specific to identify an individual with a PPGL from an individual with hypertension in the community population?

3.3 Results

3.3.1 Improving pre-operative medical preparation

Unregulated catecholamine excess causes morbidity and mortality. Although surgery remains the only cure for these tumours, surgical handling and anaesthesia can have adverse consequences if appropriate medical management is not first initiated in the form of alpha-receptor blockade +/- beta-receptor blockade[123,124]. Guidelines recommend pre-operative medical treatment with alpha-blockade for 7-14 days[12]. Yet, there is no agreed worldwide consensus on what this medical management should entail (doses, duration of treatment etc), and thus this differs from centre to centre and between countries. There are many other factors that can precipitate a hypertensive crisis aside from surgery, including a variety of medications[12]. Increasing surgical wait times place patients at risk in the community whilst awaiting their curative operation. The medications have expected side effect profiles, due to their mechanism of action, and because of these, many patients do not tolerate these medications in the community. This results in patients being under-prepared for their operation or needing to be admitted to hospital several weeks before the planned operation date to allow appropriate medical preparation, with the associated financial implications of long inpatient stays and inconvenience to patients.

This raises the question as to whether patients' compliance with medication can be improved, which should result in patients being better alpha- (+/- beta-) blocked before their operations, thus improving BP and HR control.

3.3.1.1 Phaeochromocytoma patient alert card

Aim: To design an information card for use by patients and physicians to highlight the causes of hypertensive crises to reduce the risk of these occurring.

A number of medications are known to interact and can precipitate a hypertensive crisis, therefore I designed an information card to be given to patients when they are diagnosed with a functional PPGL that describes the medications to be avoided. Patients are educated to the contents of the card, and advised to carry it at all times and show this card to all healthcare professionals (e.g. pharmacist, GP, A&E) that they interact with whilst awaiting their operation. The card was piloted on five patients with previous diagnosis of PPGL and 10 healthcare professionals to gain feedback as to what information should be included that would be helpful to avoid patient morbidity and mortality. The card was adapted to include this feedback. Figure 3.1 shows the schematic footprint of the final design of the card.

Your details

Name

DOB

Consultant

Hospital

Date of diagnosis

Date of operation

You have been prescribed

Phenoxybenzamine	Daily dose	Date started

Propranolol	Daily dose	Date started

Contact details

In an emergency:

1. Call Barts Health switchboard on **020 3416 5000** and ask for the endocrine registrar

2. Call local GP services or A&E

Non-urgent:

1. Call Barts Health switchboard on **020 3416 5000** and ask for the Endocrine Day Unit

ALWAYS CARRY THIS CARD WITH YOU

Show this card to anyone treating you

Hand this card to the pharmacist if you need an over-the-counter medicine

Healthcare professionals: medicines to avoid

Do not newly prescribe any of these medicines to this patient. If medication is required please contact the endocrine team for advice.

Medicine (this list is not exhaustive)	Prescribed for:	Class of drug
Metoclopramide* prochlorperazine*	Sickness and vertigo	Dopamine antagonists
Pseudoephedrine*	Colds and flu	Sympathomimetics
Prednisolone, dexamethasone, hydrocortisone, betamethasone	Inflammatory conditions	Corticosteroids
Morphine, pethidine, tramadol	Pain	Opiates
Amitriptyline, imipramine, paroxetine, fluoxetine	Depression	SNRI / SSRI TCA, MAO inhibitors
Sulpiride, amisulpride, tiapride, chlorpromazine	Psychosis	Dopamine antagonists
*Over-the-counter drug		

NHS Barts Health NHS Trust

Phaeochromocytoma Paraganglioma

IMPORTANT INFORMATION

Figure 3.1: Phaeochromocytoma alert card. *The figure shows the PPGL alert card that was designed and handed to patients at diagnosis, when provided with education on their diagnosis and possible interacting medications. Patients were advised to show this card to any health professional in whom they come into contact whilst awaiting their operation to avoid the prescription of any medications that may precipitate a hypertensive crisis. The card is 85 x 55 mm, tri-fold design, with patient information on the inside with medications listed that the patient is taking (and can be edited as doses are titrated for the patient's reference) and interacting medications on the back. The card is designed to be credit card size to allow it to be carried on their person at all times.*

This card was subsequently adapted by The Association for Multiple Endocrine Disorders (AMEND) for use by patients and physicians nationwide (Figure 3.2).

Figure 3.2: AMEND society PPGL alert card.

3.3.1.2 Patient preparation

Pre-operatively

Aim: To use home BP monitoring (HBPM) to personalise medication titration to improve patient compliance with medical therapy, to reduce the need for pre-operative inpatient treatment.

I prospectively recruited a cohort of 16 patients that were diagnosed with PPGL at St. Bartholomew's Hospital between September 2017 and June 2019 (intervention group) and a control group of 16 patients that were diagnosed with PPGL in the preceding five years (standard care). Demographical and clinical details of these two cohorts are provided in Table 3.1. There was no significant difference

between the two groups with regards to age at diagnosis, weight, location or size of PPGL, underlying genetics or urine metanephrine levels.

	Intervention group	Controls	p value
Number of patients	16	16	
Male [n (%)]	15 (93%)	5 (31.25%)	
Age at diagnosis (years) (mean [range])	49.8 [17-80]	51.3 [27-69]	0.797
Weight (Kg) (mean [range])	70.75 [51-101]	79.95 [65-120]	0.09
Presence of Diabetes at Diagnosis [n (%)]	8 (50%)	8 (50%)	
HbA1c (mmol/mol) (mean)	41.3	43	0.642
Location of PPGL [n (%)]			0.788
PCC	12 (75%)	12 (75%)	
Abdo PGL	3 (1.9%)	4 (25%)	
Thorax PGL	2 (1.25%)	1 (6.25%)	
Size of PPGL (mm) (mean [range])	53 [22-114]	51.9 [28-90]	0.233
Genetics tested [n (%)]	10 (62.5%)	10 (62.5%)	0.721
Genetic results:			
Negative	7 (43.75%)	7 (43.75%)	
SDHB	0	1 (6.25%)	
SDHA	2 (12.5%)	1 (6.25%)	
RET	1 (6.25%)	1 (6.25%)	
Plasma metanephrines (pmol/L) (mean +/-SEM)*:			
MN [NR <510]	4836 +/- 1582		
NMN [NR<1180]	10427 +/- 2939		
3MT [NR<180]	266 +/- 92.5		
Urine metanephrines (nmol/24hr) (mean +/-SEM):			
MN [NR <2000]	16165 +/- 5223	14433 +/- 4926	0.7825
NMN [NR<4400]	28314 +/- 9379	23302 +/- 5875	0.625
3MT [NR<2500]	3085 +/- 955	2630 +/- 1001	0.95
Duration of alpha-blockade therapy (weeks)	12.6 +/- 1.27	23.9 +/- 3.3	0.0056**
Duration of beta-blockade therapy (weeks)	11.5 +/- 1.25	13.4 +/- 4.5	0.696

*Table 3.1: Demographic and clinical details of patient cohorts. First column shows the details of the intervention group. The second column shows the details of the control group. The third column shows the comparison between the two groups for each clinical factor. Statistical analysis by Student t test for parametric data and Mann Whitney U test for non-parametric data distribution and Chi square analysis for grouped data (location of PPGL and genetics). *data on plasma metanephrines is only available for the intervention group as this test was not routinely being performed prior to 2016, thus a comparison of urine metanephrine results is also shown. MN metanephrine, NMN normetanephrine, 3MT 3-methoxytyramine*

In the intervention group all parameters of BP and HR measurements improved from diagnosis to pre-operatively (Figure 3.3). At diagnosis daytime BP was significantly higher than night-time for both systolic blood pressure (SBP) (mean 135 vs 129 mmHg, p=0.05) and diastolic blood pressure (DBP) (mean 80.4 vs 73.1 mmHg, p=0.0008). Additionally, SBP remained significantly higher during the daytime pre-operatively (mean 126 vs 118 mmHg, p=0.005), although DBP did not (mean 73 vs 63.6 mmHg, p=0.07). HR and mean arterial pressure (MAP) did not significantly differ between daytime and night-time measurements.
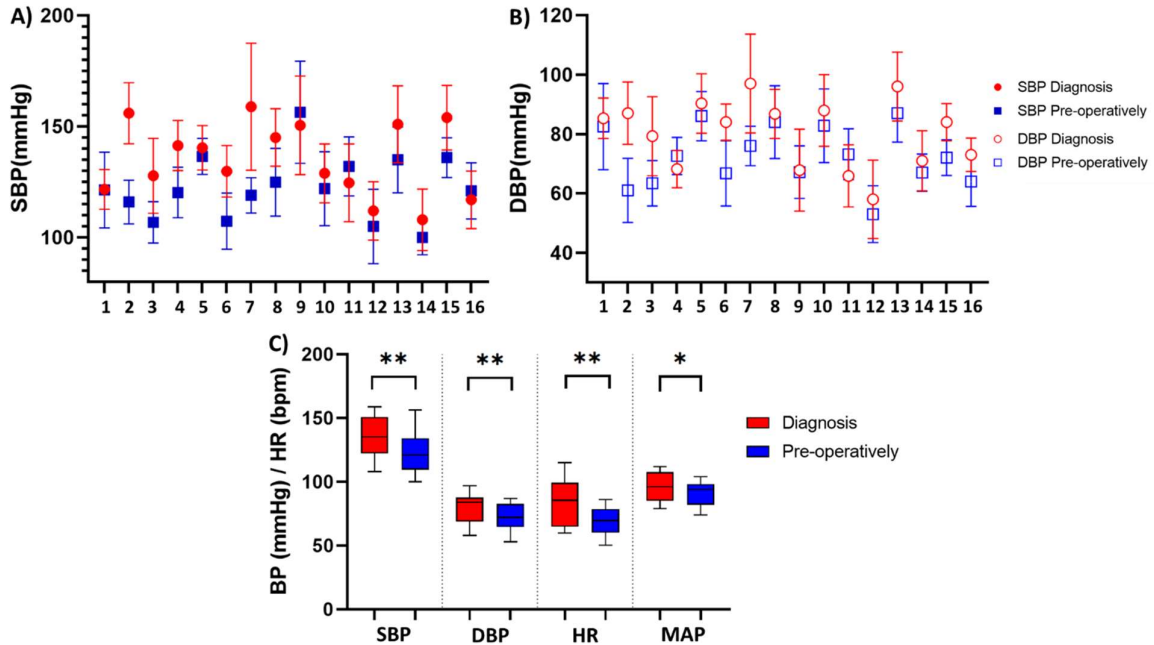
Figure 3.3: BP and HR measurements from PPGL patients in intervention cohort. *Data show box-and-whisker plot of mean, IQR and outlying points of the BP and HR measurements from ABPM at diagnosis and pre-operatively for the PPGL intervention group. A) SBP and B) DBP for each individual patient shown in pairs of diagnosis measurements (red circles) and pre-operatively measurements (blue squares). C) Mean averages of SBP (p=0.0028), DBP (p=0.0036), HR (p=0.0024) and MAP BP (p=0.044) for PPGL intervention group at diagnosis and pre-operatively. Statistical analysis by paired t test *<0.05, **<0.01. ABPM ambulatory blood pressure monitoring, SBP systolic blood pressure, DBP diastolic blood pressure, HR heart rate, MAP mean arterial pressure, bpm beats per minute*

There were no significant differences in BP or HR measurements taken via ABPM or home BP monitoring (HBPM) (7-day average) (Figure 3.4). The two methods of BP measurements showed good correlation for SBP (r=0.651, p=0.009) and DBP (r=0.651, p=0.001) and HR (r=0.486, p=0.066).
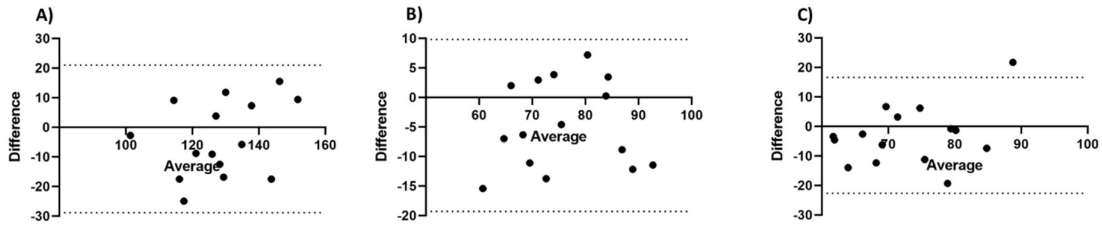
Figure 3.4: Comparison of BP and HR measurements taken by ABPM and HBPM. Data displayed as Bland-Altman plots showing the difference between the two measurements on the Y-axis and the average of the two measurements on the X-axis. A) Comparison of SBP between ABPM and 7-day HBPM (Bias -3.896, 95% limits of agreement -28.82 to 21.02), Pearson r correlation r=0.651, p=0.009. Student t test analysis p=0.559. B) Comparison of DBP between ABPM and 7-day HBPM (Bias -4.719, 95% limits of agreement -19.28 to 9.848), Pearson r correlation r=0.745, p=0.001. Student t test analysis p=0.253. C) Comparison of HR between ABPM and 7-day HBPM (Bias -32.996, 95% limits of agreement -22.63 to 16.64), Pearson r correlation r=-0.486, p=0.066. Student t test analysis p=0.69. ABPM ambulatory blood pressure monitoring, SBP systolic blood pressure, DBP diastolic blood pressure, HR heart rate, HBPM home blood pressure monitoring

Within the intervention group, there were significantly more patients that were within the targets (SBP <135 mmHg, DBP <80 mmHg and HR <80 bpm) as measured on their pre-operative ABPM compared to the one taken at diagnosis (p=0.0027). At diagnosis 50% of patients spent 50% of their time with SBP >135 mmHg compared to none pre-operatively and 35% of patients spent less than 10% of their time with a SBP >135 mmHg compared to only 10% at diagnosis (Figure 3.5).
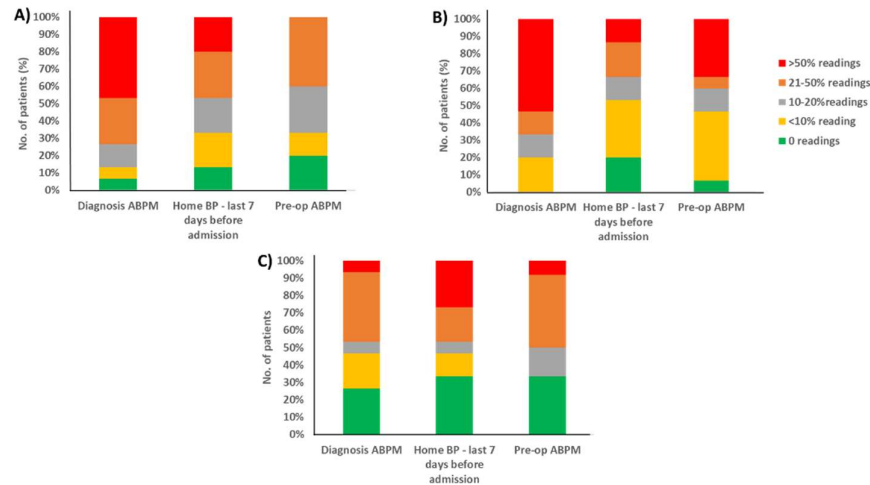
Figure 3.5: BP and HR measurements within targets. Bar charts show the number of patients (%) that have measurements above the targets on the diagnosis ABPM, HBPM of final seven days before admission and pre-operative ABPM. A) Number of patients with SBP above target of 135 mmHg. B) Number of patients with DBP above target of 85 mmHg. C) Number of patients with HR above target of 80 bpm. Statistical analysis by Chi Square test SBP p=0.034, DBP p=0.46, HR p=0.99.

Roizen criteria[109] sets out BP targets for assessing the efficacy of alpha-blockade of less than 160/90 mmHg and greater than 80/45 mmHg pre-operatively and these targets have been suggested to improve intraoperative haemodynamic stability. In our intervention cohort 75% of patients had no SBP readings above 160 mmHg or below 80 mmHg in the week before their operations, and the

remaining 25% had less than 10% of their readings outside these targets (Figure 3.6). All patients in the intervention group had a mean pre-operative ABPM of less than 160/90 mmHg. Only two patients had a mean pre-operative ABPM of greater than our outpatient target BP or HR (BP <135/80 mmHg and HR <80 bpm).
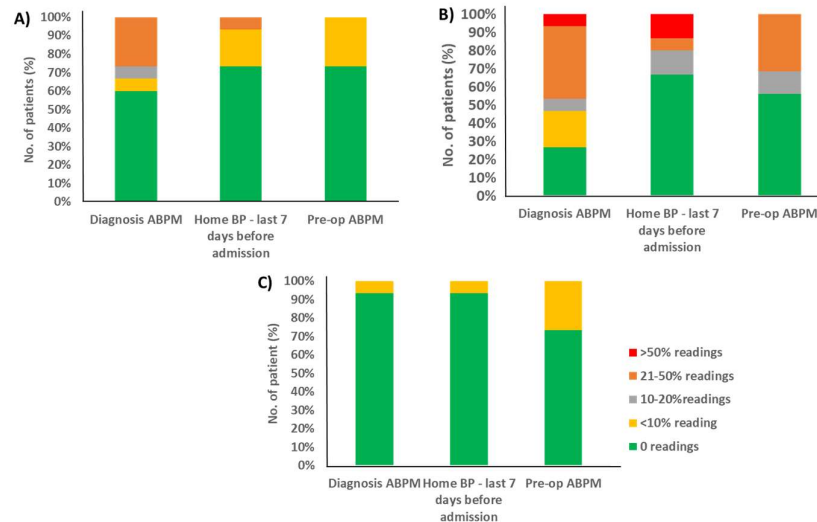
Figure 3.6: BP measurements outside Roizen criteria. *Bar charts show the number of patients (%) that have measurements outside Roizen criteria (>160/90 mmHg and <80/45 mmHg) on the diagnosis ABPM (first bar), HBPM of final seven days before admission (middle bar) and pre-operative ABPM (third bar). A) Number of patients with SBP above 160 mmHg. B) Number of patients with DBP >90 mmHg. C) Number of patients with BP <80/45 mmHg. ABPM ambulatory blood pressure monitoring, SBP systolic blood pressure, DBP diastolic blood pressure, HBPM home blood pressure monitoring. Statistical analysis by Chi Square test SBP p=0.09, DBP p=0.47, HR p>0.99.*

There was a positive correlation between plasma NMN levels and DBP from ABPM (Figure 3.7): average DBP (r=0.5, p=0.05), night DBP (r=0.537, p=0.0391) and day DBP (r=0.547, p=0.0348), maximum night DBP (r=0.511, p=0.05). There was a positive correlation between plasma NMN levels and night SBP (r=0.5, p=0.05). There was a positive correlation with plasma 3MT concentrations and HR: average HR (r=0.5394, p=0.038), day HR (r=0.45, p=0.09), night HR (r=0.6119, p=0.0153), and night maximum HR (r=0.554, p=0.0321). No correlations were observed between plasma MN concentrations and any BP or HR measurements. Measurements of plasma metanephrines were also highly correlated to the measurements of their urinary counterparts: NMN (r=0.552, p=0.0266), MN (r=0.666, p=0.0005) and 3MT (r=0.503, p=0.047).
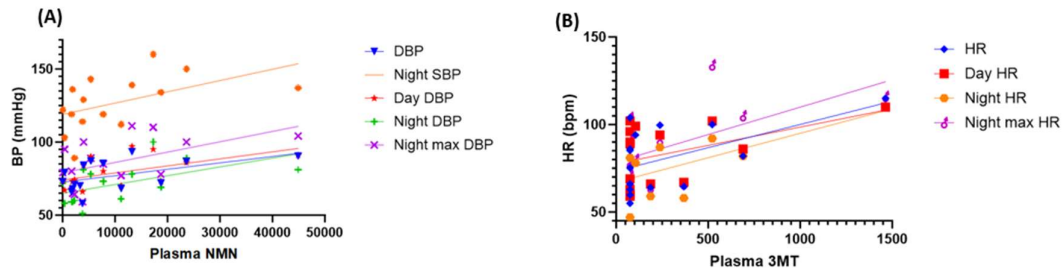
Figure 3.7: Correlations between plasma metanephrine levels and BP and HR. *A) Scatter diagram showing correlations between plasma NMN and BP for different BP measurements recorded on ABPM. Statistical analysis by spearman rank correlation: average DBP (r=0.5, p=0.05), night SBP (r=0.317, p=0.05), day DBP (r=0.547, p=0.0348), night DBP (0.537, p=0.0391), maximum night DBP (r=0.511, p=0.05). B) Scatter diagram showing correlations between plasma 3MT and HR for different HR measurements. Statistical analysis by spearman rank correlation: average HR (r=0.5394, p=0.038), day HR (r=0.45, p=0.09), night HR (r=0.6119, p=0.0153), night maximum HR (r=0.554, p=0.0321). DBP diastolic blood pressure, SBP systolic blood pressure, HR heart rate, ABPM ambulatory blood pressure measurement, NMN norepinephrine, 3MT 3-methoxytyramine.*

All patients in the intervention group tolerated phenoxybenzamine as an outpatient, compared to only 60% of the control group (p=0.0177). There was no significant difference in the doses achieved as an outpatient compared to that required pre-operatively in the intervention group (mean 132mg vs 135mg, p=0.334), but the control group required significantly higher doses of phenoxybenzamine pre-operatively to achieve adequate BP control than they had tolerated in the outpatient setting (mean 99mg vs 76mg, p=0.0018) (Figure 3.8). Significantly more of the intervention group were taking a beta-blocker as outpatients compared to the control group (100% vs 62.5%, p=0.0177). However, of the patients taking a beta-blocker as outpatients there was no significant difference in the doses required (84.62mg vs 54.38mg, p=0.08) between the two groups. On the morning of the operation there was no significant difference in the number of patients taking beta-blockade (100% vs 93.75%, p>0.999) or the doses required (80mg vs 55.45mg, p=0.11).
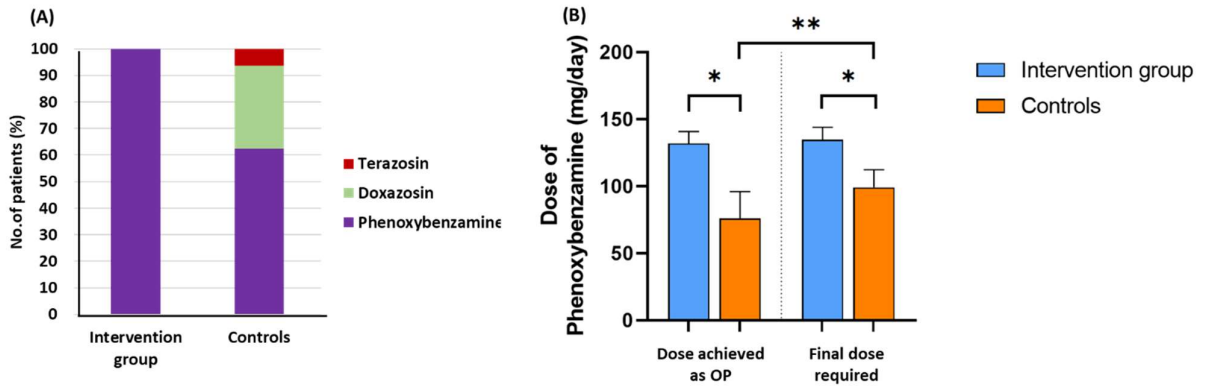
Figure 3.8: Comparison of alpha-blockade medication between intervention and control groups. (A) *Bar chart showing the number of patients in each group that tolerated phenoxybenzamine in an outpatient setting (p=0.0177, Fisher exact test). (B) Doses of phenoxybenzamine achieved in outpatient setting (p=0.0163, Mann Whitney U test) and final doses required pre-operatively (p=0.0405, Mann Whitney U test) in the intervention and control groups. There was no difference in the doses tolerated in the intervention group as an outpatient or final dose (p=0.33, paired t test). There was a significant difference between the doses tolerated in the control group in the outpatient setting compared to the dose required pre-operatively (p=0.0018, paired t test, this analysis excludes patients that did not tolerate phenoxybenzamine as outpatients). One control patient was commenced on terazosin due to intolerance of both phenoxybenzamine and doxazosin. *<0.05, **<0.01. OP outpatient*

In the three days pre-operatively the control PPGL patients had higher average SBP (mean 134.1 vs 118.8 mmHg, p=0.0136), DBP (mean 77.77 vs 70.31 mmHg, p=0.0144) and HR (mean 89.43 vs 71.68 bpm, p=0.0002) (Figure 3.9). There was no significant difference between the intervention or control PPGL group with regards to success of pre-operative blockade using Roizen criteria in the three days pre-operatively (68.75% vs 62.5%, p=0.473). The intervention group required significantly less intravenous fluids pre-operatively than the control group (mean 1.5L vs 6L, p=0.0034).
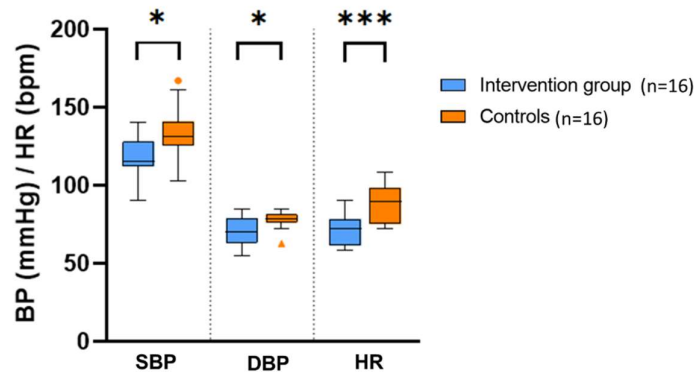
Figure 3.9: BP and HR measurements in the three days pre-operatively between PPGL intervention group and PPGL control group. *Data show box-and-whisker plot of mean, IQR and outlying points of the BP and HR measurements for PPGL intervention and control groups. Statistical analysis by Student t test *<0.05, **<0.01, ***<0.001: SBP (p=0.0136), DBP (p=0.0144), HR (p=0.002). SBP systolic blood pressure, DBP diastolic blood pressure, HR heart rate*

In summary, our data show that the intervention group had lower pre-operative blood pressures and heart rates, with less variability. This may be due to the higher doses of alpha- and beta-blockade achieved and subsequent better restoration of volume status than the control group.

Intra-operatively

Aim: To assess whether better compliance with medical therapy pre-operatively leads to lower rates of intra-operative haemodynamic instability.

Although our data suggest that the intervention group may have been better alpha-blocked pre-operatively than the control patients, whether this relates to less intra-operative HDI and better surgical outcomes is unknown. I therefore went on to investigate intra-operative parameters in the two cohorts.

There was no difference in BP or HR on the morning of the operation between the intervention and control groups. The control group had a higher SBP at the point of knife-to-skin compared to the intervention group (p=0.0375) (Figure 3.10), however there was no difference in any of the other BP or HR measurements between the intervention group and the control group intra-operatively (measurements taken at time of intubation, immediately after tumour removal, and maximum and minimum measurements intra-operatively).

There were no differences in the amount of metaraminol or norepinephrine required intra-operatively between the intervention and control groups.
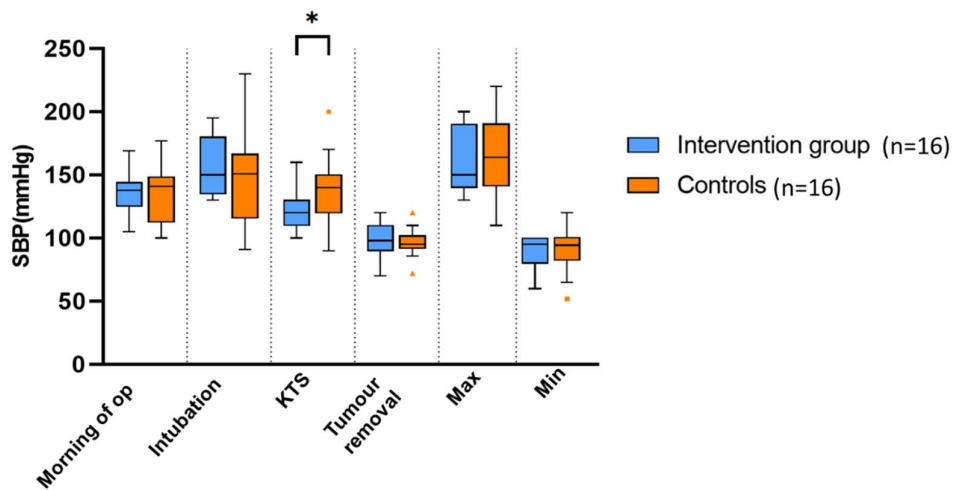
Figure 3.10: Intra-operative SBP measurements. *Data show box-and-whisker plot of mean, IQR and outlying points of the intra-operative SBP measurements for PPGL intervention and control groups. Statistical analysis by Student t test: morning of operation (p=0.895), intubation (p=0.302), KTS (p=0.0375, tumour removal (p=0.813), maximum (p=0.775), minimum (p=0.918). SBP systolic blood pressure, DBP diastolic blood pressure, HR heart rate, KTS knife-to-skin*

No universal definition has been agreed for what constitutes intra-operative HDI and therefore multiple different definitions have been used for assessing HDI across different studies. I therefore analysed our data using each of these definitions to allow comparison with published studies.

Using a definition of HDI of extreme hypertension (SBP >200 mmHg) or extreme hypotension (SBP <80 mmHg)[130,135,136] occurring intra-operatively, there was a significantly higher percentage of patients that experienced intra-operative HDI in the control group compared to the intervention group (40% vs 13%, p=0.0464) (Figure 3.11). Roizen criteria[109] was adopted as a definition for assessing the success of alpha-blockade (BP<160/90 mmHg and >80/45 mmHg), and applying these definitions intra-operatively there was no significant differences between the two groups (data not shown). An alternative definition that has previously been applied[137] is the duration of time intra-operatively that the patient spends outside the targets of SBP <160 mmHg and MAP >60 mmHg, but there was no significant difference between our intervention and control PPGL cohort using this definition (mean 5.62% vs 7.95%, p=0.2085).
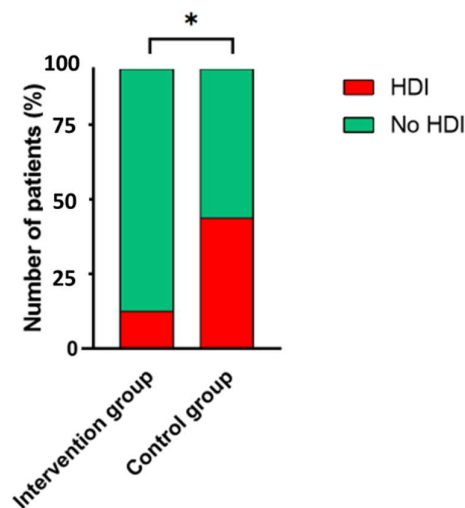
Figure 3.11: Number of patients experiencing intra-operative HDI. *Data shown as a stacked bar chart for the number of patients (%) that experienced at least one episode of HDI (SBP >200 mmHg or <80 mmHg) intra-operatively for the intervention and control groups. Statistical analysis by Chi square, *p<0.05. HDI haemodynamic instability.*

A score of intra-operative haemodynamic instability (HI-score) has previously been suggested[112,137] to include a combination of intra-operative haemodynamic variables, volume therapy and vasoactive drug usage. Using a modified version of this HI-score we demonstrated no significant difference between our PPGL intervention and control cohorts (mean 19.7 [range 0-62] vs 28.2 [range 6-69], p=0.151).

Although more intra-operative HDI was experienced within the control group, HDI did occur in both cohorts of patients. I therefore went on to combine the intervention and control PPGL patients to

investigate what factors might contribute to the development of intra-operative HDI within these cohorts. Of the total cohort of 32 PPGL patients studied eight patients (two from the intervention group and six from the control group) developed intra-operative HDI (SBP >200 mmHg or SBP <80 mmHg)[135]. The patients that experienced intra-operative HDI had higher HRs (mean 79 vs 68 bpm, p=0.014) and a trend towards higher SBP (mean 142 vs 130.6 mmHg, p=0.08) on the morning of the operation. They had higher SBP (mean 174.3 vs 144.3 mmHg, p=0.01) and DBP (mean 93.5 vs 75.5 mmHg, p=0.0077) at intubation, higher SBP (mean 145 vs 123.8 mmHg, p=0.0025) and DBP (p=0.0475, mean 82 vs 66 mmHg) and HR (p=0.0299, mean 68 vs 60 bpm) at time of knife-to skin incision (Figure 3.12). The patients in the HDI cohort also had higher modified HI-scores (38 vs 20, p=0.046) and spent a longer duration intra-operatively outside the target BP measurements (13.79% vs 4.9%, p=0.0003).
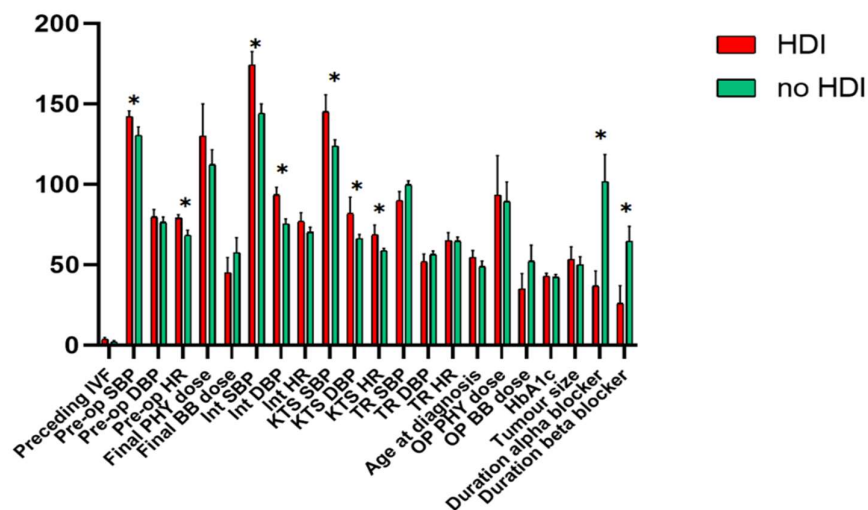
Figure 3.12: Factors affecting intra-operative HDI. Bar chart comparing different pre- and intra-operative factors in patients that experienced intra-operative HDI (SBP >200 or <80 mmHg) with those that did not. Pre-operative IVF (p=0.196), pre-operative SBP (p=0.086), pre-operative DBP (p=0.549), pre-operative HR (p=0.014*), intubation SBP (p=0.01*), intubation DBP (p=0.00787*), intubation HR (p=0.285), KTS SBP (p=0.0025*), KTS DBP (p=0.0475*), KTS HR (p=0.0299*), TR SBP p=0.0632 (90 vs 99), TR DBP p=0.297, TR HR p=0.9097, age at diagnosis (p=0.89), final PHY doses (p=0.44), final beta-blocker dose (p=0.4), OP PHY dose (p=0.555), OP beta-blocker dose (p=0.0997), Hba1c (p=0.82), tumour size (p=0.725), duration taking alpha-blocker (p=0.002*), duration taking beta-blocker (p=0.018*). Statistical analysis by Student unpaired t tests. *denotes significant results. IVF intravenous fluids, Pre-op pre-operatively, SBP systolic blood pressure, DBP diastolic blood pressure, HR heart rate, PHY phenoxybenzamine, BB beta-blocker, Int intubation, KTS knife-to skin incision, TR tumour removal, OP outpatient.

There was no difference between those patients that developed HDI compared to those who did not with regard to: age at diagnosis, tumour size, urine metanephrine levels, diabetes status, HbA1c levels, phenoxybenzamine vs other alpha-blockers, beta-blocker versus no beta-blocker, dose of phenoxybenzamine and propranolol pre-operatively, or quantity of pre-operative intravenous fluids (IVF). However, the patients that experienced intra-operative HDI were taking alpha-blockade (mean 36.86 vs 101.7 days, p=0.0021) and beta-blockade (mean 26 vs 64.57 days, p=0.0175) for a significantly

shorter duration pre-operatively than their counterparts that did not experience intra-operative HDI (Figure 3.12). Additionally, the patients that experienced HDI also showed more evidence of escape from blockade therapy (applying Roizen criteria) in the preceding three days before surgery (75 vs 26.1%, p=0.0316 Chi squared analysis).

In summary, patients in the control group experienced more intra-operative HDI than those in intervention group. When comparing patients that experienced HDI with those that did not, the main factors that contributed to this were the duration they were taking alpha- and beta- blockade. These patients could be identified by evidence of escape from therapy in the preceding days before surgery.

Post-operatively

Aim: To assess whether better compliance with medical therapy pre-operatively leads to better surgical outcomes.

There were no significant differences in the immediate post-operative BP or HR measurements between the intervention and control PPGL cohorts. There were no differences in the maximum measurements taken in the first 48 hours post-operatively, however there were significantly more control patients that experienced at least one episode of post-operative hypotension (62.5% vs 18.75%, p=0.029). There were no differences in the total number of hours that patients were given norepinephrine between the two cohorts.

The control PPGL group required more IVFs in the first six hours post-operatively compared to the intervention group (mean 912.5 vs 536.7mLs, p=0.0304) (Figure 3.13), but this difference had equalled out by 12 hours post-operatively (mean 1324 vs 1027mL, p=0.263). The control group also required significantly more IVFs in the first 48 hours they were on the ward, after step-down from HDU, compared to the intervention group (mean 5186 vs 2491 mLs, p=0.0445).
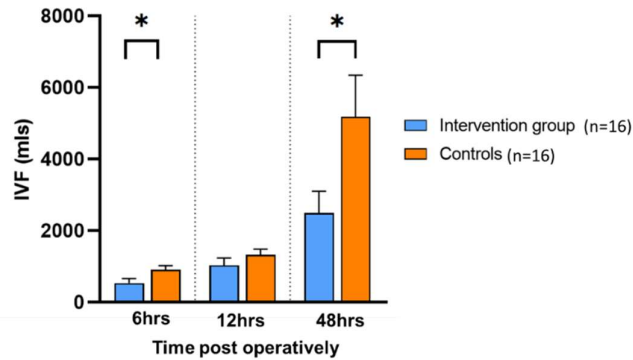
Figure 3.13: Quantity of intravenous fluid required in the first 48 hours post-operatively in the PPGL intervention group and control group. *Data show box-and-whisker plot of mean, IQR and outlying points of intravenous fluid requirements. Statistical analysis by Student t test: six hours post-operatively in HDU (p=0.0304), 12-hour post-operatively in HDU (p=0.263), 48 hours post-operatively on ward (p=0.0445). IVF intravenous fluids, hrs hours, mls millilitres.*

The intervention group required significantly fewer days in hospital compared to the control group (mean 8.17 vs 11.9 days, p=0.02), due to it being possible to admit them closer to their operation date (mean 3.25 vs 4.89 days, p=0.0034). There was no significant difference in the duration of their post-operative stays (mean 5.7 vs 7.1 days, p=0.27).
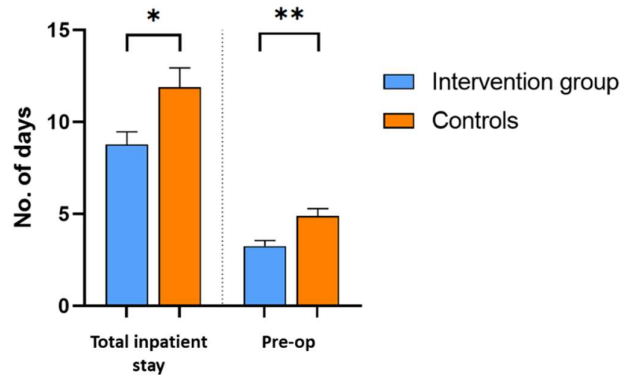
Figure 3.14: Inpatient hospital days. *Data shown as bar chart demonstrating total inpatient days (p=0.02) and pre-operatively inpatient days (p=0.0034) for intervention group vs control group (three patients were excluded from analysis in the intervention group due to one mortality and two of no fixed abode, so remained hospital patients under social services for a prolonged length of time). Statistical analysis by unpaired Student t test *<0.05, **<0.01.*

3.3.1.3 Effects on Body Composition

The value of pre-operative medical therapy with alpha-blockade has been disputed by some authors, with suggestions that an experienced and reactive surgeon and anaesthetist can prevent much of the HDI[138-140]. Nevertheless, this concept precludes any benefit that may be derived from blocking the effects of the catecholamine surges whilst awaiting surgical cure. Bioimpedance is a non-invasive measure of body composition parameters. It has been shown that adrenalectomy for treatment of PPGL improves weight, BMI and body fat distribution[141-144].

Aim: Using bioimpedance measurements to investigate whether pre-operative alpha-blockade therapy can reverse the catabolic effects of catecholamine excess.

To prospectively compare factors influenced by pre-operative medical blockade, I recruited a group of age and gender matched control subjects from a tertiary hypertension clinic at St. Bartholomew's Hospital. Demographics of the PPGL and hypertensive patient cohorts are compared in Table 3.2. There were no significant differences between the two cohorts of patients, except the hypertensive control group were heavier at baseline (91.5 vs 70.75 Kg, p=0.0014) and the follow-up duration was slightly shorter for the PPGL patients (mean 12.6 vs 16 weeks, p=0.046).

	PPGL patients	HTN controls	p value
No. of patients	16	16	
Male n (%)	15 (93%)	15 (93%)	
Age (years) (mean [range])	49.8 [17-80]	49.4 [16-79]	0.94
Weight (Kg) (mean +/- SEM [range])	70.8 +/- 3.1 [51-101]	91.5 +/- 5.3 [68.1-135]	0.008**
BMI (Kg/m²) (mean +/- SEM [range])	24.5 +/- 0.7 [22.8-29.7]	29.4 +/- 1.42 [22.8-42.9]	0.0019*
Presence of Diabetes n (%)	8 (50%)	9 (56%)	0.99
HbA1c (mmol/mol) (mean +/- SEM) **All patients** **Diabetic patients only**	41.6 +/- 2.0 48 +/- 1.1	42.3 +/- 2.9 47.7 +/- 1.2	0.91 0.88
Home BP at diagnosis (mmHg) (mean +/- SEM) SBP DBP	150 +/- 8.3 88 +/- 4.1	144 +/- 3.5 85 +/- 3.2	0.82 0.92
Clinic BP at diagnosis (mmHg) (mean +/- SEM) SBP DBP	134 +/- 3.9 79 +/- 2.8	140 +/- 3.6 89 +/- 3.7	0.61 0.31
Clinic HR at diagnosis (bpm) (mean +/- SEM)	84 +/- 4.3	77 +/- 3.6	0.49
Home BP at FU (mmHg) (mean +/- SEM) SBP DBP	130 +/- 3.3 78 +/- 2.6	138 +/- 4.1 84 +/- 3.3	0.56 0.12
Clinic BP at FU (mmHg) (mean +/- SEM) SBP DBP	127 +/- 4.2 80 +/- 3.0	141 +/- 4.2 93 +/- 3.8	0.21 0.013*
Plasma Metanephrines (pmol/L) (mean +/-SEM) **Metanephrine** [NR <510] **Normetanephrine** [NR <1180] **3MT** [NR <180]	4836 +/- 1582 10427 +/- 2939 266 +/- 92.5	243 +/- 23.7 605 +/- 96.7	0.007** 0.002**
Aldosterone (pmol/L) (mean +/-SEM)	342 +/- 61.2	368 +/- 33.2	0.711
No. of anti-hypertensive medications taking at diagnosis/baseline (mean +/- SEM)	1.4 +/- 1.3	2 +/- 2.2	0.35
Follow-up duration (weeks) (mean +/- SEM) [range]	12.6 +/- 1.3 [6.7-22]	16 +/- 0.5 [14-18]	0.046*

*Table 3.2: Demographic and clinical features of the PPGL and hypertensive patient cohorts. Second column summaries the details of the PPGL patients, third column summaries the details of the hypertensive control group and the fourth column shows the p value for the statistical comparison between the two groups (Student t test); *<0.05, **<0.01. NR normal range, SEM standard error of the mean*

There were no significant differences between the BP measurements ascertained via different methods at diagnosis for either group. There were no differences in BP measurements between the two cohorts of patients at baseline (Figure 3.15) or at follow-up (Figure 3.16).
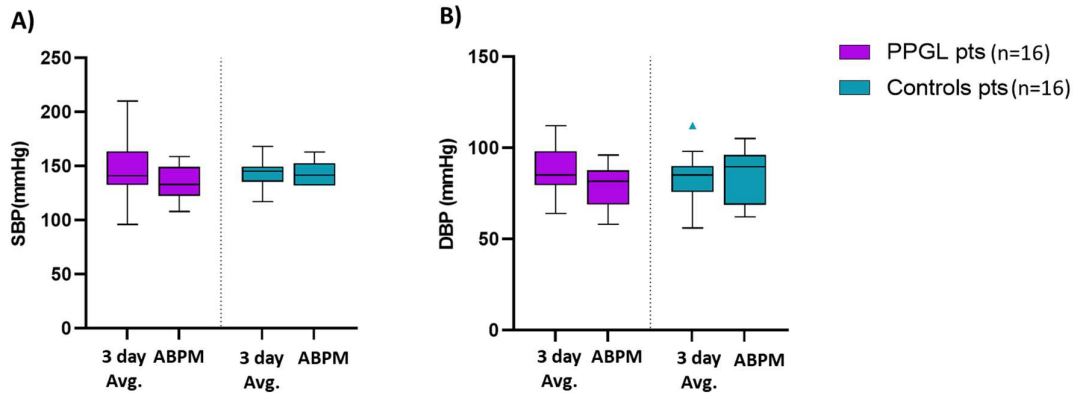
Figure 3.15: Comparison of BP readings of PPGL cohort and hypertensive control cohort at diagnosis. *Data show box-and-whisker plot of mean, IQR and outlying points of the BP and HR measurements taken via two different methods for each group: 3-day average from inpatient ward observations and 24-hour ABPM in PPGL patients (n=16) and 3-day average home measurements and 24-hour ABPM measurement for the hypertensive control group (n=16). (A) SBP ANOVA with Tukey's multi comparisons test p=0.21. (B) DBP ANOVA with Tukey's multi comparisons test p=0.368. SBP Systolic blood pressure, DBP Diastolic blood pressure, 3-day Avg. 3-day average readings from ward observations or home readings (controls), Dg Diagnosis, ABPM ambulatory blood pressure monitoring.*

There were significant improvements in BP and HR measurements in both PPGL patients and controls from measurements taken at diagnosis and follow-up (Figure 3.16). There were no significant differences to the improvements seen in SBP (p=0.23) or DBP (p=0.88) between the PPGL cohort and controls, however HR decreased significantly more in the PPGL cohort (p=0.03).
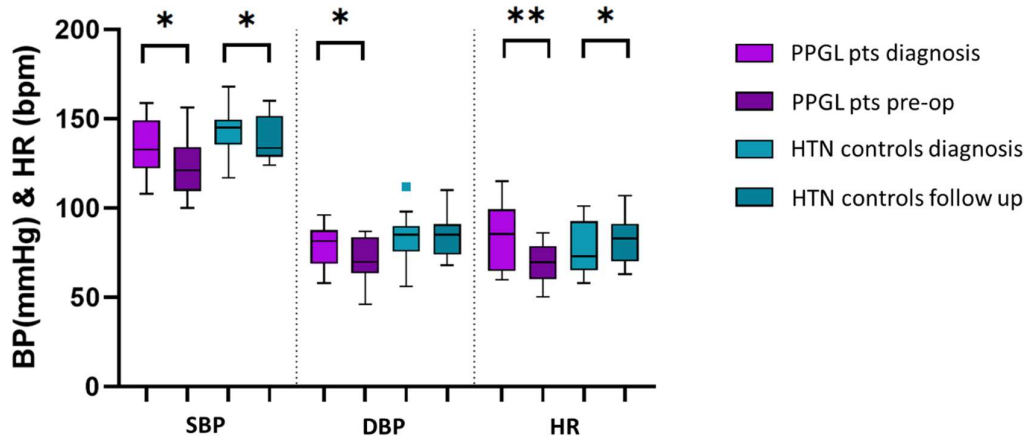
Figure 3.16: Comparison of BP and HR measurements of PPGL cohort and hypertensive control cohort at diagnosis and follow-up. *Data show box-and-whisker plot of mean, IQR and outlying points of the BP and HR measurements for 24-hour ABPM measurements for PPGL patients (n=16) and 3-day home measurements for control patients (n=16). PPGL patients: SBP p=0.0193*, DBP p=0.0415*, HR p=0.0024**. HTN control patients: SBP p=0.005*, DBP p=0.824, HR p=0.0337*. Differences in SBP (p=0.23), DBP (p=0.88), HR (p=0.003) between the PPGL and control cohorts from baseline to follow-up (statistical analysis by paired t test). SBP Systolic blood pressure, DBP Diastolic blood pressure, HR Heart rate. Follow-up measurements were taken pre-operatively in the PPGL patient group (mean 12.6 weeks [range 6.7-21]) and at an interval of 16 weeks [range 14-18] in the hypertensive control group. *<0.05, **<0.01.*

Bioimpedance markers were significantly different at baseline when PPGL patients were compared to the hypertensive controls (Figure 3.17). PPGL patients had a lower weight (mean 75.1 vs 91.5 Kg, p=0.009), BMI (mean 25.9 vs 29.7, p=0.0182), total body fat (mean 16 vs 26 Kg, p=0.007), percentage of body fat (mean 21.4 vs 25.9%, p=0.005), muscle mass (56.1 vs 63.5 Kg, p=0.022), and BMR (mean 1717 vs 1984, p=0.014). PPGL patients had a lower total body water (TBW) (mean 41.9 vs 47.7 Kg, p=0.0124), but higher proportion of TBW (mean 55.8 vs 52.7%, p=0.021) at baseline.
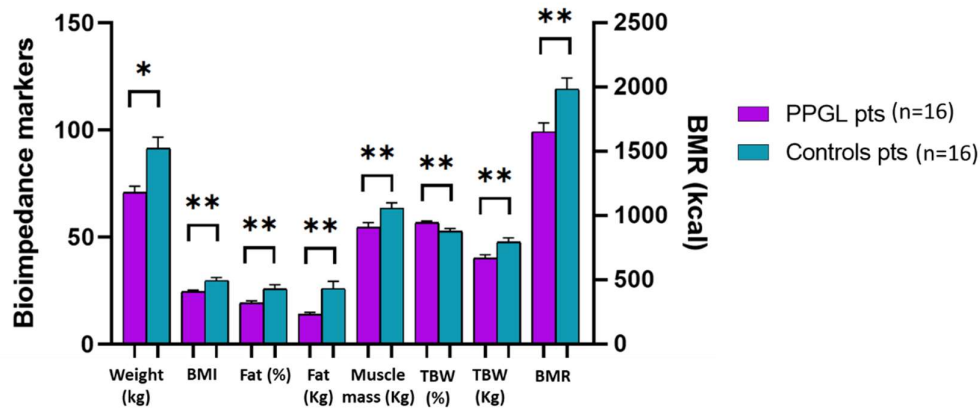
Figure 3.17: Baseline bioimpedance measurements in PPGLs and hypertensive control patients. Bar charts showing mean + SEM for each bioimpedance parameter for both cohorts. Statistical analysis by multiple paired t test (corrected for multiple comparisons by controlling false discovery rate at 1% using Benjamini, Krieger and Yekutieli two-stage setup). *<0.05, **<0.01: weight (p=0.09**), BMI (p=0.0185*), total body fat (p=0.0074**), percentage of body fat (p=0.0051**), muscle mass (p=0.0021*), BMR (p=0.0142*), TBW by weight (p=0.0214*), TBW as a percentage of weight (p=0.0214*). BMI body mass index, BMR basal metabolic rate, TBW total body water, SEM standard error of the mean.

These data suggest that patients with PPGL *in situ* are in a water depleted catabolic state compared to hypertensive controls.

I next went on to investigate whether a period of medical treatment with alpha- and beta-blockade altered any of these body composition parameters and improved PPGL patient's catabolic state. There were improvements across all of the body composition parameters when comparing measurements taken at diagnosis and pre-operatively in PPGL patients (Figure 3.18, Figure 3.19 & Table 3.3).
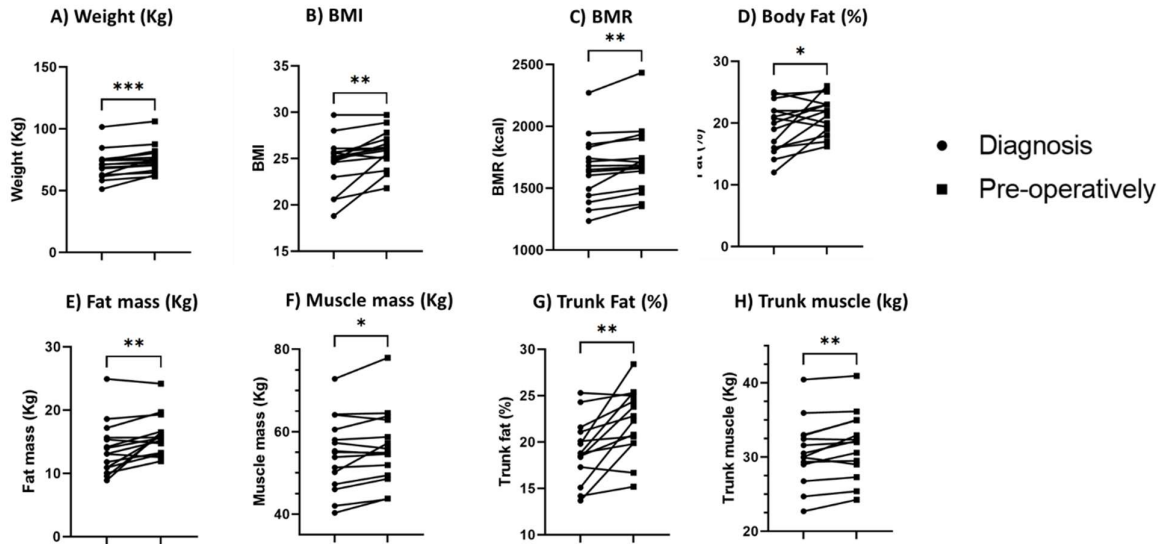
Figure 3.18: Bioimpedance parameters taken at diagnosis and pre-operatively in PPGL patients. *Data are shown as a series of paired scatter plots for each parameter showing measurement taken at diagnosis paired with the measurement taken pre-operatively for each patient. Each dot and square combination represent one patient. Statistical analysis by multiple paired t test (corrected for multiple comparisons by controlling false discovery rate at 1% using Benjamini, Krieger and Yekutieli two-stage setup). *<0.05, **<0.01, ***<0.001. (A) Weight (Kg) p=0.0002, (B) BMI p=0.0042, (C) BMR (Kcal) p=0.0025, (D) Percentage of body fat (%) p=0.0235, (E) Fat mass (Kg) p=0.0052, (F) Muscle mass (Kg) p=0.021, (G) Percentage of trunk fat (%) p=0.023, (H) Trunk muscle (Kg) p=0.0049. BMI body mass index, BMR basal metabolic rate.*
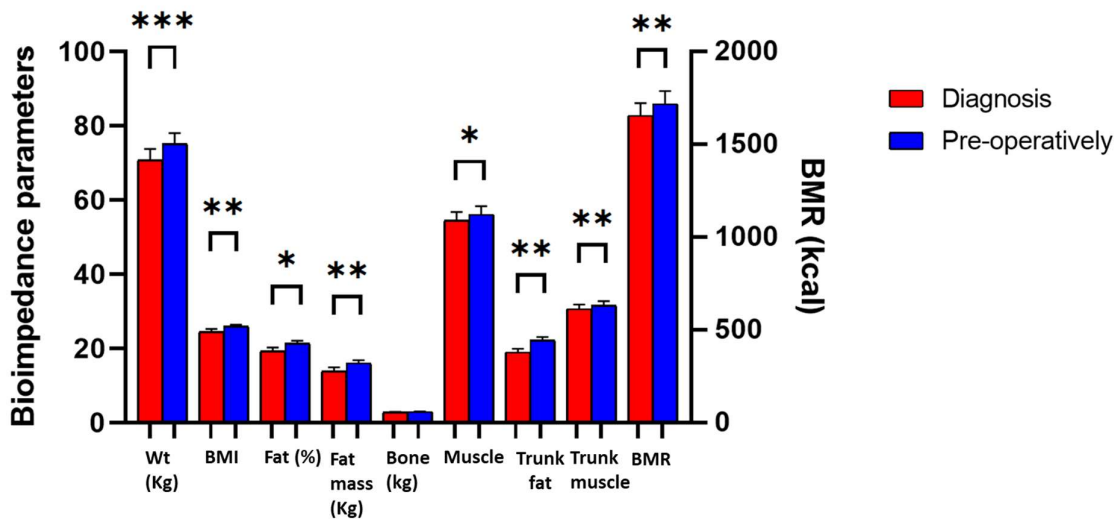
Figure 3.19: Summary data of bioimpedance parameters taken at diagnosis and pre-operatively in PPGL patients. *Data are shown as a series of bar charts for each parameter showing mean and SEM measurements taken at diagnosis and pre-operatively for PPGL patient cohort (n=16). Statistical analysis by multiple paired t test (corrected for multiple comparisons by controlling false discovery rate at 1% using Benjamini, Krieger and Yekutieli two-stage setup). *<0.05, **<0.01, ***<0.001. Weight p=0.0002, BMI p=0.0042, BMR p=0.0025, body fat (%) p=0.0235, fat mass (Kg) p=0.005, bone mass p=0.013, muscle mass (Kg) p=0.021, trunk fat (%) p=0.023, trunk muscle (Kg) p=0.0049. BMI body mass index, BMR basal metabolic rate, SEM standard error of the mean.*

It is recognised that PPGL patients are usually in a volume contracted salt and water deplete state at diagnosis[111]. Therefore, in accordance with guideline recommendations[12], PPGL patients were encouraged to drink three litres of water per day and increase their dietary salt intake to aid in expanding blood volume to combat the postural symptoms of the alpha-blockade as the vasoconstricted state is reversed. This was demonstrated in our cohort with an increase in urinary sodium levels (mean 29.5 vs 73.6mmol/L, p=0.001) and a decrease in serum aldosterone levels (mean 342 vs 197pmol/L, p=0.047) and renin activity levels (2.02 vs 0.54ng/mL/hr, p=0.07) in PPGL patients measured at diagnosis and pre-operatively (Figure 3.20).
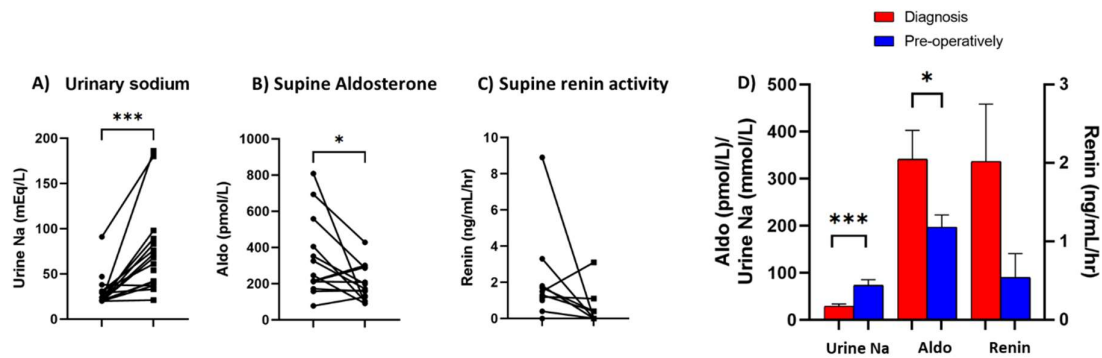
Figure 3.20: Urinary sodium, serum aldosterone and renin activity levels in PPGL patients. *Data shown as before-after scatter graphs for (A) urinary sodium levels (p=0.0001***), (B) serum supine aldosterone levels (p=0.047*) and (C) serum supine renin activity levels (p=0.07) in PPGL patients taken at diagnosis and pre-operatively. D) Bar charts showing mean + SEM for measurements taken at diagnosis and pre-operatively. Statistical analysis by multiple paired t test for parametric data (urinary sodium and aldosterone levels) and Wilcoxon matched pairs rank test for non-parametric data (renin activity levels) (corrected for multiple comparisons by controlling false discovery rate at 1% using Benjamini, Krieger and Yekutieli two-stage setup) *<0.05.. Na sodium, Aldo aldosterone, renin activity levels.*

I then proceeded to look at the effects on body water distribution in each individual (Figure 3.21). Total body water weight increased from diagnosis to pre-operatively (mean 40.1 vs 41.9 Kg, p=0.0005), mainly due to an increase in extracellular water (ECW) (mean 16.9 vs 17.5 Kg, p=0.0164), although an upward trend in intracellular water (mean 23.5 vs 24.3 Kg, p=0.051) was also observed. However, total body water as a percentage of total body weight decreased (mean 56.8 vs 55.5%, p=0.0456).
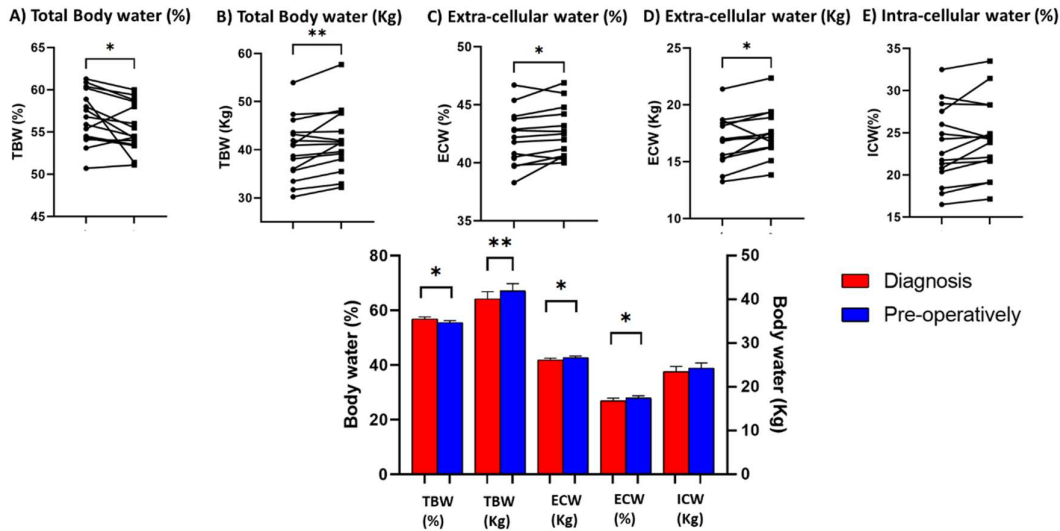
Figure 3.21: Body water distribution at diagnosis and pre-operatively in PPGL patients. *Data shown as before-after scatter graphs for (A) TBW as a percentage of total body weight (p=0.0456), (B) TBW in weight (Kg) (p=0.0005), (C) ECW as a percentage of TBW (p=0.045), (D) ECW weight (Kg) (p=0.0164), (E) ICW as a percentage of TBW (p=0.051). Bottom graph shows bar charts showing mean + SEM for measurements taken at diagnosis and pre-operatively. Statistical analysis by paired t test *<0.05, **<0.01. TBW total body water, ECW extra-cellular water, ICW intra-cellular water.*

Despite a similar improvement in BP in the hypertensive control group, there were no differences identified across any of the parameters in the control group from baseline to follow-up (Table 3.3).

Parameter	PPGL patients			HTN control patients			PPGL vs HTN at baseline
(mean +/- SEM)	Baseline	Pre-operatively	p value	Baseline	Follow-up	p value	p value
Weight (Kg)	70.8 +/-3.1	75.1 +/- 2.9	0.009**	91.5 +/- 5.3	91.4 +/- 5.1	0.92	0.009**
BMI (Kg/m²)	24.5 +/- 0.7	25.9 +/- 0.5	0.018*	29.7 +/- 1.6	29.4 +/- 1.6	0.46	0.018*
BMR (kcal)	1654 +/- 68.3	1717 +/- 70	0.014*	1984 +/- 88.4	1986 +/- 89.6	0.8	0.014*
Body Fat (%)	19.3 +/- 1.1	21.4 +/- 0.8	0.005**	25.9 +/- 1.9	25.8 +/- 1.8	0.94	0.005**
Fat mass (Kg)	13.9 +/- 1.1	16 +/- 0.8	0.007**	26 +/- 3.4	24.4 +/- 3.0	0.28	0.007**
Bone mass (Kg)	2.91 +/- 0.1	2.9 +/- 0.1	0.022*	3.3 +/- 0.1	3.32 +/- 0.1	0.31	0.022*
Muscle mass (Kg)	54.5 +/- 2.3	56.1 +/- 2.3	0.022*	63.5 +/- 2.6	63.7 +/-2.6	0.72	0.022*
Trunk fat (%)	19.1 +/- 0.9	22.2 +/- 0.9	0.002**	27.3 +/- 1.9	27.2 +/- 1.6	0.87	0.002**
Trunk muscle (Kg)	30.7 +/- 1.2	31.6 +/- 1.2	0.26	49.7 +/- 15.7	34.7 +/- 1.2	0.37	0.26
TBW (%)	56.8 +/- 0.8	55.5 +/- 0.7	0.02*	52.7 +/- 1.3	52.9 +/- 1.1	0.66	0.02*
TBW (Kg)	40.1 +/- 1.6	41.9 +/- 1.7	0.012*	47.7 +/- 2.1	47.4 +/- 2.2	0.56	0.012*
ECW (%)	41.9 +/- 0.9	42.7 +/- 0.6	0.73	41.8 +/- 0.4	41.8 +/- 0.4	0.67	0.73
ECW (Kg)	16.9 +/- 0.6	17.5 +/- 0.5	0.017*	19.7 +/- 0.8	19.8 +/- 0.8	0.41	0.017*
ICW (Kg)	23.5 +/- 1.2	24.3 +/- 1.2	0.045*	27.6 +/- 1.4	27.7 +/- 1.4	0.9	0.045*
Urinary sodium (mEq/L)	29.5 +/- 4.6	73.6 +/- 12	0.001**	68.5 +/- 11.5	78.4 +/- 12.2	0.57	0.001**
Supine Aldosterone (pmol/L)	342 +/- 61.2	197 +/- 26.2	0.39	368 +/- 33.2	309 +/- 43.9	0.34	0.39
Supine renin activity (ng/mL/hr)	2.0 +/- 0.7	0.54 +/- 0.3	0.035*	5.04 +/- 1.9			0.035*

*Table 3.3: Bioimpedance parameters at diagnosis and pre-operatively in PPGL patients and HTN control patients. Each cohort is shown over three columns: baseline data, pre-operative data and a statistical comparison between the two. The final column in the table shows the statistical comparison of the PPGL patients versus the HTN control patients at baseline. Statistical analysis by multiple paired t test corrected for multiple comparisons by controlling false discovery rate at 1% using Benjamini, Krieger and Yekutieli two-stage setup). *<0.05, **<0.01. BMI body mass index, BMR basal metabolic rate, TBW total body water, ECW extra-cellular water, ICW intra-cellular water.*

These data suggest that the changes seen in the body composition measurements of the PPGL patients are not merely an effect of improvement in BP. There were no significant changes in any of the body composition parameters in PPGL patients pre-operatively to those taken post-operatively 6-12 months later in the nine patients for whom these data was available (data not shown).

3.3.1.4 Effects on Inflammatory status

It has been shown in a series of case reports that patients with functional PPGLs have raised systemic inflammatory markers[145,146], which improve following resection of the PPGL[141,142,146].

Aim: To investigate whether patients with PPGL tumours *in situ* have evidence of systemic inflammation and whether pre-operative treatment with alpha-blockade therapy can reverse this inflammatory state.

The haematological and biochemical results for the PPGL and hypertensive control cohorts are summarised in Table 3.4. When comparing the PPGL patients with the control cohort at baseline the PPGL patients had a lower haemoglobin, haematocrit, lymphocytes, CRP and urinary sodium levels and higher PLR, ALT and Troponin T levels at baseline.

(mean +/- SEM)	PPGL patients (n=16)			HTN control patients (n=16)			PPGL vs HTN at baseline
	Diagnosis	Pre-operatively	p value	Baseline	Follow-up	p value	p value
Hb (g/dL)	132 +/- 4.5	139 +/- 3.7	0.139	150 +/- 3.5	150 +/- 3.15	0.85	0.03*
HCT (%)	0.4 +/- 0.01	0.42 +/- 0.01	0.5	0.5 +/- 0.01	0.4 +/-0.01	0.016*	0.03*
Platelets (x10⁹/L)	309 +/- 28.7	238 +/- 14.6	0.0068**	250 +/-15.1	252 +/-13.7	0.69	0.07
WBC (x10⁹/L)	7.3 +/- 0.9	5.7 +/- 0.4	0.041*	7.2 +/- 0.6	6.8 +/- 0.6	0.15	0.84
Neutrophils (x10⁹/L)	4.6 +/- 0.9	3.3 +/- 0.3	0.14	4.4 +/- 0.5	4.5 +/- 0.4	0.86	0.67
Lymphocytes (x10⁹/L)	1.5 +/- 0.2	1.6 +/- 0.1	0.71	2.0 +/- 0.1	1.9 +/- 0.1	0.39	0.047*
CRP (mg/L)	12.4 +/- 9.3	1.4 +/- 0.5	0.195	1.1 +/- 0.4	1.4 +/- 0.4	0.25	0.04*
Ferritin (ng/L)	151 +/- 32.1	96.7 +/- 17.7	0.039*	189 +/- 34.2	158 +/- 35	0.10	0.48
ALT (u/L)	49.4 +/- 9.7	29.8 +/- 5.2	0.032*	27.7 +/- 3.9	25.4 +/- 2.9	0.99	0.02*
GGT (u/L)	61.0 +/- 31.1	38.9 +/- 1.8	0.125	55 +/- 18.5	65 +/- 19.6	0.39	0.72
ACR	4.8 +/- 1.7	0.7 +/- 0.3	0.1279	11.8 +/- 8.9	13.8 +/- 8.9	0.32	0.13
HbA1c⁺ (mmol/mol)	42.1 +/- 1.9	39.6 +/- 2.1	0.047*	42.3 +/- 2.9	43.3 +/- 3.4	0.43	0.87
Urea	5.5 +/- 0.6	5.4 +/- 0.6	0.89	5.2 +/- 0.4	6.0 +/- 0.5	0.16	0.83
Creatinine	85.6 +/- 4.8	91.1 +/- 7.0	0.25	84.4 +/- 5.5	89.8 +/- 5.8	0.50	0.99
Troponin T (ng/L)	33.7 +/- 13.1 35.0 +/- 13.9+	13.9 +/- 6.6 17.9 +/- 6.9+	0.05 0.017*+	13.3 +/- 4.4	10.9 +/- 3.4	0.13	0.001**
Pro BNP (ng/L)	308 +/- 202	339 +/- 217	0.13	60.1 +/- 18.4	55.6 +/- 17.7	0.53	0.11
NLR	4.2 +/- 1.12	2.5 +/- 0.4	0.24	2.3 +/- 0.3	2.4 +/- 0.3	0.69	0.33
LMR	3.4 +/- 0.37	3.6 +/- 0.3	0.26	3.4 +/- 0.5	3.09 +/- 0.3	0.61	0.62
PLR	256 +/- 51.8	172 +/- 21	0.03*	135 +/- 10.8	138 +/- 8.6	0.94	0.04*
NPS	0.3 +/- 0.14	0.0 +/- 0.0	0.125	0.1 +/- 0.1	0.7 +/- 0.7	0.99	0.576
SII	1510 +/- 626	600 +/- 108	0.035*	595 +/- 71.3	605 +/- 57.8	0.94	0.19
Albumin (g/dL)⁺	45.6 +/- 1.4	44.2 +/- 0.9	0.253	46.8 +/- 0.8	45.8 +/- 0.8	0.19	0.46
Total Protein (g/dL)	71.4 +/- 2.8	66.1 +/- 1.3	0.061	72.1 +/- 1.7			0.69
Phosphate (mg/d/L)	1.1 +/- 0.06	1.2 +/- 0.04	0.315	1.1 +/- 0.1			0.52
PNI	53.4 +/- 1.7	52 +/- 1.2	0.35	56.9 +/- 1.09	51.9 +/- 3.8	0.21	0.14

Table 3.4: Haematological and biochemical markers of inflammatory, immune and nutritional status. Tests were undertaken at baseline and at follow-up (6.7-22 weeks later for PPGL patients and 14-18 weeks later for controls). Statistical analysis by multiple paired t test for parametric data and Wilcoxon matched pairs rank test for non-parametric data (corrected for multiple comparisons by controlling false discovery rate at 1% using Benjamini, Krieger and Yekutieli two-stage setup) for each haematological or biochemical marker is shown in the third column of each section comparing the paired results. The final column shows the p value for the comparison for each parameter between the PPGL patients and the hypertensive patient cohorts at baseline. Hb haemoglobin, HCT haematocrit, CRP C-reactive protein, ALT Alanine aminotransferase, GGT Gamma glutamyl transferase, ACR urinary albumin-creatinine ratio, HbA1c glycosylated haemoglobin C, Pro BNP B-type natriuretic peptide, NLR neutrophil-lymphocyte ratio, LMR lymphocyte-monocyte ratio, PLR platelet-lymphocyte ratio, NPS neutrophil-platelet score, SII systemic inflammatory index II, PNI prognostic nutrition index. + one patient had a proven and treated myocardial infarction was removed from analysis of Troponin T results (n=15).

Similarly to the body composition data above, I proceeded to investigate whether medical treatment with blockade had any effect on the inflammatory and immune markers in PPGL patients. PPGL patients had higher WBC, platelets, ferritin, ALT, HbA1c, Troponin T levels (Figure 3.22 & Table 3.4) at diagnosis which decreased pre-operatively. Serum based inflammatory scores have been used to predict clinical outcomes in some cancers and are based on biochemical data collected as part of routine care during diagnostic work up. Platelet-to-lymphocyte (PLR) score and systemic index (SII) score both decreased from diagnosis to pre-operatively.
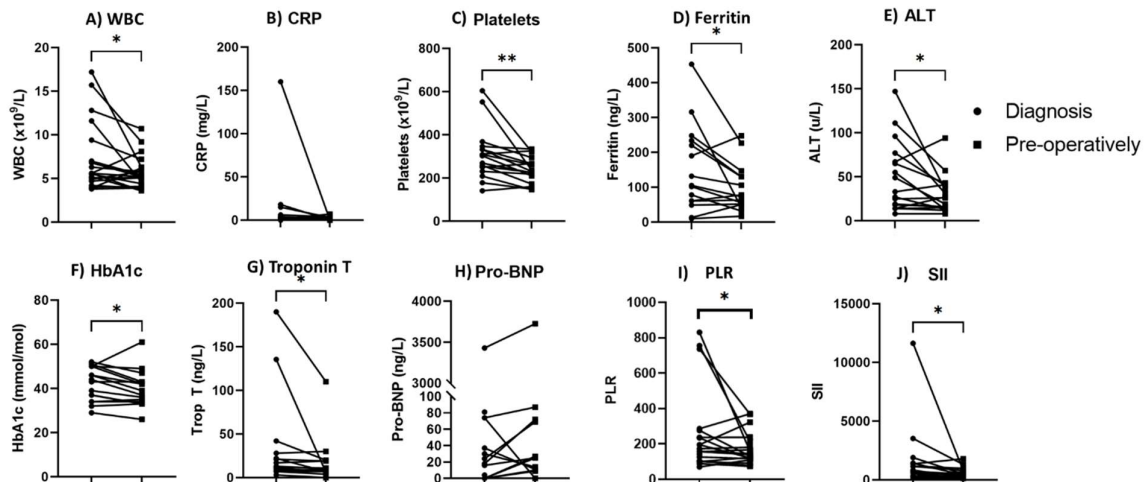
*Figure 3.22: Inflammatory and immune markers taken at diagnosis and pre-operatively in PPGL patients. Data are shown as a series of paired scatter plots for each parameter showing measurements taken at diagnosis and paired with the measurements taken pre-operatively for each patient (n=16). Each dot and square combination represent one patient. Statistical analysis by multiple paired t test for parametric data and Wilcoxon matched pairs rank test for non-parametric data (corrected for multiple comparisons by controlling false discovery rate at 1% using Benjamini, Krieger and Yekutieli two-stage setup) *<0.05, **<0.01. (A) WBC p=0.0041, (B) CRP p=0.195, (C) Platelets p=0.0068, (D) Ferritin p=0.039, (E) ALT p=0.032, (F) HbA1c p=0.047, (G) Troponin T p=0.017 (patient excluded with proven myocardial infarction), (H) Pro-BNP p=0.13. (I) PLR p=0.03, (J) SII p=0.035. WBC white blood count, CRP C-reactive protein, ALT Alanine aminotransferase, HbA1c glycosylated haemoglobin C, Pro BNP B-type natriuretic peptide, PLR Platelet-lymphocyte ratio, SII systemic inflammatory index II.*

There was no significant difference in markers of nutritional status (albumin, calcium, phosphate, PNI) at baseline between the PPGL patients and the controls (Table 3.4) or between diagnosis and pre-operatively in the PPGL patients, with the exception of an improvement in HbA1c (mean 42.1 vs 39.6 mmol/mol, p=0.0468).

There were no significant changes in any of the inflammatory, immune or markers of nutritional status in the control patient from baseline to follow-up (Table 3.4).

In summary, WBC, platelets, ferritin, ALT, HbA1c, troponin T, and systemic inflammatory scores PLR and SII all decreased in PPGL patients from diagnosis to pre-operatively. There was no change in haemoglobin, haematocrit, urea, creatinine or serum sodium concentrations suggesting that the decrease in the other inflammatory markers was not merely a dilutional effect.

3.3.2 Earlier diagnosis of patients with PPGLs - screening patients with hypertension

PPGLs can present with a vast array of symptoms and signs in different combinations and therefore correctly diagnosing it promptly can be problematic. No tools exist that can be used in the community to identify which patients warrant further investigation, therefore clinicians need to have a high index of suspicion and a low threshold for further investigations to ensure these tumours are diagnosed and treated earlier, unfortunately this is often not the case.

Aim: To design a simple tool, for use in the community setting, to identify patients in the general population earlier who may have an underlying PPGL.

We designed a questionnaire to identify discriminating symptoms in patients with a functional PPGL. We interviewed a cohort of patients with a current or history of a functional PPGL and a cohort of patients that had essential hypertension as a control group. Table 3.5 summarises the demographic information for these two cohorts.

	PPGL patients	HTN patients
Number of patients	62	74
Male [n (%)]	32 (51.6%)	39 (52.7%)
Time to presentation (months) (mean+/-SEM)	24.3 +/- 6.3	37.3 +/- 6.5
Time to diagnosis (months) (mean+/-SEM)	40 +/- 7.1	39.4 +/- 5.9
Presence of Diabetes [n (%)]	21 (33.9%)	22 (29.7%)
HbA1c mmol/mol (mean [range])	42.9 [31-61]	42.2 [26-83]
Location of PPGL [n (%)]:		
PCC	40 (64.5%)	
Abdo PGL	11 (1.8%)	
Thorax PGL	1 (0.16%)	
Pelvic PGL	1 (0.16%)	
HNPGL PGL	1 (0.16%)	
Genetics tested [No. (%)]	53 (85.5%)	
Genetic results [No. (%)]:		
Negative	25 (40.3%)	
SDHA	3 (0.48%)	
SDHB	10 (16.1%)	
SDHC	1 (0.16%)	
SDHD	1 (0.16%)	
RET	6 (9.7%)	
VHL	7 (11.3)	
Not Tested	9 (14.5%)	
No. of patients with raised metanephrines [n (%)]:		
MN only	4 (6.5%)	
NMN only	16 (25.8%)	
3MT only	7 (11.3%)	
MN + NMN	12 (19.4%)	
NMN + 3MT	10 (16.1%)	
Mixed	5 (8.1%)	
Unknown	8 (12.9%)	

Table 3.5: Demographics of the PPGL and HTN control group that completed the symptom questionnaire. *Table shows time to presentation, time to diagnosis and diabetes status for both cohorts of patients and more detailed information on the PPGL cohort on location of PPGL, underlying genetic diagnosis and type of excess catecholamine produced by tumour. MN metanephrine, NMN normetanephrine, 3MT 3-methoxytyramine, HTN hypertensive*

Patients with PPGL reported significantly more symptoms than those with essential hypertension (mean 6.4 vs 3.7, p<0.0001). A higher proportion of patients with functional PPGLs reported symptoms of diaphoresis, anxiety, constipation, tremor, abdominal pain, back pain, nausea, fatigue, weight loss, visual disturbance and a sense of impending doom (Table 3.6). Significantly more patients with PPGL reported a combination of symptoms of the classical triad (diaphoresis, headache and palpitations) than hypertensive controls (30.6 vs 6.8%, p=0.0005).

No. of patients reporting symptoms (n [%])	PPGL	HTN	p value
Total no. of patients	62	74	
No. of symptoms reported (mean +/- SEM)	6.4 +/- 0.6	3.7 +/- 0.3	<0.0001***
Headache	30 (48.3%)	38 (51.4%)	0.73
Diaphoresis	39 (62.9%)	18 (24.3%)	<0.0001***
Palpitations	30 (48.4%)	26 (35.1%)	0.12
Heart slowing	3 (4.8%)	0	0.06
Heart Pounding	17 (27.4%)	21 (28.4%)	0.90
Anxiety	26 (41.9%)	14 (18.9%)	0.003**
Constipation	16 (25.8%)	6 (8.1%)	0.005**
Diarrhoea	5 (8.1%)	4 (5.4%)	0.53
Flushing	12 (19.4%)	12 (16.2%)	0.63
Tremor	22 (35.5%)	10 (13.5%)	0.03**
Chest pain	10 (16.1%)	16 (21.6%)	0.4
Abdominal pain	12 (19.4%)	1 (1.4%)	0.0004***
Back pain	16 (25.8%)	8 (10.8%)	0.02*
Nausea	14 (22.6%)	6 (8.1%)	0.02*
Fatigue	34 (54.8%)	22 (29.7%)	0.003**
Weight Loss	19 (30.6%)	4 (5.4%)	<0.0001****
Dizziness	23 (37.1%)	21 (28.4%)	0.28
Postural symptoms	15 (24.2%)	16 (21.6%)	0.72
Dyspnoea	13 (21%)	12 (16.2%)	0.48
Visual Disturbance	19 (30.6%)	9 (12.2%)	0.008**
Paraesthesia	22 (35.5%)	18 (24.3%)	0.16
Seizure	2 (3.2%)	2 (2.7%)	0.86
Sense of impending doom	15 (24.2%)	8 (10.8%)	0.038*
Classic triad	19 (30.6%)	5 (6.8%)	0.0005***

Table 3.6: Reported symptoms. *Table showing the number of patients that reported each symptom in both the PPGL and the HTN cohorts. Third column shows the p value for the statistical analysis for comparing the two cohorts for each symptom reported. Statistical analysis by Mann Whitney U test *<0.05, **<0.01, ***<0.001, ****<0.0001.*

A regression analysis was then performed to formulate a combination of symptoms to 'score' the likelihood of a patient presenting with hypertension having a PPGL. To evaluate how well this initial model fit the data from the survey, the Akaike Information Criterion (AIC) was calculated. The AIC is a way of estimating the goodness of fit of a model. The AIC value of the initial multiple logistic regression model, when incorporating all symptoms as variables, was 171.54. The regression equation produced by backwards stepwise AIC selection (Appendix 2, equation 3) identified five positive predictive symptoms: diaphoresis, anxiety, abdominal pain, weight loss and visual disturbance, and two negative predictive symptoms: chest pain and headache. The predictive symptoms selected by this approach and their respective regression coefficients are shown in Table 3.7. All of the positive predictive symptoms were also the symptoms that were reported significantly more in the PPGL cohort than the

hypertensive control group (Table 3.6). The predicted probabilities produced by this equation for the study participants are illustrated in Figure 3.23.

Symptom	Regression coefficient	Score
Abdominal pain	2.978	3
Weight loss	1.747	2
Sweating	1.180	1
Visual disturbance	1.383	1
Anxiety	1.016	1
Headache	-1.007	-1
Chest pain	-1.849	-2

Table 3.7: Clinical Prediction Score. Table shows the seven symptoms identified by the regression model. Exact regression coefficients calculated by AIC equation (Appendix 2) for each symptom is shown in the middle column and the equivalent 'score' for each symptom is shown in the right column (calculated as the regression coefficient to the nearest integer). Possible total scores ranged from -3 to 8.
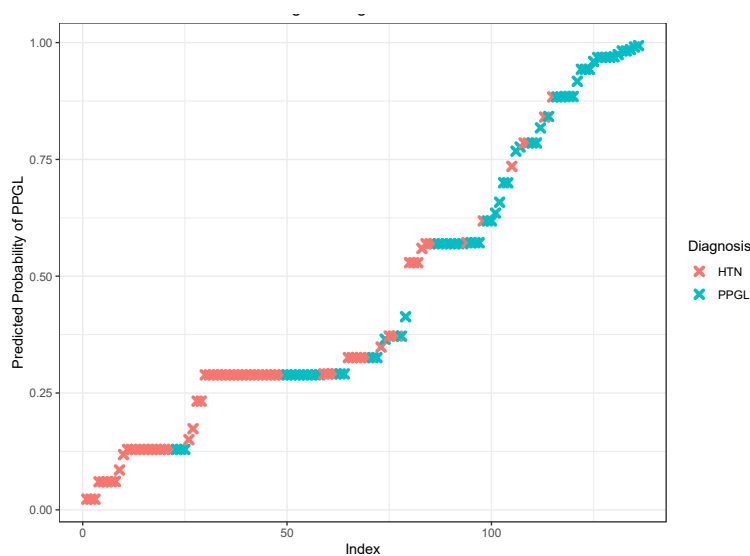
Figure 3.23: Predicted probabilities from logistic regression model. Graph showing the predicted probability of each patient having a PPGL. Each cross represents a different patient. Red crosses represent the patients with essential hypertension and blue crosses represent patients with PPGLs. Possible total scores ranged from -3 to 8.

From this regression model a clinical prediction score was developed. Each symptom was assigned a score based on the regression coefficient generated and rounded to the nearest integer (Table 3.7). Possible total scores ranged from -3 to 8. When applied to the study participants, this produced a distribution of scores shown in Figure 3.24.
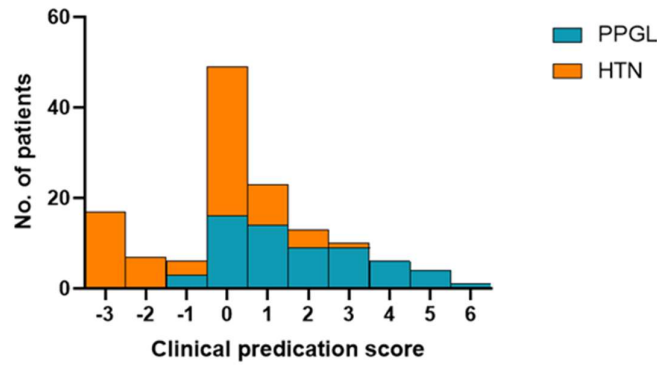
Figure 3.24: Distribution of clinical prediction scores. *Bar chart showing the distribution of PPGL and HTN patients based on the cumulative score they would have received from the symptoms reported.*

To evaluate the regression model and clinical prediction score ROC curves were applied to estimate the sensitivity and specificity of predicting the presence of PPGL in any given patient at different score thresholds. The area under the curve (AUC) was 0.829 (95% CI 0.761, 0.897) and 0.82 (95% CI 0.753, 0.886) using the exact coefficients and the clinical prediction score respectively. A symptom score of zero generated the highest sensitivity (0.952), with a specificity of 0.351 for a diagnosis of PPGL. Within our cohort 95.2% of patients that had a PPGL scored ≥0, however 64.9% of patients with hypertension also scored ≥0. A symptom score of three generated the highest specificity (0.986), with a sensitivity of 0.339, meaning a score ≥3 would be highly specific to a diagnosis of PPGL, but many diagnoses would be missed. No patient that scored < -1 had a PPGL.
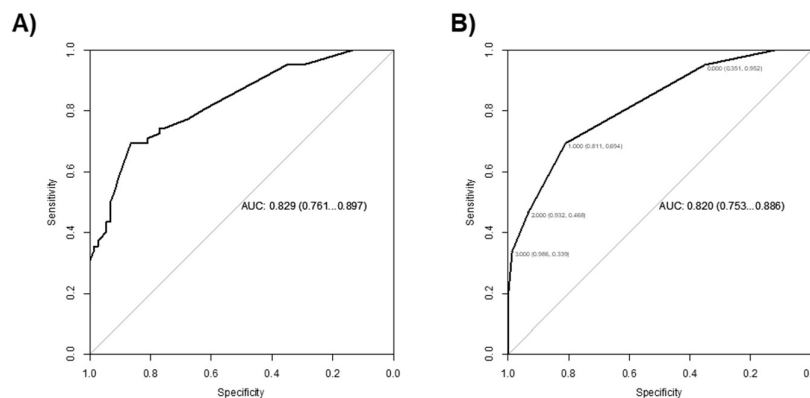
Figure 3.25: ROC curves of symptom models *Graphs show specificity and sensitivity for different scores and AUC. A) ROC curve for regression model of symptoms using coefficients generate in equation (Appendix 2). B) ROC curve for clinical prediction score highlighting symptom scores of 0-3. AUC area under the curve*

In summary, patients with a functional PPGL report more symptoms than patients presenting with essential hypertension. The most common symptoms reported were diaphoresis, anxiety, constipation, tremor, abdominal pain, back pain, nausea, fatigue, weight loss, visual disturbance and a sense of impending doom. A regression model identified anxiety, abdominal pain, weight loss, diaphoresis and visual disturbance as positive predictors of a functional PPGL.

3.4   Discussion

3.4.1   Improving pre-operative medical preparation

3.4.1.1 Patient preparation

Endocrine society clinical practice guidelines[12] recommend alpha-adrenergic blockade for 7-14 days in all patients with a hormonally functional PPGL to allow for normotension and euvolaemia to be achieved. In addition they recommend a high sodium diet and high fluid intake to prevent post-operative hypotension[12], although no specific definition is provided on what should be recommended to patients; however, this guidance assumes immediate access to operating lists. Pre-surgical treatment with medical blockade has been demonstrated to reduce perioperative mortality to less than 3%[132,147]. The necessity of pre-operative medical preparation with alpha-adrenergic blockade has been disputed by some authors over the years, with the main concerns regarding side effects and post-operative hypotension[138-140]. These concerns, however, generally focus on the need for alpha-blockade in patients that are normotensive[148] and/or do not have raised metanephrine levels or have parasympathetic PGLs or are only dopamine producing[149]. One could argue that in the hands of experienced surgeons and anaesthetists there is no need for pre-operative medical therapy in small biochemically silent tumours. Nonetheless, guidelines[12] recommend medically preparing PPGL patients with alpha-blockade +/- beta-blockade, to avoid the possible cardiovascular risks especially in patients with evidence of functional PPGLs, where benefits far outweigh the risks of treatment[150].

Previous audit work published from our centre[151] demonstrated a superiority of intravenous phenoxybenzamine over an oral preparation in intra- and post-operative outcomes. As the intravenous preparation is no longer available, we were keen to explore how to optimise medical preparation to minimise side effects and post-operative complications that have been raised as concerns against the use of these medications pre-operatively.

Firstly, these data demonstrated that oral phenoxybenzamine is a successful antihypertensive in PPGL patients. Our intervention group had lower BPs and HR with less variability pre-operatively than at diagnosis. This was likely due to the higher doses of alpha- and beta-blockade therapy tolerated. Our cohort of patients had higher BPs in the daytime compared to night-time, rather than a reverse diurnal pattern as is usually reported[152]; however, this may simply be an effect of a small sample size.

To our knowledge there are no published data implementing HBPM as a tool in managing patients with PPGLs, although it is widely used successfully in the outpatient management of patients with hypertension, both for diagnosis and subsequent monitoring for titration of medications[108]. Our data

suggest that HBPM, like for other hypertensive patients[153] is as accurate a method as ABPM for PPGL patients. Our intervention group achieved higher doses of alpha-blockade as outpatients. This may have been due to the fact that medications were gradually titrated in a personalised manner, using the home BP data. This allowed appropriate volume replacement in a step-wise approach to achieve overall better BP control whilst minimising postural side effects. Presumably it was the minimisation of the postural side effects that allowed the patients in the intervention group to tolerate higher doses and subsequently achieve better BP control. Therefore, HBPM may prove an extremely useful aid in managing PPGL patients in the outpatient setting, and also identifying at which point the addition of a beta-blocker would be beneficial and safe, if needed.

As expected we demonstrated a positive correlation with NMN levels and BP. Increasing NMN levels were correlated predominately with increasing DBP and to a lesser degree SBP. This may be due to norepinephrine exerting a greater effect on α-adrenergic receptors, over β-receptors, thus resulting in a stronger vasoconstriction rather than inotropic effect[20]. We also demonstrated a positive correlation with 3MT levels and HR. This was an unexpected finding as generally epinephrine levels are considered the driver for HR[154]. Only four of our patients had predominately epinephrine producing PPGLs and therefore this is likely too few to demonstrate a significant correlation. 3MT levels are a surrogate marker for dopamine, and this would suggest that dopamine may be contributing to patient tachycardia. Dopamine stimulation can cause smooth muscle relaxation in arterioles and thus vasodilation causing increase renal blood flow and dopamine receptors in the kidneys stimulate natriuresis[155]. These effects would result in a reflex tachycardia. Although dopamine has an inotropic action, without increasing HR, through stimulation of dopamine receptors in the heart, dopamine can also stimulate $beta_1$-receptors causing an increase in both cardiac muscle contractile force and HR[156]. A combination of these factors may explain the positive correlation we demonstrated with 3MT levels. The clinical implications of this could be in using the 3MT levels, in addition to MN levels, for assessing which patients will benefit from the addition of beta-blockade early in their management, however these results should be interpreted with caution as only a small number (n=6) of patients had raised 3MT levels.

The results from retrospective studies and case series on the best choice of alpha-blocker for medically preparing PPGL patients, have been conflicting[130,133,136,154,157-161]. The only prospective randomised study published to date, the PRESCRIPT trial[137], did demonstrate that phenoxybenzamine was superior at preventing HDI compared to doxazosin[137]. One of the main problems with phenoxybenzamine is that patients struggle to tolerate it due to its side effect profile, especially postural symptoms. Phenoxybenzamine is an irreversible inhibitor of alpha-receptors thus causing vasodilation. Therefore

the postural symptoms are caused by an inability to vasoconstrict on standing. Our data suggest that these side effects could be minimised by gradual titration of doses with appropriate salt and water repletion for volume restoration. In our cohorts the intervention group with personalised titration were more likely to tolerate phenoxybenzamine and achieved higher doses as an outpatient. This suggested that this group achieved better pre-operative blockade, supported by the fact that they also had lower SBP, DBP and HR measurements in the three days pre-operatively compared to the control group. When applying the Roizen criteria[109] to judge the success of alpha-blockade the majority of patients in our intervention group were within these targets in the week before their operations, with 75% of patients in the intervention group experiencing no SBP readings above 160 mmHg or below 80 mmHg and the remaining 25% had less than 10% of their readings outside these targets. All of the intervention group demonstrated successful alpha-blockade based on mean pre-operative ABPM measurements using Roizen criteria. We applied stricter criteria for BP and HR targets in the outpatient setting (SBP <135 mmHg, DBP <80 mmHg and HR <80 bpm)[12], but still achieved a higher proportion of patients that were within these targets (87.5% had a mean BP on pre-operative ABPM below these targets), compared to the two cohorts of patients in the PRESCRIPT trial[137], which acknowledged that 53.8% in the phenoxybenzamine cohort and 30% in the doxazosin cohort did not meet the criteria for successful pre-operative alpha blockade[137]. Our results were similar to another study into HDI in PPGL patients[135] which reported evidence of successful alpha-blockade in 75% of their patients achieving a target BP of <130/80 mmHg, based on one-off measurements taken at the final clinic, rather than ABPM averages or multiple home or ward BP measurements in the preceding days before their operation.

Successful volume restoration is a crucial part of management in these patients. Our intervention group had high aldosterone and renin levels at diagnosis, implying decreased renal blood flow in keeping with a vasoconstricted state, which decreased with medical therapy, indicating restoration of volume depletion. We also used the volume of IVF required pre- and post-operatively as a measure of volume status. In our study the intervention group required less IVF pre-operatively than the control PPGL group, suggesting that the intervention group had achieved better volume restoration as outpatients, with less need for IVF to combat postural hypotension. The intervention group also required less increase of medication doses in the three days pre-operatively to achieve satisfactory BP control. This supports the notion that the required increase in medication doses was possible in the outpatient setting as these patients were more volume replete and thus less troubled by postural symptoms. In addition post-operatively the control group experienced more hypotension and required a higher volume of IVF in the first six hours post-operatively. This was probably due to the fact that the intervention group received a more gradual titration of medication doses as outpatients.

This allowed time for physiological volume restoration. The volume of fluid required had equalled out by 12 hours post-operatively, although the control group also required significantly more IVF in the first 48 hours on the ward. This could reflect the current HDU practice to give less IVF after general anaesthesia, where it is administered in a reactive rather than proactive approach, with subsequent 'catch-up' in the first 48 hours on the ward. These data would indicate that PPGL patients should receive higher volumes of IVF proactively intra- and early post-operatively, to avoid the potential hypotension that could occur due to the abrupt decrease in catecholamines, and subsequent vasodilation, from surgical removal of the tumour.

Although intellectually it makes sense that lower BP and HR and volume repletion pre-operatively should result in less intra-operative HDI, this is difficult to prove. The only intra-operative variable that differed between our two PPGL cohorts was peak BP at knife-to-skin. Perhaps on reflection it is unsurprising that there are no significant intra-operative differences between the two groups, as both cohorts reached the same targets before their operations. For the historical control patients this was achieved by admitting the patients to hospital several days (up to a week) before their elective operation date for rapid up-titration of medication with intravenous fluid support to ensure that they were fully alpha-blocked before undergoing their adrenalectomy. This is supported by the fact that the control group had more days in hospital pre-operatively than the intervention group (5 vs 3.25 days), required a greater quantity of IVF pre-operatively (6L vs 1.5L) and required a larger increase in alpha-blockade medication (mean 42mg [0-80] vs 1.875mg [-20 -20]) and beta-blockade medication (mean 10.7mg [0-30] vs 0.94mg [-20-30]) in the three days before their operations. However, these are somewhat subjective measures as the decision as to when to admit, how much additional IVF and medication to give was made by the individual treating clinician based on the clinical situation at the time.

3.4.1.2 Haemodynamic instability (HDI)

The PRESCRIPT trial[137] is the only published prospective randomised control study looking at HDI in PPGL patients. They compared the efficacy of two different types of alpha-adrenergic blockers: doxazosin and phenoxybenzamine in 134 nonmetastatic PPGL recruited across nine centres in the Netherlands. Despite the good intentions of this study, it has several limitations and therefore the outcomes need to be interpreted with these in mind. Firstly, to include enough patients for results to be statistically significant, patients were recruited from multiple centres, meaning that different surgeons and anaesthetists were performing the operations, and presumably also different physicians were managing the patients and titrating their pre-operative medication in outpatient clinics. Although a standardised regimen for the use of intra-operative medications and IVF was used, it would

be difficult to eliminate variations between the respective surgeons and anaesthetists. Secondly, only 24.6% of the phenoxybenzamine group achieved the target BP (<130/80 mmHg and upright BP 90-110 mmHg), and 53.8% did not meet the criteria at all. This was also true for 42.4% of the doxazosin group, with 30% not meeting BP targets. Thirdly, higher doses of doxazosin were used than is licenced in the UK. They reportedly used a mean dose of doxazosin of 24mg twice daily (median 40mg [32-48]). The BNF recommends a maximum dose of 16mg/day for treatment of hypertension. Fourthly, treatment with an alpha-blocker was only started 2-3 weeks before surgery (median 14 days, maximum 20 days), in accordance with current guidelines[12]. Given these limitations it is perhaps not surprising that they did not demonstrate a difference in clinical outcomes between the two groups.

The primary end point for the PRESCRIPT trial[137] was duration of time intra-operatively spent outside of the target BP (SBP <160 mmHg and MAP >60 mmHg), and secondary end points of haemodynamic instability score (HI-score)[112] and cardiovascular complications. They found no difference in cardiovascular complications or 30-day mortality between their two cohorts. They also demonstrated no difference in the intra-operative duration of time the patients spent outside BP targets; 11.1% in the phenoxybenzamine group compared to 12.2% in the doxazosin group. In our much smaller cohort of patients, we also demonstrated no difference between our intervention and control PPGL cohorts, however we found that the duration our patients spent outside these targets to be lower (5.62% and 7.95%) for the intervention and control cohort respectively. As the final dose of phenoxybenzamine achieved in the intervention groups was not that different to that of the PRESCRIPT trial, this may be due to the patients in our intervention group being on medical therapy for a longer duration pre-operatively and thus a higher proportion achieving the pre-operative BP targets.

In addition they applied a scoring system (HI-score) to further assess intra-operative HDI designed by the same authors[112]. This score included measures of intra-operative haemodynamic variables (maximum and minimum BP and HR measurements, duration of time spent outside these targets), volume therapy and vasoactive drug usage. They demonstrated a lower HI-score in the phenoxybenzamine group compared to the doxazosin treated group (38 vs 50, p=0.02). They also showed that peak SBP, cumulative time and frequency of SBP >160 mmHg and quantity of vasoactive drugs required were lower in the group treated with phenoxybenzamine. These data imply that phenoxybenzamine was more effective than doxazosin at preventing intra-operative HDI, but whether this is associated with better clinical outcomes is unclear. We needed to modify this scoring system to apply it to our study as our anaesthetist used different vasoactive drugs and therefore we only included the usage of norepinephrine in this part of our score; due to this our results of HI-score are not directly comparable to those of the PRESCRIPT trial. We validated our modified version of this

score by demonstrating a significant difference between the patients in our cohort that developed HDI and those that did not (HI-score 38 vs 20, p=0.0003), but demonstrated no difference between our intervention and control PPGL cohorts. This may be because our sample sizes were too small to demonstrate a difference. We were, however, able to compare a number of individual variables with the results from the PRESCRIPT trial. In the PRESCRIPT trial 51.5% and 72.1% in the phenoxybenzamine and doxazosin groups respectively had at least one SBP reading >160 mmHg intra-operatively, which was similar to our study (43.75% and 62.5% in the intervention and control PPGL groups respectively). They reported an average intra-operative time spent with SBP >160 mmHg of 6% (range 0-46%) in the phenoxybenzamine treated group, which was also similar to our study (4.7% and 5.5%). However, in their cohort treated with doxazosin this figure was higher (mean 31%, range 0-89%). These data demonstrate how difficult it is to completely antagonise alpha receptors and hypertensive surges can still occur despite evidence of successful blockade[149,154], as the body continually adapts and produces more adrenergic receptors to overcome the inhibition. In support of this another interesting observation with our data was the BP spike was always at intubation, and this was true for both cohorts, reflecting the efficacy of the pre-operative oral alpha-blockade before the patients are managed intra-operatively by the anaesthetist. This maximum BP was also where the main difference was seen for those that experienced HDI compared to those that did not.

The PRESCRIPT trial reported no differences in post-operative hypotension (MAP <60 mmHg) or post-operative inotrope use (dosage or duration). However, they demonstrated a higher percentage of patients with an intra-operative MAP <60 mmHg (72.7% and 82.4% respectively) and duration of time intra-operatively with low MAP (5.8% and 6% respectively) compared to our study of 1.3% and 2.2% in the intervention and control PPGL groups respectively. This is most likely due to the shorter duration that the patients in the PRESCRIPT trial were medically prepared with the alpha-blockade medication (mean 14 days [range 13-20 days]) compared to our study (mean 88 days [range 47-147 days] for our intervention group), suggesting that the patients in the PRESCRIPT trial were less volume replete. Interestingly that biggest difference seen between the patients that experienced HDI (n=6) versus those that did not (n=26) in our study was the duration they were on alpha- and beta-blockade before their operations, rather than the actual doses achieved.

Another recently published study[135] investigated the factors that may affect haemodynamic stability during adrenalectomy in 68 patients with PPGL and also compared different types of oral alpha-blockade (labetolol vs bunazosin vs doxazosin); with 85% of the patients taking doxazosin. They defined HDI as episodes of both hyper- and hypotension occurring in the same procedure, using more extreme cut-offs of SBP >200 mmHg or <80 mmHg. Using this definition they reported 37% of patients

experienced HDI intra-operatively. Older age, higher metanephrine levels and the presence of diabetes were factors identified as promoting HDI. However, on multivariate analysis only diabetes was identified as an independent risk factor, although of note, all patients with HDI also had higher MN levels. The cohort of patients with diabetes were also older, had larger tumours and higher MN levels.

Applying the same criteria to define HDI, in our intervention group only one patient experienced an episode of intra-operative SBP >200 mmHg and another patient experienced an episode of both SBP >200 mmHg and <80 mmHg intra-operatively. In comparison to the control cohort in our study of which four patients experienced an episode of SBP >200 mmHg and three patients experienced SBP <80 mmHg intra-operatively (one patient experienced both extreme hyper- and hypotension) (40%) similar to that reported in the recent study[135]. Using Roizen criteria[109] for a definition of intra-operative haemodynamic stability of SBP <160/90 mmHg and >80/45 mmHg, seven patients (43.75%) in the intervention group experienced at least one episode of BP >160/85 mmHg and two of these patients also experienced at least one episode of BP <80/45 mmHg (12.5%). Compared to 10 control patients (66.6%) with hypertension, in addition five of these patients also experienced hypotension (33.3%) episodes. Using the more extreme definition of HDI, HDI was more likely to occur in the control than intervention group. This supports the notion that the success of medical preparation before the operation may in fact play a role in limiting intra-operative HDI, although this difference did not persist when applying the stricter Roizen criteria, but this may be due to small sample size not allowing for the difference to be demonstrated.

Although more intra-operative HDI was experienced within the control group, HDI did occur within both cohorts. When the patients that experienced intra-operative HDI (n=8) were compared with those that did not (n=24), the patients that experienced intra-operative HDI had higher SBP and heart rates on the morning of the operation. However, unlike the above study[135], we did not demonstrate that HDI was more likely with older age, higher urinary MN levels or in diabetic patients. The only differences demonstrated were that patients that experienced HDI were taking alpha-blockade medication (mean 36.86 vs 101.7 days, p=0.002) and beta-blockade medication (mean 26 vs 64.57 days, p=0.018) for significantly less time pre-operatively than their counterparts that did not experience intra-operative HDI. This is in contrast to an older retrospective study of a small number of patients that found no correlation in HDI based on the duration of treatment (five patients taking phenoxybenzamine for 14 days versus seven patients taking it for five days)[157]. To our knowledge no other studies have investigated the effects of duration of treatment. In addition, those patients that experienced intra-operative HDI also showed more evidence of escape from blockade therapy

(applying Roizen criteria) in the preceding three days before surgery (75% vs 26.1%). This knowledge could identify which patients are at higher risk of intra-operative HDI, based on evidence of escape from therapy in the preceding few days. Although this does not help identify those at higher cardiovascular risk pre-surgery, it can help forewarn surgeons and anaesthetists which patients are more at risk intra-operatively. Also if patients at higher risk can be identified a few days before their elective operations their medical therapy can be intensified as inpatients with intravenous fluid support under careful observation. These findings are different to what has been reported elsewhere where occurrence of HDI was not associated with successful attainment of target BP[135], but in this study success of alpha-blockade was assessed based on one-off BP measurement in outpatient clinic and does not compare duration of treatment.

Despite there being no significant difference in the percentage of patients that met Roizen criteria between the intervention group and control group, more patients within the control group developed intra-operative HDI. The control group experienced higher mean BP and HR in the preceding three days pre-operatively and also had more escape from targets. Although all the patients that experienced HDI had an SBP >140 mmHg on the morning of their operation, so did several patients that did not develop intra-operative HDI. Only two patients within the intervention group developed HDI, and both of these patients had a mean BP above our stricter outpatient targets on ABPM pre-operatively (BP <135/80 mmHg). Although we do not have ABPM data for the control group, given that they were taking lower doses of medication, required a greater increment in doses pre-operatively to achieve adequate BP control and more fluid support it is likely that the control patients would have demonstrated more escape from targets as outpatients than the intervention group. Potentially if Roizen criteria were modified to use stricter BP targets (<140/80 mmHg), more in line with current hypertensive guidelines[12,108] and intravenous fluid was given more proactively, much of the intra- and post-operative HDI could be avoided in these patients.

It is difficult to ascertain whether these pre- and intra-operative differences highlighted actually have any effect on clinical outcomes. Our data showed that the control group required more IVF immediately post-operatively implying more post-operative hypotension, even though they were taking lower doses of blockade medications pre-operatively. This was confirmed by a significant difference in the number of patients that experienced post-operative hypotension (18.75% vs 62.5%, p=0.029). This might, however, reflect that the doses of alpha- and beta-blockade were more rapidly up-titrated in the days before the operation to achieve the pre-operative BP control compared to the intervention group who had doses titrated more slowly over a longer duration as outpatients, allowing more time for the intervention patients to achieve euvolemia and restoration of normal physiology.

Other studies have reported higher rates of post-operative hypotension in patients treated with phenoxybenzamine[129,130], and indeed this is one of the big arguments against using this medication. The recent prospective study[137], however, did not demonstrate more severe or longer duration of post-operative hypotension in the group treated with phenoxybenzamine. Takeda *et al* reported a post-operative hypotension rate of 28%, but this did not differ between the HDI and no HDI group or between groups treated with different alpha-blockers[135].

Clinical experience, and some supportive evidence[162,163], suggests that in the hands of an experienced surgeon and anaesthetist much of the intra-operative haemodynamic instability can be overcome by reactive measures. For this reason the need for pre-operative medical preparation with alpha-blockers is sometimes disputed. Whilst this is no doubt true, these operations are performed at many centres that treat lower numbers of patients with PPGLs and therefore any measures that can be taken to reduce the risks would be beneficial. These arguments also do not consider the importance of alpha-+/- beta-blockade in the period of time between diagnosis and surgery, where the patients are at risk of a hypertensive crisis due to tumoural release of catecholamines[122,164]. Based on our data we would argue that modifying Roizen BP criteria to stricter targets could reduce intra-and post-operative HDI, and if they could be applied in the outpatient as well as the inpatient setting, could potentially reduce cardiovascular risk. This could potentially be achieved with the application of home BP self-monitoring and personalised gradual titration of mediation with appropriate fluid replacement in an outpatient setting, thus reducing the need for prolonged hospital admissions pre-operatively.

3.4.1.3 Understanding the wider benefits of medical therapy with alpha-adrenergic inhibition

Body composition

These data suggest there are additional benefits of treating patients with alpha-blocking medications beyond that of just improving haemodynamic variables.

A control group was selected from an idiopathic hypertensive population which were matched to the PPGL cohort on age, gender and diabetes status. These cohorts proved to be well matched based on baseline characteristics and baseline BP measurements. The main difference between the two cohorts was that the hypertensive control group were heavier. This difference was unavoidable as the majority of patients that are referred into a tertiary centre hypertension clinic have obesity as a contributing factor. However, there were significant, and similar, improvements in BP measurements for both cohorts from baseline to follow-up, allowing other comparisons to be made. HR decreased significantly more in the PPGL cohort than controls (p=0.003), presumably due to the use of beta-blockers in the PPGL cohort.

Bioimpedance or bioelectrical impedance analysis (BIA)[165] is a non-invasive measure of body composition. PPGL patients catabolic state at diagnosis is due to catecholamine excess driving the sympathetic nervous system causing muscle and fat breakdown[143]. When baseline measurements were compared, in addition to weight, the PPGL patients had a lower percentage of body fat and muscle mass. This has also been shown in comparison to patients with non-functioning adrenal adenoma[144,166] and healthy volunteers[143]. The PPGL patients also had a lower weight of total body water, but total body water contributed to a higher percentage of total body weight, as the PPGL patients proportionally had lower levels of muscle and fat mass presumably due to the catabolic effects of catecholamine excess. Whether weight and BMI actually correlate with metanephrine or catecholamine levels is still contested with some studies showing a negative correlation[143,167] between hormone levels and weight, and other studies demonstrating no correlation[144].

Our data showed improvements in weight, BMI, body fat and muscle mass in the PPGL cohort, but not in the hypertensive control group over the follow-up period, despite similar improvements in BP. This suggests that these catabolic effects are most likely due to catecholamine toxicity from the excess catecholamines produced by the tumours, which is potentially being reversed by blocking their effects with medical therapy. This is supported by studies demonstrating improvements in bioimpedance markers with surgical removal of the tumour[141-144,167-169]. Other historical studies have shown improvements in metabolic markers with blockade therapy, such as a decrease in free fatty acids (the breakdown product of lipolysis)[170-173]. To our knowledge this is the first study that directly demonstrates this effect on body composition parameters with medical therapy.

An increase in total body water in weight was expected due to the volume expansion required to combat the postural symptoms that occur with relaxation of vasoconstriction. The weight gain seen in these patients is often all attributed to volume therapy. However, it was surprising that total body water as a percentage of total body weight decreased. This can be explained when looking at these data in conjunction with the other body composition parameters. Both muscle mass and fat mass increase with treatment, in addition to total body water, and these data infer that muscle mass and fat mass increase to a greater extent than total body water. This implies that blockade has an important effect on reversing the catabolic state, beyond that of simply an effect of releasing vasoconstriction and reversal of hypovolaemia.

BMR unexpectedly increased in the PPGL patients from diagnosis to pre-operatively. We expected the BMR to be high on diagnosis and decrease with the effect of the alpha blockade. However, this can be explained by how BMR is calculated. BMR is calculated based on gender, weight and height of the individual and does not factor in any of the other bioimpedance measurements. Therefore BMR

increased in the PPGL as a factor of their weight increasing so significantly from diagnosis to pre-operatively with reversal of the catabolism.

There were no significant changes in any of the body composition parameters in the PPGL patients measured 6-12 months post-operatively in the nine patients for whom these data was available. This was surprising as other studies have shown big improvements in markers pre- and post operatively[142,144,168]; although of note type and/or duration of pre-treatment with alpha-blockade is not known. One might hypothesise that the maximum improvement in catabolic state is with the blocking of the adrenergic effects, but it is more likely due to the small sample size for which we have post-operative data not reaching a level of significance. Another possibility is that the duration required for full physiological recovery is longer than the point at which we took post-operative measurements. This latter theory is supported by the notion that even when comparing the body composition data post-operatively the PPGL patients still had lower muscle mass than the hypertensive control patients at baseline.

In summary, our data have demonstrated that treatment with alpha- and beta-blocking medications could potentially benefit patients beyond that of simply correcting their hypertension and tachyarrhythmias. The use of alpha +/- beta-blockade also appears to begin to reverse the catecholamine catabolic effects. Our data suggest that the reversibility of the fat and muscle breakdown with blockade is an important effect in addition to the medical effect on the reversal of the vasoconstriction. It is likely that the two weeks recommended for pre-operative medical therapy is not long enough to show these anabolic effects.

Inflammatory status

It has been demonstrated that patients with PPGLs *in situ* have evidence of systemic inflammation with studies reporting raised leukocytes, neutrophils, platelets, CRP and lower lymphocyte levels in patients with PPGL *in situ* compared to hypertensive control groups[145,146], patients with primary aldosteronism[146,174], patients with adrenocortical carcinoma[174], and healthy controls[146]. This is supported by a decrease in inflammatory markers following adrenalectomy for patients with a PPGL[141,142,146]. It is thought that increases in white blood cells occur through stimulation of β2-adrengeric receptors[175], or possibly as a systemic inflammatory response from interleukin-6 production[176-181].

Surprisingly in our cohort the haemoglobin and the haematocrit were lower in PPGL group compared to the hypertensive control cohort at baseline. This was unexpected as patients with functional PPGLs *in situ* are generally volume depleted and therefore the classic description is of polycythaemia. In our

cohort we found over half of the patients to be anaemic at diagnosis. Nine of the 16 patients with PPGL had a haemoglobin below the lower limit of the reference range (130-170 g/L) and only two patients in the PPGL cohort had haemoglobin levels of greater than 160 g/L at diagnosis. All of the PPGL patients in our cohort had haematocrit levels within the reference range (0.37-0.5), although 50% (8) had levels below 0.4. Four patients had evidence of confirmed iron deficiency anaemia with ferritin levels of less than 50 g/L, but an additional six patients (in total 62.5%) had ferritin levels less than 105 g/L (the cut-off to determine if iron deficiency exists in the setting of another illness[182]). Despite the classic description of patients with functional PPGL *in situ* having polycythaemia, many case reports document patients presenting with anaemia[176,177,181,183].

Our data demonstrated higher levels of ALT and Troponin T in the PPGL cohort compared to the hypertensive cohort at baseline, but not in the absolute leukocyte, neutrophil or platelet count as previously shown[145,146]. This may have been due to the small sample size in our cohort. Raised liver enzymes have been described in several case reports[176,184-186] and are thought to be due to stimulation of alpha-receptors in blood vessels in the liver by norepinephrine overproduction causing increased resistance in liver blood vessels resulting in decreased blood flow and oxygen supply, ultimately resulting in damage to hepatocytes[187]. Interestingly all of our patients that had raised ALT levels had pure or predominately norepinephrine secreting tumours.

Our data demonstrated improvements in many of the inflammatory markers in the PPGL cohort prior to surgical intervention. White blood count, platelets, ferritin and ALT all significantly decreased after treatment with medical therapy (mean 12.6 weeks). Surprisingly there was no significant change in haemoglobin, haematocrit, urea, creatinine or serum sodium concentrations suggesting that the decrease in the other inflammatory markers seen was not merely a dilutional effect of volume therapy. However, this was likely influenced by a number of the patients being anaemic at diagnosis, and also several being in an extreme catabolic state with low urea and creatinine levels at diagnosis. Five patients had a urea of less than 4 mmol/L at diagnosis and only one patient had a urea above 8 mmol/L. Only two patients had creatinine levels of greater than 100 µmol/L at diagnosis. Therefore it is likely that there is too much variation in a small sample size to reflect these changes. In addition on bioimpedance analysis our data demonstrated improvements in muscle mass which may have contributed to negating the expected fall creatinine and urea with fluid replenishment.

Troponin T is a marker of cardiac inflammation and/or damage. Our data demonstrated that the PPGL cohort had a higher Troponin T level at diagnosis compared to the hypertensive cohort. This could be due to subclinical cardiac inflammation likely a result of high circulating catecholamine levels stimulation of myocardial alpha- and beta-adrenoceptors[188-190] or as a direct toxic effect on

myocytes[191]. One of the patients in our cohort experienced a myocardial event before their operation, and thus had a rise in cardiac markers and was treated as an acute MI. When this patient was removed from analysis, however, there was a decrease in Troponin T levels with medical therapy. Several case reports and a case series have reported patients with PCC presenting with acute cardiac syndromes or myocarditis[192]. However, in addition to these overt cardiac effects that occur occasionally, our data supports the hypothesis that there are also subclinical cardiac effects in the majority of PPGL patients that may be amenable to reversal with blocking of the catecholamine effects.

We did not demonstrate any difference in pro-BNP markers, but this may be due to small sample size with large variations in results. Large cardiac focused studies have shown impaired LV ejection fraction, systolic and diastolic strain, and myocardial fibrosis in newly diagnosed patients with phaeochromocytoma compared to hypertensive or healthy control patients[164]. The LV ejection fraction was shown to improve following surgery, but systolic and diastolic strain persisted, which may explain why there was no improvement seen in pro-BNP markers.

No changes in any of the inflammatory markers were demonstrated in the hypertensive control group over the four month follow-up duration. This supports the concept that these inflammatory changes within the PPGL cohort are a result of catecholamine toxicity, rather than being due to the hypertension itself.

Serum based inflammatory scores have been used to predict outcomes in some cancer patients[104]. These scores are based on biochemical data collected as part of routine care during diagnostic work up (FBC, CRP, albumin), and thus are inexpensive and easily reproducible. These scores are thought to represent evidence of systemic inflammation and immunosurveillance status of the patient[193]. Neutrophilia in cancer is most likely caused by tumour cells secreting myeloid growth factors or other cytokines, or due to tissue destruction causing cancer-related inflammation. Whereas lymphocytes are important in mediating anti-tumour activity and therefore low levels may represent evidence of immunosuppression[104,193]. Thus these scores are thought to represent an ineffective immunological tumour response, which may aid tumour invasion, thus relating to poor clinical outcomes[104]. In general increased PLR, NPS, NLR and SII and low LMR are associated with poor clinical outcomes, and have been applied to other tumours such as meningiomas[194] and gliomas[195], craniopharyngiomas[196], pituitary adenomas[193] and neuroendocrine tumours[197-200] to predict surgical outcomes. In our cohort of patients, the absolute lymphocyte count was lower in the PPGL cohort at baseline and the PLR, and absolute platelet count were higher in the PPGL group than the hypertensive controls. Leucocytes, platelets, PLR and the SII, decreased in the PPGL cohort following a period of medical therapy. These findings support the idea that catecholamines induce a systemic inflammatory response. If left

101

untreated this could potentially increase patients vulnerability to infection during and following surgery, and likely slow post-operative healing. As far as we are aware no other study has demonstrated these improvements in inflammatory markers specifically with medical therapy before surgical intervention; however, two case studies have noted a decrease in leucocytosis following treatment with an alpha-blocker alone[181] or with the addition of an anti-inflammatory agent[184], supporting our findings.

The inflammatory and immune markers and correlations with clinico-pathological features will be discussed in more detail in the next chapter where I investigated inflammatory and immune markers in the PPGL tumour microenvironment in a larger cohort of patient tumours.

3.4.2   Earlier diagnosis of patients with PPGLs - screening patients with hypertension

Early diagnosis of patients with PPGL is important to avoid the long-term cardiovascular and metabolic effects of excess catecholamines. Diagnosis is relatively cheap and uncomplicated with plasma or urine metanephrines to confirm biochemical presence of a PPGL before undergoing localisation imaging studies. However, as patients with PPGLs do not conform to a specific set of symptoms and signs clinicians must have a high index of suspicion and low threshold for further investigations. Although the likelihood ratio is very high (6.3-14.6) if a patient presents with the classical triad of headache, diaphoresis and palpitations[201,202], few patients actually present with this classic symptom triad, with figures reported as low as 4%[121]. This triad of symptoms are also reported in a significant proportion of patients that do not have a PPGL[201,203,204].

Our aim was to create a tool that could be used in the community setting to identify which patients that presented with hypertension required further investigation to rule out a diagnosis of PPGL. We wanted to identify if there were any discriminating symptoms that patients with functional PPGLs experience that separate them from individuals that suffer with hypertension from other causes. Our data demonstrated that patients with PPGL report more symptoms than patients with essential hypertension, but similarly to a recent review[202], there was no clear-cut set of symptoms to distinguish between them. Nonetheless, we did identify several symptoms that PPGL patients experience more frequently. These included diaphoresis, anxiety, constipation, tremor, abdominal and back pain, nausea, fatigue, visual disturbance, weight loss and an impending sense of doom, consistent with a recently reported observational study[203].

From these data using a regression analysis model, a set of symptoms were identified and allocated each with a score (between -2 and +3) on how likely it was that each particular symptom was caused by a PPGL. Many of the same symptoms that were reported significantly more by the patients with

PPGL were also identified as positive predictive symptoms in the regression model (abdominal pain, weight loss, diaphoresis, visual disturbance and anxiety), supporting the importance of these symptoms in diagnosis. We found that the higher the score the more likely the patient had a PPGL. Within our cohort 98.6% of patients that scored ≥ 3 had a PPGL, but this only included 33.9% of all the patients that actually had a PPGL. We found a score of greater than zero gave the highest sensitivity, with 95.2% of patients with a PPGL within our cohort scoring ≥ 0. However, it should be noted that these are preliminary data on a relatively small cohort of patients and that the evaluation of the regression model and clinical prediction score is based on the same population that they were fitted to (in-sample evaluation). This is likely to overestimate the performance of the model due to overfitting, and therefore the sensitivity and specificity figures presented are relevant to our cohort only and not the general population. Our cohort consisted of PPGL and HTN patients in a 1:1 ratio, which obviously does not reflect the general population. Reports suggest that less than 1% of hypertension is due to PPGL[12], and a recent prospective study found a prevalence of 11.8% of patients investigated for PPGL were actually diagnosed with one (245 of 2065 patients)[203]. Therefore, to validate these data and refine the symptom score the control group would need to be increased at least 10-fold and it would require external validation. However, despite these limitations in the study design the symptoms we identified were consistent to those found in other studies[202,203].

It was surprising that diabetes proved to be a negative predictor to a diagnosis of PPGL. On further reflection, this is likely to reflect the choice of control group including patients with metabolic syndrome as a main contributory factor to their hypertension. We, therefore, chose to exclude diabetes from the further analysis when evaluating the symptoms to formulate the score card, although the presence of new onset diabetes in a patient with other suggestive symptoms should heighten a clinicians' suspicion to the possible diagnosis.

There is very little in the literature examining the types of signs and symptoms that patients with PPGLs present, and fewer still that have a comparative group. The original studies by Manager in 1977[113], and two further reports in the 1980's[201,204], identified the classic triad of diaphoresis, palpitations and headache to be dominant presenting features. More recently a systematic review[202] supported these earlier findings, and an observational study[203] identified palpitations, but not headache. Interestingly our data identified headache as a negative predictive symptom, and palpitations, although reported more frequently by the PPGL population, did not reach significance between our cohorts. This may be due to the choice of control group being a hypertensive population, as approximately 50% of each cohort reported headaches, and it is the high BP component that is thought to drive the symptom of headaches in PPGL patients. Despite headache being a negative

predictive symptom in our regression model, 30% of patients with PPGL in our cohort reported the classic triad of symptoms. This was significantly higher than those in the control group, suggesting that although this presentation is not common, it is highly specific, in keeping with other studies[113,201-204]. Our data demonstrated similar percentages of patients reporting other symptoms[113,120]. Geroula *et al*,[203] also demonstrated that reported symptoms differ depending on the dominant type of excess catecholamine secreted, and this may explain some of the variation between different reports.

A recent prospective observational study[203] similarly attempted to establish a clinical prediction model. In addition to five positive predicative symptoms (diaphoresis, tremor, nausea, palpitations, pallor) they added a point for BMI ≤25 Kg/m^2 and HR ≥85 bpm and a negative point if obese. They reported a 5.8-fold likelihood of having a PPGL with score ≥ 3, which increased to 11.5-fold increase when surveillance and incidentaloma patients were excluded. Higher scores also correlated with high metanephrine levels.

Also of note, surprisingly, neither of the two recent reviews highlight hypertension as an important factor on multivariate analysis[202,203]; however, this may reflect limitations in study designs (e.g. use of office BP missing paroxysms, high general prevalence of HTN when defined as BP >140/80 mmHg and thus not factoring in the often more severe HTN observed). Both studies found HTN to be a significant presenting symptom on univariate analysis with 80.7% and 94.5% of symptomatic PPGL patients having HTN respectively[202,203]. We cannot compare our data to this as we used a hypertensive control group, and did not measure BP at the time of interview. The reason for the choice of a hypertensive control group in this study was that many of symptoms/signs experienced by patients with PPGL are thought to be due to hypertension, secondary to catecholamine excess and we wished to try and establish whether there were any symptoms or combination of symptoms that could discriminate patients with PPGL, that were beyond those caused by hypertension alone.

3.5   General conclusions and future work

In conclusion we have shown that pre-operative medical therapy with alpha +/- beta blockade has additional benefits beyond those of improving haemodynamic parameters. We suggest that the use of home blood pressure monitoring is a useful tool in the outpatient management of PPGL patients. Its use allows personalised titration of medications, allowing physiological adaptation to occur more slowly, minimising side effects and thus improving compliance. The longer duration of treatment with alpha-blockade, rather than dose *per se*, appears to be an important factor in reducing intra-operative HDI and frequency of post-operative hypotension. In addition, we have highlighted that medical therapy with alpha +/- beta blockade is potentially able to reverse both the inflammatory and catabolic

effects of catecholamine excess. Seven to fourteen days is unlikely to be a long enough duration for these anabolic effects to occur. These data would therefore support the notion that patients with PPGL would benefit from a longer duration of medical therapy with alpha +/- beta-blockade (the shortest duration any of our patients were treated was six weeks) before undergoing their surgical cure, and this could be achieved with the use of HBPM.

3.5.1 Limitations

As with all studies involving rare conditions there are several limitations to this work, mainly the small sample number included. Nonetheless, despite the small number of patients included in the prospective study, statistical significance was reached for some elements. To strengthen the statistical significance, ideally, we would have had double the number of controls than patients. Unfortunately, due to the pandemic situation, time for data collection was limited. To minimise the effect of this limitation, I opted to use a matched hypertensive control group, to allow a direct comparison of bioimpedance and inflammatory parameters. Patients were matched on age, gender and diabetes status. Ideally we would have also matched patients on weight, but due to the nature of the disease studied this was not possible as PPGL patients are generally in a catabolic state, as shown by our data and others[203]. By contrast the majority of patients referred to a tertiary hypertensive clinic have obesity as a contributory factor. Ideally urine sodium content would have been assessed using 24-hour urine collection instead of a morning spot urine collection for a more accurate assessment.

As we used hypertensive patients as our control group, we do not truly have normative comparison data from healthy controls. Therefore, our data demonstrates for example that PPGL patients are salt and water deplete, but this is in comparison to a control group with an abnormal physiological condition of salt and water retention. A hypertensive control group was chosen to allow for comparison in parameters, which took into account a change in BP. Ideally we would have also had a second control group of 'healthy' volunteers; although this would have obviously not matched for BP. Healthy volunteers could have been used to compare baseline bioimpedance and inflammatory baseline markers to provide normative data; but it would not have been useful to use a healthy control group to look at changes to these parameters over time. The hypertensive control group underwent ABPM at baseline, but did not have a repeated measure at follow up, thus limiting the direct comparison of ABPM measurements; however, both cohorts utilised HBPM. Despite these limitations, we believe our data are valid as in addition to the comparison with the control group, both cohorts provided their own internal controls as parameters were compared at two time points. Unfortunately,

post-operative data was only available for 60% of the PPGL cohort as data collection was limited due to COVID restrictions.

Assessing intra-operative HDI as a marker as to the efficacy of alpha-blockade is somewhat problematic as it will be affected by the reactive measures of the surgeon and anaesthetist. We attempted to control for this by selecting cohorts of patients that were operated on by the same surgeon and anaesthetist, as well as recording norepinephrine and metaraminol usage. In addition assessing post-operative complications is difficult, as due to the nature of the condition studied all the patients were electively admitted to HDU post-operatively, and thus immediate post-operative care was undertaken by teams outside of our department.

The only way of truly demonstrating the necessity of pre-operative medical preparation with alpha-blockade would be to perform a prospective randomised blinded study of patients that received pre-operative alpha-blockade and those that did not. However, this has never been undertaken as not only would it be logistically difficult to undertake, but there are also ethical implications regarding the safety aspects of the patients not receiving treatment. As this has not been undertaken, there is no set way of assessing the efficacy of alpha-blockade, and different studies have attempted this in different ways[131,135,137]. Therefore to allow comparison with published data we analysed our data using several different definitions.

Many of the limitations of the symptom questionnaire are discussed above. Ideally this type of study would be prospective to eliminate recall bias. In addition measurements of BMI, BP and HRs should be recorded using home, rather than clinic measurements, to reflect true average BP and HR as well as identifying measurements at the time of paroxysms, if they occur. A comparative cohort is important, but the choice of type of control group is problematic and different studies have approached this in different ways. In our current study we used patients referred to a tertiary hypertensive clinic, but the majority of these patients had long standing hypertension and were already taking a number of medications. Ideally the control group would also be prospectively recruited at diagnosis of hypertension before the initiation of medication. Due to the low prevalence of PPGL and the high prevalence of hypertension in the general population the ratio of patients with PPGL to control group needs to be increased considerably, aiming for 1:10 or higher. Also using the study design we employed with use of a regression model analysis, external validation would be required using a separate dataset before it could be piloted in the community. Unfortunately, we did not have the time or resources to acquire a second dataset to externally validate these data and our sample was too small to split the data into statistical valid training and testing datasets. Finally, it must not be forgotten that not all patients with PPGL are hypertensive, and in fact some studies have

reported that hypertension is not a useful positive predictive symptom[202]. These may be biased, however, by the high prevalence of hypertension and studies not differentiating between 'mild' hypertension and 'severe' levels of hypertension or paroxysmal hypertension, and therefore both the level of hypertension and whether it is sustained, paroxysmal and/or postural should be taken into account.

3.5.2 Future work

Further work is required to explore these areas in more detail. We have proposed adopting stricter BP targets and by applying these to larger cohorts, it may be possible to work out more specific cut-off BP figures that predict intra-operative HDI. In an ideal setting it would be possible to predict those at risk of HDI much earlier. Use of HBPM may be able to aid in this, and thus allowing intervention to prevent HDI from occurring. If patients could be confidently risk stratified, pre-operative hospital admission could be reduced, with the subsequent financial health benefits, in addition to the benefits to patients of minimising the duration they are required to be in hospital.

Our data implies that patients with PPGL *in situ* can develop systemic inflammation. We have discussed some preliminary results suggesting that some of this may be due to direct effects of catecholamine excess and that medical therapy with alpha-blockade can reverse these changes. However, many of the mechanisms underlying these are still speculative, nor is it clear if these benefits are dose dependant. An avenue of future work would be to investigate the mechanism underpinning the improvements seen in diabetes status, muscle and fat metabolism and the inflammatory markers, and if higher doses tolerated and/or longer duration of treatment resulted in further improvements. In addition alternative methods for analysing body composition should be used which could include for example, using thickness of subcutaneous fat in triceps and thigh circumference, as well as measurements of insulin. To aid in investigating underlying mechanisms subsequent bioimpedance data at intervals post-operatively would be interesting to analyse, as in our cohort at the point of post-operative analysis PPGL had not reached baseline parameters of controls. Additionally specific durations of pre-operative medical therapy need to be investigated further to identify exactly what is the optimal duration of treatment for which these benefits are attained. The patients in the presented cohort were treated for 6-22 weeks, but the minimum duration of treatment may be less than this.

Systemic inflammation, especially if long standing, could potentially make patients more vulnerable to infection during and following surgery, and likely slower to heal. Future work could investigate this further to see if these preliminary results hold true for a larger cohort and if improvements in inflammation pre-operatively reduce rates of post-operative infections and wound healing times.

The development and use of the PPGL alert card was popular with patients and the idea was adopted by the AMEND society, but its use needs to be audited before widespread implementation.

Chapter 4. Succinate Dehydrogenase disease and surveillance

4.1 Background

4.1.1 Surveillance screening in patients with known *SDH* germline mutations

With more widespread access to genetic testing, an increasing number of apparently sporadic PPGLs are now being identified as familial (current estimates suggest 40-50%[24,205]). Cascade genetic screening of relatives is, in turn, leading to the identification of increasing numbers of gene mutation carriers, the vast majority of whom are asymptomatic. These genetic advances open up the potential for direct clinical benefit in as many as half of people are destined to develop PPGL disease. To realise this benefit, it will be necessary to formulate screening protocols that identify PPGLs at an early stage, prior to the development of symptoms and/or metastatic spread. When this work was undertaken there was no consensus on screening or the follow-up of asymptomatic *SDH* mutation carriers and each country and institution approached this in their own way. Important barriers to the development of consensus guidelines for screening include uncertainties, for each subunit, regarding the site, rate of growth and potential for metastasis of PPGL; and (particularly for *SDHB*) a growing realisation, as more asymptomatic carriers are identified, that previous prevalence estimates were erroneously high. Together with the resource/health economic considerations that arise from intensive radiological screening protocols for increasing numbers of often asymptomatic individuals, these issues have led to markedly different strategies being employed between centres, both nationally and internationally. Recently a new international consensus statement[229] has been published towards which this work contributed.

Recent guidelines[12] combine evidence and expert opinion to guide the appropriate course of management in the ongoing care and monitoring for recurrence or metastatic disease of patients with PPGL disease. Workable algorithms have been produced based on presenting phenotype to identify the most likely underlying causative gene in the index case. However, the appropriate modality and frequency of imaging for the gene carriers identified via cascade screening remains paradoxically, more difficult.

Once an *SDH* mutation carrier has been identified, it is universally accepted that inclusion in a screening protocol is appropriate and that such a protocol should include a comprehensive clinical evaluation with biochemical testing for abnormal catecholamine production (plasma and/or urine metanephrines). However, a significant proportion of *SDH*-associated PPGLs remain clinically and

biochemically silent for a prolonged period due to lower tumoural production of catecholamines[23,206,207], and the majority of parasympathetic PGLs never produce excess quantities of catecholamines[208]. In recent years there has been increasing evidence that size of tumour correlates with malignant potential[206,209,210]. It seems clear, therefore, that imaging must play the central role in screening asymptomatic *SDH* gene carriers, to identify tumours at early, smaller stages.

A number of studies and guidelines have suggested potential surveillance protocols for managing *SDH* gene mutation carriers[12,13,18,31,53,58,59,64,65,69,79,92,211-219]. Most of these, however, do not differentiate between the follow-up of asymptomatic carriers and those that have (or have previously had) tumours. Very few suggest 'tailor made' surveillance imaging protocols based on specific *SDH* subunit gene mutations. *SDHB*-associated RCCs are now recognised as a unique subtype of RCC[68,72-74], with clear cell pathological features and are reported to behave differently from other forms of RCC[30,66,71]. It stands to reason therefore that different surveillance regimens may be warranted for disease caused by different mutations of the *SDH* genes.

4.1.2 Uses of SDHB immunohistochemistry (IHC)

With the current knowledge on the percentage of patients with PPGLs having an underlying genetic germline mutation, genetic testing is now recommended in all at risk patients[12]. Not every patient that presents with a PPGL, however, meets the criteria for genetic testing in the UK and genetic testing also has financial implications to the healthcare system. Protein expression of SDHB in tumour tissue has been shown to be an accurate and reliable marker for identifying patients harbouring underlying germline *SDH* mutations regardless of the *SDH* subunit affected. It has been validated in multiple studies investigating retrospective cohorts of PPGL tissue from patients known to harbour an *SDH* mutation[114,220-222], with reported sensitivity and specificity of 100% and 84% respectively[222] and good inter-observer reliability[114]. An absence of SDHB staining in tumour cells corresponds to a likely underlying *SDH* mutation, as a mutation in any one of the *SDH* genes, causes absence or destabilisation of the SDH proteins[114,222]. False negative results have been reported in some VHL-related PCCs and one NF1-related PGL, therefore reducing specificity[114,223]. PPGLs due to underlying *SDH* mutations, all show loss of SDHB protein expression, but PPGLs due to mutations in *SDHB, D,* and *C* genes show normal SDHA immunoreactivity, whereas PPGLs due to an *SDHA* mutation show loss of SDHA protein expression in addition to SDHB[114]. Abnormal SDHB protein expression is also reported in *SDHD*-related PPGLs, although often as a decreased diffuse cytoplasmic expression rather than complete absence[224,225]. The reliability of absence of SDHB staining for *SDHD* germline mutations appears less reliable than for the other subunits[114,221]. SDHB immunohistochemistry has now been widely adopted

in most centres for prospective analysis of PPGL tissue to identify those at risk of carrying underlying germline *SDH* mutations.

4.1.3 Pathogenicity of different mutations

At the discovery of a new gene mutation it is not known whether the specific variant is truly causative of disease or a coincidental occurrence. It is clinically important to establish whether each specific variant is pathogenic as this has implications not only to the patient and their family, but to the geneticist and clinician to decide on when cascade genetic testing is appropriate and subsequent surveillance screening of asymptomatic carriers of these mutations. It is difficult to prove definitely whether any specific variant is pathogenic and therefore guidelines recommend that this decision must be based on an accumulation of evidence, combining the clinical picture and laboratory techniques as to the function of the mutation and the damage it may cause to the resulting protein structure[102]. In a 2015 review, there were 445 different germline *SDH* mutations reported and 403 of these have been described in patients with PPGL[226]. Of these 35% were missense mutations, 26% splice site, 15% nonsense, 13% large deletions and 11% frameshifts. As with any new genes, until there are clinical cases with proven causal links to specific gene mutations, VUSs will exist. Bioinformatic tools exist (e.g. SIFT, Polyphen and Mutation Assessor) to predict *in silico* the functional impacts of different mutations. There are also several databases (e.g. ClinVar, Varsome[227]) that connect reported variants with clinical associated phenotypes. Matching SDHB/A IHC data and *in silico* analysis were available for 145 of these reported mutations and 92% were consistent[226]. The nature of the second hit was reported for 85 of these mutations and 73% had inactivation of the wild type allele by LoH. In 9% there was retention of heterozygosity and in 14% of cases the second hit was a separate somatic mutation. This demonstrates that LoH is the predominant mechanism of inactivation in these tumour suppressor genes[226]. According to the Leiden Open Variation Database (LOVD) there are now 876 unique public DNA variants reported across all the *SDH* subunits[52]. As *SDHB* and *SDHD* mutation carriers are more common more of these specific mutations have been investigated. For *SDHA, SDHC* and *SDHAF2* the causal links of VUS are less well known[99,228].

4.1.4   Gaps in current knowledge to be addressed in this chapter

I.   The clinical implications of our new detailed knowledge on the genotype-phenotype correlations of the different *SDH* subunits has not been fully studied. There is very little research on how these correlations can be translated directly to benefit patients. There is no universal consensus on the most appropriate surveillance regimen for asymptomatic non-proband carriers of these mutations.

II.   The usefulness of SDHB IHC in clinical practice for identifying historical cases at risk of underlying *SDH* mutations.

III.   The pathogenicity of certain mutations currently recorded as VUS.

4.2   Aims

I.   **Surveillance protocols in *SDH* carriers**

To analyse the published literature and our large cohort of individuals carrying *SDH* mutations to propose individualised screening strategies for each *SDH* subunit.

Question: What is the optimal surveillance strategy for *SDH* mutation carriers, and should this differ depending on the subunit in which the mutation occurs?

II.   **Historical PPGL patients**

To use SDHB immunohistochemistry to investigate historical PPGL tumour tissue samples to identify patients at risk of carrying underlying *SDH* mutations.

Question: Can SDHB immunohistochemistry be used retrospectively on historical PPGL tumour samples to identify patients and their relatives at risk of carrying germline *SDH* mutations?

III.   **Pathogenicity of mutation variants**

To investigate whether various reported variants of unknown significance in our cohort are pathogenic.

4.3   Results

4.3.1   Surveillance protocols in *SDH* carriers

Aim: To analyse the published literature and our large cohort of individuals carrying *SDH* mutations to propose individualised screening strategies for each *SDH* subunit.

The majority of individuals now identified as carriers of gene mutations in one of the *SDH* subunits are asymptomatic. Therefore, there is much controversy over the best way to manage these individuals, without disease or symptoms, and who may never be affected by disease. Therefore, there must be a carefully sought balance between recognition of disease early, so it can be promptly treated, if it does occur, but not negatively impacting these individuals lives too much by laborious investigations. Given that we know that disease characteristics differ between different *SDH* subunits, this then raises the question; what is the ideal surveillance strategy for *SDH* mutation carriers, is a 'one size fits all' approach really in the best interests of the patients or should surveillance strategies differ depending on the subunit in which the mutation occurs?

When this work was undertaken there was no consensus on screening or the follow-up of asymptomatic *SDH* mutation carriers and each country and institution approached this in their own way. Since then a new international consensus statement[229] has been published to which this work contributed.

To begin to address these questions I first analysed the clinical outcomes of the large cohort of patients carrying *SDH* mutations at our institution, and then collected and analysed data of all the published cohorts readily available.

Clinical data of all the patients treated for PPGL at our institution was gathered and a summary of the characteristics of this cohort is presented in Table 4.1 and Figure 4.1.

Total no. of patients [n (%)]	302
Male	145 (48%)
Female	157 (52%)
Mean age at diagnosis [years (range)]	45 (10-80)
Deceased	36 (11.6%)
Hypertensive at diagnosis	163 (54%)
Single PPGL	229 (76%)
Multiple PPGLs	70 (23%)
Metastatic	34 (11.4%)
Secretory	145 (48%)
Resected	254 (84%)

Table 4.1: Summary of the cohort of patients diagnosed with PPGL and managed at St. Bartholomew's Hospital. *This includes all patients diagnosed with PPGL, it does not include any individuals with known gene mutations that do not have disease.*
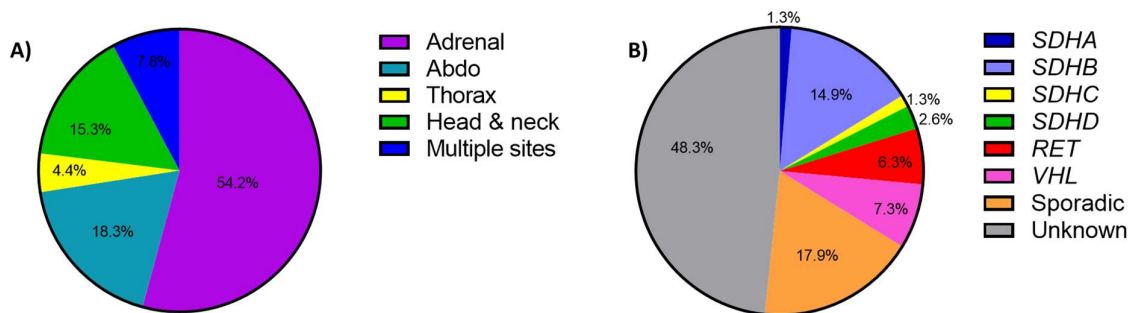
Figure 4.1: Characteristics of the PPGL cohort. *The graphs show the distribution of sites at which PPGLs occurred in this cohort of patients and the genetic status of these patients. A: Pie chart showing the different sites of PPGL development in this cohort. B: Pie chart showing the spectrum of genetic diagnosis of the cohort of patients with PPGL.*

4.3.1.2 SDH cohorts

SDHB cohort

The cohort of patients with *SDHB* mutations diagnosed and managed at St. Bartholomew's Hospital up until August 2016 (Appendix 3) consisted of 92 patients from 36 kindreds, consisting of both index patients (that presented with tumours) and asymptomatic carriers (identified through cascade genetic testing). The details of the kindreds are summarised in Appendix 3. They had 22 different mutations spanning exons 1-7 of the *SDHB* gene (Table 4.3). There were 23 paediatric patients. Five of these 23 children, aged 1-11 years, were awaiting their first imaging at the time of analysis and therefore are excluded from the results below. All have now undergone at least two rounds of surveillance imaging and no tumours have been identified.

	Total	Adults	Children
No. of patients	87	69	18
Male	42	34	8
Female	45	35	10
Index patients	27	21	6
Patients in surveillance screening	60	48	12
No. of Patients with tumours	42	35	7
- Index patients	27 (100%)	21	6
- Surveillance patients	15 (25%)	14	1
Total No. of *SDHB*-related tumours	67	47	20
- Index	52	33	19
- Surveillance	15	14	1
Deceased	7		

Table 4.2: Summary table of the cohort of patients with SDHB germline mutations. This table presents the data in two ways: the number of patients with tumours (row 6) and the total numbers of tumours (row 7). Some patients have developed multiple tumours. These data are also separated out to show tumour occurrence in adults and children. The percentages, in brackets, demonstrate the number of patients from that subgroup that developed tumours (e.g. 100% of index patients and 25% of surveillance patients).

Table 4.3 shows the 22 different mutations and the number of associated tumours.

Type of *SDHB* mutation (22)	No. of families (36)	No. of patients per mutation within cohort (92)	No. of index cases per mutation (27)	No. of patients with PGL tumour (38)	No. of patients with other tumours (7)	Total No. of *SDHB-related* tumours (67)	No. of PGL (62)	No. other tumours (10)	No. of patients with malignant PGL (11)	Youngest age at diagnosis (years)	*Notes*
Splice Exon 1	3	11	1	1	0	1	1	0	0	15	*Index patients for two families diagnosed and treated elsewhere*
Missense Exon 6	1	2	1	1	0	1	1	0	0	15	
Frame shift Exon 4	1	5	2	2	0	2	2	0	0	12	*2 index cases within same family presenting separately before genetic diagnosis known*
Frameshift Exon 4	1	8	1	2	0	2	2	0	1	29	
Nonsense Exon2	2	9	1	3	1	4	3	1 (GIST)	1	18	*Index patient for two families diagnosed and treated elsewhere*
Deletion whole Exon 1	4	13	3	4	1	9	8	1 (RCC)	0	25	*Index patient for one family diagnosed and treated elsewhere*
Nonsense Exon 2	1	3	1	1	1	4	2	4 (2 RCC/ 1TCC/ PTC)	1	10	
Missense Exon 2	3	5	1	2	1	12	12	1 (TCC)	1	10	*Index patient for one family diagnosed and treated elsewhere*
Missense Exon 2	3	10	3	4	1	6	5	1 (RCC)	1	28	
Missense Exon 4	1	4	1	3	0	5	5	0	2	19	

Type of *SDHB* mutation (22)	No. of families (36)	No. of patients per mutation within cohort (92)	No. of index cases per mutation (27)	No. of patients with PGL tumour (38)	No. of patients with other tumours (7)	Total No. of *SDHB-related* tumours (67)	No. of PGL (62)	No. other tumours (10)	No. of patients with malignant PGL (11)	Youngest age at diagnosis (years)	*Notes*
Missense Exon 6	2	3	1	3	0	4	4	0	1	24	*Index patient for one family diagnosed and treated elsewhere*
Frame shift Exon 7	1	2	1	1	1	1	1	(RCC before genetic diagnosis)	0	42	*One patient presented with RCC 7 years before genetic diagnosis was known & therefore not included*
Missense Exon 4	1	2	1	1	0	2	2	0	1	47	
Missense Exon 6	1	1	0	0	0	0	0	0	0		*Index patient for family diagnosed and treated elsewhere*
Missense Exon 4	2	2	1	1	0	1	1	0	1	44	*Index patient for one family diagnosed and treated elsewhere*
Splice Intron 4	2	2	2	2	0	2	2	0	0	32	*unrelated 2 separate index cases*
Nonsense Exon 2	1	1	1	1	0	1	1	0	1	33	
Missense Exon 5	1	1	1	1	0	4	4	0	0	40	
Nonsense Exon 3	2	3	2	2	1	3	3	1 (PTC)	0	43	
Splice Intron 6	1	1	1	1	0	1	1	0	0	27	

Type of *SDHB* mutation (22)	No. of families (36)	No. of patients per mutation within cohort (92)	No. of index cases per mutation (27)	No. of patients with PGL tumour (38)	No. of patients with other tumours (7)	Total No. of *SDHB-related* tumours (67)	No. of PGL (62)	No. other tumours (10)	No. of patients with malignant PGL (11)	Youngest age at diagnosis (years)	*Notes*
Splice exon 4	1	3	1	1	0	1	1	0	0	34	
Deletion of entire *SDHB* gene	1	1	0	1	0	1	1	0	0	54	

Table 4.3: Genotypes within the SDHB cohort and associated disease. *Prevalence of the different types of tumours is shown for each mutation. Columns 3 and 4 show the total number of patients and number of index patients within the cohort for each genetic mutation. Columns 5 and 6 show the total number of patients with PGL tumours and other types of tumours (e.g. RCC, GIST, PTC, TCC). Columns 7-9 show the total number of tumours. Column 10 shows the number of patients with malignant PGL disease for each genotype. The sum total of each column is shown in brackets beneath the heading. PGL Paraganglioma; RCC renal cell carcinoma; GIST Gastrointestinal stromal tumour; PTC Papillary thyroid carcinoma; TCC Transitional cell carcinoma of the bladder*

The majority of the index patients presented with a sympathetic PGL. Nine index patients had multiple tumours and nine developed metastatic disease. Twenty-five percent of the surveillance patients had a tumour identified on screening (Table 4.4).

	Index Patients = 27	Surveillance Patients = 60	Total = 87
No. of patients identified with all tumours [n (%)]	27 (100%)	15 (25%)	42 (48.2%)
No. of *SDHB -related* tumours	52	15	67
No. of patients with PGL [n (%)]	27 (100%)	11 (18.3%)	38 (43.7%)
No. of PGLs [n (%)]	**51**	**11**	**62**
- Head and Neck PGL	10 (19.6%)	1 (9%)	11(17.7%)
- Thoracic PGL	6 (11.7%)	3 (27%)	9 (14.5%)
- Abdominal PGL	21 (41.2%)	6 (54.5%)	27 (43.5)
- Phaeochromocytoma	8 (15.7%)	0	8 (12.9%)
- Pelvic PGL	3 (5.9%)	0	3 (4.8%)
- Bladder PGL	3 (5.9%)	1 (9%)	4 (6.4%)
RCC	1	3	4
GIST	0	1	1
Patients with multiple tumours	4 at diagnosis 5 subsequently	0	9
Patients with malignant disease+	9 (2 at diagnosis)	2 (1 at diagnosis)	11
Other tumours identified in cohort (not counted above)	1 PTC	1 PTC (micro) 1 TCC 1 Prostate	4

Table 4.4: Summary of the different types of tumours identified in both the index and surveillance patients. This table shows the total number of patients that developed tumours and the total number of different types of tumours that occurred in each patient subgroup, subdivided into PGL tumours and other SDHB-related tumours. Other tumours that were identified in patients are also shown. The number of patients that developed multiple tumours and malignant disease is also shown. + Malignant disease defined as an aggressive tumour with local invasion into surrounding structures or metastasis with widespread dissemination or occurrence at a site where neural crest cells are not usually found. SDHB succinate dehydrogenase subunit B mutation; PGL paraganglioma; RCC renal cell carcinoma; GIST gastrointestinal stromal tumour; PTC papillary thyroid carcinoma; TCC transitional cell carcinoma of the bladder; mets disseminated metastatic disease

Index patients

There were 27 index patients (21 adults, 6 children) presenting between 1975 and 2015. All had symptoms of catecholamine excess or mass effect and these 27 patients have had a total of 52 tumours (43 PGLs, 8 PCCs, 1 RCC). Median age at diagnosis was 33 years (range 10-68 years), with a linear spread across this age range. Obviously, some index cases predate the introduction of this surveillance screening protocol and therefore there was variable routine follow-up for some of these earlier patients until the mutation was identified.

The 21 adult index patients (13 men, 8 women) had a total of 34 PGLs identified and one papillary thyroid carcinoma. Of these, four presented with multiple tumours at diagnosis and a further three developed multiple tumours subsequently. The 34 PGLs consisted of nine abdominal PGLs and six PCCs, nine head and neck PGLs (HNPGL), five thoracic, three bladder and two pelvic PGLs. Four patients are deceased (three related to their metastatic disease, including a suicide due to the uncertainty associated with their diagnosis, and one following a haemorrhagic stroke).

Six index patients were diagnosed in childhood (two boys, four girls). They were diagnosed between 1982 and 2011 and aged between 10-15 years. All had single tumours at presentation, with no evidence of metastatic disease. Three had abdominal PGLs, one a PCC, one a thoracic PGL and one a pelvic PGL. Two of these children went on to develop multiple tumours (including 11 further PGLs and one papillary RCC) and subsequent disseminated metastatic disease in adulthood, both have subsequently died of their disease. The time from diagnosis to development of further disease was 13.0 and 16.5 years. The remaining four children have had no further disease to date; with duration of follow-up between 2-19 years.

Twenty-five of the 27 index patients underwent surgical resection. The two patients who did not have a successful primary surgical resection developed metastatic disease three and six years later.

Appendix 4 shows a breakdown of the 13 index cases that developed multiple tumours and/or had malignant disease. Nine of these patients had malignant PGLs (two at diagnosis). If defined as non-malignant at diagnosis the time to development of metastases was 3-25 years (mean 9 years). Fourteen of the 27 index patients had single non-malignant PGLs and have had no further tumours identified on subsequent surveillance imaging. These 14 patients have a mean duration of follow-up since original diagnosis of 10.5 years (range 5-27 years). Five patients went on to develop metachronous PGL tumours (including three that subsequently also developed metastatic disease). The mean time to the development of a second primary was 7.2 years (range 0.6-17 years). One patient had multifocal papillary thyroid carcinoma identified on his first post-operative scan.

The mean ongoing follow-up for the index patients is 8 years (2-20 years).

Surveillance patients

A total of 65 patients were identified through genetic testing: 48 adults and 17 children. Five of these children were awaiting their first surveillance imaging at the time of analysis; therefore 60 patients had completed at least one round of surveillance. Forty-three patients (71.6%) have not had any tumours identified on surveillance to date.

Fifteen patients (25% of screened carriers) have had a total of 15 new *SDHB*-related tumours identified through the surveillance programme including eleven PGLs, three RCC and one GIST. Table 4.5 summarises the details of the 15 asymptomatic patients that had tumours identified by surveillance imaging. Of the eleven PGLs, six were abdominal, three were thoracic, with one bladder and one HNPGL. In addition to these eleven PGLs, four lesions have been identified as probable PGLs with characteristic findings on radiology. These are all <1 cm and therefore are currently under surveillance. These four patients are all asymptomatic with negative metanephrines. For clarity these four lesions have not been included in the statistical analyses.

The cumulative total years of surveillance across this cohort of 60 asymptomatic *SDHB* mutation carriers was 328 years; during which 15 new *SDHB*-related tumours were identified.

Ten of these 15 tumours were identified on the first surveillance imaging (five abdominal and three thoracic PGLs, one HNPGL and one GIST). Only two of these 15 patients had raised metanephrine levels. One of the 15 patients developed metastatic disease and subsequently died; this occurred 18 months after the initial diagnosis of a 6.5 cm abdominal PGL on first surveillance scan, with negative biochemistry. Five tumours were identified after a negative first screen on subsequent surveillance scans 2-6 years later and all these patients had negative urine and plasma metanephrines. These included one abdominal PGL (4 years), one bladder PGL (6 years) and three RCCs (2, 2 & 4 years) (Table 4.5). Median age at diagnosis of these 15 patients was 35 years (range 16-83 years).

Additionally, one aggressive transitional cell bladder carcinoma (TCC), which has subsequently metastasised, one micropapillary thyroid carcinoma and one prostate carcinoma (he had previously been treated for TCC) were identified during surveillance. A further patient had treatment for RCC seven years before his *SDHB* mutation was identified.

The most common incidental findings were nodular thyroid and adrenal disease, renal and liver cysts, lung nodules and lymphadenopathy.

The mean follow-up for the surveillance group was 5.7 years (0-14 years).

Our cohort had an overall penetrance of 43.7% for the development of PPGL tumours (38 patients with PGLs). When the index patients are removed the penetrance falls to 18.3% risk of developing a PPGL (11 of 60 patients).

Patient No.	SDHB Mutation	Age at diagnosis (years) + gender	Family History	Diagnosis	Tumour size (mm)	First scan	No. of years into surveillance imaging	Scan no. of specific area where tumour identified	Plasma / urine metanephrines	Malignant disease	Other lesions	Outcome	Years of subsequent disease free follow-up
28	Nonsense exon 2	26 M	Brother of index. 4 family members with tumours within kindred	Abdo PGL	65	Positive	0	1	Negative			Primary tumour surgical resection	
				metastasis			1.5			Y		Deceased from metastatic disease	
31	Nonsense exon 2	40 F	Sister of index. 4 family members with tumours within kindred	Thoracic PGL	51	Negative	4	1	Negative			Surgical resection	8
50	Nonsense exon 2	35 M	Sister of index. 2 family members with tumours within kindred	RCC	25	Negative	4	3	Negative		TCC bladder	Developed metastatic disease from TCC RCC resected	5
45	Deletion whole exon 1	19 M	Son of index. 2 family members with tumours within kindred	Abdo PGL	14	Negative	4	2	Negative			Awaiting surgical date	
60	Missense exon 2	24 M	Son of index. 3 family members with tumours within kindred	Thoracic PGL	11.7	Positive	0	1	Negative			Surgical resection	7
61	Missense exon 3	76 M	Father of index. 3 family members with tumours within kindred	RCC	28	Negative	2	2	Negative		Prostate ca	Under surveillance - clinical decision based on age and size of tumour	4

Patient No.	*SDHB* Mutation	Age at diagnosis (years) + gender	Family History	Diagnosis	Tumour size (mm)	First scan	No. of years into surveillance imaging	Scan no. of specific area where tumour identified	Plasma / urine metanephrines	Malignant disease	Other lesions	Outcome	Years of subsequent disease free follow-up
68	Missense exon 4	83 M	Father of index. 3 family members with tumours within kindred	Abdo PGL	60	Positive	0	1	Positive			Under surveillance. Not operated on due to patient age, co-morbidities and difficulty of operation. Patient asymptomatic	9
71	Missense exon 6	46 M	Brother of index (not in this cohort). 3 known family members with tumours in this kindred	Abdo PGL	35	Positive	0	1	Negative			Surgical resection	8
72	Missense exon 6	80 F	Mother of index (not in this cohort). 3 known family members with tumours in this kindred	Thoracic PGL	38	Positive	0	1	Negative			MIBG treatment. Patient choice over surgical resection	9
21	Frameshift exon 4	30 M	Son of index. 2 family members with tumours within kindred	Bladder PGL	5	Negative	6	6	Negative			Surgical resection	4
39	Deletion whole exon 1	62 F	Aunt of index. 2 family members with tumours within kindred	RCC	12	Negative	2	2	Negative			Under surveillance	2
56	Missense exon 2	18 F	Daughter of index (not in this cohort). 2 family members with tumours within kindred	Abdo PGL	11	Positive	0	1	Negative			Awaiting surgery	

Patient No.	*SDHB* Mutation	Age at diagnosis (years) + gender	Family History	Diagnosis	Tumour size (mm)	First scan	No. of years into surveillance imaging	Scan no. of specific area where tumour identified	Plasma / urine metanephrines	Malignant disease	Other lesions	Outcome	Years of subsequent disease free follow-up
69	Missense exon 4	16 M	Son of index. 3 family members with tumours within kindred	Abdo PGL	65	Positive	0	1	Positive	Y		Surgical resection	6
92	Deletion of entire SDHB gene	54 M	Son has PCC (not in this cohort)	HNPGL	27		1	1	Negative			Awaiting surgical resection/radiotherapy	
35	Nonsense exon 2	28 M	2 family members with PGL (not in this cohort)	GIST	45		1	1	Negative			Surgical resection	

Table 4.5: Tumours identified in surveillance screening of patients with SDHB mutations. *This table describes the demographic details, genotype, tumour details, biochemistry and outcomes for the patients that had tumours identified by surveillance imaging. PGL paraganglioma, Abdo PGL abdominal paraganglioma, PCC phaeochromocytoma, GIST gastrointestinal stromal tumours, RCC renal cell carcinoma, TCC transitional cell carcinoma of bladder, HNPGL head & neck paraganglioma*

SDHA cohort

The cohort consisted of six index cases and five asymptomatic carriers. The six index cases were originally diagnosed between 1973 and 2011 and had histologically proven PPGL, who subsequently underwent genetic testing during the course of their follow-up and were confirmed to have an underlying *SDHA* germline mutation. I performed a retrospective analysis of their notes and describe their clinical outcomes. From these six index cases, cascade genetic testing occurred and identified a further five asymptomatic carriers of *SDHA* mutations. All patients are now being followed-up in specialised endocrine clinics and are undergoing annual screening, including annual clinical and biochemical assessment and cross-sectional imaging, although the frequency and modality of imaging differs between centres.

Appendix 5 provides a detailed summary of the patients described.

The six index patients originally presented aged 18, 34, 36, 46, 47 and 68 years. Five patients presented with a single lesion at diagnosis: intra-thyroidal PGL, thoracic PGL, PCC and two abdominal PGLs. One patient (patient 3) presented with two synchronous lesions: she had a carotid body tumour producing excess 3MT and a thoracic PGL producing excess norepinephrine. All patients underwent surgical resection of the primary tumours. Two patients developed recurrence in the surgical bed and both patients went on to develop metastatic disease 16 and 37 years later (patients 8 and 9). One of these two patients (patient 8) also developed an additional five metachronous lesions 7-10 years after original diagnosis.

The five asymptomatic carriers identified through cascade screening have not had any tumours identified in surveillance imaging and all have negative biochemistry. They have had a total of 17 years surveillance. Additionally, patient 8 has one adult son who has been undergoing clinical and radiological screening with no tumours identified to date but has not yet undergone genetic testing. Patient 11 has three children and one sister (who has breast carcinoma) that are awaiting genetic testing but have no history of PPGL.

Table 4.6 combines the evidence that suggests pathogenicity for each of the described mutations. SDHA IHC was performed on tissue that was available.

Pt. No.	SDHA Mutation	Type	In silico analysis	Immunochemistry analysis	EXAC database population frequency	ACMG Classification[102] (analysed by Varsome database[227])	Published reports on pathogenicity
1	c.91C>T exon 2	Frameshift	ExPASy translate tool - premature stop codon resulting in a truncated protein	PGL tissue unavailable for analysis. Breast tissue immunopositive for SDHA and SDHB	0.2 per 1000 individuals (south Asian population). 0.3% of Dutch controls	Pathogenic	Korpershoek et al. 2011. JCEM 96(9):E14[230] Casey et al. 2017. Molecular Genetics & Genomic Medicine[231]
3	c.1338delA exon 10	Frameshift	ExPASy translate tool: premature stop codon resulting in a truncated protein	PGL immunonegative for SDHA	<1 per 1000 individuals 0.00001499	Pathogenic	Casey et al. 2017. Molecular Genetics & Genomic Medicine[231]
7	c.1753C>T exon 7	Missense	PolyPhen2 programme with a score of 1.000 (damaging) SIFT programme, with a score of 0.00 (deleterious)	PGL Immunonegative for SDHA Parathyroid tissue immunopositive for SDHA	<1 per 1000 individuals 0.0000248	Pathogenic	Korpershoek et al. 2011. JCEM 96(9):E14[230] Casey et al. 2017. Molecular Genetics & Genomic Medicine[231] Papathomas et al. 2015. Modern Pathology 28, 807-821[114]
8	c.923C>T exon 8	Missense	PolyPhen2 programme with a score of 1.000 (damaging) SIFT programme, with a score of 0.00 (deleterious)	PGL tissue unavailable for analysis Tissue specimen from bone biopsy immunopositive for SDHA and heterogenous SDHB immunochemistry. Not enough tissue available for LoH analysis	Not reported	Uncertain significance	Casey et al. 2017. Molecular Genetics & Genomic Medicine[231]

Pt. No.	*SDHA* Mutation	Type	*In silico* analysis	Immunochemistry analysis	EXAC database population frequency	ACMG Classification[102] (analysed by Varsome database[227])	Published reports on pathogenicity
9	c.91C>T exon 2	Frameshift	ExPASy translate tool - premature stop codon resulting in a truncated protein	PGL tissue unavailable for analysis	0.2 per 1000 individuals	Pathogenic	Korpershoek *et al.* 2011, JCEM 96(9):E14[230] Casey *et al.* 2017. Molecular Genetics & Genomic Medicine[232]
11	c.91 C>T exon 2	Frameshift	ExPASy translate tool - premature stop codon resulting in a truncated protein	PGL tissue unavailable for analysis	0.2 per 1000 individuals	Pathogenic	Korpershoek *et al* 2011, JCEM 96(9):E14[230] Casey *et al.* 2017. Molecular Genetics & Genomic Medicine[232]

Table 4.6: Investigations of pathogenicity for SDHA mutation variants. *In silico analyses were performed on each missense variant using programmes SIFT and PolyPhen2 in order to predict pathogenicity of the DNA variants. The variants were classified as probably damaging by PolyPhen2 programme with a score of 1.000 (scores 0.0-1.00, with the most damaging at 1.000), (sensitivity 0.00; specificity 1.00) and classified as deleterious by SIFT programme with a score of 0.00 (scores 0.0-1.0, with the most damaging at 0.0). Column five shows immunohistochemistry analysis of tissue (where available). Column six shows population frequency from the EXAC database and column seven showed the ACMG classification. References for where mutations have been previously published are shown in the last column.*

4.3.1.3 Synthesis of published cohorts

Surveillance strategies differ between individual centres and countries. The majority of the cohort of patients with *SDH* mutations at St. Bartholomew's Hospital carry *SDHB* mutations (described above) and therefore to address the question of whether surveillance should be individualised for each *SDH* subunit cohorts more data were required for the other subunits. I therefore proceeded to gather data from all the published cohorts containing patients with *SDH* mutations that are readily available. These results include our published cohorts of patients with *SDHB* and *SDHA* mutations[65,233] from St. Bartholomew's Hospital as outlined above.

SDHB cohorts

The combined cohorts on individuals carrying *SDHB* mutations provide data on 1341 asymptomatic *SDHB* carriers and demonstrate a tumour detection rate of 15.4% (207 asymptomatic carriers with PPGLs identified on screening), when index cases are excluded.

Where data are available in the literature[18,53,54,58,59,64,65,69,92,114,216,234-237] the breakdown of PPGLs that occur by specific tumour locations has been calculated. This combined cohort consists of 392 patients with 471 PPGLs (Table 4.7 & Figure 4.2).

	SDHB mutation carriers		
	No. of patients with tumour* [% (n)]	No. of tumours+ [% (n)]	Risk of malignancy by location$ [% (n)]
Total	349 patients	471 (in 392 patients)	344 total PPGLs, 95 developed malignancy
HNPGL	35.5% (124)	35.2% (166)	12% (11/92)
Thoracic PGL	8.3% (29)	7.0% (33)	17.2% (5/29)
PCC	15.1% (53)	12.3% (58)	34.1% (14/41)
Abdo PGL	34.7% (121)	40.6% (191)	32.9% (54/164)
Pelvic PGL	2.8% (10)	2.1% (10)	30% (3/10)
Bladder	3.4% (12)	2.8% (13)	87.5% (7/8)

*Table 4.7: Tumour site frequency in SDHB mutation carriers. Data are presented in two ways and applies to patients that have developed a PPGL tumour: the first column shows the percentage chance the PPGL occurring at any given site (based on 349 patients). The second column shows the breakdown of PPGL occurrence by each tumour location as a percentage of the total number of tumours (471 total PPGL tumours occurring in 392 patients). If a study did not specify the number of tumours in a given patient it was assumed there was a single tumour. If a patient had multiple tumours at different locations, these are counted separately. Due to availability of clinical data and the way it is presented for different studies, there are more patients included in the data showing the breakdown by the total number of tumours and this includes patients that had multiple tumours. Risk of malignancy is given as a percentage of the number of malignant PGL at each site of disease. Pelvic PGLs are divided into those that arise in the bladder and those that arise outside the bladder as, from the reported data, it is possible that the bladder PGLs have a particularly high malignancy rate which is worthy of note. PPGL phaeochromocytoma and paraganglioma tumours, PCC phaeochromocytoma, Abdo PGL abdominal paraganglioma, HNPGL head & neck paraganglioma. $Risk of malignancy given as % of total for that location (number of malignant PGL/total reported in that location). *Based on studies[53,54,58,59,62,64,65,69,82,92,234-237], +Based on studies[53,54,58,59,62,64,65,69,92,114,216,234-237]. $Based on studies [53,54,58,59,62,65,82,89,92,235,237].*
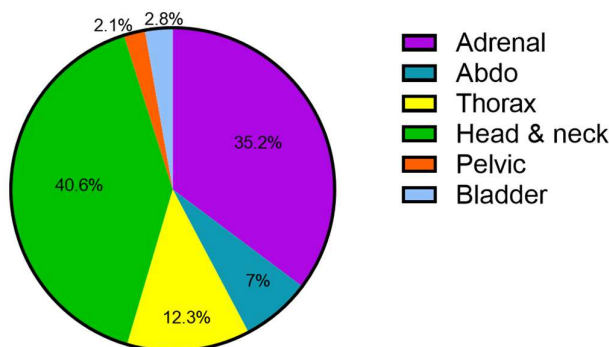
Figure 4.2: Tumour site frequency in SDHB mutation carriers. Pie chart representing all patients that develop a tumour and the percentage of PPGLs occurring at any given site (based on 349 patients).*

For a smaller cohort of combined studies[53,54,65,69,92,114,234,236,237] totalling 191 PPGLs, the median age at diagnosis for each site was calculated. This did not differ significantly for PPGLs occurring at adrenal, extra-adrenal abdominal, thorax, bladder or pelvic sites (median ages at diagnosis 32, 30.5, 33, 27, 29.5 years respectively), but median age of diagnosis was older for those with HNPGLs at 42.5 years (range 21-93 years).

Where detailed clinical information was available[53,54,59,62,65,69,92,235,237] malignancy risk by tumour location has been calculated (Table 4.7 & Figure 4.3). This included a total of 344 tumours, where 95 cases were associated with malignancy (27.6%).
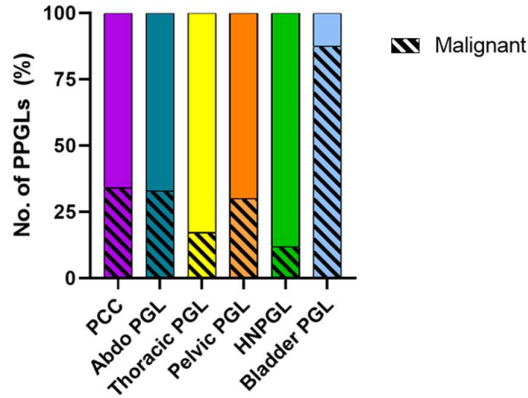
Figure 4.3: Risk of malignancy in SDHB mutation carriers of different PPGL based on site of occurrence. *The graph shows the risk of malignancy for each PPGL tumour location in SDHB mutation carriers, as a percentage of the total number PPGLs occurring at each site of disease. Total number of tumours is normalised to 100%. PCC (n=41), abdo PGL (n=164), thoracic PGL (n=29), pelvic PGL (n=10), HNPGL (n=92), bladder PGL (n=8). These figures are derived from a total of 95 malignant PPGLs (with a malignancy rate of 27.6%). We have divided pelvic PGL into those that arise in the bladder and those that arise outside the bladder as, from the reported data, it is possible that the bladder PGLs have a particularly high malignancy rate which is worthy of note. PCC phaeochromocytoma, Abdo PGL abdominal paraganglioma, HNPGL head & neck paraganglioma*

In summary, the tumour detection rate with surveillance screening was 15.4% in the asymptomatic carriers. The risks of developing a PPGL in the head or neck were just as high as in the abdomen in *SDHB* carriers. The risk of developing a PCC was only 15.1%, and risks of PPGL development at other sites were lower still (thoracic 8.3%, pelvis 2.8% and bladder 3.4%). The risk of malignant transformation was highest for PGLs occurring in the bladder, followed by abdominal and pelvic regions. Risk of malignant transformation was lowest in the head and neck.

The combined cohorts published in the literature on individuals carrying *SDHD* mutations provide data on 257 asymptomatic *SDHD* carriers and demonstrate a tumour detection rate of 52.9%. Table 4.8 & Figure 4.4 show the risk of tumour formation at different sites from the synthesised published cohorts [53,54,84,86,89,92,114,207,211,216,234,238-244].

	SDHD mutation carriers		
	No. of patients with tumour* [%/(n)]	No. of tumours+ [%/(n)]	Risk of malignancy by location$ [%/(n)]
Total	363 patients	787 in 535 patients	413 total PPGLs, 28 developed malignancy (6.7%)
HNPGL	83.1% (320)	65.4% (515)	7.5% (24/319)
Thoracic PGL	5.5% (21)	4.6% (36)	5.3% (1/19)
PCC	35.8% (138)	19.9% (157)	4.5% (2/45)
Abdo PGL	9.4% (36)	6% (47)	3.9% (1/26)
Pelvic PGL	0.3% (1)	0.5% (4)	0 (0/4)
Bladder	NR	NR	NR

Table 4.8: Tumour site frequency SDHD mutation carriers. *Data are presented in two ways and applies to patients that have developed a PPGL tumour: the first column shows the percentage chance the PPGL occurring at any given site (based on 363 patients). The second column shows the breakdown of PPGL occurrence by each tumour location as a percentage of the total number of tumours (787 PPGLs in 535 patients). If a study did not specify the number of tumours in a given patient there was assumed to be a single tumour. If a patient had multiple tumours at different locations, these are counted separately. Due to availability of clinical data and the way it is presented for different studies, there are more patients and tumours included in the data showing the breakdown by the total number of tumours and this includes patients that had multiple tumours. Risk of malignancy is given as a percentage of the number of malignant PGL at each site of disease. PPGL phaeochromocytoma and paraganglioma tumours, PCC phaeochromocytoma, Abdo PGL abdominal paraganglioma, HNPGL head & neck paraganglioma, NR not reported.* *[53,54,82,84,86,89,92,211,234,238-245], +[53,54,82,84,86,89,92,211,216,234,238-245], $[53,54,56,82,84,89,92,211,235,242-245]
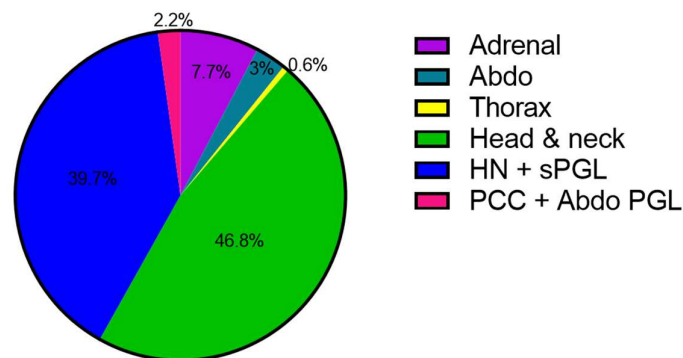
Figure 4.4: Tumour site frequency in SDHD mutation carriers. *Pie chart representing patients that develop a tumour and the percentage of PPGLs occurring at any given site. Adrenal/ PCC phaeochromocytoma, Abdo abdominal paraganglioma, HN head & neck paraganglioma, sPGL sympathetic paraganglioma.*

Where clinical data were available[53,54,56,84,89,114,207,235,242,244,246] this has been analysed to provide data on malignancy risk by tumour location (Table 4.8 & Figure 4.5). This included a total of 413 tumours, where 28 cases were associated with malignancy (6.7%).
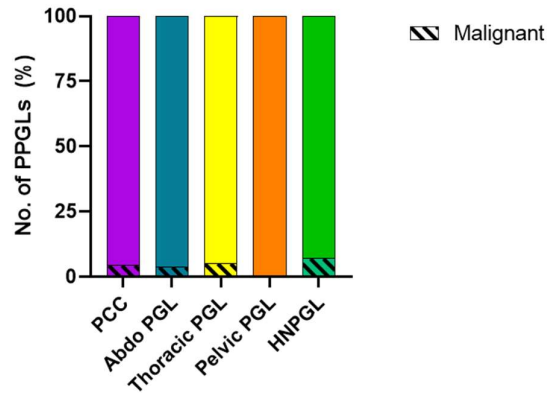
Figure 4.5: Risk of malignancy in SDHD mutation carriers of different PPGLs based on site of occurrence. The graph shows the risk of malignancy for each PPGL tumour location in SDHD mutation carriers, as a percentage of the total number PPGLs occurring at each site of disease. Total number of tumours is normalised to 100%. PCC (n=45), abdo PGL (n=26), thoracic PGL (n=19), pelvic PGL (n=4), HNPGL (n=319). These figures are derived from a total of 95 malignant PPGLs (with a malignancy rate of 27.6%). PCC phaeochromocytoma, Abdo PGL abdominal paraganglioma, HNPGL head & neck paraganglioma

In summary, prevalence of PPGL is higher in *SDHD* carriers, with a tumour detection rate of 52.9% in asymptomatic carriers. Of those that develop tumours the majority occur in the head and neck region; however, just under 20% of the PPGLs that occurred were found in the adrenal gland. Risks at other sites were lower. Malignancy transformation is lower for PPGLs that occur in *SDHD* carriers (6.7%), but not insignificant and malignancy has been reported at all sites except the pelvis.

There are fewer cases reported of patients with *SDHA, SDHC* and *SDHAF2* mutations. Table 4.9 summarises all the cases reported for these other *SDH* subunits at the time of analysis.

	SDHA	*SDHC*	*SDHAF2*
Total no. of patients with PPGLs	63	127	49
Total no. of PPGLs (n)	75	166	78
PCC [%(n)]	25.4% (17)	22% (28)	2% (1)
Abdo PGL [%(n)]	37.3% (25)	11% (14)	0
HNPGL [%(n)]	35.8% (24)	69.3% (88)	94% (46)
Thoracic PGL [%(n)]	8.9% (6)	4.7% (6)	2% (1)
Intra-thyroidal PGL [%(n)]	4.8% (3)	0	2% (1)
No. of patients with multiple PPGLs [%(n)]	11.9% (8)	36% (46)	53% (26)
No. of patients with malignant PPGLs [%(n)]	13.4% (7)	5.5% (7)	0
Median age at diagnosis (years) (range)	37.7 (12-66)	45 (12-84)	33 (20-59)
No. of RCC reported	0	8	0
No. of pituitary adenoma reported (n)	2	2	1
No. of GISTs reported	7 in germline mutations, numerous somatic mutations	numerous	0

Table 4.9: Tumour site prevalence in SDHA, SDHC, SDHAF2 mutation carriers. *Table shows the occurrence of PPGLs at different locations for SDHA, SDHC and SDHAF2 mutation carriers. Figures are presented as a percentage of patients presenting with tumours for each of these SDH subunits with the figure in brackets being the number of patients with at least one PPGL at this site. PPGL phaeochromocytoma and paraganglioma tumours, PCC phaeochromocytoma, Abdo PGL abdominal paraganglioma, HNPGL head & neck paraganglioma. Collated cohorts: SDHA[5,228,230,231,247-250], SDHC[3,7,56,64,83-92], SDHAF2[5,50,100,101].*

4.3.2 Historical PPGL patients

Surveillance screening programmes are important for individuals that are known carriers of gene mutations, but it is only in recent years that knowledge about underlying genetic mutations has advanced and different causative mutations have been identified. There are numerous cases of patients that have been diagnosed and treated for PPGLs historically, that may or may not be undergoing follow-up. Many of these patients may now be deceased, but follow-up on the family members is important. There are two implications to consider; firstly, individuals that harbour genetic mutations they are unaware of, that subsequently develop disease that could have been detected and treated at an earlier stage, and secondly, family members that are unnecessarily under surveillance as they do not carry the underlying mutation. It will be time consuming and costly to track all these individuals and counsel them as to the benefit of genetic screening, without the important considerations of the burden this will add to the genetics services. This therefore raises the question as to how to identify higher risk patients and families.

Aim: To use SDHB immunohistochemistry to investigate historical PPGL tumour tissue samples to identify patients at risk of carrying underlying *SDH* mutations, to allow family screening and prevention of morbidity in future generations.

Historical patients were identified from the PPGL database. Slides were cut from FFPE tumour blocks and stained for SDHB and then scored. Figure 4.6 demonstrates the different scoring of SDHB IHC from selected cases.
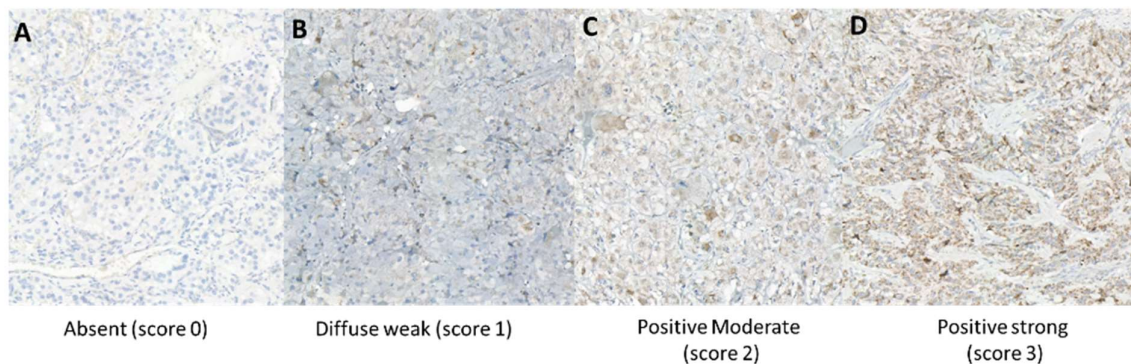
Figure 4.6. Examples of SDHB IHC. *Four different SDHB IHC staining results are shown from selected cases to demonstrate the different scores. A) absent staining (score 0), B) diffuse weak staining (score 1), C) positive moderate staining (score 2), D) positive strong staining (score 3).*

SDHB IHC was performed prospectively on all new cases of PPGL from 2016 onwards. Of the 276 total historical cases from the PPGL database, 54.7% (151) had already undergone genetic testing. Of the remaining 125 cases 62.4% (78 cases) should have undergone genetic testing at the time this work

was undertaken based on UK NHS criteria: all patients with PGL, any patient with a personal or family history of PPGL, or any patient with a PCC less than 50 years old. Of these cases, historical pathology blocks were available for 41 (53%) cases. SDHB IHC was performed on these 41 cases. In addition (as part of the TMA) a further 26 samples have been tested in patients with known *SDHB, SDHD, RET or VHL* mutations. Of the patients with a known *SDH* mutation, all had negative SDHB staining, as expected indicating absence of the SDHB protein. Additionally, all four patients with known *VHL* mutations had negative SDHB staining and the four patients with RET mutations had moderate staining (presence of the SDHB protein).

Of the 41 historical samples 32% (13) had weak or absent SDHB staining (8 weak, 5 absent). Of those that were scored as weak, 70% had heterogenous staining with patchy areas of immunopositive cells, making it more difficult to score accurately. Of these 13 patients, 5 have, so far, undergone genetic testing and three had negative genetic testing and two were found to have confirmed *SDHB* mutations.

Prospectively we have performed SDHB staining on 29 PPGL cases from 2016 to 2020. Of these 60.7% (18) had normal expression of SDHB and 39.3% (11) have weak or absent staining of SDHB. Twenty-one (72.4%) of these cases have been referred for genetic testing. For three patients their genetic status was known at the time of their operation (2 *RET*, 1 *SDHB*) and these PPGLs were identified on surveillance screening. The five patients not referred either do not meet the criteria for genetic testing in the UK (three patients, adrenal PGL >50 years) or declined testing (one patient) and one patient died two weeks post operatively. Of the 11 patients that had weak or absent SDHB staining in the tumour tissue, genetics were unknown at the time of diagnosis and subsequent genetic testing identified eight patients had a genetic mutation identified on the gene panel analysis: 2 *SDHA*, 4 *SDHB*, 1 *SDHC,* 1 *FH*.

4.1.1   Pathogenicity of genetic variants

It is clinically important to establish whether each mutation is pathogenic as this has implications on whether cascade genetic testing is offered to family members and whether surveillance screening should subsequently be offered if the individual is found to carry the mutation. The American College of Medical Genetics and Genomics (ACMG) and the Association for Molecular Pathology guidelines recommend variant classification from pathogenic through to benign based on an accumulation of evidence[102]. SDHB IHC, described above, is one such method, and based on negative SDHB staining patients have been referred for genetic testing. On occasion genetic testing yields inconclusive results, with the variant labelled as a VUS. For the clinician it is difficult to know how to manage these

individuals and their family members, and the uncertainty about whether this gene variant may pre-dispose them to tumour development can be very distressing for the individual. To decide on whether cascade genetic testing of family members and subsequent surveillance screening should be undertaken further analysis of novel VUSs is required[102].

Aim: To investigate whether specific genetic mutations labelled as VUS are causative of the patient's PPGL in our cohort.

The details of the VUS mutations that have been further analysed in this work are outlined in Table 4.10. Further clinical detail on the patients' case histories are given in each subsection for each described VUS.

Gene	Mutation	Mutation type	Tissue sample	Experiments	ACMG classification [102]	*In silico* analysis	SDH IHC	outcome
TMEM127	c.245-10C>G	Intronic (near start of exon 3)	Blood PA PGL	*In silico* analysis, LoH, RNA splice analysis	Likely benign	Probably no affect on splicing (HSF)	N/A	Patient blood heterozygous for the mutation. No LoH demonstrated in either the PA or PGL tissue. No disruption of splice site demonstrated.
SDHA	c.923C>T p.Thr308Met	Missense (exon 8)	Blood PGL	*In silico* analysis, LoH, SDHB/A IHC	Uncertain significance	Damaging (Polyphen2)	Weak SDHB expression, normal SDHA expression	DNA too degraded
SDHB	c.298T>C p.Ser100Pro	Missense (exon 4)	Blood PA PGL	*In silico* analysis, LoH, SDHB IHC	Likely pathogenic	Damaging (Polyphen2)	SDHB expression absence in PGL, but normal expression in PA	Patient blood heterozygous for the mutation. No LoH demonstrated in PA or PGL tissue.

Table 4.10: VUS mutations. *The table shows the different mutations that have been investigated and the outcomes. TMEM127 transmembrane protein 127, SDH succinate dehydrogenase, PA Pituitary adenoma, PGL paraganglioma, LoH loss of heterozygosity, IHC immunohistochemistry, HSF human splice finder analysis*

4.3.2.1 TMEM127 c.245-10C>G variant

This gene encodes the transmembrane protein 127 (TMEM127) and is situated on chromosome 2q11.2. This transmembrane protein is a negative regulator of the mechanistic target of rapamycin (mTOR) pathway. The *TMEM127* gene is made up of four exons with a linear DNA length of 22806 base pairs and mRNA length of 4593 base pairs coding for a 238 amino acid protein. It acts as a tumour suppressor gene and recently mutations in this gene were identified as causing a hereditary predisposition to developing PCC[251]. Mutations in *TMEM127* occur in both germline and somatic forms and account for approximately 1% of all PPGLs[252], but until now have not yet been associated with pituitary adenomas, which are known to occur in other familial PPGL syndromes.

Patient clinical history

A 70-year-old Swiss female presented to Luzerner Kantonsspital hospital with visual field loss and was diagnosed with a pituitary macroadenoma. She had a history of an abdominal PGL. Both lesions were surgically resected.

The patient underwent genetic testing at the Royal Devon and Exeter laboratory, aged 68 years, which revealed a heterozygous novel intronic mutation in intron 2, close to the start of exon 3 (c.245-10C>G), within the *TMEM127* gene (Figure 4.8). This variant was judged as a VUS. Mutation analysis of all coding regions and exon/intron boundaries by targeted next generation sequencing for *FH, MAX, RET, SDHA, SDHAF2, SDHB, SDHD* and *VHL* were negative. The *TMEM127* variant was confirmed with Sanger sequencing. This mutation replaces a pyrimidine with a purine. This nucleotide is not conserved across all species, with a Thymine (T) present instead of Cytosine (C) in pig, cow, cat and dog species; however, a pyrimidine is always conserved at this position amongst species.

This variant is not listed in the Exome Aggregation Consortium (ExAC) or Exome variant server or Genome aggregation (gnomAD) databases. *In silico* analysis predicts that the mutation probably has no impact on splicing, as no significant splice motif alteration was detected on human splice finder (HSF) analysis. The ACGM guidelines classify this variant as likely benign[227].

Optimisation of methods

The patient's blood and tissue samples from both the PGL and pituitary adenoma were sent to our laboratory from Luzern with the patients consent for further analysis.

Genomic DNA extraction (Table 4.11) was performed from the patient's blood using Illustra DNA extraction kit BACC2 (GE Healthcare), as outlined in the methods section and this was stored at -20°C. Genomic DNA was extracted from four FFPE slides, cut to 10 µm thickness for both paraganglioma and

pituitary adenoma tissue using QIAamp DNA FFPE tissue kit (Qiagen) following manufacturer's instructions, as outlined in the methods section. These slides were reviewed by a senior pathologist and the appropriate area of tumour to be extracted was identified on a sequential H&E slide (Figure 4.7). Samples were stored at -20°C.
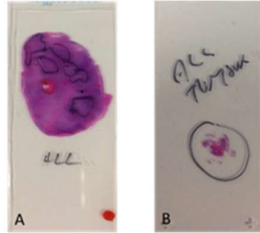
Figure 4.7: H&E slide showing macroscopically the PGL (A) and pituitary adenoma (B) tissue. *The circles highlighted in the PGL tissue represents small areas of necrosis that were avoided in tissue collection for DNA.*

Sample	DNA concentration (ng/µL)	260/280
Blood	27.4	1.58
Pituitary adenoma tissue	138.3	1.99
Paraganglioma tissue	56.7	1.93

Table 4.11: DNA concentrations achieved on DNA extraction. *DNA was extracted from whole blood using Illustra DNA extraction kit BACC2 (GE Healthcare) and from four FFPE slides of tumour tissue using QIAamp DNA FFPE tissue kit (Qiagen) of both the paraganglioma and pituitary adenoma. The table shows the DNA concentration achieved and the purity of the samples (260/280).*

First, I designed primers to flank the intronic *TMEM127* mutation based on the gene sequence obtained from NCBI (NG 027695.1) (Figure 4.8) to produce a product size of 323 base pairs.

Figure 4.8: TMEM127 variant primer design. *The primers designed using PRIMER3 Plus Software for the identified mutation are highlighted in purple. The gene sequence was obtained from NCBI (NG 027695.1). Exon two is highlighted in green and exon three is highlighted in blue. The mutation (highlighted in red) is a C to G point mutation. Dots represent intronic sequence not shown. Product size was 323 base pairs.*

These primers where then optimised using a temperature gradient on a G-storm thermocycler machine (Figure 4.9).

Thermocycle conditions		*Temperature gradient (°C)
Hot start	95°C 2mins	58.2
Start cycle	X35	59.6
Temp	95°C 30secs	61.1
Annealing Temp	*Gradient	62.7
Elongation temp	68°C 30secs	64.4
End cycle		65.1
Temp	68°C	67.2
Store	10°C	67.8
		68.2
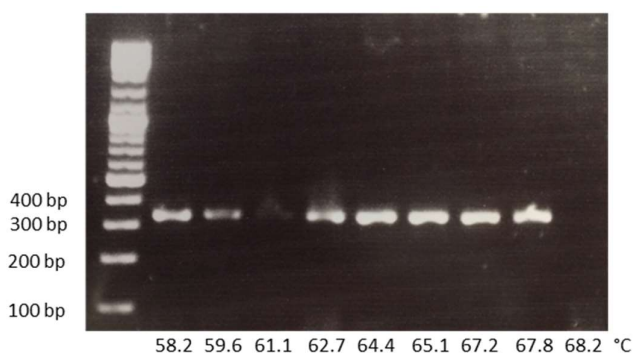
Figure 4.9: Optimisation of TMEM127 primers *The table shows the thermocycler conditions and temperature gradient used for optimisation of these primers using a G-storm thermocycler machine. The figure shows the PCR products ran on a 2% agarose gel demonstrating the bands achieved at different annealing temperatures. Product size was 323 base pairs.*

Optimum annealing temperature to use these primers was 63°C. Primers were used at 10μM.

I amplified the DNA samples by PCR under the conditions shown in Table 4.12.

Reagents	Volume (μL)	Thermocycler conditions	
		Heat lid	105°C
Forward Primer	0.5	Hot start	95°C 2mins
Reverse Primer	0.5	Start cycle	X35
dNTPs	0.5	Denaturation Temp	95°C 30secs
Taq buffer	2.5	Annealing Temp	63°C 30secs
Polymerase	0.125	Elongation temp	68°C 30secs
Water	19.875	End cycle	
Total volume	24	Final extension Temp	68°C 5min
		Store	10°C

Table 4.12. PCR conditions for amplification. *The table outlines the reagents, concentrations and the G-storm thermocycler conditions used for DNA amplification.*

PCR product bands were visible on the agarose gel for the patient's blood DNA, but not for either tumour tissue (Figure 4.10).

Well 1 – patient blood

Well 2 – patient blood

Well 3 – Pituitary adenoma

Well 4 – Pituitary adenoma

Well 5 – PGL

Well 6 - PGL
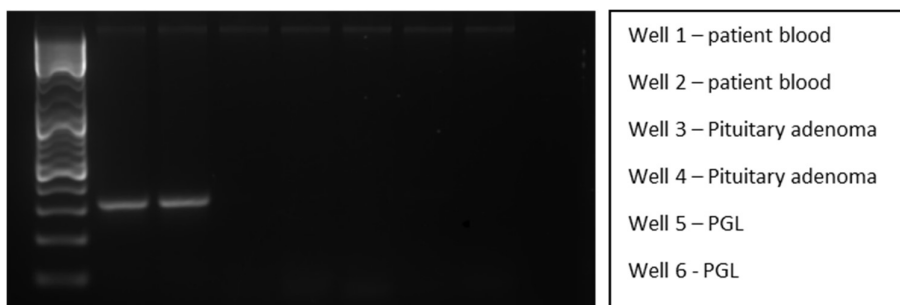
Figure 4.10: PCR gel for TMEM127 c.245-10C>G mutation. *The positive control, in duplicate (patient's blood sample), shows a band at the correct size (323bp), but no band is visible for either of the tumour tissues.*

I repeated this experiment using double concentrations of reagents: dNTP, primers and Taq polymerase enzyme, to increase the amplification of the DNA product, but was still unsuccessful.

This suggested the possibility that the product length was too large for the fractionated DNA obtained from the FFPE tumour tissue. I tested this hypothesis using a different primer set, with a smaller product for a different gene (*PRKAR1A* gene, product size 141bp) on the same samples and under the same conditions. This demonstrated successful PCR with the smaller amplicon primers (images not shown).

I therefore designed new primers for this variant with a shorter product size of 165 base pairs (Table 4.13 and Figure 4.11).

	Sequence	Temp (°C)	GC (%)	Length (bp)
Forward Primer	GGTGGAGGGGAATCAAACTCC	67.7	57.1	20
Reverse Primer	ACTACACAGGATGCCCAGGA	64.6	55	20
Product size = 165 base pairs				

Table 4.13: Shortened product TMEM127 Primers. Table outlines the details of the redesigned primers to create a smaller product.

ACAGCGTCCTCCAGAACTGCCCTGGCTCCCAGGACTGT**GGTGGAGGGGAATCAAACTCC**TTCTAGGTGGG
GACTTCCTGCACCAAGTGTTACTTGGGGCCGTGAAAATTTGGTTCT**C**CCTCTACAGATTTCTGCATGAAT
CCCCAGACAGTGCTGCTCCTGCGGGTCATCGCCGCCTTCTGTTTCCTGGGCATCCTGTGTAGTCTCTCCG
CTTTCCTTCTGGATGTCTTTGGGCCGAAGCATCCTGCTCTGAAGATCACTCGTCGCTATGCCTTCGCCCA
TATCCTAACGGGTAAGCCGTGAGCCTGCTCACAGTGGGAGAGGAACTGCTACAGGGTGGGGGCATCCTGT

Figure 4.11: Position of primers for shortened product. The position of the new primers creating a smaller product are shown within the gene sequence. Exon three is highlighted in blue. The mutation (highlighted in red) is a C to G point mutation and the new primers are highlighted in purple. Product size was 165 base pairs.

The same conditions and temperature gradient were used as above (Table 4.12) to optimise the new primers. Optimum annealing temperature to use these primers was between 59.6 and 61.1°C (Figure 4.12).

Temp: 58.2, 59.6, 61.1, 62.7, 64.3, 66.1, 67.2, 67.8, 68.2   °C
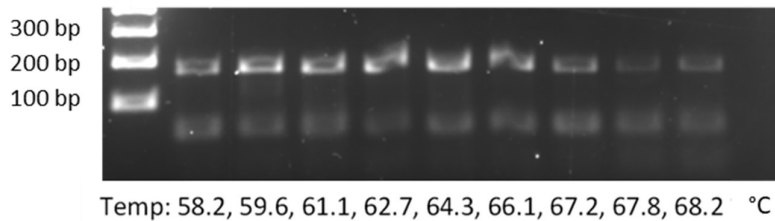
Figure 4.12: Results of optimisation of shortened primers for TMEM127 c.245-10C>G variant. PCR products produced from different annealing temperatures using the new primers were ran on a 2% agarose gel. The brightest bands seen at 59.6°C and 61.1°C suggest these to be the optimum annealing temperatures. Product size 165 base pairs.

I repeated the above PCR experiment, using the following conditions (Table 4.14) and 2µL of tissue DNA and doubled the concentration of dNTPs, Taq polymerase and primers.

Reagents	Volume (µL)	Thermocycler conditions	
Forward Primer	1.0	Heat lid	105°c
Reverse Primer	1.0	Hot start	95°C 2mins
dNTPs	1.0	Start cycle	X 40
Taq buffer	2.5	Denaturation Temp	95°C 30secs
Polymerase	0.25	Annealing Temp	60°C 30secs
Water	17.25	Elongation temp	68°C 30secs
Total volume	23	End cycle	
		Final extension Temp	68°C 5min
		Store	10°C

Table 4.14: PCR conditions for amplification. *The table outlines the reagents, concentrations and the G-storm thermocycler conditions used for DNA amplification for the shortened product length.*

Bands of the correct product size were demonstrated for DNA from both tumour tissues and the patient's blood (Figure 4.13).
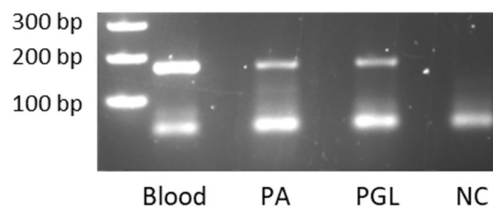
Figure 4.13. Results from PCR of TMEM127 c.245-10C>G mutation. *The gel shows bands at the correct product size for each of the DNA samples (165bp). The bands at the bottom are due to primer dimerization and are not true products. PA pituitary adenoma, PGL paraganglioma, NC negative control.*

These PCR products were then purified using QIAquick PCR purification kit (Table 4.15) and were sequenced by Sanger sequencing under standard conditions (Figure 4.14).

Sample	DNA concentration (ng/µL)	260/280
Blood	21.5	1.58
Pituitary adenoma tissue	13.8	1.95
Paraganglioma tissue	12.6	1.96

Table 4.15: DNA concentrations achieved after purification. *The table shows the DNA concentrations of the patient's blood sample and the pituitary and paraganglioma tissue and the purity of the samples (260/280).*
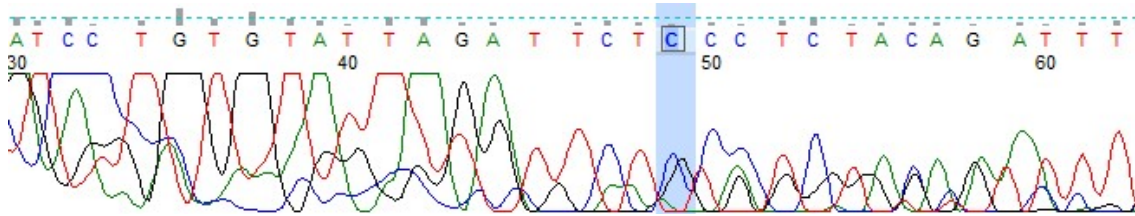
Figure 4.14: Sanger sequencing results of PGL DNA. The figure shows the Sanger sequencing of the DNA product from the paraganglioma tissue. Multiple peaks are demonstrated suggesting possible contamination.

Sanger sequencing did not show clear results, suggesting a possible contamination with the purification step. Therefore, I repeated the experiment, using the same conditions, which demonstrated the bands at the expected product size.

Findings

If LoH is present in the tumour tissue then the 'normal' wild type allele will be lost, leaving only the remaining mutated allele at this position, suggesting loss of this section of the chromosome. Sanger sequencing results from the patient's blood sample (Figure 4.15) confirms heterozygosity; the patient carries a germline mutation with one normal allele 'C' and one mutated allele 'G'. The gel electrophoresis (Figure 4.16) demonstrates amplification of the correct region.
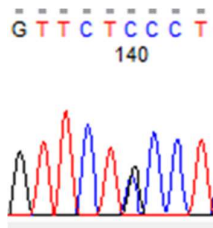
Figure 4.15: Sanger sequencing results of serum blood sample. Figure shows Sanger sequencing results from patient's blood sample showing the patient is heterozygous for the mutation in her blood: two peaks at position c.245-10 (g.16007) demonstrating the 'normal' wild type allele C base pair (blue peak) and in addition an overlapping second peak demonstrating the mutated G base pair (black peak).
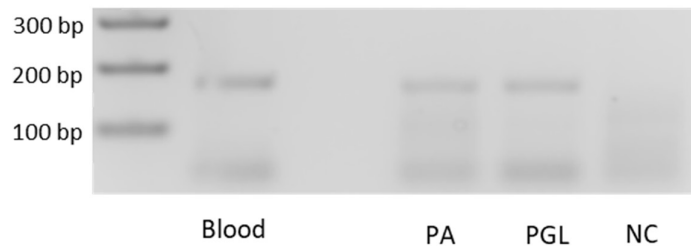
Figure 4.16: Agarose gel showing results of PCR for TMEM127 c.245-10C>G mutation. Bands can be seen at the expected product size (165bp) for the patient's blood sample, pituitary adenoma (PA) and paraganglioma (PGL) with a negative control (NC).

I purified the DNA from both the remaining PCR product and the gel bands (Table 4.16) using QIAquick PCR purification kit, according to the manufacture's protocol, as outlined in the methods. The PCR products were sequenced by Sanger sequencing under standard conditions (Figure 4.17).

Sample	DNA concentration from PCR product (ng/µL)	DNA concentration from gel product (ng/µL)
Blood	22.9	8.7
Pituitary adenoma tissue	19.6	2.8
Paraganglioma tissue	19.6	3.0

Table 4.16: DNA concentration achieved after purification from both PCR product and gel.
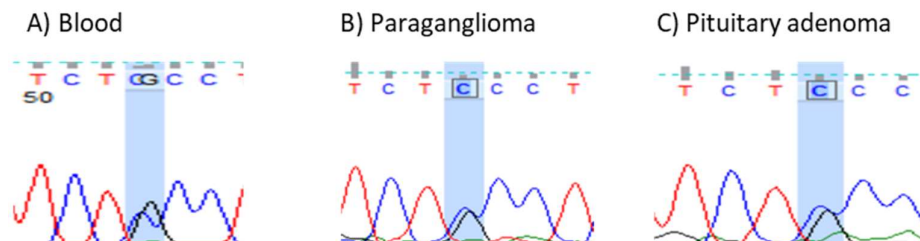
Figure 4.17: Sanger sequencing of products from PGL, pituitary tissue and patient's blood sample. *Sanger sequencing results for A) patients' blood, B) paraganglioma tissue and C) pituitary adenoma tissue. The heterozygosity is demonstrated in the patient's blood sample showing two peaks representing the two alleles at the same location: the normal wild type 'C' base (blue peak) and the mutated base 'G' (black peak). Both the paraganglioma and the pituitary demonstrate two peaks of the same base 'C', without loss of one of the alleles.*

No LoH is demonstrated in either the paraganglioma or the pituitary adenoma as two peaks can be seen in both. To confirm this finding RNA splicing analysis was performed.

RNA splicing experiment

There are other mechanisms by which a mutation may become pathogenic, so in some cases even if LoH is not present the variant may still be pathogenic due to another mechanism. In this case as this mutation is near the acceptor splice site, it may cause disruption in the coding at the acceptor splice site resulting in abnormal splicing, and thus an abnormal protein.

Optimisation of methods

I extracted RNA from the patient's whole blood using PAXgene blood RNA kit, as outlined in the methods. I designed primers to produce a product size of 242 base pairs (Figure 4.18).

GACTGCGAACCCGGAGCGTTGCTATCCTCCACCGGACTGTCAGGCTCTGCGCGCCCCGCGGAGGTCGGCG
GCGACCAGCAGCGACTGCGGAGCGACGGCGGGCGGCCCCGGGCATGTACGCCCCCGGAGGCGCAGGGCTG
CCCGGCGGGCGCCGGCGGAGGAGCCCGGGAGGCAGCGCTCTGCCCAAGCAGCCGGAGCGTAGCCTGGCCT
CGGCCCCTGCCTGGCGCCCTGTCTATCACGGCGCTGTGCACTGCCCTCGCCGAGCCCGCCTGGTTGCACAT
CCACGGAGGCACCTGTTCGCGCCAGGAGCTGGGGGTCTCC**GACGTGTTGGGCTATGTGC**ACCCGGACCTG
CTGAAAGATTTCTGCATGAATCCCCAGACAGTGCTGCTCCTGCGGGTCATCGCCGCCTTCTGTTTCCTGG
GCATCCTGTGTGTAGTCTCTCCGCTTTCCTTCTGGATGTCTTTTGGGCCGAAGCATCCTGCTCTGAAGATCAC
TCGTCGCTATGCCTTCGCCCATATCCTAACGGTTCTGCAGTGTGCCACCGT**CATTGGCTTTTCTTATTGG
GC**TTCTGAACTCATCTTGGCCCAGCAGCAGCAGCATAAGAAGTACCATGGATCCCAGGTCTATGTCACCT
TCGCCGTTAGCTTCTACCTGGTGGCAGGAGCTGGTGGAGCCTCAATCCTGGCCACGGCAGCCAACCTCCT

Figure 4.18. mRNA sequence for TMEM127 mutation. *Primers were designed using Primer3 plus software to flank exon three. The figure shows the mRNA sequence, taken from NCBI. Exon two is highlighted in green, exon three is highlighted in blue and part of exon 4 is highlighted in grey. Primer positions are highlighted in purple. Product size is 242 base pairs.*

I then optimised the primers using the same thermocycler conditions as outlined in Table 4.12 and temperature gradient shown in Figure 4.19. The brightest single band visible with the least smear was identified at 64°C, therefore this was selected as the optimum annealing temperature for the primers (Figure 4.19).
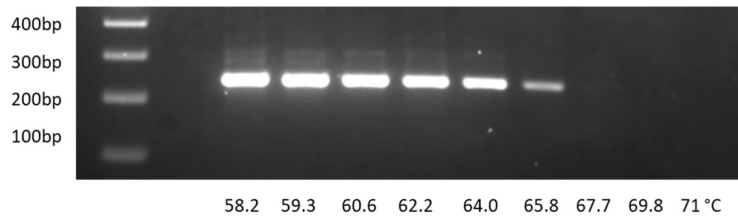
Figure 4.19. Results of optimisation of mRNA primers for TMEM127 c.245-10C>G mutation. *Agarose gel image shows bands at the expected product size (242bp) and clearly visible for annealing temperatures from 58.2-65.8°C.*

	Thermocycler conditions
Lid temp	100°C
Hot start	95°C 2mins
Cycles	x30
Denaturation temp	95°C 30secs
Annealing temp	64.5°C 30secs
Elongation temp	68°C 30sec
Final extension	68°C 5min

Table 4.17: Final optimised thermocycler conditions for TMEM127 mRNA primers

Findings of RNA splicing experiment:

Two bands were present across both the patient samples and the healthy controls, which were also visible (and stronger) with GAPDH primers. Light bands are visible for the negative RT samples,

suggesting environmental contamination. Bands are not well spread and therefore require longer electrophoresis to separate further before evaluation.
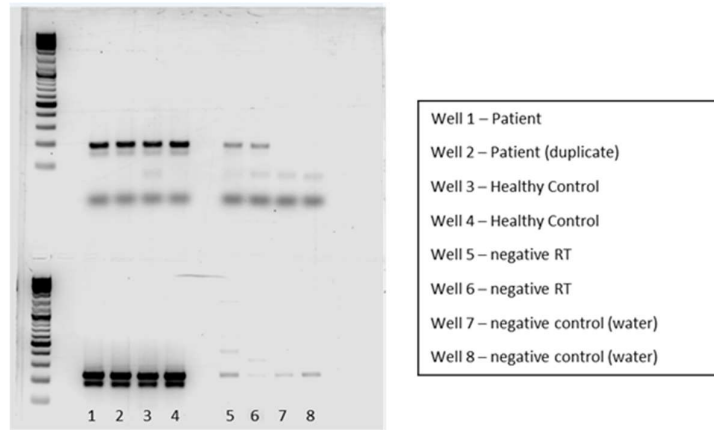
Figure 4.20: PCR gel on patient's blood sample showing TMEM127 primers (top) and GAPDH primers (bottom). The top figure shows the products using the TMEM127 primers on RNA extracted from patient's blood. The bottom figure shows housekeeping GAPDH primers on the same samples tested in duplicates. Wells 1-2 is patient blood sample, wells 3-4 contain healthy control blood samples, wells 5-6 contain negative RT samples, wells 7-8 negative control (water). RT reverse transcription enzyme, negative RT does not contain the reverse transcription enzyme.

I repeated the experiment after first exposing the water, PCR tubes, pipettes and tips to UV light. The experiment was also performed under a UV hood to minimise contamination. Products were visible at the expected product size for the patient's blood samples and the healthy control sample, although a further band was visible at a position of less than 100 base pairs product size.
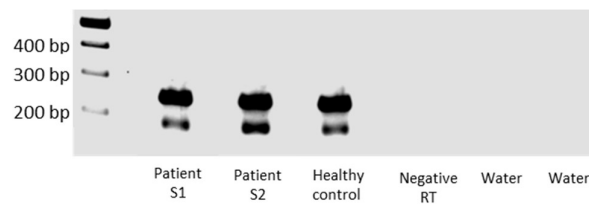
Figure 4.21: TMEME127 RNA PCR gel. The agarose gel shows two visible bands for both patient samples (wells 1&2) and healthy control (well 3), but nothing visible in negative controls (wells 4-6). Bands visible at expected product size of 242 base pairs with an additional band visible at <100bp.

Both bands were cut out of the gel, purified (Table 4.18) and sent for Sanger sequencing.

	DNA concentration (ng/μL)		
	Sample 1	Sample 2	Control
Band 1	4.9	15.8	6.1
Band 2	8.2	17.2	2.6

Table 4.18: DNA concentrations of gel bands after purification.

Using ContigExpress software sequences from the control and the patient's samples were compared to the TMEM127 reference sequence. No disruption is demonstrated at the expected site between exons two and three (Figure 4.22).

Figure 4.22: ContigExpress comparing TMEM127 sequences. *The first, third and seventh lines of sequencing are the reference sequence for the TMEM127 gene, the second line represents the control sample, the fourth line represents band 1 from the patient and the eighth line represents band 2 from the patient. The red box outline highlights the exon 2 and exon 3 junction, with four base pairs outlined from the end of exon 2 and four base pairs at the start of exon 3 (AAAGATTT). The mutation lies in the intron in-between (close to start of exon 3) and would be expected to cause a disruption at this site. The figure shows the same sequence of eight bases (AAAGATTT) from the reference sequence are also present for the patient's samples.*

In summary, it is unlikely that the TMEM127 germline mutation identified in the patient's blood is responsible for the paraganglioma or pituitary adenoma as no LoH was demonstrated in the DNA of either tumour and RNA analysis did not demonstrate any disruption to the transcript sequence.

4.1.1.1 SDHA c.923C>T p.Thr308Met mutation variant

This missense mutation replaces a wild-type 'C' base with a 'T' at position 923 in cDNA (mRNA) causing an amino acid substitution of Threonine replaced by Methionine within exon 8. *In silico* analysis using Polyphen2 and SIFT software predicted this mutation to be probably damaging with a score of 1.00 (0.00-1.00). This mutation had not been reported in the ExAC database at the time of analysis.

Patient clinical history

A male originally presented aged 46 years with symptoms of catecholamine excess and was diagnosed with a 50x30 mm left para-adrenal PGL. This was successfully resected. Unfortunately, he presented one year later with a new abdominal PGL (70x70x40 mm), which was also resected. He underwent genetic testing which identified a novel missense mutation (c.923C>T) in the *SDHA* gene, of unknown significance. He remained well for six years until two further abdominal PGLs (15 mm and 34 mm) were identified on surveillance imaging. At this time two spinal metastatic deposits were also evident on imaging. He underwent EBRT 50Gy in 25 fractions followed by cyberknife radiotherapy (14Gy in 1#) when an increase in size on the metastatic bone lesions was noted 10 years later.

Proving pathogenicity of variant

IHC was performed on the PGL tumour tissue for SDHB and SDHA proteins. This showed SDHB to be only weakly expressed, but normal expression of SDHA protein was seen (Figure 4.23).
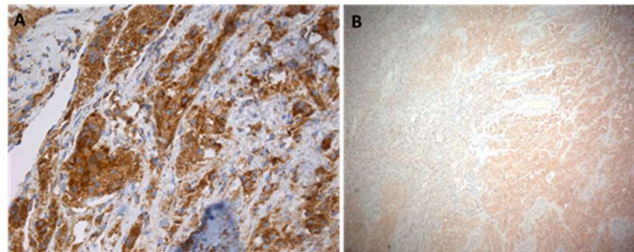
Figure 4.23: SDHA (A) and SDHB (B) IHC of PGL tissue. *Figure A demonstrates normal protein expression of SDHA. Figure B shows weak expression of the SDHB protein.*

DNA was extracted from the patient's whole blood sample and from FFPE slide of tumour tissue (Figure 4.24).

Sample	DNA concentration (ng/µL)	260/280
Blood	290	1.82
Paraganglioma tissue	506.6	1.78

Figure 4.24: Macroscopic image of FFPE PGL slide and DNA concentrations achieved This slide has been annotated by the pathologist showing the area of tissue to be extracted. The table shows the DNA concentrations achieved following extraction from whole blood and FFPE tissue.

Primers were designed to create a product that was 185 base pairs in length (Figure 4.25) and optimised using a temperature gradient (Figure 4.26). The optimised annealing temperature was 56.9°C with the brightest and clearest band seen at this temperature (Figure 4.26).

CTGTGCAGTTTTGCACATAATGCCTTCTGCTTATCTTTTTCCTTCTTTCCTGCAAAGAATGTCTTGAAAAAAATAA
TGCATTTGAAATAGAGATCTAGCAATTGTTAGGTAATAAATATGTGTGGTTTTTTGCAGGCATATATGGTGCTGG
TTGTCTCATTACGGAAGGATGTCGTGGAGAGGGAGGCATTCTCATTAACAGTCAAGGCGAAAGGTTTATGGAGCG
ATACGCCCCTGTCGCGAAGGACCTGGCGTCTAGAGATGTGGTGTCTCGGTCCATGACTCTGGAGATCCGAGAAGG
AAGGTGCGTGTGATTTACCACCAGCACTGTCTGAGCGGGCACACGGGCCGGGGTTGCTTCTGTGAGTTTCAGCAC

Figure 4.25. Part of the SDHA gene sequence Gene sequence from NCIB (NG 012339.1:4983-43842). Exon eight is highlighted in green. The designed primers are highlighted either side of the mutation in purple. The point mutation is highlighted in red. PCR product is 185 base pairs.

	Thermocycle Conditions
Lid temp	105°C
Hot start	95°C 2mins
Cycles	X40
Denaturation temp	95°C 30secs
Annealing temp	Gradient
Elongation temp	68°C 30sec
Final extension	68°C 5min
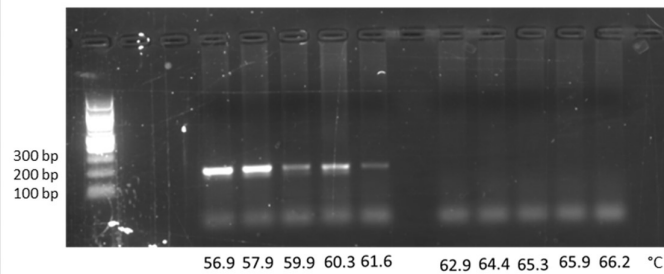
Figure 4.26: Optimisation of primers for SDHA c.923C>T mutation. The table summarises the thermocycler conditions used for optimisation of the primers. The figure shows the results of the optimisation using a temperature gradient. The brightest clearest band is seen at an annealing temperature of 56.9°C.

Findings

The experiment was then undertaken at a temperature of 56.9°C with the DNA extracted from the patient's blood sample and PGL tumour tissue. No band was seen for the PGL tissue, suggesting the DNA was too degraded in this sample (Figure 4.27). This was repeated using the same DNA sample with the same result (image not shown).
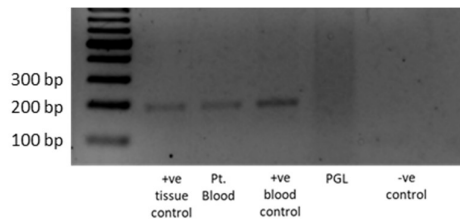
Figure 4.27: Results of experiment for SDHA c.923C>T mutation. Figure shows image of PCR products run on a 2% agarose gel demonstrating expected PCR product (185bp) for the patient's blood sample and positive control; however, no band was seen for the PGL tissue.

To distinguish if there was a problem with the primers or whether the DNA was too degraded for any amplification, this experiment was repeated using a set of primers to a different gene (*PRKAR1A* gene) with a slightly smaller product size (141 bp). Both sets of primers demonstrated successful

149

amplification bands for the patient's blood sample and the positive control, but not for the DNA taken from the PGL tissue (Figure 4.28). This confirmed that the DNA from the PGL tissue was degraded.
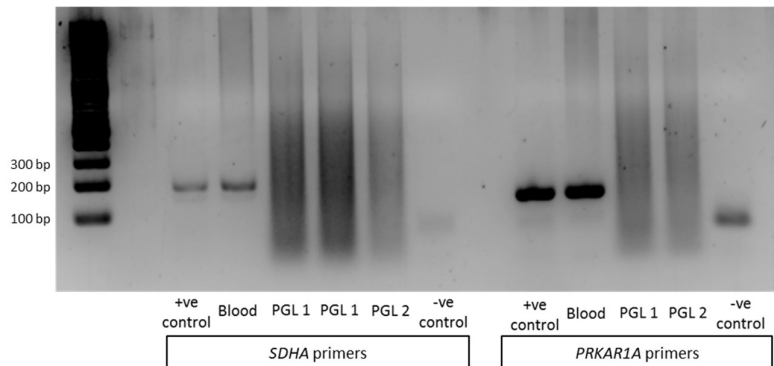
Figure 4.28: Results of control experiment using PRKAR1A gene. *The figure shows the image of PCR products run on a 2% agarose gel using same SDHA primers as above (left 5 columns) and primers for the PRKAR1A gene (right 5 columns). The same smear effect is seen for the DNA from the PGL tissue for both sets of primers confirming the DNA from the tumour tissue was degraded. PRKAR1A Protein Kinase CAMP-Dependent Type I Regulatory Subunit Alpha. SDHA Succinate dehydrogenase subunit A, PGL paraganglioma.*

This experiment was repeated using tumour tissue extracted from a different pathological block, but the result was the same indicating the DNA was degraded in the tumour tissue.

4.1.1.2 SDHB c.298T>C p.Ser100Pro mutation variant

This missense mutation results in a substitution of a Serine for a Proline amino acid. Polyphen2 *in silico* analysis predicts this mutation to be damaging. This variant is not reported in the GnomAD database.

Patient clinical history

A 56-year-old postmenopausal women presented with a nine month history of bitemporal hemianopia. An MRI revealed a large pituitary mass, for which she underwent surgical resection and histology was in keeping with a lactotroph adenoma. Her father had a metastatic spinal PGL and was known to be a carrier of an *SDHB* mutation c.298T>C.

Proving pathogenicity of the mutation

SDHB IHC was undertaken and showed loss of granular cytoplasmic SDHB staining in the patient's father's PGL, but normal expression in her pituitary adenoma (Figure 4.29).
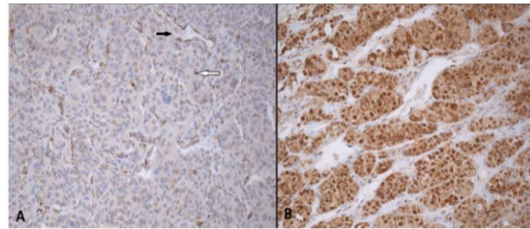
Figure 4.29: SDHB IHC of PGL and pituitary adenoma. *(A) SDHB IHC of the PGL tissue demonstrating loss of expression of the SDHB protein. The black arrow shows positive endothelial cells (positive internal control) and the white arrow indicates the negative tumour cells. (B) Normally expressed SDHB protein in pituitary adenoma.*

We proceeded to investigate whether either of the tumour tissues showed LoH**.** DNA was extracted from the patient's blood sample and pituitary tumour tissue and her father's PGL tumour tissue (Figure 4.30).
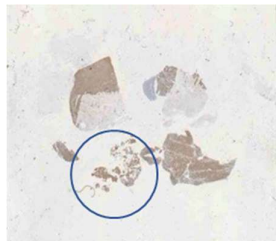
Sample	DNA concentration (ng/µL)
Blood	326
Pituitary adenoma tissue	3.9
Paraganglioma tissue	27.6

Figure 4.30: Macroscopic image of pituitary tissue and DNA concentrations achieved *The pituitary adenoma is circled, the remaining tissue is normal adenohypophysis. The table shows the DNA concentrations achieved.*

TCAAGCCATTAGAACCACATTCGAGGCAGGAAGAAGGAAGGGAGAAAAGCCAACAGGCACCTCTGT
CAGAGGAATGTTGCATGTCAGTGCTGCCCCTGATGGCA`CAGCAAGGAGGATCCAGAAG`AAAGTATTTGGG
GCAGGACTGATTCCGGATATGGGTGAGGATGTGTTAAATGTGTGTCTCTTTCAG`GCATCTGTGGC`T`CTTG`
`TGCAATGAACATCAATGGAGGCAACACTCTAGCTTGCACC`CGAAGGATTGACACCAACCT`CAATAAGGTC`
`TCAAAAATCTACCCTCTTCCACACATGTATGTGATAAAGGATCTTGTTCCC`GTGAGTTTCTGCATCTCTC
TGGTTTTGTTTTTATTTGCATGGGGGGCAGTGCTATGTGTGTTACGCTATTAGTTTTTCAGGGCAGGATT

Figure 4.31. Part of SDHB gene sequence from NCIB. *Exon four is highlighted in blue. The site of the mutation is highlighted in red and the selected primers are highlighted in yellow. Product size = 162bp*

These primers were optimised using thermocycler conditions outlined in Figure 4.26. These *SDHB* primers worked across the full range of annealing temperatures. The clearest band was visible at 64.4°C and therefore this was the annealing temperature used in further experiments.

56.9 57.9 59.9 60.3 61.6 62.9 64.4 65.3 65.9 66.2 °C
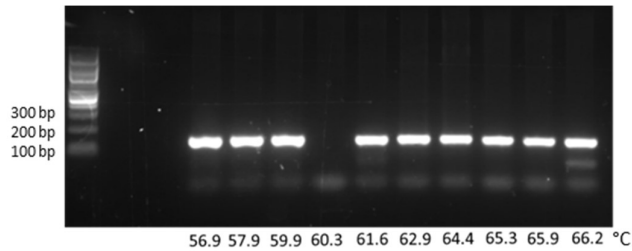
Figure 4.32: Optimisation of primers for SDHB c.298T>C mutation. *PCR gel showing temperature gradient for SDHB primers. Bright bands were visible across the full range of annealing temperatures; however, the clearest band visible was at 64.4°C.*

Findings

Bands were visible at the expected product size for the patient's blood sample, both the tumour tissue samples and the positive controls (Figure 4.33). PCR products were sent for Sanger sequencing (Figure 4.34) after DNA quantification (Table 4.19).

Blood   PA   PGL   -ve   +ve   +ve
                   control control control
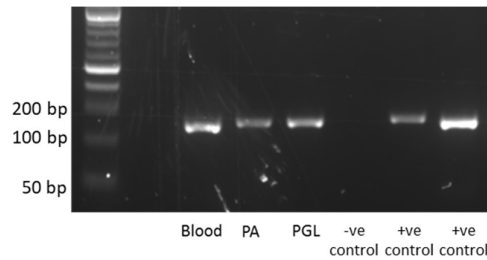
Figure 4.33: Results of PCR for SDHB c.298T>C variant. *Gel image shows PCR products run at an expected size of 162bp for patient's blood sample, PA and PGL tumour tissue. PGL paraganglioma, PA pituitary adenoma, +ve control tissue (pituitary adenoma), +ve control (healthy volunteer blood).*

Sample	DNA concentration (ng/µL)	260/280
Blood	9.1	1.89
PA tissue	14.4	1.74
PGL tissue	14	2.09

Table 4.19: DNA concentrations after purification of PCR product for SDHB c.298T>C variant. *Table shows the DNA concentrations achieved of the PCR products of the patient's blood sample, the PA and PGL tumour tissue and the purity of the samples (260/280). PA pituitary adenoma, PGL paraganglioma*

152

The patient's blood sample showed heterozygosity for the mutated base as expected (Figure 4.34a); however, both the patient's pituitary tumour tissue and her father's PGL tumour tissue unexpectedly also showed heterozygosity (Figure 4.34b&c).
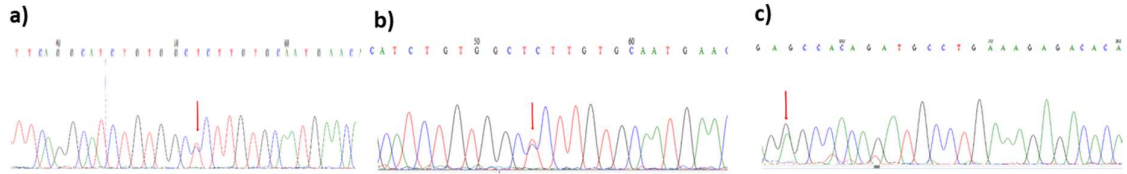
Figure 4.34: Sanger sequencing results. *a) Patient's blood sample showing heterozygosity with two bases detected at the mutated site (arrowed: mutated 'C' (blue peak) and the wild type 'T' (red peak)). b) The patient's father's PGL tissue showing heterozygosity with two peaks visible. c) Patient's pituitary tissue (reverse sequence) showing heterozygosity with two peaks visible.*

In summary, SDHB IHC was negative in the father's PGL, but positive in the patient's pituitary adenoma. LoH analysis confirmed heterozygosity in the patient's blood; however, no LoH was identified in either the patient's pituitary adenoma or the patient's father's PGL.

4.4 Discussion

4.4.1 Surveillance protocols

When this work was undertaken there was no consensus on screening or the follow-up of asymptomatic *SDH* mutation carriers and each country and institution approached this in their own way. Since then a new international consensus statement[229] has been published to assist in decision making as to when and how these individuals should be followed up. This work contributed to the production of these new guidelines. As a result of this the discussion is divided into multiple sections, the first sections discuss these data in the context of the situation during which it was undertaken for each subunit and then radiological imaging options, concluding with a suggested model for surveillance screening based on these data. A concluding section is then provided discussing these data in light of research published since this work was undertaken and the current guidelines.

4.4.1.1 SDHB

The importance of surveillance screening in asymptomatic relatives is highlighted when analysing studies that separate out the asymptomatic carriers/relatives from the index cases demonstrating a detection rate of 15.4% and 52.9% in carriers of *SDHB* and *SDHD* mutations respectively. Individual studies for *SDHB* carriers report a tumour detection rate ranging from 3.5-35%[53-56,58,63-65,92,216,236,237], similar to our results (25%) and 52.9% for *SDHD* carriers[53,54,56,63,89,92,211,216,219,242,243]. The most recent analysis on penetrance of *SDHB* disease[56] is based only on clinically apparent disease at the time of genetic testing, so these figures will be underestimating the true penetrance, as they do not factor in asymptomatic disease.

The majority of studies combine all PGLs that occur in sympathetic locations, and this can bias the subsequent translation of these figures to clinical practice and individual patients. To be able to advise patients on their individual risk it is important to understand the likelihood of tumour development at different sites, chance of recurrence and aggressiveness of individual tumour behaviour (e.g. likelihood of a particular tumour developing metastatic lesions). The data are presented in two ways; firstly, the percentage of patients that develop at least one tumour at any given site, which enables one to define the clinical risk to the patient and secondly, the percentage of tumours that occur at each site, which enables one to define which sites warrant surveillance imaging.

Interestingly, while it is widely recognized that the most likely site to develop a PGL is extra-adrenal abdominal, the combined data suggest the risk of developing HNPGL is just as high. The risk of developing a PCC appears to be low and the occurrence of bilateral PCC in *SDHB* carriers is rare. These

figures are not dissimilar to a previous review reporting only 12% of patients that developed a tumour had a PCC[3]. The large cohort of *SDHB* patients reported in the PGL.EVA study also had a high rate of HNPGL with more than 50% of patients with tumours having a HNPGL[216]. It is possible that the combined data above is skewed by the inclusion of cohorts containing a large number of patients with Dutch founder mutations (exon 3 deletion and c.423+1G>A splice site mutation), with an apparent predominance of HNPGLs. If the three large Dutch studies are removed[58,69,237] 18.75% of patients presented with PCC, 37.5% with at least one extra-adrenal abdominal PGL, 20.4% with at least one HNPGL and 10.8% with a thorax PGL, with similar figures for pelvic and bladder PGLs. Therefore, surveillance screening needs to include imaging to cover all of these sites.

Median age at diagnosis for each site did not differ significantly for PPGLs occurring at adrenal, abdominal, thorax, bladder or pelvic sites (median ages at diagnosis 32, 30.5, 33, 27, 29.5 years respectively), but median age of diagnosis was older for those with HNPGLs at 42.5 years (range 21-93 years). This may be influenced by the majority of HNPGLs being biochemically silent tumours and therefore being detected later, and that historically they were not thought to be important in *SDH* disease and therefore were not looked for in the early studies. The oldest patient identified was 93 years old with a HNPGL identified on surveillance imaging[236].

Recent attempts have been made to define a genotype-phenotype correlation in *SDHB* mutation carriers. Ricketts *et al*[80] compared truncating mutations predicted to cause absent or unstable protein with missense mutations that cause no loss of protein stability. Although more recently these same authors[56] have extended their cohort and report no difference in age-related risks of PPGL between missense and truncating mutations, they did suggest a non-significant trend towards higher overall penetrance in carriers of the mutation predicted to cause the most severe protein instability (p.Ile127Ser). They suggested that there was a higher risk of HNPGL specifically with the p.Gly96Ser missense mutation (causing abnormal splicing) and that there was a non-significant trend towards an increased risk of malignancy at age 60 years when mutations occurred in the first 300 nucleotides than with more 3' mutations. Recently Jochmanova *et al*[55] have suggested that there is a difference in age-related penetrance between genders, with a penetrance of 71.8% at age 75 years in males compared to 30.8% in females. They further analysed the most common six mutations (of the 48 identified) in their cohort and suggested a possible (but not statistically significant) slower rate of disease in four mutations (Ile127Ser, IVS1+G>T, exon 1 deletion, Arg90Stop) when compared to patients harbouring mutations Val140Phe and Arg46Stop. Further definition of any genotype/phenotype correlations, if present, could enable adaptation of screening protocols on a genotype basis.

A detailed systematic review and meta-analysis was undertaken[253] and included nine cohorts of *SDHB* mutation carriers with malignant disease. The pooled risk for incidence of malignancy was 17% for all *SDHB* mutations carriers (including both index cases and asymptomatic carriers). The combined data show a malignancy rate of 27.6%, in keeping with previous reports[59-61]. More clinical relevance may be found in assessing the malignancy risk as a percentage of the total tumours that occurred at each site. These data suggest that the risk of malignant transformation is the same for both PCC and abdominal PGLs in *SDHB* carriers. The notable exception is bladder PGLs; although the series were small, concern has been raised about their substantial malignant potential (estimated at approximately 50%)[254,255]. Another key finding is that the risk of malignant transformation of HNPGL in *SDHB* carriers appears to be lower compared to PPGLs that develop at other sites. These data should be interpreted with caution as the numbers of tumours at some sites is small.

4.4.1.2 SDHD

The combined cohorts of individuals carrying *SDHD* mutations confirms that the most common site of disease in *SDHD* carriers is within the head and neck, where multiple PGLs can occur, as previously reported. It does highlight that there is a high risk of patients developing a PCC (35.8%) or abdominal PGL (9.4%) and a small, but significant risk of developing PGLs at other sympathetic sites, so any surveillance screening should include these sites and not be exclusive to the head and neck.

Some studies have attempted to elucidate phenotypes related to specific mutations. Ricketts *et al*[80] demonstrated mutations that affect protein stability were associated with earlier age of onset and a higher risk of developing PCC. Additionally Heesterman *et al*[243] found that individuals with p.Leu139Pro mutations had a higher penetrance and higher risk of multiple tumours (when compared to the most common mutation in this cohort, p.Asp92Tyr). A recent paper[56] confirmed the *SDHD* missense mutation p.Pro81Leu had a low risk of sympathetic PGL, although similar risk to other mutations of *SDHD* (one PPGL and 37 HNPGL in cohort of 53 carriers) and of note, two of these individuals with HNPGL developed metastases. This mutation is predicted *in silico* to have only a mild effect on protein stability and the authors suggest this may mean that the tumourigenesis process may be different between sympathetic and parasympathetic tumours. A study following the natural growth rate of 28 *SDHD*-associated HNPGL radiologically demonstrated growth in only five tumours (17.9%) during 3.2 years (+/-2.5years) follow-up [243]. Therefore, suggesting that surveillance protocols could in the future be further refined based on specific genotypes with *SDH* subunit mutations, but more data is needed.

It is recognised that PPGLs occurring in *SDHD* carriers run a more benign course. The results here show a combined malignancy risk of 6.7%, in keeping with a previous detailed meta-analysis[253] of 10 cohorts of *SDHD* mutation carriers with malignant disease, though malignancy has been reported across a spectrum of *SDHD* mutations[245].

4.4.1.3 SDHA, SDHC, SDHAF2

There is less published data available for individuals who carry *SDHA, SDHC* and *SDHAF2* gene mutations and therefore these results should be interpreted with caution in regard to targeting specific surveillance programmes. For *SDHA,* unlike with *SDHB* and *SDHD*, in the described combined cases there is no obvious predilection to any specific body site for a tumour to occur. In our cohort two out of six of the index patients have developed distant metastatic PPGLs. Time to disseminated disease was 16 and 37 years, and occurred following development of recurrent disease, suggesting a long duration of disease before onset of metastases. This finding has now been confirmed by other reported cases[5,231,256]. A cautious approach must be used before ascribing definite pathogenicity to newly identified mutations due to the high frequency of VUS[99,257]. One sample demonstrated positive SDHA IHC. It has previously been described that SDHA IHC may be positive in the presence of a definitive mutation on rare occasions when there is disparity between molecular genetic aberrations of a tumour suppressor gene and retention of protein expression[114,226,258]. It has been hypothesised that this may be due to the second hit in the *SDH* gene in the tumour tissue resulting in an inactive SDH complex with preservation of antigenicity[114].

4.4.1.4 Other surveillance programmes

Recommendations for screening have often been based on studies looking at sensitivity and specificity of different imaging modalities in comparison to each other[11,216,259,260]. Some recommendations regarding specific imaging modalities and frequencies were appropriate when there was less knowledge and an assumed higher penetrance, but these would no longer be considered valid by the recommending centres. An understanding of the different sensitivities and specificities is important but must be interpreted in the setting of the clinical goal of surveillance in a particular cohort. The goal of a surveillance programme is to detect all tumours before they cause morbidity or undergo malignant transformation, thereby allowing therapeutic intervention at the correct time (which may be after a period of more focused surveillance). Historically, surveillance recommendations have included the use of MRI or CT for surveillance screening of head and neck, chest, abdomen and pelvis. Some recommendations include the routine or first screen use of whole body scintigraphy (metaiodobenzylguanidine (MIBG), ^{111}In-diethylene triamine pentacetic acid-pentetreotide

(Octreoscan), ^{68}Ga-Dodecanetetraacetic acid-Octreotate (DOTATATE), Fluorodeoxyglucose (FDG), or Fluoro-dihydroxyphenylalanine (F-DOPA) positron emission tomography (PET)[12,13,18,53,54,58,69,79,86,89,92,211,212,215,216,219] (Appendix 6). There are advantages and disadvantages of different imaging techniques used in different surveillance programmes. The first divide is between cross-sectional imaging (e.g. CT or MRI) and functional imaging techniques. Functional imaging modalities are based on the increased glucose uptake in tumours (e.g. 18F-FDG PET) or the preferential uptake of substrates in the PPGL processing pathways (e.g., MIBG, 6-[18F]-fluorodopamine (18F-FDA), and 18F-DOPA techniques)[12,214,216,217,219,243,261-265]. Arguments have been made for the use of techniques reliant on tumour hypermetabolic activity, rather than PPGL specific metabolism, to increase sensitivity for less differentiated tumours[219]. Functional imaging using ^{18}F-FDG has been shown to be more sensitive in the detection of PPGLs in *SDHB/D* carriers compared to ^{123}I-MIBG, and is more sensitive in the detection of *SDHB/D* related metastases compared to non *SDH*-related disease[214,219,264]. ^{68}Ga-DOTATATE PET/CT has been shown to be superior in the localization of *SDHB*-associated metastatic PPGLs[217] and HNPGLs[266,267]. The multicentre PGL.EVA study[216] is a large study that compared four methods of radiological screening in 238 subjects (113 index patients and 125 asymptomatic carriers) with mutations in all *SDH* subunits (124 *SDHB,* of which 85 were carriers), with a follow-up period of three years. They compared head & neck gadolinium enhanced magnetic resonance angiography (HNMRA), together with contrast enhanced CT TAP to functional imaging using ^{123}I-MIBI and somatostatin receptor scintigraphy (SRS) with ^{111}In-labeled pentetreotide scintigraphy. They demonstrated a 91.7% sensitivity of tumour detection with the combined use of cross-sectional imaging using HNMRA + CT TAP and functional imaging with SRS when centrally reported and concluded that initial screening of patients should be with this combination. This conclusion, however, does not factor in the requirement for lifelong screening, often from a young age, through reproductive years, and the potential cumulative lifetime radiation exposure. A retrospective sub-analysis of the PGL.EVA cohort evaluated the use of a rapid contrast-enhanced angio-MRI, which has a much shorter duration of scanning of 5 to 10 minutes, in detecting HNPGL in *SDH* mutation carriers and found no difference in performance with standardized MRI[268]. The most sensitive method in the evaluation of sympathetic primary PPGLs is suggested to be 18F-fluorodopamine PET, but availability is limited[12]. Both MIBG[216,243,269] and Octreoscan[12] have been shown to be less useful in *SDH* surveillance imaging.

It has been previously recommended that CT or MRI are sufficient to detect an adrenal lesion and have similar sensitivities for detection of PPGLs[11,13,120]. It is argued that CT may offer better spatial resolution detecting smaller lesions, but MRI provides better soft tissue contrast and thus offers unique information for tumour characterization and delineation[261]. MRI is considered more favourable for

localising extra-adrenal PGLs, in pregnant and paediatric patients and in patients whom radiation exposure should be limited[11,120]. Asymptomatic carriers of *SDH* mutations fall in this latter category, and therefore MRI, rather than CT, should be the imaging of choice for surveillance in this group.

MRI only studies

Very few other studies have solely used MRI for surveillance imaging. A previous study in Utah[64], evaluated the results of 45 rapid sequence MRIs in 37 *SDH* carriers, of whom 28 were asymptomatic. Patients had 1-3 MRI scans to assess tumour pick-up rate. They identified six new *SDH*-related tumours in five patients. In this small study they identified one true PGL that was not identified on initial MRI reading and one PGL that was later deemed not a PGL. Both of these results were altered at the second MRI reading. The authors concluded a sensitivity of MRI for surveillance of 87.5% and specificity of 97.7% and highlighted the importance of double reporting of MRIs.

A recent UK study[92] reported on the use of rapid sequencing MRI for the long-term monitoring of individuals with *SDH* mutations. They analysed a cohort of 47 patients (of whom 35 were asymptomatic carriers) with known *SDH* mutations over a 10-year follow-up period. Patients underwent two yearly surveillance MRIs and they identified six PPGLs in the asymptomatic carriers. The authors concluded that biannual rapid-sequence non-contrast MRI is an effective method to monitor individuals with *SDH* mutations. Our results demonstrate similar detection rates in asymptomatic carriers of 25%. As expected, the majority of disease is identified on the first surveillance scan, but our results show subsequent surveillance scans are important in identifying further disease following a negative initial screen. Of our cohort only two of these asymptomatic carriers had raised metanephrine levels. Cumulatively these three cohorts provide data on 181 individuals with *SDH* mutations (161 *SDHB*), including 128 asymptomatic carriers (120 *SDHB*) which supports the use of non-ionising imaging for surveillance in the form of rapid sequence MRI, as a safe and reliable modality for monitoring and identifying new disease. The importance of reviewing images in a specialist centre on more than one occasion is highlighted throughout all studies to ensure no disease is missed. All the MRIs at our centre are double reported by specialist radiologists to minimise the risks of missing small *SDH*-related lesions, previously reported to be 5%[216]. If a lesion is noted on the second MRI report, previous scans are reviewed again to identify if the lesion can be seen. Several cases of this have occurred before the double reporting system was introduced, or original scans were done at outside centres and sent to radiologists at our centre for the second report, which has subsequently identified a lesion.

Radiation risks

With the known evidence regarding long-term risks of radiation[270-272], more centres are adopting radiation free methods for surveillance imaging in asymptomatic carriers, with MRI being the logical choice, in alignment with the Endocrine Society guidelines[218]. The use of MRI avoids the possible risk of radiation induced tissue injury in this susceptible cohort. Females incur greater damage than males from radiation injury[270,272]. Although all organs demonstrate a relative increase in radiation induced cancer risk, the most significant for this cohort is the thyroid, breast and ovary[270]. Children have about twice the risk of radiation induced cancer compared to adults in their thirties and about five times the risk compared to adults in their sixties for both sexes[270,272]. The lifetime risk of radiation induced cancer in children (0-19 years) is estimated as 8-14% per Sievert (Sv) of radiation exposure, and 4.22-8.54% for adults 20-49 years[270] (). Typically, in practical terms, this confers a lifetime radiation induced fatal cancer risk of 1:2000 for an adult and 1:1000 for a child undergoing a CT scan of the chest, abdomen and pelvis. One of the concerns about sole use of radiological imaging (e.g. CT/MRI) in screening is missing tumours, particularly in the thorax and some authors have suggested that nuclear imaging could be used to detect these[216], although of note the lower sensitivity in detecting PGL in the thorax with CT in the study was ameliorated by a second imaging review in expert hands.

Age at which to commence surveillance screening is also highly debated. Our results suggest that surveillance should commence at age five years, as these were the earliest tumours detected (*SDHB* carriers: six years with abdominal PGL[273], nine years with an PCC[53] or HNPGL[80] and 15 years with a thoracic PGL[53] and five years with *SDHD* mutations[54]). However, the modality of imaging used in children will have to be tailored to the individual child and their families. Early studies recommended commencing at age 10 years or at least 10 years before the earliest age of diagnosis within each family[13,53]; however, without a clear genotype-phenotype correlation within each subunit, the utility of this is unclear. Another study[58] using a more statistical approach calculated an optimal age to start imaging for HNPGL as 27 years; although of note no children were included in this study.

4.4.1.5 A suggested model for subunit specific surveillance screening

Appendix 6 summarises suggested surveillance programmes that have been recommended by different centres and are highly variable. Very few studies separate out the different *SDH* subunits in terms of surveillance screening. Most use *SDHB* mutation carriers as the basis of their screening programmes, as this group make up the bulk of the affected population in the majority of centres. Regular clinical and biochemical review of *SDH* mutation carriers is universally recommended. If an imaging surveillance programme is sensitive enough, all lesions should be detected before they have

a clinical or biochemical correlate. It is recognised that *SDH*-related PPGLs remain clinically and biochemically silent for a prolonged period due to lower tumoural production of catecholamines[23,206,207], and the majority of parasympathetic PGLs are non-functional[208]. In recent years there has been increasing evidence that size of tumour correlates with malignant potential [206,209,210], emphasising the importance of sensitive imaging regimens to identify tumours before they reach malignant potential. As novel and more sensitive and specific biomarkers are discovered, less reliance on imaging techniques is likely to occur in the surveillance of asymptomatic carriers; however, for the time being imaging plays a central role.

Table 4.20 outlines a model for a suggested surveillance protocol that could be adopted for asymptomatic carriers, based on the data presented in this chapter for the specific underlying *SDH* subtype.

Table 4.20: SDH-subunit specific surveillance proposals. *The table outlines suggestions for surveillance protocols for each SDH subunit. These proposals are based on the data from the literature and the data presented in this chapter. It is advised here, along with the Endocrine Society guidelines[11], that imaging surveillance should be with the exclusive use of MRI for all SDH surveillance screening, with radiation modalities reserved for the further characterization of tumours identified on screening, treatment planning if required and the detection and surveillance of known or potential metastatic disease (e.g. after the excision of a large SDHB-related PPGL where metastatic disease is a possibility).*

SDH subunit	Surveillance screening proposals			Rationale	Additional comments
	First screen	**Subsequent surveillance**			
SDHB	Clinical review and education. Assessment of metanephrine levels. Non-contrast MRI with additional DWI sequences including head and neck (with one section through the pituitary), thorax, abdomen and pelvis.	Annual clinical review Annual assessment of biochemistry (plasma or 24 hour urinary metanephrines)	Non-contrast MRI with additional DWI sequences skull base to pelvis every 2 years	Malignancy rate is high Sites of tumour development is broad Screening for this group should be the most frequent and most comprehensive. By detecting a tumour early, this allows focused monitoring to enable intervention at the appropriate point in time	When a potential tumour is identified but not suitable for immediate removal, this should be followed more closely. Possible *SDH*-related RCC should necessitate urgent specialist review and early intervention due to the more aggressive behaviour that is reported compared to their sporadic counterparts[130,52]
SDHD (of paternal inheritance)			Non-contrast MRI with additional DWI sequences for head and neck every 3 years with additional thorax, abdomen and pelvis every 5 years*	High penetrance High risk of multiple tumours The goal is to detect tumours at an early stage so that monitoring can be focused. Clinical priority is to define when and how to intervene to minimize patient morbidity, given the growing consensus that fractionated or stereotactic radiation is highly effective and avoids the inevitable cranial nerve morbidity of surgical resection and the recognised slow growth rate HNPGLs[64,67,131,132]	When an asymptomatic tumour is identified, we would recommend more frequent surveillance imaging to assess growth rates so that timing of intervention can be planned. For HNPGLs, the frequency of scanning and timing of intervention should also take into account the site, recognising the reported increased aggressiveness and malignancy rates of jugular and vagal PGLs, over carotid body PGLs[64]
SDHC			As per *SDHD* recommendations	There is insufficient evidence to define a distinct surveillance strategy for this subtype. *SDHC* mutations appear to have sites of disease and malignancy rates that are similar to *SDHD.*	As more data accumulates the interval of these surveillance scans is expected to increase (relative to *SDHB&D*) given the lower penetrance of disease
SDHA			As per *SDHB* recommendations	There is insufficient evidence to define a distinct surveillance strategy for this subtype. The sites of disease are similar to *SDHB;*	

162

SDH subunit	Surveillance screening proposals			Rationale	Additional comments
	First screen	Subsequent surveillance			
				however, penetrance and malignancy rates are lower.	
SDHAF2 (of paternal inheritance)			MRI head and neck every 3 years with MRI of other body sites if metanephrines raised or clinical concern	High penetrance of HNPGL, very low risk of other sites. No malignancy reported.	

MRI magnetic resonace imaging, DWI diffusion weighted imaging, SDHA succinate dehydrogenase subunit A, SDHB succinate dehydrogenase subunit B, SDHC succinate dehydrogenase subunit

C, SDHD succinate dehydrogenase subunit D, SDHAF2 succinate dehydrogenase subunit AF2

[*]Given the above figure of 35% of SDHD mutation carriers developing a PCC, any clinical and/or biochemical suspicion should prompt earlier abdominal imaging.

4.4.1.6 Recent literature and conclusions

As described in this chapter, over the past decade genotype-phenotype correlations have emerged for the different subtypes of *SDH* mutations; however, more recent work has proposed that variant type (truncating versus missense) may predict phenotype[274]. In a cohort of 950 clinical cases, truncating mutations (predicted to have a profound effect on protein structure and function) were over-represented, contributing 60% of *SDHB* variants and 77% of *SDHD* variants. With truncating mutations occurring in a higher proportion of patients with PPGLs and malignant disease and missense mutations (result in a single amino acid change) occurring in a higher proportion of HNPGL cases. Patients with truncating mutations also had earlier age of PPGL diagnosis. In a further report the same authors[275] propose several hypotheses for why specific tissues have differing tolerances to the metabolic disruption caused by *SDH* variants. They hypothesise that different types of variants (i.e. truncating versus missense) may result in differing levels of succinate and ROS-mediated toxicity. They suggest that truncating variants may block succinate oxidation more so than missense variants leading to higher levels accumulating compared to missense variants and that there may be a succinate 'threshold' for tumourigenesis. Alternatively, they propose that sympathetic paraganglia may have weaker anti-oxidative defence compared to parasympathetic tissues, and that there may be a selective ROS-mediated toxicity in the more vulnerable tissues[275]. New research suggests that metastatic progression in *SDH*-related PPGLs is due to immortalization-related mechanisms such as TERT activation or *ATRX* mutation within the primary tumour[276]. Although these recent studies have clearly advanced the *SDH* genotype-phenotype field, there are some discrepancies with earlier similar studies[55,80], and there is still much work to be done before it can be translated back to improving clinical care.

The largest cohort of *SDHC* mutation carriers has recently been published (n=91)[277]. This confirmed the presented data with 65.2% having an isolated HNPGL, but demonstrated a slightly higher rate of metastatic disease at 19.6%. Similarly, they report the median age of diagnosis as 43 years, but demonstrated a lower occurrence of metachronous tumours. GIST, PA and RCCs were all documented within their cohort. They report a tumour incidence of 40.5% at age 40 years and 94.6% at 60 years in probands and 4.4% and 6.7% respectively in carriers[277] (all tumours in carriers were identified on first surveillance screening).

Other recent work has focused on the spectrum of tumours, beyond PPGLs, that occur in *SDH* carriers[278]. Stomach GISTs are the second most common tumour to occur in *SDH* carriers. They present with multifocal tumours along the stomach wall and have a characteristic histological epithelioid appearance. They have a high rate of metastatic spread, but clinical course of disease remains

unpredictable. Despite this, as the lifetime penetrance of GIST in *SDH* carriers is not known, specific screening programmes for GISTs are not yet recommended[278]. *SDH* GISTs predominantly occur in *SDHA* carriers (47% of reported SDH-deficient cases), whereas *SDH* RCCs predominantly occur in *SDHB* carriers; although they have also been reported in *SDHA*, *SDHC* and *SDHD* carriers. SDH deficient RCC also have a distinct morphology of intracytoplasmic inclusions and intra tumour mast cells[279]. Up to 26% are thought to be bilateral and 33% metastatic[278]. Pituitary adenomas are still thought to be a rare occurrence in *SDH* carriers. Prevalence is reported at 0.3-1.8% in unselected PA cases; with the majority of these being lactotropinomas or somatotropinomas. Although it is described that when they do occur they tend to have a more aggressive phenotype. The situation with regards to thyroid carcinoma is still unclear. Five cases of epithelial thyroid carcinoma have been reported and 63 cases of differentiated thyroid carcinoma, but none demonstrated negative SDHB immunoreactivity[278], so the presence of thyroid carcinoma in *SDH* carriers may be incidental.

Our group[280], and another group[281] have also separately put forward surveillance suggestions specifically for the paediatric cohort of *SDH* mutation carriers, some of which has contributed to the new international consensus guideline[229].

The national genomic test directories (https://www.england.nhs.uk/publication/national-genomic-test-directories/) have recently been updated for the criteria for NHS referrals for patients with PPGL. This now states that patients should be referred for genetic testing if they have: a unilateral PCC aged <60 years, or PGL or bilateral PCCs occurring at any age, or PPGL with loss of SDH expression on IHC, or PCC occurring with RCC at any age or PPGL at any age if ≥1 relative has had a PPGL, RCC or GIST.

Since this work was undertaken new international consensus guidelines[229] have been published towards which this work contributed. In conclusion I will briefly summarise the consensus findings and current recommendations. The consensus concluded that tumour screening should be performed in all individuals with a *SDHA, SDHB, SDHC, SDHD* (paternal inheritance), but not in the case of maternal inheritance of *SDHD* where development of a tumour is rare (the consensus does not include *SDHAF2* in its recommendations)[282]. Tumour screening should commence between ages 6-10 years for *SDHB* carriers and 10-15 years in carriers of other *SDH* subunits. Genetic screening should only be performed if the child falls into the category that they would proceed to tumour screening if found to be genetically positive, and newly published age specific reference ranges for plasma metanephrines should be used for the paediatric population[283]. In adulthood annual measurement of plasma metanephrines is the preferred option, but in children measurement of urinary metanephrines can be used if there is a desire to avoid venepuncture. With regards to imaging; first line imaging should be done with MRI for abdominal and pelvic regions and PET-CT for visualisation of the thoracic region in

adults; accepting that this will expose the individual to a one-off radiation dose of 8mSv for benefit of a baseline 3D image of the whole body. MRI should be used in children wherever possible, but ultrasound is an option in children who do not tolerate MRI. If functional imaging is required PET-CT should be used instead of ^{123}I-MIBG or ^{111}In-pentetreotide. Regular follow-up should take place with plasma or urinary metanephrines annually in adults and every two years in children with MRI every 2-3 years, which can be reduced to five yearly after the age of 70 years, with cessation at age 80 years. Extra screening should take place before planning a pregnancy due to morbidity and mortality risk of functional PPGL during pregnancy[284,285]. Finally, the consensus agreement concluded that genotype-phenotype relationships were still not well established as phenotypes can vary greatly with the same mutation and within the same family. Therefore, the current guidance is that surveillance strategies should not differ based on mutation type or if metastatic disease has occurred within a family.

4.4.2   Historical PPGL patients

Genetic testing is now recommended for all 'at-risk' patients; but current guidelines do not address how historical cases should be handled. Absence of protein expression of SDHB and SDHA in PPGL tumour tissue has been shown to be a reliable marker for identifying those tumours that are due to underlying *SDH* germline mutations[114,220-222], and thus identifying which patients would benefit from further genetic screening. We applied this method to investigate a cohort of historical PPGL cases, to identify which patients were at higher risk of having an underlying *SDH* germline mutation and may benefit from genetic testing, or if the index case was deceased whether family members would benefit from this testing.

Our data showed that all our proven cases with *SDH* germline mutations did demonstrate completely absent or very weak immunostaining. We also identified a number of cases that had negative or weak immunostaining, but genetics did not highlight a known underlying mutation. This could be due to these being intronic mutations or somatic mutations in the tumours. There have also been a few reports where there has been a definitive mutation with a disparity between molecular genetic aberrations of a tumour suppressor gene and retention of protein expression[114,226,258]. These cases, along with several other genetic negative cases from our cohort suspected to have a familial syndrome, subsequently contributed to a collaborative pilot study run at another site investigating the prevalence of somatic driver mutations in PPGL[286], which identified two somatic *EPAS* mutations, and one somatic mutation in each of *KIF1B, FGFR3, TP53, SDHA, RET* and *VHL* genes. All are classified as VUS, except for one of the *EPAS* mutations which is classified as likely pathogenic.

There are potential pitfalls in the use of SDHB and SDHA IHC. Despite early reports on it having 100% sensitivity, with complete absence of SDHB immunostaining in *SDHB* mutated PPGLs[222], it is now recognised that SDHB and SDHA protein expression is not an all or nothing phenomenon, with heterogeneous expression reported[114], as well as false positive and false negative results. Caution needs to be used when interpreting SDHB IHC with regards to possible underlying *SDHD* and *VHL* mutations, as false positives occur (e.g. SDHB immunostaining in the presence of an underlying *SDHD* mutation)[221]. In this cohort *VHL* samples had mostly absent SDHB immunostaining. This pattern has been shown in other studies[114,220,287]. In one large study, 11 of 37 *VHL* samples showed abnormal SDHB immunostain; with six being immunonegative and a further five having discordant scoring between observers, due to heterogeneity and/or weak diffuse staining patterns, as well as one malignant NF1 case[114]. Due to the small possibility of these false positive findings, it is advised that if genetic testing of *SDH* genes fails to identify a mutation, further investigation to explore mutations in *VHL*/*NF1* and *SDHC* promoter methylation should be sought[114].

A number of the historical cases for which we undertook SDHB immunostaining demonstrated patchy weak staining making it difficult to score; this 'indeterminant' staining has been reported in other studies[114,287] . This may have been due to the IHC being unreliable in older tissue samples or may be because these mutations cause incomplete depletion of the protein, and therefore some staining was still seen. We found this to be particularly true for historical samples more than eight years old and older samples than this often also showed weak staining in the surrounding control tissue. This suggests that the widespread use of SDHB IHC for testing historical samples may have only limited utility for identifying historical cases where familial screening would be indicated. Also, SDHB immunostaining can only identify mutations in *SDH* genes and therefore this does not aid in identifying other potential underlying genetic causes of these historical cases.

Numerous studies have been undertaken investigating the usefulness of SDHB IHC in retrospective cohorts of PPGL tissue in correlating IHC results with underlying germline mutation in the *SDH* genes [114,220-222]. Yet few translate this back to clinical practice to the direct benefit of the patients and their relatives to look at uptake into specialised screening programmes and clinical outcomes of these surveillance programmes. Due to time limitations and clinical restrictions due to the COVID pandemic, not all the historical cases with negative SDHB immunostains have undergone genetic testing and this work is ongoing.

4.4.3 Pathogenicity of different mutation variants

Establishing whether specific variants are pathogenic is clinically important due to implications on decisions regarding cascade genetic testing and surveillance screening. A cautious approach must be used before ascribing definite pathogenicity to newly identified variants[102]. It is difficult to prove definitely whether any specific variant is pathogenic and therefore guidelines recommend that variants are classified into five categories: pathogenic, likely pathogenic, uncertain significance, likely benign and benign, based upon accumulated, and sometimes contradictory, evidence[102]. This should take into account the clinical picture and molecular analysis as to the function of the mutation.

4.4.3.1 TMEM127 c.245-10C>G variant

The germline mutation was confirmed in the patient's blood sample. The patient has had two tumours known to be associated with underlying genetic mutations but are also known to occur sporadically. The patient had no reported family history. No LoH was identified in either the pituitary or the paraganglioma tumour tissue. The mutation occurred 10 base pairs from the beginning of exon 3 and is further within the intron than commonly reported splice acceptor site mutations. In vitro splicing experiments revealed no changes in the splicing pattern. Although two bands appeared to be visualised on the agarose gel, all the samples from both bands for the patient had the same sequence as the *TMEM127* reference with no missing sections, suggesting that these are in fact not two separate bands, but part of the same band. This suggests that this mutation is not causing a splice change and is unlikely to be pathogenic.

Reports mostly link mutations in this gene to PCC formation[252,288], although there have been a handful of cases of patients developing PGLs[289,290]. Qin *et al* first identified the *TMEM127* gene to confer susceptibility to PCC in 2010 and identified 3% of apparently sporadic PCC to have underlying *TMEM127* mutations. They demonstrated LoH in all 19 PCC tumour samples tested, with loss of the wild-type allele. Yao *et al* subsequently examined a further 124 tumour samples and confirmed LoH for a further four new mutations[288]. More recently, a large prospective study analysing data from 972 unrelated registrants without mutations in the classic genes (*VHL, RET, NF1, SDHB,C,D*) from the European-American-Asian Pheochromocytoma-Paraganglioma Registry, found 2.1% had underlying *TMEM127* mutations, but no LoH analysis was performed on the tumour samples to prove pathogenicity[290]. The authors estimated penetrance at 40 years of age to be 41% for *TMEM127* mutation carriers[290]. Multiple tumours are common and malignant PPGLs has been reported to occur in approximately 10% of patients[290,291]. To date there have been no reported cases of pituitary adenomas occurring in patients carrying underlying *TMEM127* mutations. This variant is reported in

the ClinVar database to be of uncertain significance and it is categorised as likely benign by the ACMG classification[102,227]. On balance it is unlikely that this VUS is pathogenic and the cause of this patient's pituitary adenoma and PGL, which may both be sporadic tumours that have coincidentally occurred in the same patient.

4.4.3.2 SDHA c.923C>T p.Thr308Met variant

This patient's first presentation was at a relatively young age and subsequently has developed multiple PGLs and now has metastatic disease confined to his bones. Although recurrence of tumours at the same site of the previous resection is possible if not all tumour is successfully removed in the operation, it is unusual for patients with truly sporadic tumours to develop metachronous and synchronous tumours. This gentleman has two sons both of whom are well but have not been offered genetic testing as his mutation has been labelled as a VUS. Due to the high index of suspicion that this is familial disease, both are undergoing regular surveillance screening despite not having a confirmed genetic test. SDHB IHC results are suggestive of dysfunction of the SDH enzyme, but surprisingly the SDHA stain showed normal expression of the protein. Absence or weak diffuse staining of SDHB is common in mutations in any of the *SDH* subunits; however, absence of SDHA staining is specific to *SDHA* mutations[114] and would have been expected in this case. It has previously been described that SDHA IHC may be positive in the presence of a definitive mutation on rare occasions where there is disparity between molecular genetic aberrations of a tumour suppressor gene and retention of protein expression[114,226,258]. It has been hypothesised that this may be due to the second hit in the *SDH* gene in the tumour tissue resulting in an inactive SDH complex with preservation of antigenicity[114]. This mutation has not been reported in the ExAC database, but had the most aggressive phenotype in our *SDHA* cohort[233] and there has also been another recently reported metastatic case carrying the same *SDHA* mutation[232]. These authors performed structural analysis of the effects of this mutation (using DUET scoring) and predicted it would cause mild destabilisation of the protein promoter region and part of the substrate binding region and therefore likely to affect protein stability. This variant is reported in the ClinVar database to be likely pathogenic and it is classified as of uncertain significance by the ACMG guidelines[102,227].

We were unable to demonstrate LoH in the PGL tissue, despite attempts using different pathological specimens, as the tumour samples were old and therefore the DNA was too degraded for further analysis. Ideally the patient's two children would be tested for the presence of this mutation in serum, but currently they have not consented to this due to underlying anxiety about the implications if they are proven to be carriers, especially in the context of this mutation currently being classified as a VUS.

4.4.3.3 SDHB c.298T>C p.Ser100Pro variant

Presentation with an isolated pituitary macroadenoma is rare in *SDHB* carriers[53,77]. This is only the fourth published case[292]. This mutation has previously been reported in a patient with a PGL[293], and is classified as likely pathogenic by the ACMG classification[102,227]. We demonstrated SDHB IHC to be negative in the father's PGL, but positive in the patient's pituitary adenoma. Heterozygosity was confirmed in the patient's blood; however, no LoH was identified in either the patient's pituitary adenoma or the patient's father's PGL. In in vitro studies, the p.Ser100Pro substitution did not show elevated succinate levels, but had an increased succinate/fumarate ratio[293]. Previous reports of this mutation have demonstrated faint SDHB expression and presence of LoH in PA tissue[77]. This suggests that this mutation may not be the cause of these tumours in this family. However, although the majority of second hits in *SDHB* tumours are caused by LoH (85%), a minority are caused by other second hit phenomena such as somatic mutations at a different point in the allele. Additionally, there was very little pituitary adenoma tissue to extract DNA from and this was amongst normal adenohypophysis tissue and therefore there remains the possibility of tumour DNA contamination with normal pituitary tissue.

4.5   General conclusions and future work

The overarching aim of any *SDH* surveillance programme must be to identify disease at an early stage with small tumour sizes in order to allow intervention at the appropriate time, improve cure rates and limit the chance of malignant transformation. A consensus statement has now been published with guidance on specific surveillance programmes for each of the *SDH* subunits[229]. Lifelong surveillance has significant implications in terms of time, frequency, cost, incidental findings and anxiety for the carriers. As new research becomes available it is likely that it will be possible to further modify these programmes for specific mutation variants, moving towards more personalised tailored surveillance screening. It is the hope that in time it will become possible to delineate specific mutation variants that cause more aggressive disease requiring more intensive surveillance. Equally important will be to identify specific mutation variants that cause only benign disease in specific locations, alleviating anxiety experienced by individuals that carry these mutations as well as decreasing the burden of surveillance screening they are required to undergo.

4.5.1   Limitations

These studies were undertaken retrospectively. At the time our *SDH* cohort comprised predominately of *SDHB* subtype, with proportionally more index cases than would reflect the general population. The

inclusion of index cases in penetrance figures tends to overestimate them. Therefore, we also analysed the 'asymptomatic carriers' separately, but this unavoidably decreases the sample number. We have considerably smaller cohorts for the other *SDH* subunits and therefore have provided a more descriptive analysis of these. To calculate accurate penetrance figures very large cohorts are required. We have therefore combined data of clinical cases reported in the literature that were readily available. It should be noted that this was limited to publications in the English language and was therefore limited to mainly countries of Europe and America. The data was extracted from the available published literature and not taken from primary sources.

It would be valuable for any surveillance programmes to undergo prospective auditing and validation so that successful programmes can be more widely adopted.

Many of the pathological samples used to analyse the historical cases and investigate the pathogenicity of the variants of uncertain significance were old samples that had been stored in archives for many years. One of the biggest problems encountered was unreliability in the immunostaining of the old pathological samples making accurate interpretation of the SDHB staining difficult. Reduced availability of pathological specimens resulted in fewer historical samples being tested than planned.

Finally, due to the pandemic situation during which this work was undertaken time was limited to locate and test more historical samples or locate additional pathological specimens to complete investigations of all the VUSs when DNA was found to be too degraded in the specimens tested. This resulted in the process of contacting individuals and families where historical samples were found to be high risk of *SDH* mutation to be greatly delayed. This work still needs to be undertaken.

4.5.2 Future work

One of the most pressing areas for further work lies within linking genotypes to phenotypes. If it was possible to be sure that certain variants only caused benign disease and/or tumours in certain tissues then surveillance programmes could be greatly curtailed and personalised towards individuals and families. This would mean that surveillance imaging could be targeted, with consequential lessening of pressure on health resources.

Another area where research is currently lacking, is the psychological effect on individuals and families. We currently do not know the mental health impact of these vigorous surveillance programmes, or that of being carriers of mutations with an unpredictable clinical course. Research

into these issues to establish the extent of distress caused and how this can begin to be rectified would be beneficial.

When investigating the historical patients the data presented was limited to only investigating for the likely presence of an underlying *SDH* mutation using SDHB immunohistochemistry. There are, however, many other known causative mutations and use of immunohistochemistry methods may be beneficial for investigating these in historical case cohorts to identify patients and relatives at risk of a predisposition to developing PPGLs.

Finally, another important area for future research lies in identifying novel treatments for malignant disease. Rates of metastatic disease are high in *SDHB* carriers, and much of this disease appears to remain resistant to conventional treatments.

Chapter 5. Immune cells in the tumour microenvironment of phaeochromocytoma and paraganglioma tumours

5.1   Background

Surgical resection is the only known cure for PPGLs, but 15-20% are associated with metastases and all should be considered as having malignant potential. Unlike other neoplasms, there are no known pathological or biochemical markers that can identify or predict which tumours have malignant potential, malignancy in PPGLs is defined once metastases are already present[294], by which time surgical cure is not an option. Only 30-60% of patients with metastatic disease live five years after initial diagnosis, although there is heterogeneity in tumour behaviour, with some PPGLs behaving more aggressively and others more indolently[295]. The reasons for these differences are largely unknown, although some PPGLs with underlying mutations in some genes, e.g. *SDHB*, *FH* and *MAX,* are known to behave more aggressively. Treatment options for metastatic PPGL (mPPGL) are limited. Historically chemotherapy with cyclophosphamide, dacarbazine and vincristine was used, but only a small number of patients demonstrated a response to treatment, with overwhelming toxicity being a major drawback[296]. In recent years more therapies have been explored. ^{131}I-MIBG[297], tyrosine kinase inhibitors (cabozantinib[298], temozolamide[299,300]) and peptide receptor radionuclide therapy (PRRT, 177-Lutetium-dotatate)[301,302] have been shown to be beneficial for some patients, but results of these small trials are conflicting.

In recent years there has been interest in whether manipulating the immune response to cancer could create more treatment options. Early attempts at immunotherapy for PPGLs using interferon alpha-2b, which activates natural killer cells, had to be suspended due to the high levels of side effects including renal failure, liver toxicity and decreased quality of life[303,304]. More recently, immune therapies such as immune checkpoint blockade (ICB) has shown promise in some cancer treatments[305]. These drugs inhibit the binding of programmed cell death 1 (PD-1) on the T cell to programmed death-ligand 1 (PD-L1) on the tumour cell and thereby permits the T cell to kill the tumour cell. Recent reports suggest that PPGL tumours caused by pseudohypoxia-related genes may particularly benefit from PD-L1 inhibition therapy as it was shown that increased expression of PD-L1 occurs via HIF-dependant mechanisms increasing the ability of tumour cells and surrounding stroma to repress T cell activity, thus suggesting T cell suppression is promoted by pseudohypoxia[306]. A recent phase II clinical trial which investigated the PD-L1 inhibitor pembrolizumab[307] demonstrated a modest

anti-neoplastic activity in mPPGLs. Despite this, treatment options for mPPGL are still lacking and therefore other targets for therapies need to be investigated.

PPGLs have one of the lowest rates of somatic mutations[24]. This leads to the expectation that they have a low immunogenic antigen density and minimal inflammation[307,308]. Historically they have been described as immunologically 'cold tumours' due to the minimal infiltration of tumour infiltrating lymphocytes (TILs)[309], but a small number of studies have demonstrated immune cells infiltrating into these tumours[307]. Cells of the innate immune system express both α- and β-adrenoreceptors and these have been reported to directly modulate innate immune cell functions[310,311]. In addition, catecholamines contribute to the chronic inflammatory response. Acute effects of catecholamine exposure are thought to be largely immunosuppressive[145], but continued exposure leads to heightened proinflammatory response of monocytes upon differentiation and re-stimulation[145]. The intra-tumoural effects has not been well studied.

5.1.1 Introduction to the tumour microenvironment and immune cells

Solid tumours are complex tissues consisting not only of tumour cells but other surrounding and supporting cells, such as endothelial cells, immune cells, fibroblasts, stromal cells, pericytes and extracellular matrix (ECM)[312] (Figure 5.1). The combination of these tumours cells and stromal cells together forms the tumour microenvironment (TME). Emerging evidence suggests that the TME plays a critical role in tumourigenesis; initiation, growth and metastasis[313]. Intercellular communication is driven by a complex network of cytokines, chemokines and inflammatory enzymes within the local ECM[312], and within the tumour these elements can promote cell trafficking, modulation of immune and stromal cells, angiogenesis, invasion and metastatic ability[312]. The TME appears to be highly specific to each tumour type[314]. Tumour evasion of immunosurveillance is a hallmark shared by all types of cancer[315]. Tumour-infiltrating immune cells have been identified in numerous solid tumours and densities of them have been found to correlate to clinical outcomes[316]. The discovery of immune cell populations in their TME may open up new treatment strategies[317].
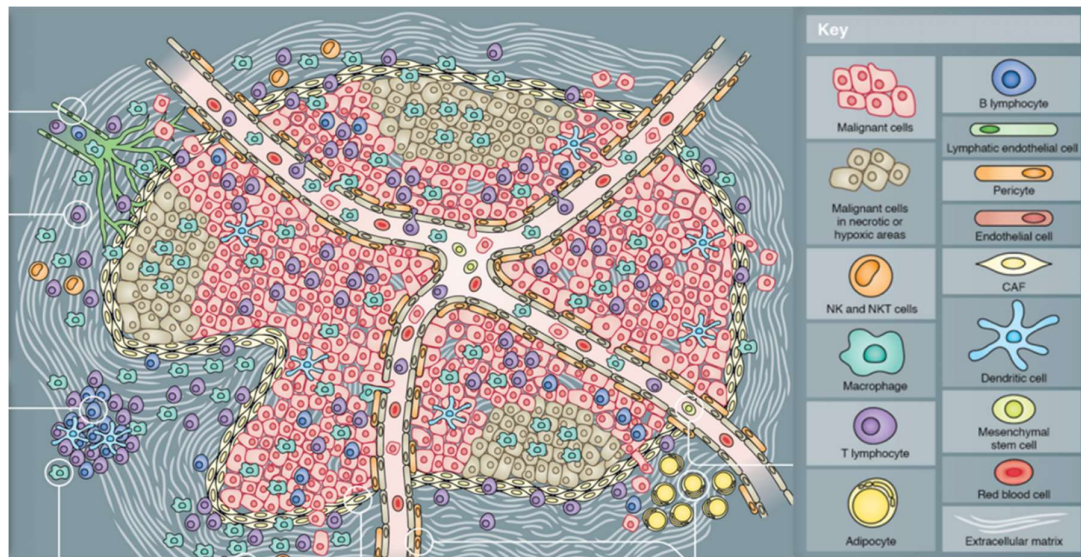
Figure 5.1: Diagrammatic representation of the tumour microenvironment. *Adapted from Balkwill et al[312], showing the different components of the TME.*

5.1.1.1 Macrophages

Macrophages play a major role in the TME as a component of immune cell infiltrate in tumours. There is evidence to suggest that macrophages undergo marked phenotypic changes when exposed to hypoxia and express a number of mitogenic and proangiogenic cytokines[318]. There are classically two main groups of macrophages: 'M1' (classically activated macrophages) and 'M2' (alternatively-activated or tumour associated macrophages (TAMs)). This distinction is important due to their differing biological properties. M1 arise following stimulation with Th1 cytokines (e.g. interferon-gamma (INFγ) and tumour necrosis factor alpha (TNFα)) or exposure to bacterial proteins (e.g. lipopolysaccharide). They secrete proinflammatory cytokines (e.g. interleukins (IL) IL1, IL6, IL8, IL12, IL23, and TNFα) and are associated with bactericidal and tumouricidal effects. TAMs (M2) are stimulated by Th2 cytokines (e.g. IL4, IL10, IL13), transforming growth factor beta (TGFβ) and glucocorticoids[319]. They secrete high levels of IL10 and IL1 receptor antagonist (IL1ra) and are associated with ECM remodelling, cell proliferation, immunosuppression and evasion, tumour progression, and they have a role in regulating the epithelial-mesenchymal transition (EMT) pathway. M2 macrophages are reported to be the most represented immune cell in human malignancies such as breast, bladder and prostate[320,321]. Macrophages can be found in all tissues of the body, but acquire specialised phenotypes depending on the local microenvironment[318]. Thus, depending on the stimuli from the TME, they can switch from an aerobic profile based on oxidative phosphorylation to an anaerobic one based on glycolysis and back again[322]. Gene mutations within the TCA cycle create a 'pseudohypoxic' TME, which could potentially support the phenotypic change in macrophages.

Little is known about the actions of macrophages in PPGL tumours. A small number of previous studies have been performed investigating immune infiltration in PPGLs and showed increased macrophage infiltration and lymphocyte depletion[308,317,323]. These studies suggest that macrophage infiltration may influence PPGL tumour behaviour, such as increased aggressiveness similar to other neoplasms such as breast[324,325], prostate[326], ovarian[326,327], thyroid[328,329] and neuroendocrine tumours (NETs)[330].

5.1.1.2 Lymphocytes

Various populations of T lymphocytes exist in the TME and draining lymph nodes. Cytotoxic CD8+ memory T cells are strongly associated with a good prognosis as they are capable of killing tumour cells[331]. Some studies show that a higher density of CD8 T cells predicts a better response to immune checkpoint inhibitor therapy[332]. CD4+ T cells are further subdivided into T helper 1 (Th1), Th2 and Th17 cells. Th1 lymphocytes support CD8 T cells and are also associated with a good prognosis[312,333]. They produce the cytokines IL2 and interferon gamma (INF-γ). Other T lymphocytes are thought to promote inflammation and tumour growth, such as Th2 cells which support B-cell function and produce immunosuppressive cytokines IL4, IL5 and IL13, and Th17 lymphocytes which produce IL17A, IL17F, IL21 and IL22[333]. Additionally immunosuppressive T regulatory cells (Tregs) are often reported to be tumour promoting[312]. These cells express forkhead box P3 (FOXP3) and CD25 and produce IL10 and TGFβ and exhibit cell-mediated contact through cytotoxic T lymphocyte antigen 4 (CTLA4) inhibiting recognition and clearance of tumour cells by the immune system[312,334]. B lymphocytes are found mainly in lymph nodes and reports on whether they correlate with a good or bad prognosis in different cancers are mixed[312]. Natural killer cells can infiltrate tumoural stroma, but they are not found in contact with tumour cells. They are generally thought to predict a good prognosis through their cell-killing activity, although there have been reports that this function can be inhibited by malignant cell-derived TGFβ[312,333].

In ACC, high levels of infiltrating T cells have been reported to correlate with better survival[335], but generally in the few studies that have looked at lymphocyte infiltration in PPGLs lymphocyte depletion has been reported[308,317,323].

5.1.1.3 Neutrophils

Neutrophils are a type of white blood cell usually found in the blood stream and form part of the innate immune response. They are highly mobile and one of the first responders to migrate towards the site of inflammation drawn by IL8 signals. IL8 is a proinflammatory cytokine produced in response to inflammation or environmental stress such as hypoxia[336]. Intra-tumoural expression of IL8 is proposed to be a key regulator of infiltrating neutrophil recruitment into the TME, which may then

promote metastasis[337]. However, the role of tumour-associated neutrophils is controversial[312] and no reports in the literature could be found on the contribution of neutrophils in the TME of PPGLs.

5.1.1.4 The role of cytokines in the TME

With growing interest in the role of the TME in cancer development in the last decade, the role of cytokines has been demonstrated in different cancers such as breast, prostate, melanoma, oesophageal, non-small cell lung, bladder and pancreatic cancer[312,338], and more recently in endocrine tumours such as thyroid cancer[339] and NETs[314].

Cytokines are secreted proteins that mediate communication between cells. They include chemokines, growth factors, interferons, interleukins and angiogenic factors (Table 5.1). They can act in a paracrine or autocrine manner and have different functions with some providing host defence and others promoting cell growth[315]. It has been suggested that a pro-inflammatory cytokine population in the TME may promote local invasion[340] and transmigration[341] of tumour cells.

Chromaffin cells release catecholamines and peptides in response to various stress related signals. Cytokines secreted by immune cells can modulate the amount and composition of the adrenal medulla output, but conversely secretions from the adrenal medulla can have wide ranging actions on immune cell functions[342]. Adrenal medulla peptides can be either immunosuppressive (vasoactive peptide (VIP), pituitary adenylate cyclase-activating polypeptide (PACAP), enkephalin, galanin) or immunostimulatory (cortisol-releasing hormone (CRH), substance P (SP)) by direct action of immune cells or indirectly through stimulating adrenal cortex steroid production[342]. The best described cytokines associated with the adrenal medulla are IFNα, IL6, IL1 and TNFα[342].

Classification of cytokines by immune response	
Immune response	**Members**
Adaptive immunity	IL-2, IL-3, IL-4, IL-5, IL-7, IL-9, IL-13, IL-15, IL-21, GM-CSF, G-CSF, M-CSF, EPO, TSLP
Pro-inflammatory signalling	IL-1 (IL-1α, IL-1β, IL-1ra), IL-6, IL-11, IL-17A, IL-18, IL-25, IL-31, IL-33, IL-36, IL-36ra, IL-37, IFNα, IFNβ, IFNγ, IFNλ, IFNκ, TNFα, TNFβ, CNTF, CT-1, LIF, OPN, OSM
Anti-inflammatory signalling	IL-10, IL-12, IL-19, IL-20, IL-21, IL-22, IL-24, IL-26, IL-27, IL-28, IL-29, IL-35

Classification of cytokines by main source, target cell and primary function				
Family	**Cytokine**	**Main source**	**Target cell**	**Primary function**
Interleukins	IL-1	M, DC, B cells	B, NK and T cells	Pyrogenic, pro-inflammatory, proliferation, differentiation, angiogenic
	IL-2	T cells	B, NK and T cells	Proliferation, cell activation (Th1 cytokine)
	IL-3	T cells, NK cells	B and T cells, SC	Haematopoietic precursor proliferation and differentiation
	IL-4	Th cells	B cells, T cells, M	Proliferation of B and T cells, stimulation of IgG and IgE production, enhances MHC class II expression
	IL-6	Th cells, fibroblasts, M	Activated B cells, plasma cells	Differentiation into plasma cells, IgG production, pro-inflammatory, proliferation (Th1 cytokine), angiogenic
	IL-7	BM stromal cells, EC	SC	B and T cell growth factor, thymocyte growth, survival T cells, haematopoiesis
	IL-8	M	Neutrophils	Chemotaxis, pro-inflammatory
	IL-9	T cells	T cell	Cell growth and proliferation
	IL-10	T cells	M, B cells	Inhibits cytokine production and mononuclear cell function, anti-inflammatory (Th2 cytokine)
	IL-11	BM stromal cells	B cells	Differentiation, induction of acute phase proteins
	IL-12	T cells	NK cells	Activation of NK cells, pro-inflammatory (Th1 cytokine)
	IL-13	T cells	M, B cells	Inhibits cytokine production and mononuclear cell function, anti-inflammatory (Th2 cytokine)
	IL-15	Monocytes	T, NK and mast cells	Mast cell growth, NK cell development and activity, T cell proliferation
	IL-18	T cells	B, NK and T cells	Proliferation, cell activation (Th1 cytokine)
	IL-21	T cells	B cells	Inhibits B cell proliferation
Tumour Necrosis Factor	TNF-α	M, monocytes	M, tumour cells	Phagocyte cell activation, endotoxic shock, Tumour cytotoxicity

	TNF-β	T cells	Phagocytes, tumour cells	Chemotaxis, phagocytosis, oncostatic, induction of other cytokines
Interferons	IFN-α	Leukocytes	Various	Anti-viral, anti-angiogenic
	IFN-β	Fibroblasts	Various	Anti-viral, anti-proliferative, anti-angiogenic
	IFN-γ	T cells	Various	Anti-viral, macrophage activation, increase neutrophil function, increase expression of MHC
Colony Stimulating factors	G-CSF	Fibroblasts, endothelial cells	SC in BM	Granulocyte production
	GM-CSF	T cells, M, fibroblasts	SC in BM	Granulocytes, monocytes and eosinophils production
	M-CSF	Fibroblasts, endothelial cells	SC in BM	Monocyte production and activation
	EPO	Endothelial cells	SC in BM	Red blood cell production
Others	TGF-β	T and B cells	Activated T and B cells	Inhibit T and B cell proliferation, inhibit haematopoiesis, promotes fibrosis and wound healing
	FGF	Various	Fibroblasts	Angiogenic, promotes fibrosis and wound healing, cell proliferation and differentiation, fibroblast proliferation
	VEGF	Various	Endothelium	Angiogenic, lymphangiogenesis, chemotaxis

Table 5.1: Classification of cytokines. Classification shown is based on immune response and family to which they belong. Main source of each cytokine, it's target cell and primary function are provided. Adapted from Pedro Marques with permission. BM bone marrow, CNTF ciliary neurotrophic factor, DC dendritic cells, EC epithelial cells, EPO erythropoietin, FGF fibroblast growth factor, G-CSF granulocyte-colony stimulating factor, GM CSF granulocyte macrophage colony stimulating factor, IFN interferon, Ig immunoglobulin, IL interleukin, LIF leukaemia inhibitory factor, M macrophages, MHC major histocompatibility, NK natural killer cells, OPN osteopontin, OSM oncostatin, SC stem cells, TSLP thymic stromal lymphopoietin, TGF transforming growth factor TNF tumour necrosis factor, VEGF vascular endothelial growth factor

IFNs are secreted by a variety of cell types including macrophages, monocytes, lymphocytes, fibroblasts, glia and neurons, but are not secreted by chromaffin cells[342]. Chromaffin cells are responsive to IFNs, which appear to have an inhibitory influence on secretory activity and can activate the protein kinase C (PKC) dependent ERK1/2 pathways[342]. It has also been suggested that IFNγ can induce apoptosis in these cells via the STAT3 signalling pathway[342].

IL6 levels are low in healthy individuals but rise rapidly in response to infection or tissue damage[342]. IL6 is produced by adrenal cortical cells and in single cells in the human medulla[343]. A stress response release of cortisol and catecholamines promotes IL6 production. IL6 regulates immune reactions, haematopoiesis and acute and chronic inflammatory responses and is associated with systemic inflammatory syndrome[342]. The classical inflammatory response is mediated by local cytokines IL1 and TNFα. IL1 plays an important role in neuroendocrine adaptation to acute and chronic stressors, and is

present in chromaffin cells[344]. IL1 has a wide spectrum of inflammatory, metabolic and immunological properties and can promote growth and maintenance of tumours[344]. Succinate acts as an inflammatory signal, and it has been shown to induce IL1b production via HIF1α[345]. IL1b has been shown to promote malignant transformation in other forms of cancer including colorectal and oral cancers[346,347]. Cytokines, including IL6 and IL1, are able to induce activation of inducible nitric oxide synthase[176]. Nitric oxide is a potent systemic vasodilator, but at a tumour level it could potentially alter the TME by creating a local inflammatory response, allowing easier dispersion of tumour cells.

TNFα is a multifunctional proinflammatory cytokine with widespread actions. It is expressed within steroid producing cells within the zona reticularis and medulla, but not within chromaffin cells themselves. TNFα induces neuropeptide expression and secretion from chromaffin cells, with activation of the NFκB pathway. PACAP released from stimulated splanchnic nerves, enhances the ability of TNFα to upregulate galanin and VIP expression in chromaffin cells. TNFα and IL6 have a role as intra-adrenal factors that regulate adrenal steroid production. TGFα expression has been demonstrated in the majority of PCCs[348].

There are a handful of case reports documenting cytokine release from PCCs[176,178-180,349-354], and one recent small case series[355], mainly relating to IL6 production, although IL-1[344], TNFα[142,356] and IL8[142] have also been reported. When these cytokines are systemically distributed, and levels are detected in the plasma the patients often experience fever and other symptoms of an inflammatory syndrome including weight loss, anorexia and malaise. One interesting study showed that plasma IL6 and TNFα were substantially higher in patients undergoing laparoscopic adrenalectomy than laparoscopic cholecystectomy and remained high for at least five days post-operatively in the former. This suggests that these cytokines are being released from either the PCC tumour cells themselves or TME, rather than this just being a response to the stress of surgery[357]. No studies examine local cytokine production and the effect this may have on the TME in PPGLs and if this may affect their migration and invasiveness ability. One study[358] looking at the distribution of growth factors and cytokines in PGL tissue has shown that the extent and distribution varied between specimens. Whereas IL6, TNFα and IGF-1 were present in both chromaffin and sustentacular cells, leukaemia inhibitory factor (LIF) was restricted to chromaffin cells in tumours and endothelial growth factor (EGF) to sustentacular cells only. EGF was seen in some but not all tumours.

Craniopharyngiomas are another non-glial tumour of the nervous system, that are deemed benign, but are locally invasive and thus have high morbidity. It has been shown that the TME of craniopharyngiomas is rich in cytokines[359], specifically IL6, IL8 and MCP1[360]. Recently it has been

suggested that this is in part due to the upregulated expression of the ion channel P2X7R in these tumours. The authors demonstrated that P2X7R activation promoted local cytokine production[360].

Few studies have looked at the TME in *SDH* disease. It has been demonstrated in mouse cell line models that the TME (in this case represented by the presence of cancer-associated-fibroblasts (CAFs)) can induce metabolic changes and increase proliferation in *SDHB*-silenced neuroblastoma cells[361] and more recently that this same TME can upregulate the migration and invasion ability of *SDHB*-silenced spheroid PCC cell cultures, due to increased secretion of lactate by CAFs[362].

Conventional methods to assess cytokine levels utilises enzyme-linked immunosorbent assay (ELISA); however, this method is limited as only one cytokine can be measured at a time. Protein arrays now exist that can simultaneously quantify multiple different cytokines.

The commonalities in TME's across many neoplasms suggest that targeting cells in the TME and their mediators could have applications for treatment options[312].

Little is known about the important components of the TME in PPGL tumours and the contribution the different elements of the TME have on the developing PPGL tumours, and to my knowledge this has never before been compared to non-pathological medulla.

5.1.1.5 Serum inflammation-based scoring

Inflammation is an important process in cancer physiology with both effects of promoting carcinogenesis and protective effects of initiating immune responses to tumour cells[104]. It has been suggested that catecholamines can cause subclinical and even mild systemic inflammation with a study showing higher levels of leukocytes, neutrophils and CRP[141] in patients with PCC compared to patients with primary aldosteronism or essential hypertension, with a decrease in levels post adrenalectomy[146]. Catecholamines can cause a neutrophilia[363,364] and there have been case reports on persistent neutrophilia being the presenting symptoms of PCC[365]. Studies have shown that serum inflammation scores can correlate with clinical outcome in some cancers[104,366]. This has also been applied to study some endocrine tumours including thyroid carcinoma[367,368], NETs[197-200], crainopharyginomas[196,369] and pituitary adenomas[193]. Several scoring based systems have been used which utilise values obtained from standard blood tests: Neutrophil-to-Lymphocyte Ratio (NLR)[104,370,371], Platelet-to-Lymphocyte Ratio (PLR)[104,372], Lymphocyte-to-Monocyte Ratio (LMR)[373,374], Neutrophil-Platelet Score (NPS)[106] and Systemic Immune-Inflammation Index (SII)[105]. The prognostic nutrition index (PNI) and the Glasgow Prognostic score (GPS) assess the nutritional status of patients[104,366,375]. Increased NLR, PLR, NPS, SII and GPS and low LMR and PNI are associated with poor clinical outcomes[104,370,374,375]. To my knowledge only two studies have looked at applying these

inflammation scores in patients with PPGLs[145,174] and both of these had small patient numbers and were unable to investigate differences within the PCC group, but overall found higher proinflammatory responses compared to controls. This suggests PPGLs do cause a systemic inflammatory response and serum markers may be useful in predicting clinical outcome.

5.1.2 Somatostatin receptors in PPGL

Many neuroendocrine tumours express one or more somatostatin receptor subtype (SSTR1-5). Somatostatin (SST) is a neuropeptide with an affinity for all five receptor subtypes and can inhibit both hormone secretion and cell proliferation. SST analogues have long been used to achieve symptomatic relief in other neuroendocrine tumours such as gut or pancreatic secretory NETs. In randomised multinational studies, SST analogues (Octreotide, Octreotide LAR, Lanreotide, Pasireotide) have also been shown to have anti-proliferative effects and prolong the time to progression of disease for inoperable NETs that express SSTRs[376,377]. They have been used to both slow tumour growth and promote tumour regression[377-379].

The anti-proliferative effects of SST analogues in patients with NETs were clearly demonstrated in the PROMID (Octreotide LAR)[377] and CLARINET (Lanreotide)[376] studies. Anti-proliferative effects are thought to occur by direct binding of the SST analogues to SST receptors (SSTR). This induces apoptosis and cell cycle arrest through regulation of phosphotyrosine phosphatase and mitogen-activated protein kinase and blocking the effects of growth factor receptor stimulation, resulting in increased production of cell cycle inhibitor P27 and affect the P13K/Akt/mammalian target of rapamycin (mTOR) pathways[380].

PGLs are neuroendocrine in origin and although the original discovery of SSTR overexpression in PPGLs occurred in the 1990's[381], further studies into this have been limited and conflicting. Although some case reports have suggested a certain level of success in the treatment of metastatic PPGLs with SST analogues[382,383], a small placebo controlled study demonstrated no antisecretory effects[384]. In studies looking at reduction/stability of disease, rather than symptomatic control, results have been variable[301,302], and underlying genetic status is often not known. Studies have demonstrated the usefulness of using SSTR IHC as a method of predicting responsiveness to SST therapy in other tumours[116].

Previous studies have confirmed all PPGLs immunostain strongly positive for SSTR1 and negative for SSTR4 and SSTR5[385] and therefore the work presented here focuses on SSTR2 and SSTR3 where previous reports have been conflicting.

5.1.3 Gaps in current knowledge to be addressed by this thesis

I. The types of cytokines present in the PPGL TME and the effect this may have on malignant potential.

II. What comprises the immune cell components of the TME of PPGLs.

III. Use of serum-based inflammatory scores in PPGLs and whether they can predict clinical outcomes.

IV. Whether SSTR expression in PPGLs differs due to underlying germline mutations and correlates with malignant potential.

5.2 Aims

I. To characterise the TME in PPGL tumours

To characterise the different cytokines and infiltrating immune cell types present in the TME of PPGL tumours and non-pathological adrenal medulla.

To investigate whether genetic status influences the immune TME.

To characterise circulating immune and inflammation-based scores and ascertain whether these correlate with the TME of PPGL tumours and can be used to predict prognosis in patients with PPGL tumours.

ii. To characterise SSTR expression in PPGL tumours

To use SSTR immunohistochemistry to investigate whether there are any differences between PPGLs due to *SDH* germline mutations and sporadic PPGLs.

To use SSTR immunohistochemistry to investigate whether there are any differences between different *SDH* subunits and between malignant and benign PPGL tumours.

5.3   Results

5.3.1   Primary culture of PPGL and non-pathological medulla cells

A primary culture of PPGL tumour cells and cells from non-pathological adrenal medulla tissue was established. Non-pathological adrenal medulla tissue was harvested from adrenal glands removed from patients with PPGLs and adrenal cortical primary aldosteronism tumours, to investigate which cytokines predominate in the TME of non-pathological and tumour chromaffin tissue. The clinical details of the patients from whom the tumours were removed are shown in Table 5.2 and included three PCCs and four PGLs from two males and five female patients. All of the PPGLs were functional and produced norepinephrine and in addition two also co-secreted epinephrine and one dopamine.

	PPGLs	Non-pathological medulla
Total	7	5
Cultured in CM	5	3
Cultured in 1% media	7	5
Gender [n(%)]	2M (29%)	4M (80%)
Type [n(%)]:		
PCC	3 (42%)	
PGL	4 (57%)	
Location [n(%)]:		
PCC	3 (43%)	
Abdo PGL	2 (29%)	
Pelvic PGL	1 (14%)	
HNPGL	1 (14%)	
Genetics [n(%)]:		
Negative	3 (43%)	
NT*	2 (29%)	
Positive	2 (29%)	
FH	1 (14%)	
SDHB	1 (14%)	
Functional [n(%)]:	7 (100%)	
Plasma MN	2 (29%)	
Plasma NMN	7 (100%)	
Plasma 3MT	1 (14%)	
Plasma Metanephrines (mean + SD):	1088 +/- 2208	
Plasma MN	9583 +/- 7519	
Plasma NMN	31.16 +/- 76	
Plasma 3MT		
Age at diagnosis: (years) (mean + range)	46.9 (18-69)	
Ki67: (%) (mean + range)	<1% (0-5%)	
Size of PPGL: (mm) (mean + range)	49.4 (22-100)	

Table 5.2: Clinical characteristics of the tumours cultured. *In total seven PPGL tumours and five non-pathological medulla tissue were cultured in either complete media (CM, containing 10% bovine serum) or 1% serum media (containing 1% bovine serum). The table shows the type of tumour, location, underlying genetic diagnosis, whether the tumour was functional and what hormones it was producing. *genetics not tested as patients did not meet the age criteria for NHS testing. CM complete media), PCC phaeochromocytoma, PGL paraganglioma, Abdo abdominal, HNPGL head & neck paraganglioma, NT not tested, FH fumarate hydratase, SDHB Succinate dehydrogenase subunit B, MN metanephrine, NMN normetanephrine, 3MT 3-methoxytyramine*

In total, I studied seven PPGL tumours and five non-pathological medulla tissue samples. To ascertain the viability of the cells in culture they were initially cultured in complete media (containing 10% bovine serum) for one week, cell density (Figure 5.4) and metanephrine levels were measured daily to assess the survival rate of the cells (Figure 5.5). Media was removed and replaced with fresh media every 24 hours to remove dead cells and replenish nutrients. There were higher levels of all three metanephrines in the cells cultured from the PPGLs than the non-pathological medulla. Concentrations of metanephrines dropped dramatically after day two (48 hours in culture), this is in keeping with the microscopy photographs (Figure 5.2) and the results of the cell density assay (Figure 5.4) that show similar numbers of cells for the first two days, then a rapid decline, suggesting a high cell death rate from this time. Microscopy photographs demonstrated larger cells of varying shapes from day five onwards, suggesting the introduction of fibroblasts (Figure 5.2 D5&D7), which are also demonstrated on the immunofluorescence images (Figure 5.6, Figure 5.7). Concentrations of NMN and MN did not decrease to zero over one week, suggesting some chromaffin cells remained alive over this time period. Concentrations of 3MT were very low in non-pathological medulla culture and dropped to zero at day two and dropped to zero on day four in PPGL cultured cells (Figure 5.5).
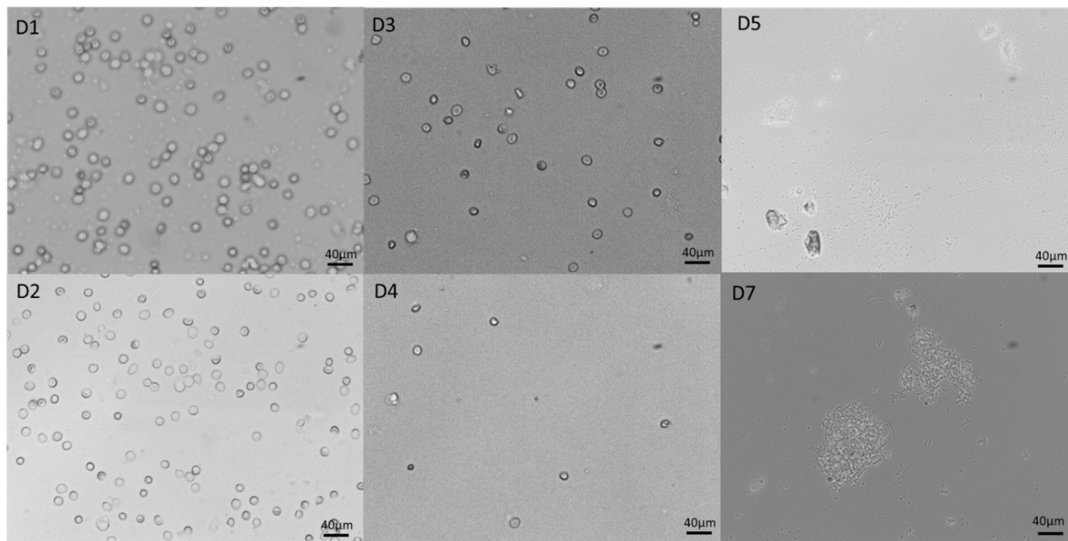
Figure 5.2: Light microscopy photographs of cultured PPGL cells. Cells were cultured and allowed to adhere for 36 hours, media was then replaced with fresh media every 24 hours. Photographs taken over seven days at x20 magnification.
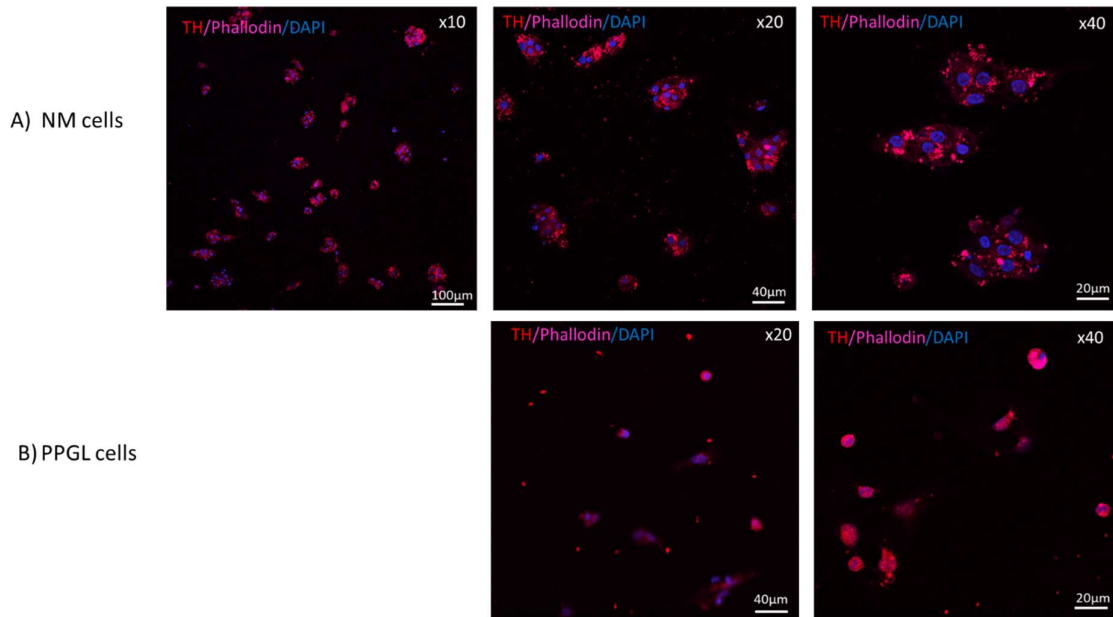
Figure 5.3: Merged immunofluorescence images of cultured non-pathological medulla cells and PPGL cells at different magnifications. *A) Cultured non-pathological medulla cells showing cell clusters at x10, x20 and x40 magnification. B) Cultured PPGL cells showing single tumour cells at x20 and x40 magnification. Cells were cultured and allowed to adhere for 36 hours and then fixed and stained for tyrosine hydroxylase (TH, red), phalloidin (magenta) and counterstained with DAPI (blue). NM non-pathological medulla, PPGL phaeochromocytoma and paraganglioma.*
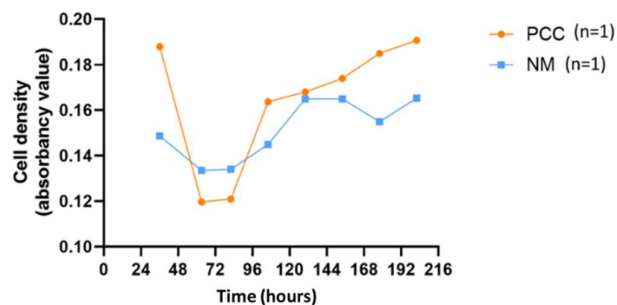
Figure 5.4: Cell density in cultured PPGL tumours and non-pathological medulla cells over one week. *Cells were cultured and allowed to adhere for 36 hours, old media containing dead cell was removed and fresh media was then given every 24 hours. Cell density measured using crystal violet assay. PCC phaeochromocytoma, NM non-pathological medulla.*
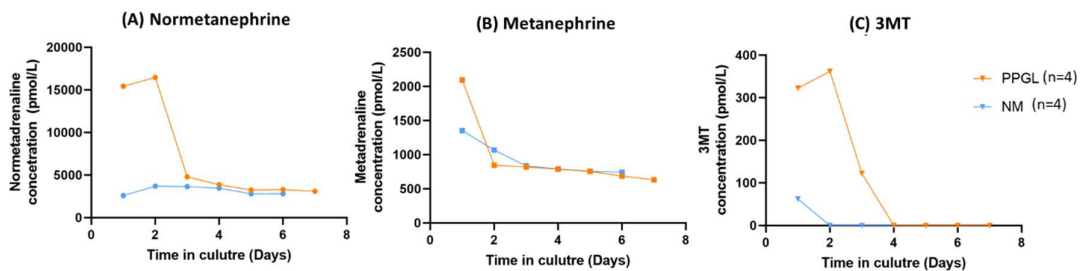
Figure 5.5: Concentration of metanephrines in supernatant of cultured PPGL tumours and non-pathological medulla cells over one week. *Cells were cultured and allowed to adhere for 36 hours, fresh complete media (containing 10% bovine serum) was then given every 24 hours and samples were taken at 24-hour intervals. 3MT 3-methoxytyramine, PPGL phaeochromocytoma and paraganglioma, NM non-pathological medulla.*
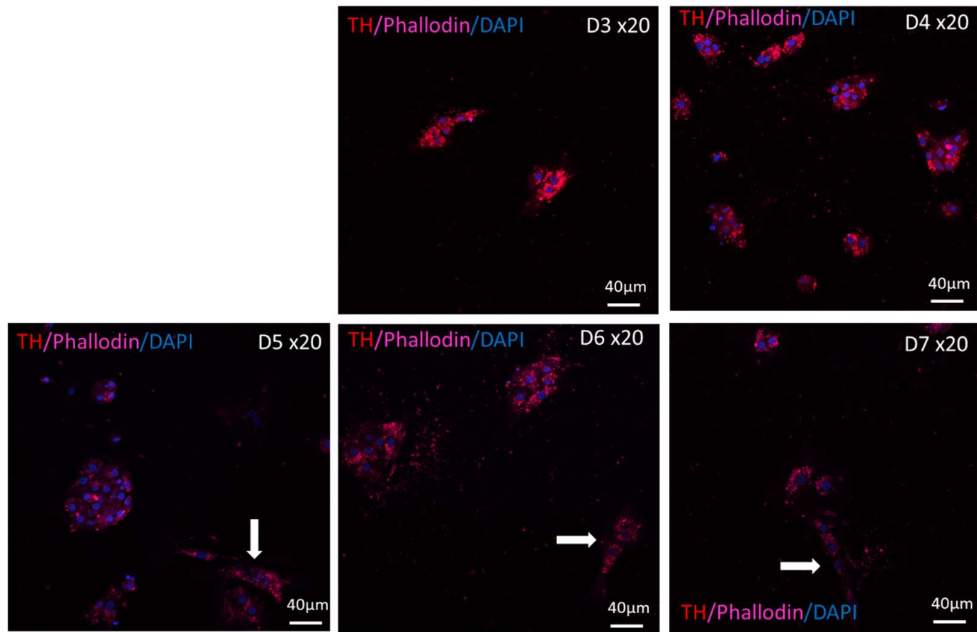
Figure 5.6: Merged immunofluorescence images of cultured non-pathological medulla cells. Images show microscopy photographs of merged immunofluorescence images of cultured non-pathological medulla cells at x20 magnification over seven days. Cells were cultured and allowed to adhere for 36 hours and then fixed and stained for tyrosine hydroxylase (TH), phalloidin and counterstained with DAPI. White arrows show fibroblasts emerging on day 5 onwards. D3 day 3.
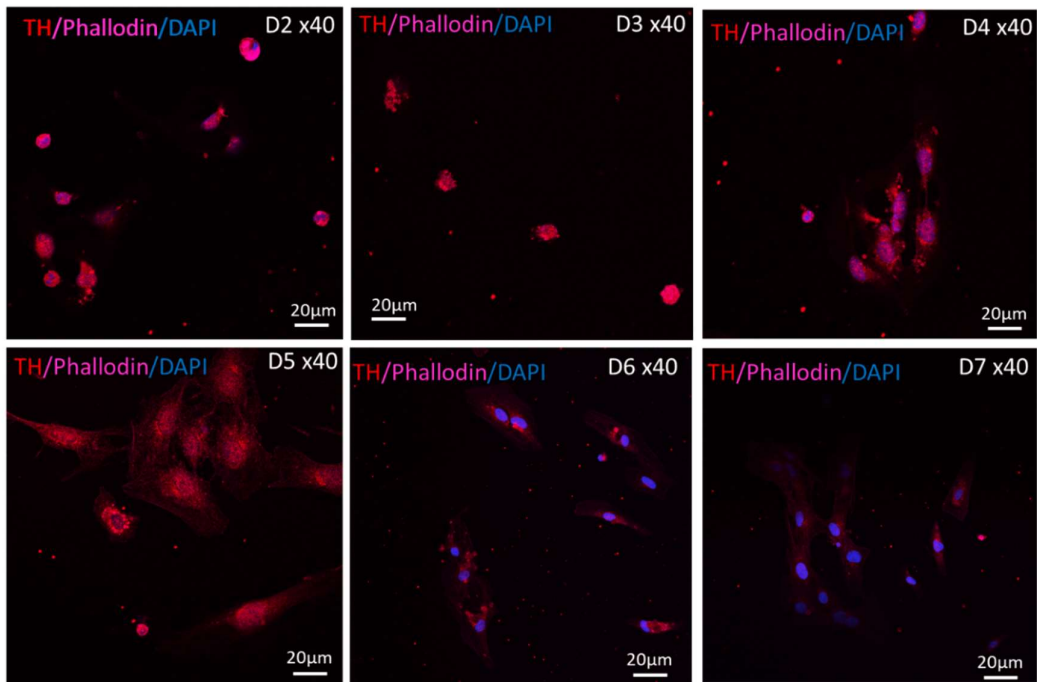
Figure 5.7: Merged immunofluorescence images of cultured PPGL cells. Images show microscopy photographs of merged immunofluorescence images of cultured PPGL cells at x40 magnification over seven days. Cells were cultured and allowed to adhere for 36 hours and then fixed and stained for tyrosine hydroxylase (TH), phalloidin and counterstained with DAPI. Fibroblasts are emerging from day 5 onwards. D2 day 2.

For the cytokine analysis cells were cultured in complete media (containing 10% bovine serum) for 36 hours to allow cells to adhere, this was then changed to 1% serum media for 24 hours before collecting supernatant for cytokine analysis. Subsequent analysis showed that the cells did not survive long in the 1% media (Figure 5.8) and therefore further experiments were undertaken using complete (containing 10% bovine serum) media.
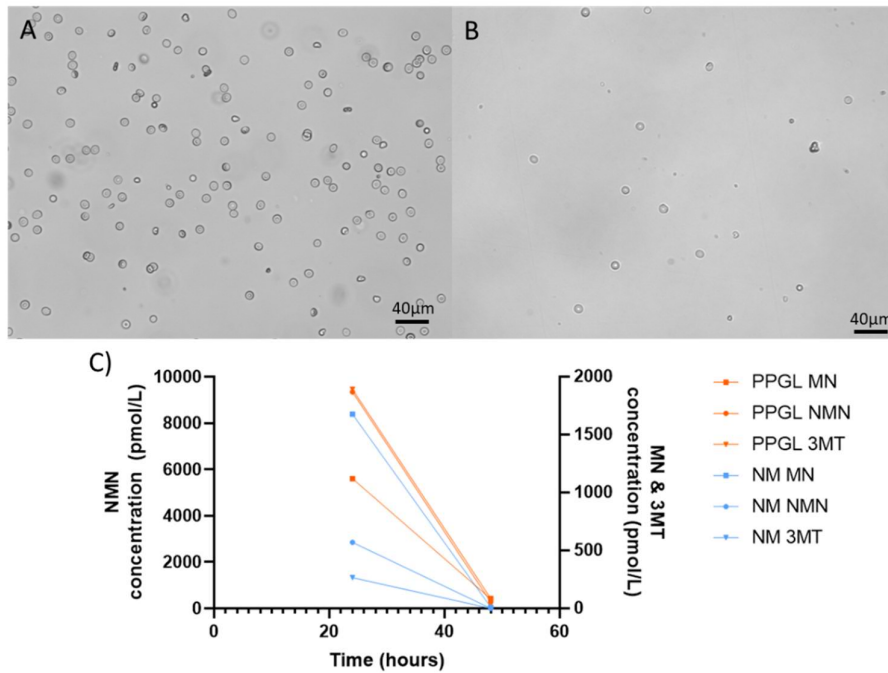
Figure 5.8: Cultured PPGL cells in 1% serum media. *Images show the deleterious effects when PPGL cells were cultured in 1% serum media. Cells were cultured in complete media (containing 10% bovine serum) for 24 hours and then changed to 1% serum media. A) microscopy photograph showing PPGL cells cultured in complete media for 24 hours. B) microscopy photograph showing PPGL cells cultured in complete media for 24 hours and then changed to 1% serum media for 24 hours. C) metanephrine concentrations in cultured PPGL cells at 24 hours and then after a further 24 hours in 1% serum media. PPGL phaeochromocytoma and paraganglioma, NM non-pathological medulla, MN metanephrine, NMN normetanephrine, 3MT 3-methoxytyramine.*

5.3.2 The cytokine profile of PPGL TME

The cohort of patients described above (Table 5.2) were used to assess the cytokine profiles in PPGL and non-pathological medulla TME. The concentrations of 42 cytokines were assessed in fresh supernatant of cultured cells from seven PPGLs and five non-pathological medullas. As a result of the majority of the cells dying after 24 hours in 1% serum media the data has been divided into two subsets showing the eight cultured specimens (five PPGL tumours and three non-pathological medulla) measured in complete media in which the majority of cells remained viable for the duration of the experiment, and for completion the original 10 cultures (six PPGL tumours and four non-pathological medulla) cultured in 1% media.

The number of tumours or non-pathological medulla that produced any detectable cytokines (taken as producing concentration levels above the lowest standard curve point in the serum) is shown in the table below (Table 5.3). As the lowest curve point was zero for many of the cytokines, a cut off at the second standard point of the curve was used to identify cytokines that were produced at higher levels. In general interleukins were either not secreted at all or secreted in tiny amounts, with the exceptions of IL6, IL8 and IL18 (all of which were secreted at levels above point two on the standard curve). All of the tumours secreted FGF, MDC, IL6, IL8, IP10 and MCP1. In addition, FGF, MDC, IL8 and IP10 were also secreted by all the non-pathological medulla samples. No cytokine or chemokine was secreted solely by the cultured non-pathological medulla cells.

PPGLs tumours are more often secretory than non-pathological medulla (52% vs 32%, p<0.0001).

	No. > standard 1		No. > standard 2	
Cytokine/ Chemokine	NM (n=3)	Tumour (n=5)	NM (n=3)	Tumour (n=5)
EGF	3 (100%)	5 (100%)	2 (66%)	4 (80%)
FGF	3 (100%)	5 (100%)	3 (100%)	5 (100%)
GCSF	1 (33%)	4 (80%)	1 (33%)	2 (40%)
GROα	3 (100%)	5 (100%)	3 (100%)	4 (80%)
MCP3	2 (66%)	2 (40%)	2 (66%)	2 (40%)
MDC	3 (100%)	5 (100%)	3 (100%)	5 (100%)
PDGF-AA	0	3 (60%)	0	4 (80%)
IL6	1 (33%)	5 (100%)	1 (33%)	5 (100%)
IL8	3 (100%)	5 (100%)	3 (100%)	5 (100%)
IP10	3 (100%)	5 (100%)	3 (100%)	5 (100%)
MCP1	3 (100%)	5 (100%)	1 (33%)	5 (100%)
MIP-1α	2 (66%)	4 (80%)	1 (33%)	3 (60%)
IL-18	1 (33%)	4 (80%)	1 (33%)	3 (60%)
GM-CSF	3 (100%)	5 (100%)	0	1 (20%)
IFNγ	0	5 (100%)	0	0
IL-10	0	3 (60%)	0	1 (20%)
IL-12P40	3 (100%)	5 (100%)	0	0
IL-1RA	2 (66%)	4 (80%)	0	1 (20%)
IL-1B	1 (33%)	4 (80%)	0	0
IL-4	3 (100%)	5 (100%)	0	1 (20%)
MIP-1B	2 (66%)	3 (60%)	0	1 (20%)
RANTES	0	3 (60%)	0	3 (60%)
TNFα	1 (33%)	4 (80%)	0	3 (60%)
VEGF-A	2 (66%)	4 (80%)	0	2 (40%)
TOTAL	45 (62.5%)	102 (81.6%)	24 (32%)	65 (52%)
p value	p<0.0001		p<0.0001	

Table 5.3: Detectable cytokines/chemokines in supernatant of cultured PPGL tumour or non-pathological medulla cells grown in complete media. Cytokine/chemokine profile determined from human Millipore MILLIPLEX Cytokine-42-Plex array. Eotaxin, TGFα, Flt-3L, Fractalkine, INFα2, IFNγ, IL12P40, IL12P70, Il13, IL15, PDGFβ, IL1α, IL9, IL2, IL3, IL5 and IL7 were not detected (e.g. below lowest concentration on standard curve). Number (and percentage) of samples that produced each cytokine/chemokine is shown. Statistical analysis performed with Chi squared (p<0.0001). NM non-pathological medulla

All of the cultured cells, both tumour and non-pathological medulla secreted some concentration of EGF, FGF, GROα, MDC, IL8, IP10, MCP-1, GM-CSF, IL-12P40, IL4 and PDGF-AA, IFNγ, IL10, RANTES were secreted only by the cultured tumour cells. Eotaxin, TGFα, Flt-3L, Fractalkine, INFα2, IFNγ, IL12P40, IL12P70, Il13, IL15, PDGFβ, IL1α, IL9, IL2, IL3, IL5 and IL7 were not detected. There were significantly higher concentrations of MDC (p=0.02), IP10 (p=0.01), IL-18 (p=0.02) and IFNγ (p<0.001) derived from PPGL tumour cells than non-pathological medulla cells cultured in complete media (Table 5.4, Figure 5.9). There was a trend towards a higher concentration of FGF (p=0.07) and IL-1β (p=0.09) in the PPGL cells. Cytokines/chemokines were not detected in the cell free complete media samples except GROα,

MCP3 and IP10, and even for these cytokines/chemokines concentrations were higher in culture samples (>10x) with the exception of MCP3.

Cytokine/ Chemokine	Concentration in cell free media (pg/mL)	Tumour (n=5) (pg/mL)		Non-pathological medulla (n=3) (pg/mL)		p value
		Mean	+/- SEM	Mean	+/- SEM	
EGF	0.00	7.4	0.5	5.5	1.2	0.12
FGF	0.00	77.6	23.9	6.9	2.8	0.07
GCSF	0.00	10.9	7.7	10.9	7.4	1.00
GROα	8.57	134.1	64.1	18.6	10.3	0.23
MCP3	4.52	4.2	0.68	7.0	1.6	0.11
MDC	0.00	83.3	10.3	29.9	12.9	*0.02
PDGF-AA	0.05	3.8	1.4	15.4	15.3	0.34
IL6	0.00	117.0	75.7	3.9	3.8	0.31
IL8	0.11	985.0	411.1	74.0	70.7	0.15
IP10	1.67	34.8	4.8	8.8	4.2	*0.01
MCP1	0.00	344.8	168.1	35.0	20.0	0.22
MIP-1α	0.00	20.7	8.9	29	2.5	0.19
IL-18	0.00	4.2	0.9	0.5	0.3	*0.02
GM-CSF	0.46	2.7	0.6	1.3	0.2	0.15
IFNγ	0.32	1.1	0.06	0.5	0.1	*<0.001
IL-10	0.16	1.47	0.7	0.24	0.09	0.23
IL-12P40	0.00	1.65	0.3	1.28	0.07	0.42
IL-1RA	0.00	7.87	6.4	0.74	0.3	0.44
IL-1β	0.12	1.59	0.4	0.38	0.2	0.09
IL-4	0.00	2.19	0.8	0.87	0.3	0.28
MIP-1β	0.00	3.06	1.4	0.8	0.4	0.29
RANTES	0.00	5.07	2.4	0	0	0.16
TNFα	0.00	4.44	1.7	0.43	0.4	0.12
VEGF-A	0.00	4.42	2.3	0.55	0.2	0.26

*Table 5.4: Concentrations of secreted cytokines/chemokines in cultured tumour or non-pathological medulla cells grown in complete media. Cytokine/chemokine profile determined from human Millipore MILLIPLEX Cytokine-42-Plex array. Eotaxin, TGFα, Flt-3L, Fractalkine, INFα2, IFNγ, IL12P40, IL12P70, Il13, IL15, PDGFβ, IL1α, IL9, IL2, IL3, IL5 and IL7 were not detected (e.g. below lowest concentration on standard curve). Mean concentrations are shown (pg/mL) +/- SEM for PPGL tumours (n=5) and non-pathological medulla (n=3). P value is shown for a comparison between the tumour and non-pathological medulla, *denotes significant results.*

Although statistical significance was not reached with this low number of samples, there was >10 times higher mean concentrations of IL6 (29x), IL8 (13x), MCP1 (10x), TNFα (10x) and FGF (11x) in the cultured tumour cells compared to the non-pathological medulla. Only PDGF-AA and MCP3 were secreted in higher levels in non-pathological medulla cells than PPGLs and similar concentrations of GCSF were secreted in both.
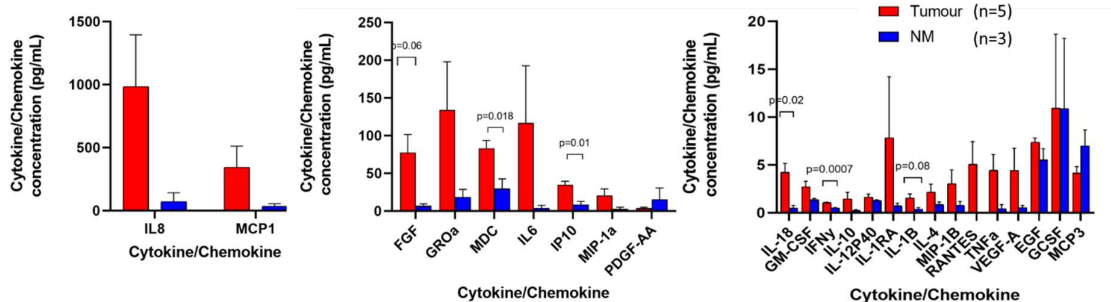
Figure 5.9: Cytokine/chemokine profiles of cultured PPGL tumour or non-pathological medulla cells grown in complete media. Cytokine/chemokine profile determined from human Millipore MILLIPLEX Cytokine-42-Plex array. Graphs show the top 25 secreted cytokine/chemokines. Shown across three graphs as y-axis varies. Statistical analysis completed using a Student's t-test.

In general, concentrations of cytokines were lower in both the PPGL and non-pathological medulla cells culutred in 1% serum media compared to those cultured in complete media, agreeing with a lower density of live cells in the 1% serum media as shown above (Figure 5.8). IL6, IP10, GM-CSF and IL4 concentrations were marginally higher in the supernatant from the cells cultured in 1% media. This implies that the secretion of these particular cytokines may be induced by high stress (in this case by the low percentage of serum in the media). There were no significant differences between the cytokine profiles in PPGLs (n=7) and non-pathological medulla (n=4) cultured in 1% serum media (Figure 5.10).
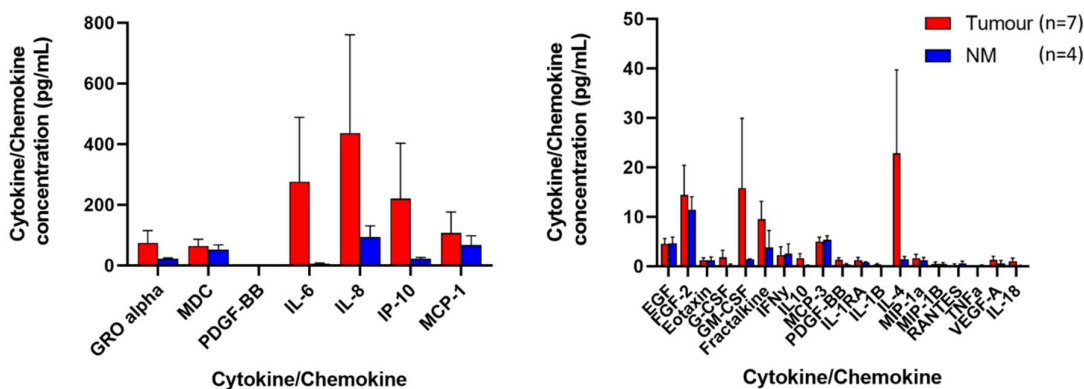
Figure 5.10: Cytokine/chemokine profiles of cultured PPGL tumour or non-pathological medulla cells grown in 1% serum media. Cytokine/chemokine profile determined from human Millipore MILLIPLEX Cytokine-42-Plex array. Graphs show the top 25 secreted cytokine/chemokines. Shown across two graphs as y-axis varies. Statistical analysis using a Student's t-test showed no significant difference between PPGLs and non-pathological medulla for any of the cytokines/chemokines.

These data suggest that PPGLs are immunologically active tumours and generate a local inflammatory response.

5.3.3 Infiltrating immune cells in the TME of PPGLs

To investigate which immune cells were present in the TME of PPGLs compared to non-pathological adrenal medulla, 65 tumour samples and 20 non-pathological adrenal medulla samples were analysed using immunohistochemistry. Table 5.5 shows the clinical characteristics of the patients from whom these PPGL tumours were resected. For comparison 20 tissue samples of non-pathological medulla were analysed. Non-pathological adjacent medulla was analysed from 10 of the patients that had undergone adrenalectomy for PCC and a further 10 samples of non-pathological medulla were analysed from 10 patients that had undergone adrenalectomy for a primary aldosterone tumour arising from the adrenal cortex (and hence not involving the adrenal medulla).

Total PPGLs	**65**
Total no. of patients	**61**
Gender [n (%)]**:**	
Male	44 (71%)
Female	18 (29%)
Age at diagnosis (years) (mean [range])	40 (14-80)
Size of tumour (mm) (mean [range])**:**	55.2 (10-235)
PCC (n=38)	49.1 (10-114)
Abdo PGL (n=17)	64 (19-235)
Thorax PGL (n=5)	70.4 (45-117)
Pelvic PGL (n=3)	41 (30-52)
HNPGL (n=2)	70 (30-110)
No. of primary PPGLs [n (%)]	56 (86%)
No. multiple PGLs [n (%)]	4 (6%)
No. recurrent PGLs [n (%)]	5 (8%)
Functional [n (%)]**:**	
Yes	49 (75.3%)
No	8 (12.3%)
Unknown	8 (12.3%)
Raised metanephrines > ULN [n (%)]:	
MN	21 (32%)
NMN	30 (46%)
3MT	5 (2%)
Urine metanephrine levels (nmol) (n[%]):	44 (67.7%)
MN (mean+/-SEM) [NR <2000]	11122+/-2840
NMN (mean+/-SEM) [NR <4400]	22760+/-4930
3MT (mean+/-SEM) [NR <2500]	2775+/-478
Plasma metanephrine levels (pmol/L) (n[%]):	23 (35.4%)
MN (mean+/-SEM) [NR <510]	3475+/-1175
NMN (mean+/-SEM) [NR <1180]	9814+/-2421
3MT (mean+/-SEM) [NR <180]	155+/-71.3
Malignant (n[%])	15 (23%)
Benign (n[%])	50 (77%)
Genetics tested (n[%]):	53 (83%)
Positive	33 (50%)
Negative	21 (32%)

Table 5.5: Clinical characteristics of patients from whom the PPGLs were resected. *MN metanephrine, NMN normetanephrine, 3MT 3-methoxy-tyramine*

The tumour characteristics of this cohort are shown in Table 5.6 and Figure 5.11. I investigated 50 benign tumours and 15 malignant tumours which were compared to 20 non-pathological medulla samples. Of these tumours 58.5% were located in the adrenal gland (PCCs), 38.5% of tumours were sympathetic PGLs and 3% were parasympathetic PGLs (HNPGL). Of the sympathetic PGLs 28% were located in the abdomen, 7.7% in the thorax and 3% in the pelvis. Half of this cohort had a known underlying genetic diagnosis, a further 32% had undergone genetic testing but no germline mutation had been identified and the remaining 20% had not undergone genetic testing as they did not meet the UK criteria for testing (due to age at diagnosis).

Total no. of tumours	65
Malignant tumours [n (%)]	15 (23%)
Benign tumours [n (%)]	50 (77%)
Total no. of non-pathological medulla samples [n (%)]:	20
Adjacent NM	10 (50%)
Independent NM	10 (50%)
Location of primary tumour [n (%)]:	
PCC	38 (58.5%) [2M]
All PGLs:	27 (41.5%) [10M]
Abdominal PGL	18 (28%) [7M]
Thorax PGL	5 (7.7%) [1M]
Pelvic PGL	2 (3%) [1M]
HNPGL	2 (3%)[1M]
Genetics [n (%)]:	
SDHB	20 (30%) [9M]
RET	6 (9%)
VHL	4 (6%)
SDHA	2 (3%) [1M]
FH	1 (1.5%)
Negative	21 (32%) [2M]
Not tested	13 (20%) [3M]

Table 5.6: Tumour characteristics of the 65 PPGLs and 20 non-pathological medulla samples. [M] = number of malignant tumours within each subgroup. SDH succinate dehydrogenase, FH fumarate hydratase, VHL von Hippel Lindau, RET rearranged during transfection proto-oncogene (RET), negative (when tested on a 10 gene panel), NT genetics not tested.
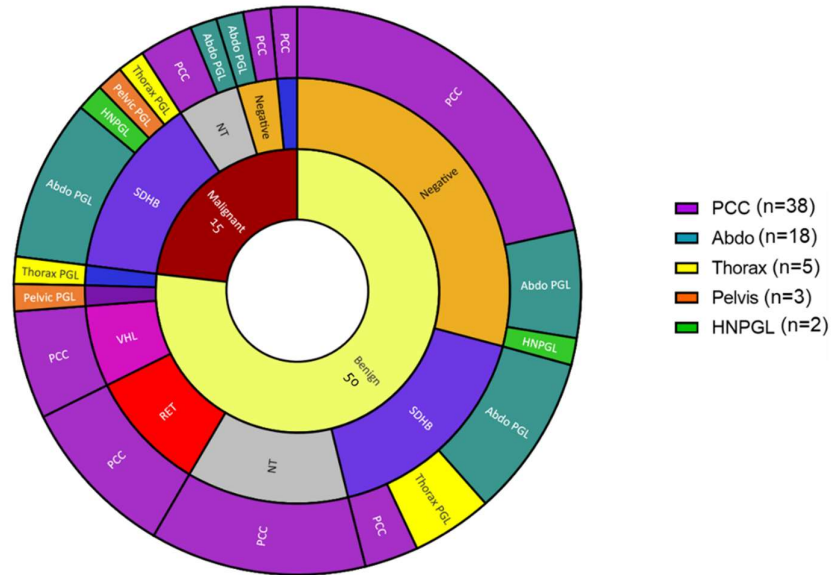
Figure 5.11: Tumour characteristics of the 65 PPGL tumours. *An expanded pie chart showing the breakdown of the benign and malignant tumours into underlying genetic status of the patient and location of the tumour. Inner circle shows the number of benign (n=50) and malignant (n=15) PPGLs included in the cohort. The middle circle shows the breakdown of both the benign and malignant PPGLs individually into their underlying genetic status and the outer circle shows the location of the tumour for each genetic subtype.*

The immune cells assessed included macrophages, lymphocytes, and neutrophils. There is a significant concentration of infiltrating immune cells in the TME of PPGLs, with a prominence of macrophages.

Figure 5.12 demonstrates examples of immune cell staining in tumours and non-pathological medulla.
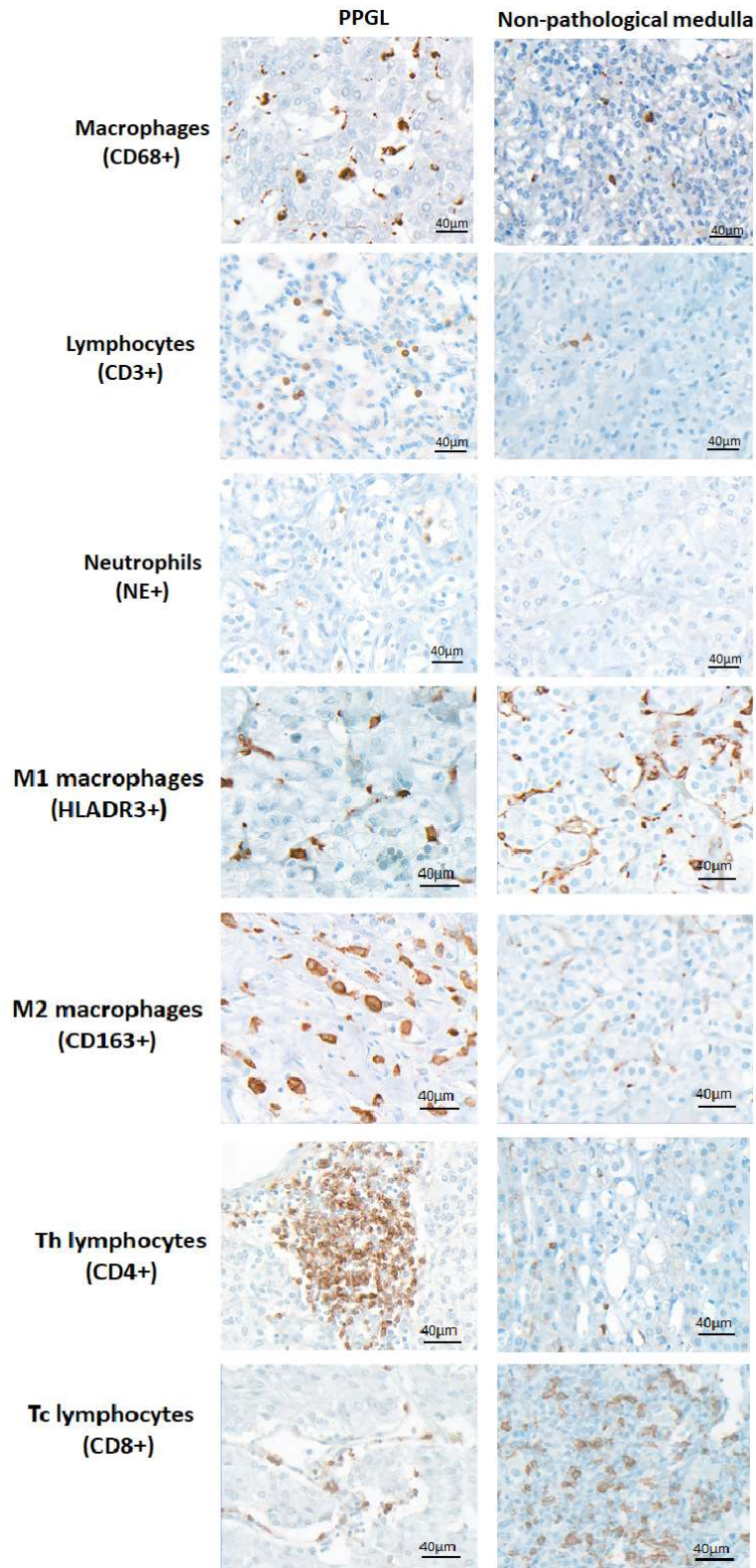
Figure 5.12: Immunohistochemical panels of immune markers. *Immune cells analysed: macrophages (CD68+), lymphocytes (CD3+), neutrophils (NE, neutrophil elastase+), M1 macrophages (HLADR3+), M2 macrophages (CD163+), Th T helper lymphocytes (CD4+), Tc cytotoxic T lymphocytes (CD8+). First column shows staining in PPGL tumour tissue and second column shows staining in non-pathological medulla tissue.*

PPGL TME contain infiltrating immune cells and there are significant differences between the concentration of different immune cell types (Figure 5.13).
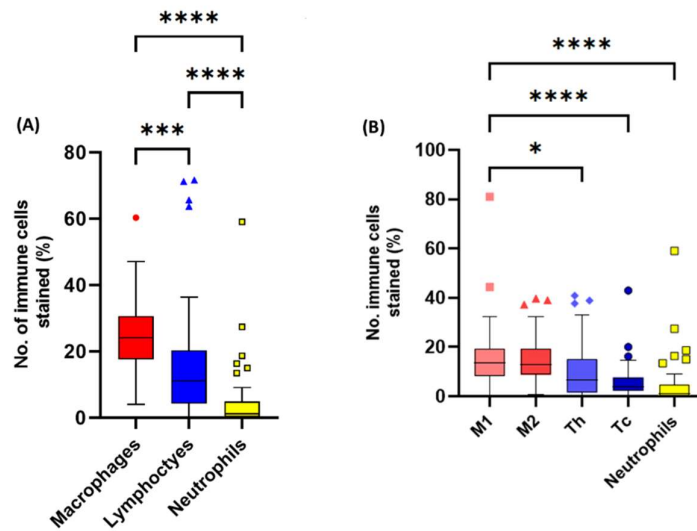
Figure 5.13: Immunohistochemical analysis of immune cells in PPGL tumours. *Immune cells analysed: macrophages (CD68+, M1 HLADR3+, M2 CD163+), lymphocytes (CD3+, Th CD4+, Tc CD8+), neutrophils (NE, neutrophil elastase+). Data show box-and-whisker plot of mean, IQR and outlying points of the percentage of immunopositive cells as a proportion of the total number of cells for PPGL tumour tissue (n=65). (A) Comparison between major immune cell types. Statistical analysis by one-way ANOVA with Tukey's multi comparisons test p<0.001. Macrophages vs lymphocytes p=0.0002, macrophages vs neutrophils p<0.001, lymphocytes vs neutrophils p<0.0001. (B) Subsets of macrophages (M1, M2) and lymphocytes (Th, Tc). Statistical analysis by one-way ANOVA with Tukey's multiple comparisons tests (p<0.001), *p<0.05, ***p<0.001, ****p<0.0001. Th T cell helper lymphocyte, Tc T cell cytotoxic lymphocytes*

Figure 5.14 shows there is a higher concentration of infiltrating immune cells in tumour tissue compared to non-pathological adrenal medulla tissue. PPGL tumour cells contain more infiltrating macrophages, lymphocytes and neutrophils compared to non-pathological adrenal medulla tissue (Figure 5.14). There were very few neutrophils identified within the non-pathological adrenal medulla tissue.
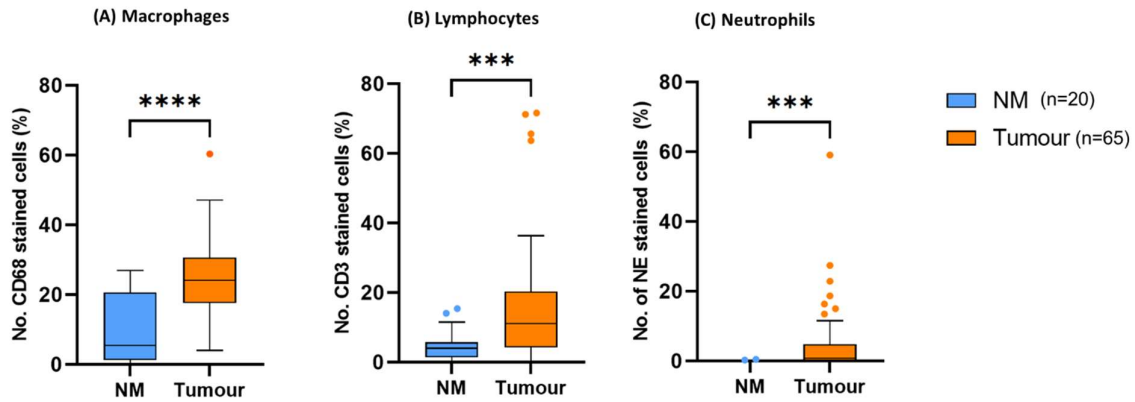
Figure 5.14: Immunohistochemical analysis of immune cells in PPGL tumours compared to non-pathological adrenal medulla. *Immune cells analysed: (A) macrophages (CD68+), (B) lymphocytes (CD3+), (C) neutrophils (NE, neutrophil elastase+). Data show box-and-whisker plot of mean, IQR and outlying points of the percentage of immunopositive cells as a proportion of the total number of cells for PPGL tumour tissue (n=65) and non-pathological adrenal medulla tissue (NM n=20). Macrophages are normally distributed data and were analysed using a Student's two-tailed t test, p<0.0001. Lymphocytes (p=0.0003) and neutrophils (p=0.0004) are non-parametric data and were analysed using a Mann-Whitney U test.*

Non-pathological medulla tissue taken from the same specimen that contained a PCC tumour (referred to as adjacent (Ad) NM) shows a higher infiltration of macrophages, but not lymphocytes or neutrophils, compared to NM tissue taken from an independent adrenal medulla (Ind NM) (Figure 5.15). There is a higher infiltration of macrophages into PPGL TME compared to independent NM, but not in the adjacent NM from the tumour specimen. As there was a significant difference in the macrophage infiltration in the adjacent NM compared to the independent NM, further comparisons use the independent NM only, unless otherwise stated.
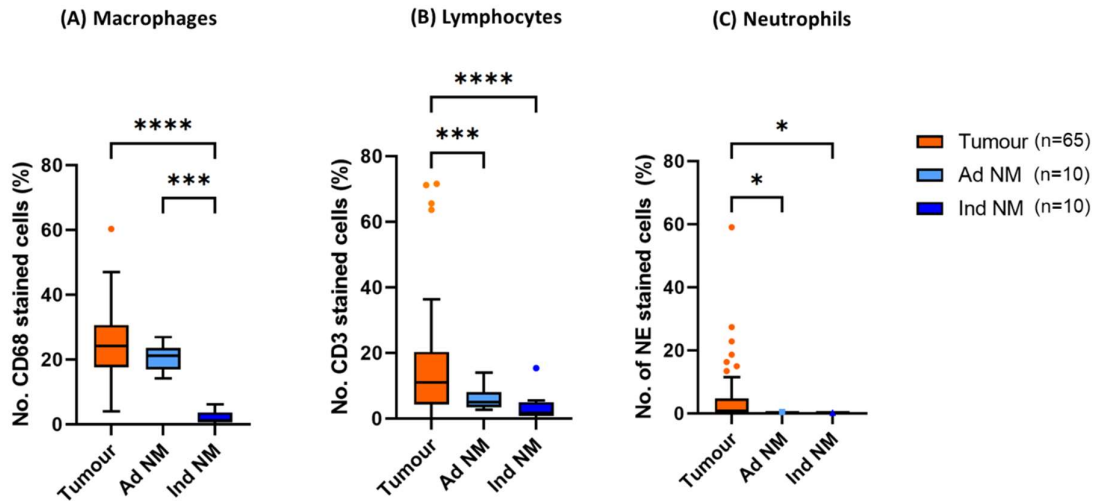
Figure 5.15: Immunohistochemical analysis of immune cells in PPGL tumours compared to non-pathological adrenal medulla. *NM tissue taken from adjacent tissue (Ad NM) to PCC tumour and NM taken from independent adrenal medulla (Ind NM). Immune cells analysed: (A) macrophages (CD68+), (B) lymphocytes (CD3+), neutrophils (NE, neutrophil elastase+). Data show box-and-whisker plot of mean, IQR and outlying points of the percentage of immunopositive cells as a proportion of the total number of cells for PPGL tumour tissue (n=65) and normal adrenal medulla tissue from adjacent tissue (Ad NM n=10) and independent NM (Ind NM n=10). ****p<0.0001, ***p<0.001, **p<0.01, *p<0.05 (Welch's one-way ANOVA with Dunnett's T3 multiple comparisons test was used to analyse parametric macrophage data and Kruskal Wallis test with Dunn's multiple comparisons test was used to analyse non-parametric lymphocyte and neutrophil data). Macrophages ANOVA p<0.0001, Lymphocytes Kruskal Wallis p<0.0001, Neutrophils Kruskal Wallis p<0.0001, Macrophage Ad NM vs Ind NM p=0.001, lymphocyte tumour vs Ad NM p=0.005, Neutrophils tumour vs Adjacent NM p=0.04, Neutrophils tumour vs Independent NM p=0.02.*

To further explore whether the immune cell infiltration corresponded to the aggressiveness of the tumour the immune cell infiltration was analysed in benign and malignant tumours separately. Immune cell infiltration was similar in malignant tumours compared to benign tumours, although both benign and malignant tumours contained significantly higher levels of immune cells compared to non-pathological medulla tissue (Figure 5.16).
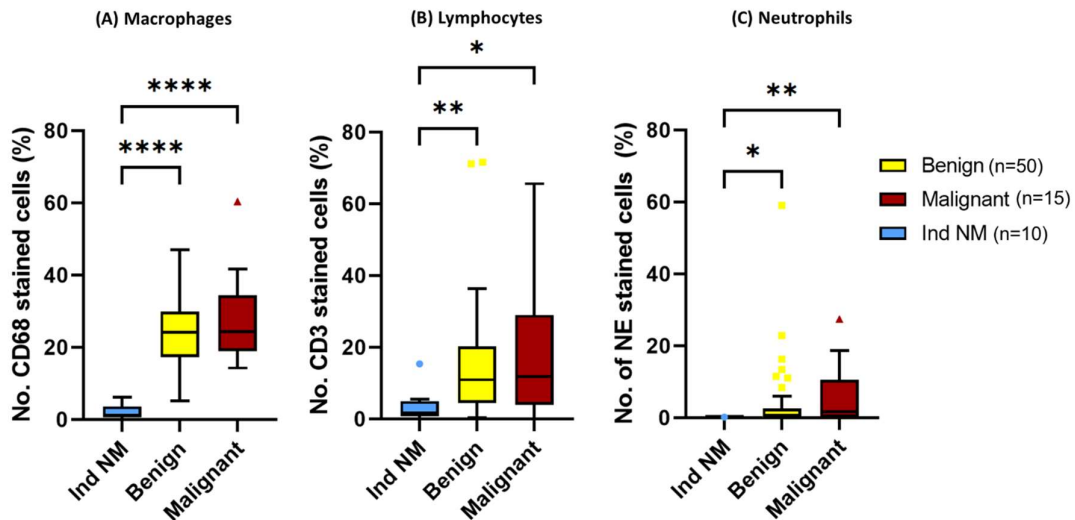
Figure 5.16: Immunohistochemical analysis of immune cells in benign and malignant PPGL tumours compared to non-pathological adrenal medulla. *Immune cells analysed: (A) macrophages (CD68+), (B) lymphocytes (CD3+), (C) neutrophils (NE, neutrophil elastase+). Data show box-and-whisker plot of mean, IQR and outlying points of the percentage of immunopositive cells as a proportion of the total number of cells for benign tumour (n=50), malignant tumour (n=15) and independent NM (NM n=10). ****p<0.0001, *p<0.05 (Welch's one-way ANOVA with Dunnett's T3 multiple comparisons test was used to analyse the parametric macrophage data and the Kruskal Wallis test with Dunn's multiple comparisons test was used to analyse the non-parametric lymphocyte and neutrophil data). CD68 ANOVA p<0.0001, CD3 Kruskal Wallis p=0.0022, NE Kruskal Wallis p=0.0034, CD3 Ind NM vs benign tumours p=0.0028, CD3 Ind NM vs malignant tumours p=0.0129, neutrophils Ind NM vs benign tumours p=0.0178, NE Ind NM vs malignant tumours p=0.0027), non-significant results of benign vs malignant tumour tissue CD68 p=0.358, CD3 p=0.999, NE p=0.53.*

It is believed that the aggressiveness of the tumour can correlate with the location of the tumour and underlying genetic status[23,62], specifically *SDHB* mutations are known to be more aggressive than tumours caused by other genetic mutations, and extra-adrenal sympathetic PGLs are thought to be more aggressive than those that arise within the adrenal gland or parasympathetic chain. Therefore, it was investigated whether the immune cell infiltration differed depending on these clinical features.

Firstly, PCCs were compared with all extra-adrenal PGLs. There were similar levels of immune cell infiltration in PCC and extra-adrenal PGL tumours. There was a higher level of infiltration of immune cells in both PCCs and PGLs individually compared to NM (Figure 5.17).
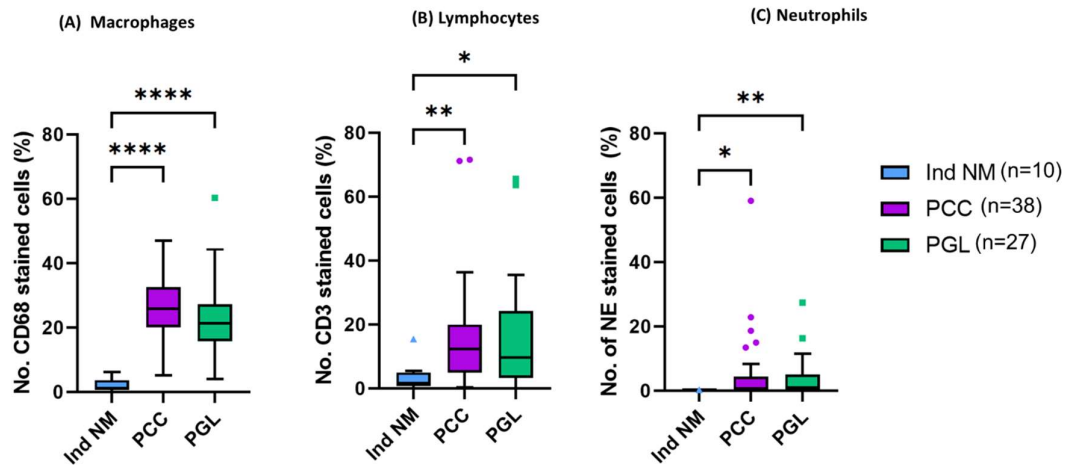
Figure 5.17: Immunohistochemical analysis of immune cells in PCCs compared to PGLs and non-pathological adrenal medulla. *(A) macrophages (CD68+), (B) lymphocytes (CD3+), (C) neutrophils (NE, neutrophil elastase+). Data show box-and-whisker plot of mean, IQR and outlying points of the percentage of immunopositive cells as a proportion of the total number of cells for PCC (n=38), PGL (n=27) and Independent non-pathological adrenal medulla tissue (Ind NM n=10). ****p<0.0001, ***p<0.001, *p<0.05 (Welch's one-way ANOVA with Dunnett's T3 multiple comparisons test used for parametric macrophage data (p<0.0001) and Kruskal Wallis test with Dunn's multiple comparisons test for lymphocyte (p=0.0025) and neutrophil (p=0.0054) non-parametric data). Non-significant results of PCC vs PGL CD68 p=0.588, CD3 p=0.999, NE p=0.969.*

Next, the immune cell infiltrate was evaluated at more specific tumour locations. There was a similar level of macrophage infiltration between the different PPGL tumour sites (Figure 5.18). There were differing levels of lymphocyte infiltration, with the highest levels in the HNPGLs (29.4% +/- 0.35), followed by abdominal PGLs (18.6% +/- 4.85), and PCC (16% +/- 2.6), with the lowest levels detected in the pelvic PGLs (3.22% +/- 0.13) though these differences were not statistically significant. The data for the pelvic and HNPGL should be interpreted with caution as the number of tumour samples of these types was low. There was no significant difference in the levels of neutrophil infiltration in the PPGL tumours that arose at different locations.
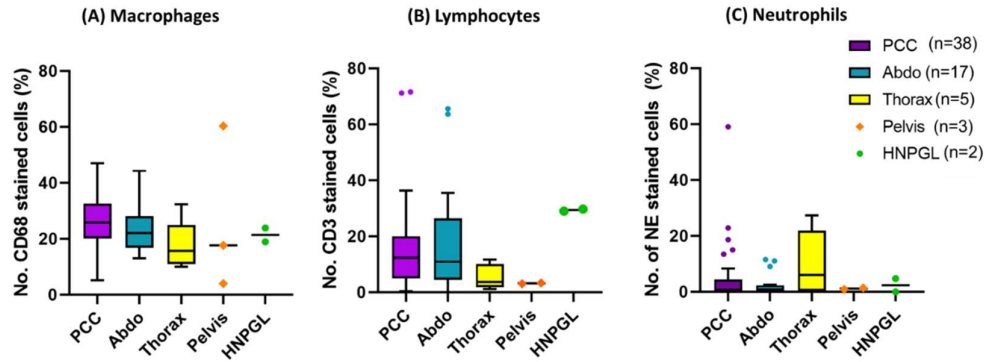
Figure 5.18: Immunohistochemical analysis of immune cells in PPGL tumours that arose in different locations and non-pathological adrenal medulla. *(A) macrophages (CD68+), (B) lymphocytes (CD3+), (C) neutrophils (NE, neutrophil elastase+). Data show box-and-whisker plot of mean, IQR and outlying points of the percentage of immunopositive cells as a proportion of the total number of cells for PCC (n=38), Abdominal PGL (Abdo n=17), Thorax PGL (n=5), Pelvic PGL (n= 3), Head & neck PGL (HNPGL n=2) and non-pathological adrenal medulla tissue (NM n=20). Welch's one-way ANOVA with Dunnett's T3 multiple comparisons test used for parametric macrophage data (p=0.3788) and Kruskal Wallis test with Dunn's multiple comparisons test for lymphocyte (p=0.1646) and neutrophil (p=0.255) non-parametric data. Data from pelvic PGLs and HNPGLS were removed from statistical analysis as sample size was too low.*

5.3.3.1 Genetics

The mutational landscape from which these tumours arise is diverse and may contribute to the variable immune infiltration, thus it was explored whether the immune profiles of the tumours differed depending on the underlying genetic status of the patient. There were no significant differences in immune profiles between tumours from patients with positive genetic diagnosis and those with negative.
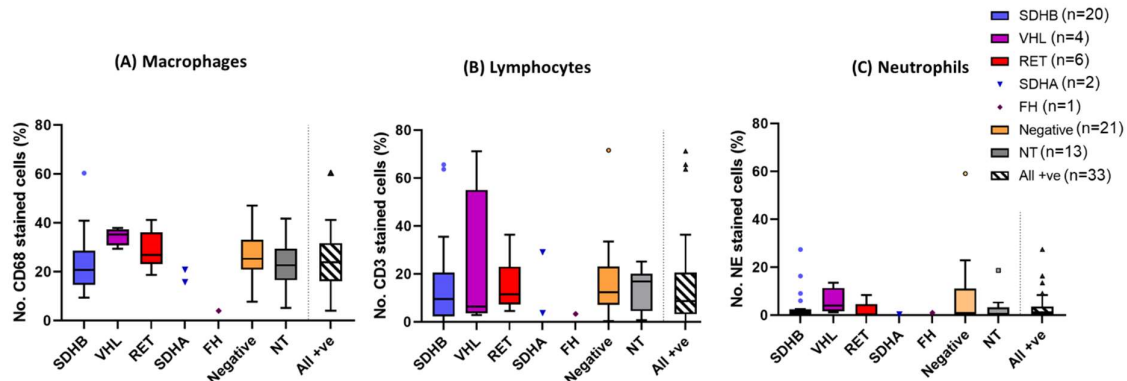
Figure 5.19: Immunohistochemical analysis of immune cells in PPGL tumours that arose in patients with different underlying germline genetic diagnosis. *(A) macrophages (CD68+), (B) lymphocytes (CD3+), (C) neutrophils (NE, neutrophil elastase+). Data show box-and-whisker plot of mean, IQR and outlying points of the percentage of immunopositive cells as a proportion of the total number of cells for SDHB (n=20), VHL (n=4), RET (n=6), SDHA (n=2), FH (n=1), negative genetics (n=21), not tested (NT n=13) and all patients with genetic mutation included (all +ve, n=33). One-way ANOVA with Tukey's multiple comparisons test was used to analyse the parametric macrophage data (p=0.342) and the lymphocyte data (p=0.985). The Kruskal Wallis test with Dunn's multiple comparisons test was used to analyse the neutrophil (p=0.413) non-parametric data. Data from FH and SDHA were not included in statistical analysis as sample size was too low. SDH succinate dehydrogenase, FH fumarate hydratase, VHL von Hippel Lindau, RET rearranged during transfection proto-oncogene (RET), NT genetics not tested.*

There was no significant difference between immune cell infiltration depending on the underlying genetic diagnosis. There was also no significant difference between immune cell infiltration between cluster 1 and cluster 2 PPGLs (data not shown) for lymphocytes or neutrophils. There was a trend towards a higher infiltration of macrophages in cluster 1b compared to cluster 1a PPGL tumours (p=0.09, one-way ANOVA).

As macrophages were the dominant immune cell type in the PPGL TME, I then investigated whether there was a difference in the type of macrophages that were present. M1 macrophages are generally considered pro-inflammatory and M2 macrophages as anti-inflammatory and are also commonly referred to as tumour-associated macrophages (TAMs)[322,386]. There was a significantly higher number of M1 macrophages in non-pathological medulla compared to tumour (mean 25.9% vs 15.7%, p=0.0008) and a significantly lower number of M2 macrophages (9.97% vs 15.2%, p=0.025). Furthermore, there was a significantly higher number of M1 macrophages in benign compared to malignant tumours (16.3% vs 8.29%, p=0.0001). There was a significantly higher ratio of M2:M1 macrophages in PPGL tumours compared to non-pathological medulla (Figure 5.20A). As there was no difference in the ratio of M2:M1 in tissue taken from adjacent and independent NM (Figure 5.20B), all the samples from NM were used for subsequent analysis. Sub-analyses were undertaken for adjacent NM and independent NM separately and both showed the same significant results when compared to benign and malignant tumours (data not shown). There was a significantly higher ratio of M2:M1 macrophages in malignant PPGLs compared to benign (1.68 vs 1.06, p=0.0099), but still a higher ratio in benign tumours compared to non-pathological medulla (1.06 vs 0.314, p=0.0003) (Figure 5.20C).

M2 macrophages predominate in the PPGL TME, with the highest levels occurring in malignant tumours.
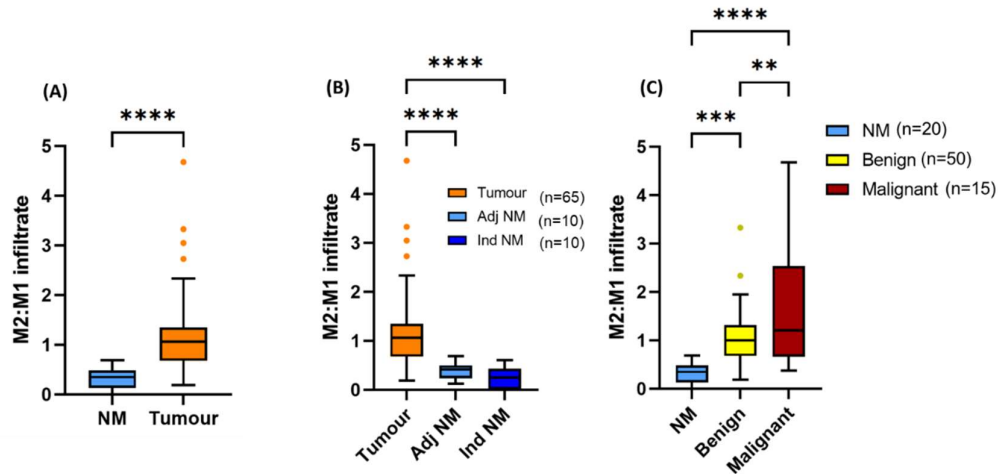
*Figure 5.20: Immunohistochemical analysis of subsets of macrophages in PPGL tumours compared to non-pathological adrenal medulla. Immune cells analysed: M1 (HLADR3+), M2 (CD163+). (A) All non-pathological medulla (n=20) vs PPGL tumours (n=65), (B) PPGL tumour vs adjacent non-pathological medulla (Adj NM n=10) and independent (Ind NM n=10), (C) All non-pathological medulla (n=20) vs benign PPGL tumours (n=50) and malignant PPGL tumours (n=15). Data show box-and-whisker plot of mean, IQR and outlying points of the ratio of M2 macrophages: M1 macrophages. ****p<0.0001, ***p<0.001, **p<0.01, *p<0.05 (Welch's t test (A) or Welch's one-way ANOVA test with Dunnett's T3 multiple comparisons test (B and C)).*

This suggests that the ratio of subpopulations of macrophages is potentially related to the behaviour of the TME rather than the absolute values of infiltrating cells.

I then investigated whether the type of macrophage infiltration differed at different locations of PPGLs. As with the other types of immune cells there was a significantly higher ratio of M2:M1 cells in PCC (p<0.0001) and PGL tumours (p<0.0001) compared to NM tissue, with more M2 macrophages occurring in the PPGL tumours and higher levels of M1 macrophages in NM tissue. There was no significant difference in the infiltration of the different macrophage subtypes at different locations of PPGL tumours.
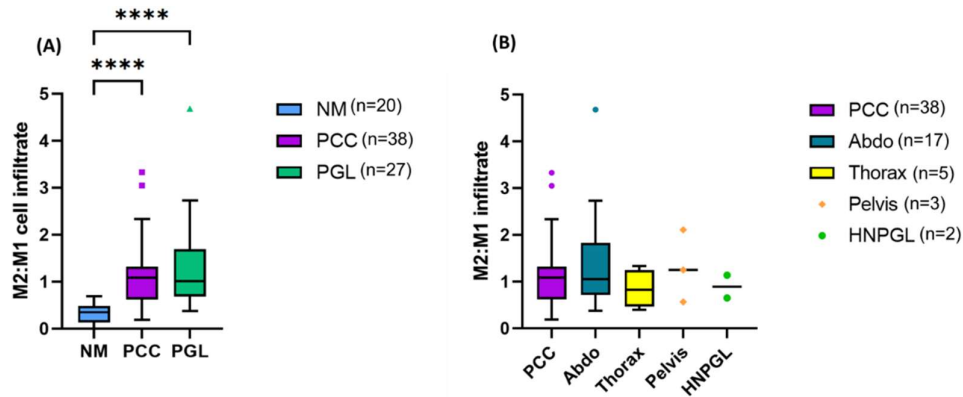
Figure 5.21: Immunohistochemical analysis of subsets of macrophages at different PPGL tumour sites. *Immune cells analysed: M1 (HLADR3+), M2 (CD163+). (A) All non-pathological medulla (n=20) vs PCC (n=38) vs PGL (n=27), (B) M2:M1 cell infiltrate of PPGL tumours arising at different locations. Data show box-and-whisker plot of mean, IQR and outlying points of the ratio of M2:M1 macrophages. Statistical analysis using Kruskal Wallis ANOVA test with Dunn's multiple comparisons test as data is non-parametric. (A) p<0.0001, (B) p=0.613, pelvic PGL and HNPGL excluded from statistical analysis due to low sample number.*

There was also no difference in the type of macrophage infiltration depending on the specific underlying genetic diagnosis (data not shown). There was a higher proportion of M2:M1 macrophages in cluster 1 compared to cluster 2 (Table 1.1) PPGLs (mean 1.95 vs 0.635, p=0.017), with the highest number in cluster 1a (mean 1.99 vs 1.7 vs 0.635) (Figure 5.22).
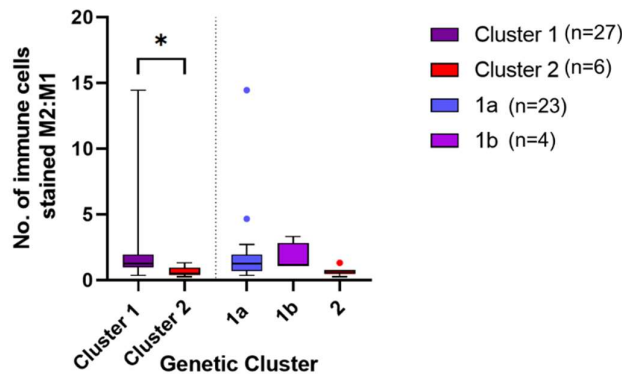
Figure 5.22: Immunohistochemical analysis of subset of macrophages infiltration in PPGL tumours by genetic cluster. *Immune cells analysed: M1 (HLADR3+), M2 (CD163+). Data show box-and-whisker plot of mean, IQR and outlying points of the ratio of M2:M1 macrophages. Cluster 1 vs Cluster 2 p=0.017 (Mann Whitney U test). Cluster 1a vs Cluster 1b vs Cluster 2 p=0.06 (Kruskal Wallis ANOVA test with Dunn's multiple comparisons test).*

Next I investigated whether the lymphocyte infiltrate in the TME comprised of different subtypes of lymphocytes. Cytotoxic memory T cells (Tc) are strongly associated with a good prognosis as they are capable of killing tumour cells[331]. T helper (Th) lymphocytes are further subdivided into T helper 1 (Th1), Th2 and Th17 cells. Th1 lymphocytes support Tc cell function and are also associated with a good prognosis[312,333], whereas Th2 lymphocytes are thought to promote inflammation and tumour growth and produce immunosuppressive cytokines[333].

There was a significantly higher density of T helper cells in tumour compared to non-pathological medulla (p=0.0015, mean 10.7% vs 3.7%) and benign compared to malignant PPGLs (p=0.039, mean 8.5% vs 1.1%). There was also higher density of Th cells in PCCs compared to PGLs (p=0.039, mean 7.6% vs 3.7%), but no differences were observed in the absolute number of Tc cells (Figure 5.23).
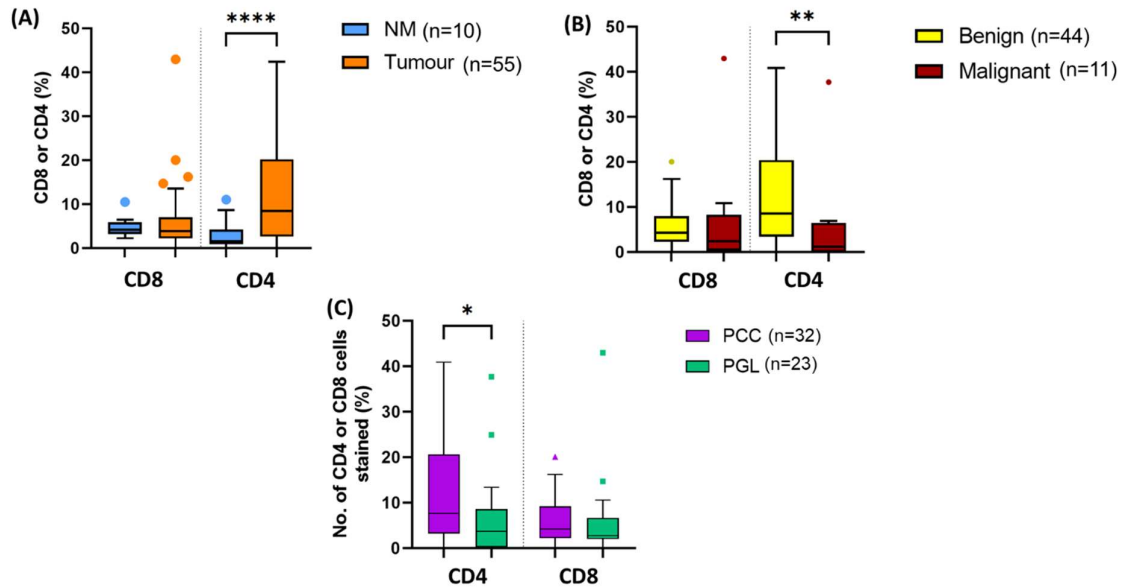
Figure 5.23: Immunohistochemical analysis of subset of lymphocytes infiltration in PPGL tumours. *Immune cells analysed: T helper lymphocytes (CD4+), Cytotoxic T cells (CD8+). Data show box-and-whisker plot of mean, IQR and outlying points. (A) PPGL tumour vs non-pathological medulla for Tc (CD8) p=0.4 Th (CD4) p<0.0001 (Welch's t-test). (B) Benign vs malignant PPGL tumours for Tc (CD8) p=0.25, Th (CD4) p=0.01 (Mann Whitney U test). (C) PCC vs PGL for Tc (CD8) p=0.52, Th (CD4) p=0.0039** (Mann Whitney U test). ****p<0.0001, ***p<0.001, **p<0.01, *p<0.05*

Some differences were observed when investigating the underlying germline mutations of the PPGL tumours (Figure 5.24). There was a lower density of T helper cells in PPGLs with an underlying *SDHB* mutation compared to *VHL* mutations (p=0.05, mean 2.7% vs 22.5%), and genetic negative PPGLs (p=0.04, mean 2.7% vs 12.39%). There was higher density of Th cells in genetically negative PPGLs compared to those with a known genetic mutation (p=0.0274, mean 13.39% vs 4.78%). There was a higher density of Tc cells in PPGLs with negative genetics compared to those with a known genetic cause (p=0.047, mean 6.9% vs 5.2%), and also when compared to only those with *SDHB* mutations (p=0.0033, mean 6.9% vs 5.17%).
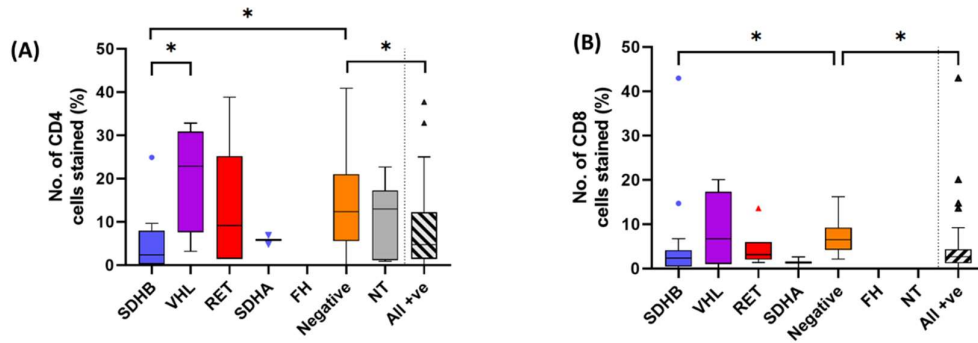
***Figure 5.24: Immunohistochemical analysis of subset of lymphocytes infiltration in PPGL tumours with
different underlying germline mutations.*** *Immune cells analysed: T helper lymphocytes (CD4+), Cytotoxic T cells
(CD8+). Data show box-and-whisker plot of mean, IQR and outlying points. (A) Th (CD4+) cell infiltration of PPGLs
with different genetic mutations p=0.0315 (Kruskal Wallis ANOVA test with Dunn's multiple comparisons test),
SDHB vs VHL p=0.05, SDHB vs negative p=0.04, All positive (+ve) vs negative p=0.0274. (B) Tc (CD8+) cell
infiltration of PPGLs with different genetic mutations p=0.0185 (Kruskal Wallis ANOVA test with Dunn's multiple
comparisons test), Genetics negative tumours vs tumours with known underlying germline mutations p=0.047,
SDHB vs negative p=0.033. ****p<0.0001, ***p<0.001, **p<0.01, *p<0.05. SDH succinate dehydrogenase, FH
fumarate hydratase, VHL von Hippel Lindau, RET rearranged during transfection proto-oncogene (RET), NT
genetics not tested.*

I therefore went on to investigate whether the ratio of cytotoxic T cells to T helper cells (Tc:Th) had a
further influence within the TME, in a similar fashion to the macrophage subtypes. There was a
significantly higher ratio of Tc:Th cells in the non-pathological medulla compared to the tumour
(p=0.0092, mean 3.38 vs 0.879) (Figure 5.25), but no significant differences were observed between
the benign and malignant tumours. There were no significant differences observed based on the
location of the tumour or the underlying genotypes.
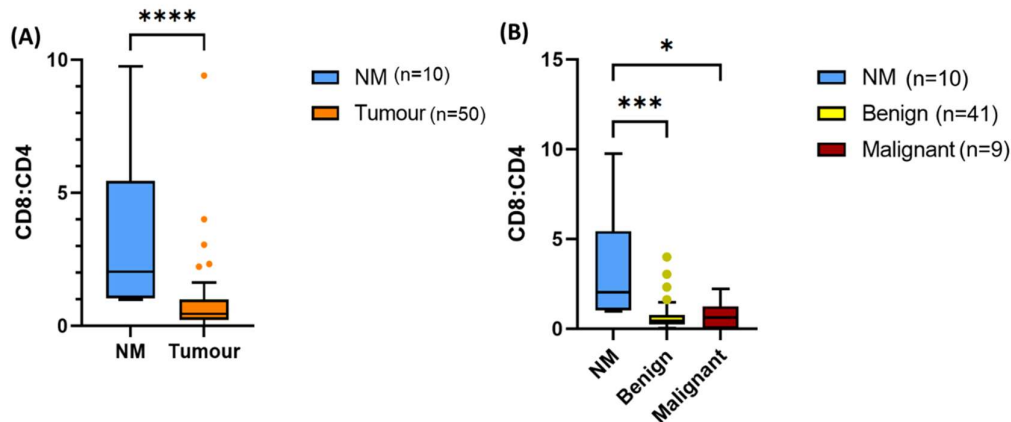
***Figure 5.25: Immunohistochemical analysis of subsets of lymphocytes in PPGL tumours compared to normal
adrenal medulla.*** *Immune cells analysed: T helper lymphocytes (CD4+), Cytotoxic T cells (CD8+). Data show box-
and-whisker plot of mean, IQR and outlying points of the ratio of Tc lymphocytes: Th lymphocytes (CD8:CD4).
Where Tc cells were zero, these samples were excluded from analysis as mathematical calculation of ratio was
invalid. (A) non-pathological medulla (n=10) vs PPGL tumours (n=50), p<0.0001 (Mann Whitney U test). (B)
Benign PPGL vs malignant PPGLs compared to non-pathological medulla (p=0.0006, one-way ANOVA with Dunn's
multiple comparisons test). ****p<0.0001, ***p<0.001, **p<0.01, *p<0.05*

As malignant tumours in this cohort occurred only in patients with *SDHB* mutations, negative genetics or those that have not undergone genetic testing, these subgroups were analysed independently (Figure 5.26). There was a higher infiltration of macrophages in malignant *SDHB* tumours compared to benign tumours (p=0.029, mean 30% vs 18.3%) and higher M2:M1 ratio (p=0.02, mean 3.57 vs 1.17), as well as a higher Ki67 proliferative index (p=0.03, mean 15.4% vs 4.36%). In the negative genetics group, there was no significant difference in immune cell infiltration between benign and malignant tumours. There were no differences in the patients whom genetic diagnosis was undetermined (data not shown). All PPGLs that arose in patients with *RET* and *VHL* mutations were benign tumours.

In PPGL tumours from patients with underlying *SDHB* mutations there is a higher infiltration of macrophages in malignant tumours than benign tumours, specifically of the M2 pro-inflammatory subtype.
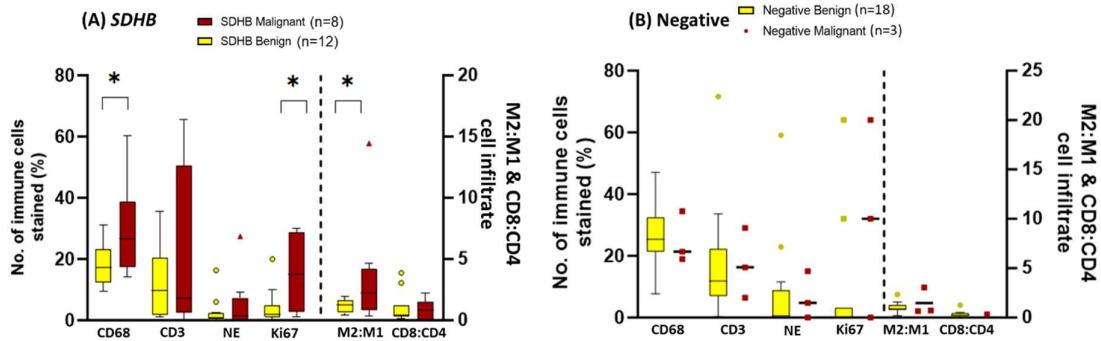
Figure 5.26: Immunohistochemical analysis of immune cell markers in PPGL tumours that arose in patients with either SDHB or negative genetic diagnoses. *Immune cells analysed: macrophages (CD68+), (B) lymphocytes (CD3+), (C) neutrophils (NE, neutrophil elastase+), M2:M1 (CD163+:HLADR3+) macrophages, Tc:Th (CD8:CD4) lymphocytes, Ki67 proliferative index. Data show box-and-whisker plot of mean, IQR and outlying points of the percentage of immunopositive cells as a proportion of the total number of cells. (A) Immune cell infiltration in benign (n=12) and malignant (n=8) PPGLs in patients with SDHB mutations. Macrophages p=0.029 (Student's t test), lymphocytes p=0.45 (Welch's t test), neutrophils p=0.955 (Mann Whitney U test), M2:M1 p=0.02 (Mann Whitney U test), CD8:CD4 p=0.868 (Mann Whitney U test), Ki67 p=0.03 (Welch's t test). (B) Immune cell infiltration in benign (n=18) and malignant (n=3) PPGLs in patients with no known underlying genetic mutations; macrophages p=0.759 (Student's t test), lymphocytes p=0.974 (Student's t test), neutrophils p=0.656 (Mann Whitney U test), M2:M1 p=0.648 (Welch's t test), Ki67 p=0.079 (Mann Whitney U test).*

Ki67 is a proliferation index that for some tumour types is considered a marker of aggressiveness. Within this PPGL cohort there was a significantly higher Ki67 in malignant PPGLs compared to benign (p=0.039), but there was no difference in Ki67 proliferative index between the different tumour locations (Figure 5.27).
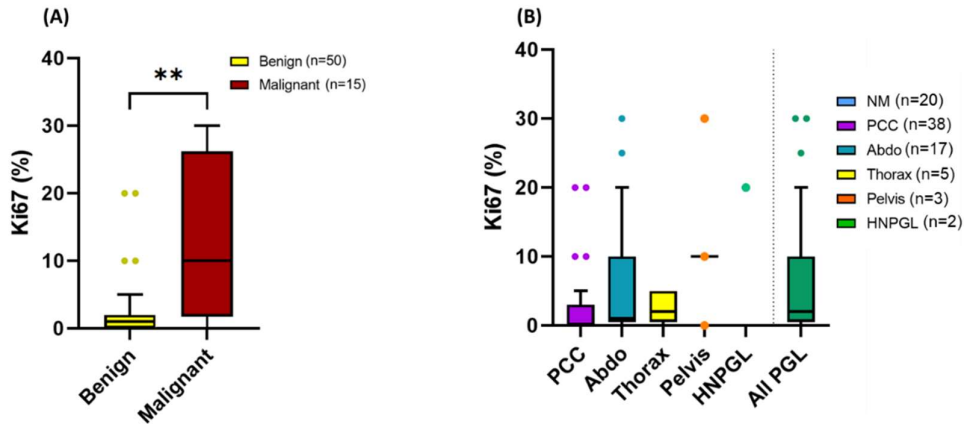
Figure 5.27: Immunohistochemical analysis of Ki67 proliferative index Data show box-and-whisker plot of mean, IQR and outlying points of Ki67 proliferative index (A) benign and malignant tumours, Welch's t test p=0.0039. (B) at different PPGL tumours sites, Kruskal Wallis ANOVA test p=0.078, pelvic PGL and HNPGL excluded from statistical analysis due to low sample number.

There was no significant difference between Ki67 index and immune cell infiltration, although there was a trend towards a positive correlation with Ki67 and macrophage infiltration (p=0.07). There was also a downwards trend in lymphocyte count and an upward trend in M2:M1 with increasing Ki67 index up to 10% (Figure 5.28).
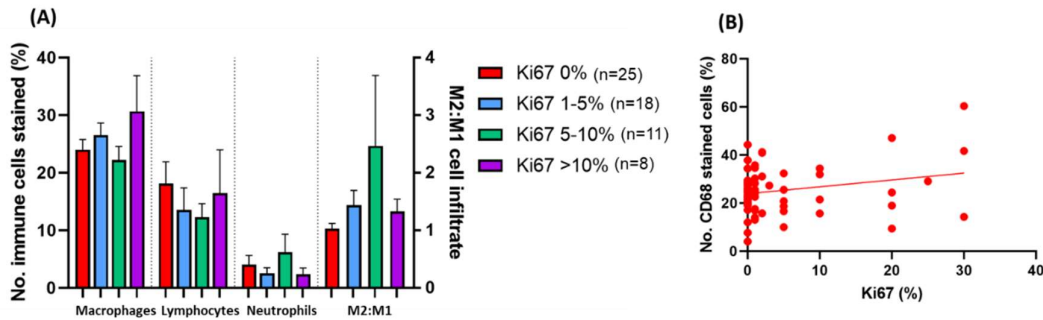
Figure 5.28: Immunohistochemical analysis of Ki67 proliferative index and immune cell infiltration in PPGL tumours. (A) Bar chart showing immune cell infiltration in different categories of Ki67 proliferative index. Ki67=0 (n=25), Ki67=1- <5% (n=18), Ki67 = 5-<10% (n=11), Ki67 = ≥10% (n=8). Statistical analysis using Welch's one-way ANOVA test (macrophage's (p=0.434) and lymphocytes (p=0.733)) and Kruskal-Wallis ANOVA test (neutrophils (p=0.092) and M2:M1 (p=0.536)). (B) Scatter diagram of macrophage (CD68) infiltration against Ki67 proliferative index (Pearson r=0.229, p=0.073).

There was no correlation between tumour size and Ki67 index or tumour size and immune cell infiltration (Figure 5.29). There were no significant differences between tumour size of benign and malignant tumours (mean 44 vs 58 mm, p=0.314), although there was a trend to malignant tumours being larger when recurrent tumours were removed (44 vs 64 mm, p=0.075). Recurrent tumours are identified at smaller sizes and usually before they become active as they are often identified on surveillance screening[65]. Therefore, a further sub-analysis was performed with recurrent tumours removed. With recurrent tumours removed from the analysis (n=4) there is a significant correlation

210

between increasing number of lymphocytes with increasing tumour size (p=0.045) and a trend towards increasing macrophage infiltration with increasing tumour size (p=0.083) (Figure 5.29).
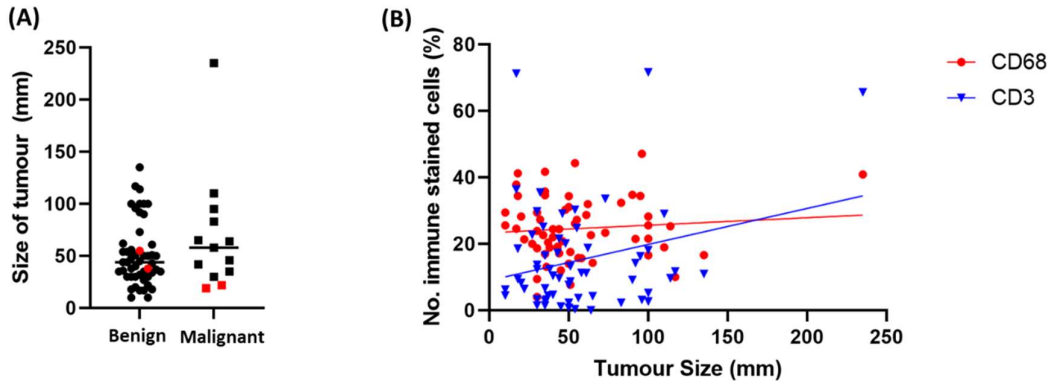
Figure 5.29: Sizes of benign and malignant PPGL tumours and relation to immune cell infiltration. *(A) Scatter plot showing sizes of benign and malignant tumours. Red dots identify those tumours that were recurrent and removed from subsequent analysis (p=0.314 Mann Whitney U). (B) Scatter diagram of macrophage (CD68 Pearson r=0.009, p=0.083) and lymphocyte (CD3 Pearson r=0.259, p=0.045)) infiltration in tumours relating to their sizes, with recurrent tumours removed.*

There was a positive correlation between neutrophil infiltration and M2:M1 cell infiltration (p=0.01) and a trend towards a positive correlation between Ki67 and macrophage infiltrate (p=0.06), but not between the other immune cells or tumoural factors (Figure 5.30).
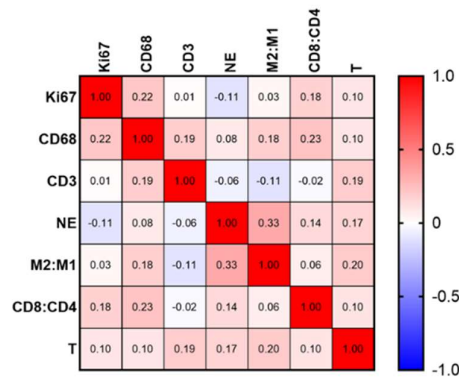
Figure 5.30: Heat map correlation between tumoural variables. *Bar on righthand side shows intensity of correlation with gradient of colour between blue -1.0 (negative correlation) through to white 0 (no correlation) and red +1.0 (positive correlation). Ki67 proliferation index, macrophages (CD68+), lymphocytes (CD3+), neutrophils (NE), M2:M1 macrophages (M2:M1), cytotoxic T cells: T helper cells (CD8:CD4), tumour size (T). Figures represent Pearson r correlation values (-1.0 to 1.0).*

5.3.3.2 Effect on the PPGL TME immune profile by tumoural function

In most centres metanephrine concentrations (the breakdown products of catecholamines) are now used as a marker of excess hormone production of PPGLs, as they are more reliable and easier to measure than catecholamines themselves[22].

In total data for 57 (88%) PPGLs were available on the functional status of the tumours (Table 5.5). Plasma metanephrines were available for 25 (38%) of the PPGLs, urine metanephrines for 45 (69%) and for an additional five (7.7%) only urinary catecholamine data were available. The vast majority (75.3%) were functional (taken as metanephrine/catecholamine level above the upper limit of local laboratory reference range) (Figure 5.31A). Twenty-one (32%) had a raised MN level, 30 (46%) had a raised NMN level, but only five (2%) had a raised 3MT levels (Figure 5.31B).
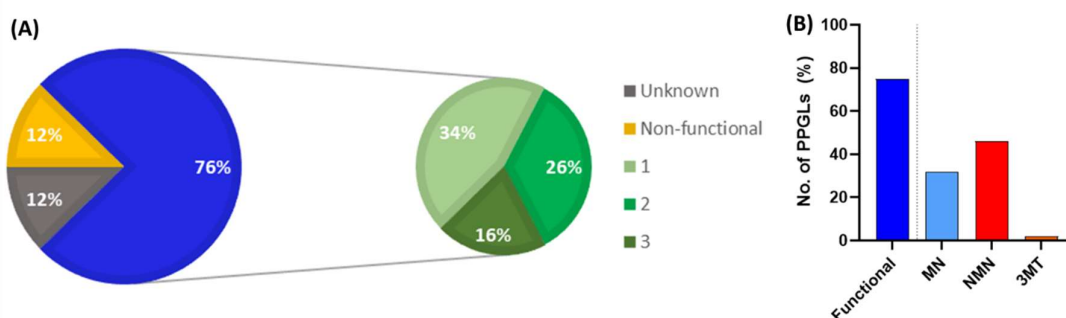
Figure 5.31: Functional status of PPGLs. *(A) Pie chart showing functional PPGLs (n=49), non-functional PPGLs (n=8), unknown functional status (n=8). Smaller pie chart shows an expanded view of the functional PPGLs demonstrating whether they are producing 1, 2 or 3 of the catecholamines (epinephrine, norepinephrine, dopamine) in any combination, measured as their corresponding metanephrine concentrations (MN, NMN, 3MT). (B) Bar chart showing the percentage of PPGLs producing different metanephrines as a proportion of the total number of PPGLs (note some tumours produce more than one metanephrine). Functional = PPGL producing excess catecholamines above the ULN reference range, MN metanephrine, NMN normetanephrine, 3MT 3-methoxytyramine.*

As there was heterogeneity between the sources of the hormone data, including results from plasma and urine metanephrines and urine catecholamines, the results were analysed as a proportion of the upper limit of the normal reference range and in addition the plasma and urine metanephrines were analysed separately.

More of the benign PPGLs were functional when compared to the malignant PPGLs (83 vs 55%) (Figure 5.32A&D). More of the benign PPGLs produced MN, whereas a higher proportion of malignant PPGLs produced 3MT (Figure 5.32B&C).

212
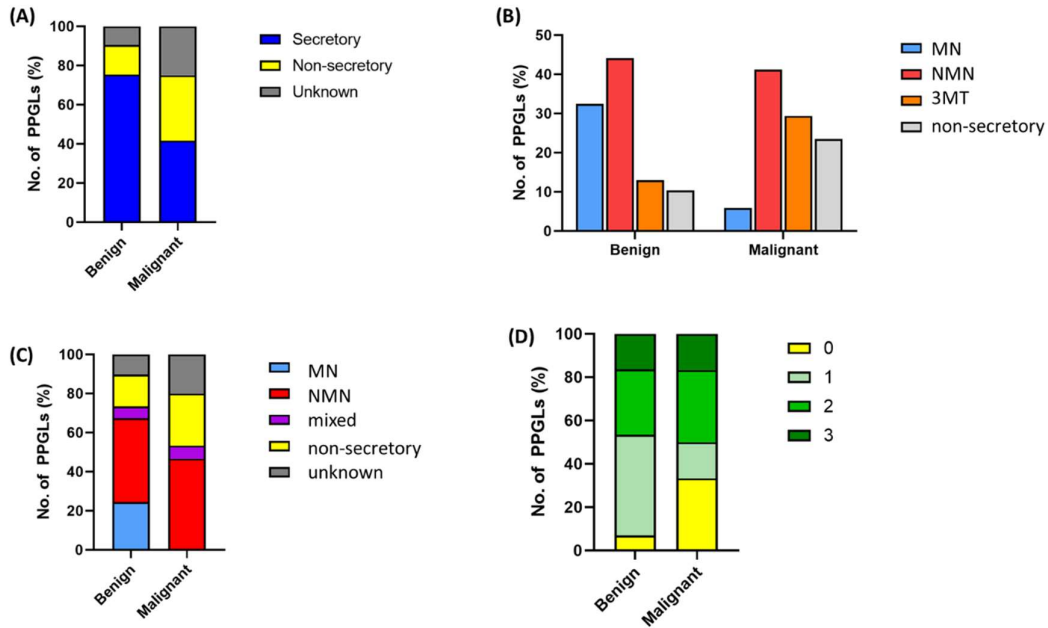
Figure 5.32: Functional status of benign and malignant PPGLs. *(A) Stacked bar chart showing functional status of benign (n=40) and malignant (n=8) PPGLs, as a proportion of the total number of PPGLs. (B) Stacked bar chart demonstrating the number of the metanephrines produced by each tumour as 0, 1, 2 or 3 in any combination (metanephrine, normetanephrine and 3-methoxytyramine (3MT)) for benign and malignant PPGLs. (C) Bar chart showing the total metanephrines being produced by benign and malignant PPGLs (note some PPGLs produced more than one metanephrine, figure D). (D) Stacked bar chart showing the dominant metanephrines being produced by benign and malignant PPGLs as a proportion of the total of number of PPGLs. 'Dominance' was determined by the highest concentration for each individual tumour. Tumours were only assigned to the 'mixed' category when metanephrine and normetanephrine levels were equally raised with a ratio of 1.0.*

There was a good correlation between plasma and urine MN and NMN levels (Figure 5.33) in the 21 PPGLs for which both of these sets of data were available.
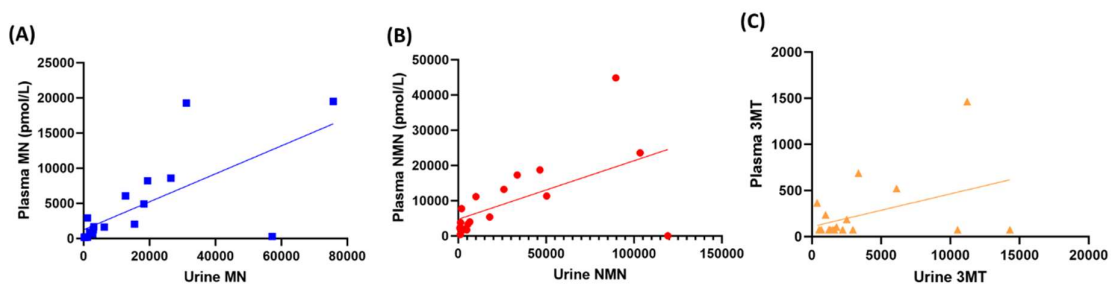
Figure 5.33: Plasma and urine metanephrine results. *(A) Concentration of plasma metanephrine (MN) plotted against concentration of urine metanephrine for each individual PPGL (n=21), (Pearson r = 0.69, p=0.001). (B) Concentration of plasma normetanephrine (NMN) plotted against concentration of urine normetanephrine for each individual PPGL (n=21), (Pearson r=0.565, p=0.015). (C) Concentration of plasma 3-methoxytyramine (3MT) plotted against concentration of urine 3MT for each individual PPGL (n=21), (Pearson r=0.42, p=0.06).*

There was a significant correlation between the size of the PPGL and the concentration of normetanephrine (p=0.009), but not for metanephrine (p=0.27) or 3MT (p=0.9) (Figure 5.34).
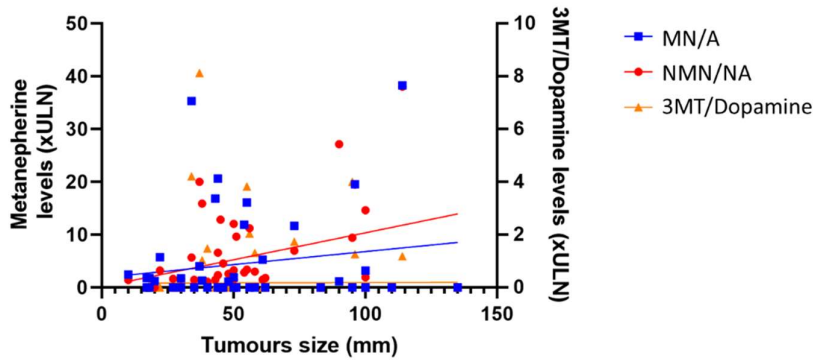
Figure 5.34: Metanephrine or catecholamine levels for different tumour sizes. Hormone levels are plotted as a proportion of the upper limit of the normal reference range (xULN) as data are pooled from plasma metanephrine results (n=23), urine metanephrine results (n=65) and urine catecholamine results (n=5). Metanephrine (MN)/Epinephrine (A) p=0.27 (Goodness of fit R=0.167), Normetanephrine (NMN)/Norepinephrine (NA) p=0.009 (Goodness of fit R=0.147), 3-methoxytyraime (3MT)/dopamine (A) p=0.9 (Goodness of fit R=0.0038).

Next the immune infiltration in the TME was analysed to determine how it is affected by the functional status of the PPGL (Figure 5.35). There was a significantly higher ratio of M2:M1 macrophages in non-functional PPGLs compared to functional PPGLs (p=0.044), with high levels of M2 macrophages in non-functional tumours. There was a significant difference in the macrophage infiltration depending on the dominant hormone being produced (p=0.0431), with higher levels in the PPGLs producing high levels of both MN and NMN (mixed category) (but data did not reach significance for individual comparisons). There was also a significant difference in the lymphocyte infiltration between PPGLs producing different dominant hormones with the lowest levels in the tumours producing the mixed hormones and the highest levels in the tumours producing MN (p=0.04).
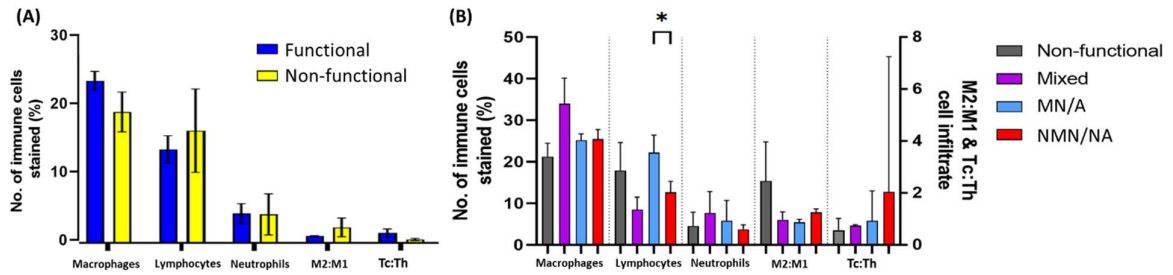
Figure 5.35: Immune cell infiltration depending on PPGLs functional status. *Immune cells analysed: macrophages (CD68+), lymphocytes (CD3+), neutrophils (NE, neutrophil elastase+), M2:M1 macrophages (CD163+:HLADR3+). (A) Bar charts showing immune cell infiltration in functional (n=47) and non-functional (n=9) PPGL tumours as a proportion on the total number of cells stained. Functional tumour is any tumour with any hormone (MN, NMN, 3MT) above the upper limit of the normal reference range. Macrophages p=0.183, lymphocytes p=0.61, neutrophils p=0.98, M2:M1 p=0.044, Tc:Th p=0.874 (Student's unpaired t tests). (B) Bar chart showing immune cell infiltration in PPGL tumours based on the dominant hormone production. A/MN n=15, NMN/NA n=28, mixed n=4 (NMN and MN levels were equally raised with a ratio of 1.0). Dominance was determined by the highest concentration for each individual tumour. Macrophages p=0.0431 (Welch's ANOVA with Tukey's multiple comparisons test), lymphocytes p=0.0417, neutrophils p=0.384, M2:M1 p=0.46, Tc:Th p=0.9 (Kruskal-Wallis ANOVA test with Dunn's multiple comparisons test). MN metanephrine, NMN normetanephrine, 3MT 3-methyoxytyramine, A epinephrine, NA norepinephrine, Tc cytotoxic T cell lymphocytes, Th T helper cell lymphocytes*

There were positive correlations between the different hormones produced by the PPGLs (Figure 5.36). There was a positive correlation between neutrophil infiltration and MN levels (p=0.002) and tumour size and NMN levels (p=0.01). There was a trend towards a negative correlation between lymphocyte infiltration and normetanephrine levels (p=0.07).
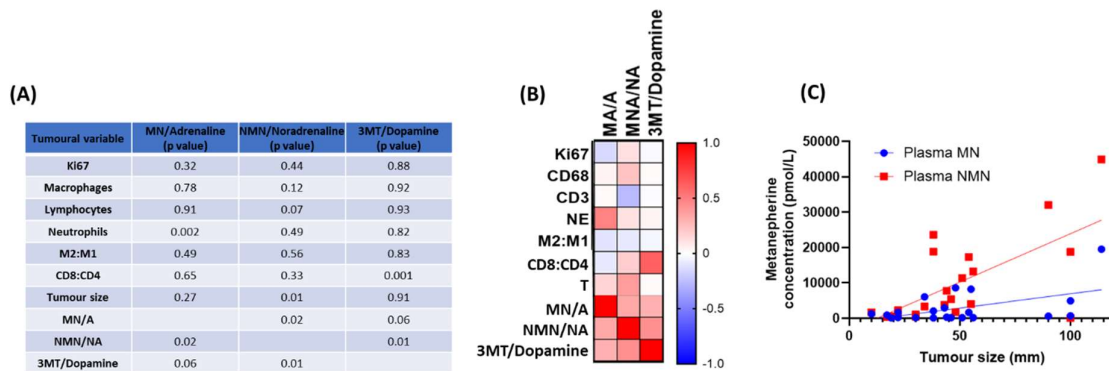
Figure 5.36: Correlation between tumoural variables and hormone levels. *(A) Table showing p values for the different correlations between the tumoural factors and hormone levels (Pearson r correlation). MN/A, NMN/NA, 3MT/Dopamine. (B) Heat map showing correlation between tumoural variables and hormone levels. Bar on righthand side shows intensity of correlation with gradient of colour between red -1.0 (negative correlation) through to white 0 (no correlation) and blue +1.0 (positive correlation). Ki67 proliferation index, macrophages (CD68+), lymphocytes (CD3+), neutrophils (NE), M2:M1 macrophages (M2:M1). (C) Scatter diagram showing the positive correlation between tumour size and plasma normetanephrine levels (Pearson r=0.384, p=0.01) and metanephrine levels (Pearson r=0.167, p=0.27). MN metanephrine, NMN normetanephrine, 3MT 3-methyoxytyramine, A adrenaline/epinephrine, NA noradrenaline/norepinephrine, T tumour size.*

215

When PPGLs with plasma metanephrine data available were analysed separately (n=21) there were positive correlations between tumour size and plasma MN (p=0.016) and plasma NMN (p=0.001) (Figure 5.36C) and neutrophil infiltration and plasma MN (p=0.004) and plasma NMN (p<0.0001). A similar positive correlation was identified between neutrophil infiltration and urine MN levels (p=0.06) when PPGLs with urine metanephrine data was analysed separately (n=44). In addition, a positive correlation between macrophage infiltration and urine NMN (p=0.02) was identified.

Attempts were made to validate these data using immunofluorescence double staining on a cohort of six malignant PPGLs, six benign PPGLs and five non-pathological medulla samples (Figure 5.37). Firstly, tissues were immunolabelled with a macrophage marker (CD68+) paired with a lymphocyte marker (CD3), and subsequently investigated for macrophage (CD68+, CD163+), and lymphocyte (CD4+, CD8+) subtypes.
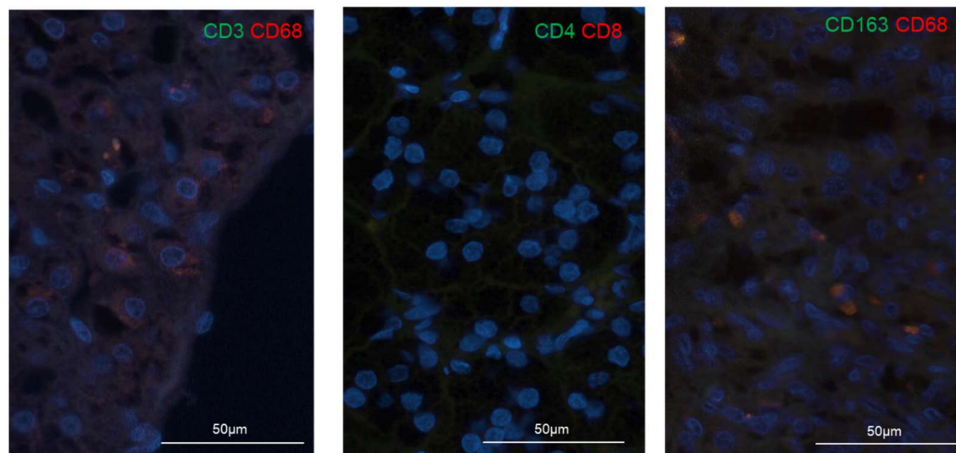
Figure 5.37: Immunofluorescence microscopy images of immune cell markers in PPGLs. *Immune cells analysed: macrophages (CD68+) M2 macrophages (CD163+), Lymphocytes (CD3+), T helper 1 cells (CD4+), Cytotoxic T cells (CD8+)*

This qualitative assessment did confirm that macrophages were the dominant immune cell type and lymphocytes were sparse; however, this method was not successful as there were high levels of background staining and autofluorescence observed making it impossible to carry out further analysis.

5.3.4 Patient serum inflammatory markers

In an ideal world it would be possible to identify patients at higher risk of malignant transformation earlier in the diagnostic process. The ideal method would be to have biochemical markers that could be used to predict the behaviour of the tumour and subsequent patient prognosis. I investigated whether biochemical and haematological markers measured in the patients' serum, taken as a blood test at diagnosis and one day before their operation could be used to predict tumoural factors or immune infiltration.

There was a positive correlation between the tumour Ki67 score and the patients' serum pre-operative prognostic nutrition index (PNI) (p=0.05) and neutrophil-platelet score (NPS) (p=0.011) scores, and between both pre-operative (p=0.02) and diagnosis lymphocyte-monocyte ratio (LMR) (p=0.05) and tumour neutrophil infiltrates. There was a trend towards a negative correlation between tumour macrophage infiltration and both pre-operative (p=0.07) and diagnosis LMR (p=0.06). There was a positive correlation between age and SII at diagnosis with older patients scoring higher (Figure 5.38).
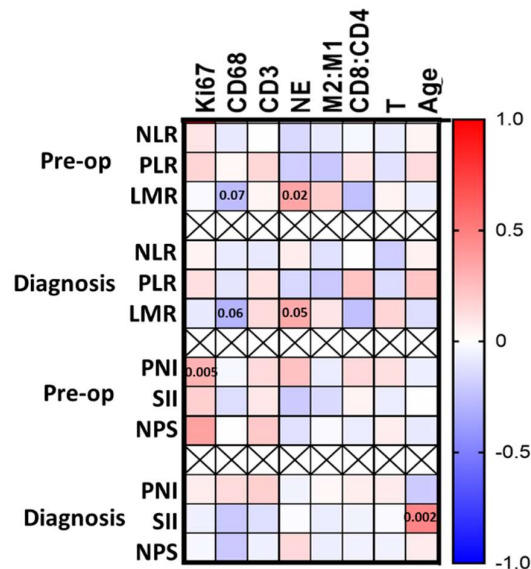
Figure 5.38: Heat map demonstrating correlation between tumoural variables and patient serum inflammatory scores. Bar on the right hand side shows intensity of Pearson r correlation with gradient of colour between blue -1.0 (negative correlation) through to white 0 (no correlation) and red +1.0 (positive correlation). Ki67 proliferation index, macrophages (CD68+), lymphocytes (CD3+), neutrophils (NE), M2:M1 macrophages (M2:M1), tumour size (T), NLR neutrophil-to-lymphocyte ratio, PLR platelet-to-lymphocyte ratio, LMR lymphocyte-to-monocyte ratio, PNI prognostic nutrition index (albumin+(5xlymphocytes)), SII systemic inflammation score (NLR x total platelet count), NPS neutrophil-platelet score (score 0 if neutrophils<7.5 and platelet <400, score 1 if neutrophils >7.5 or platelets >400, score 2 if neutrophils >7.5 and platelets >400). Significant p values are shown on the heat map. Bloods taken at diagnosis were taken at first reported high metanephrine levels, 'pre-op' blood tests were taken one day before adrenalectomy.

There was a significant difference in NLR (p=0.05, mean 3.325 vs 1.865) and PLR (p=0.0364, mean 208.6 vs 134.3) scores between benign and malignant tumours at diagnosis; with higher scores in benign PPGLs. There were no differences in scores between benign and malignant PPGLs for the other serum inflammatory markers at diagnosis (WBC, platelets, neutrophils, lymphocytes, LMR, PNI, SII and NPS). There were significantly higher levels of serum WBC pre-operatively in malignant PPGLs than benign, no differences were observed in the other inflammatory markers taken pre-operatively.
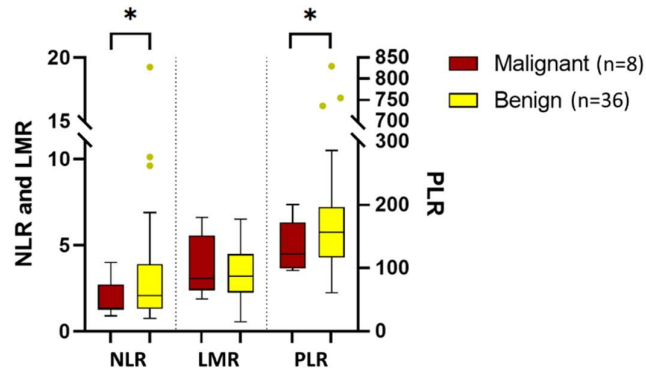
Figure 5.39: Patient serum inflammatory scores at diagnosis in benign and malignant PPGLs. *Data show box-and-whisker plot of mean, IQR and outlying points of NLR, LMR and PLR serum inflammatory scores taken at the time of diagnosis of benign and malignant PPGLs. NLR p=0.045, LMR p=0.544, PLR p=0.0364 (Welch's t test). NLR neutrophil-lymphocyte ratio, LMR lymphocyte-monocyte ratio, PLR platelet-lymphocyte ratio.*

These data indicate that patients' serum inflammatory scores may be able to aid in prognostic scoring.

5.3.5   SSTR expression in PPGL tumours

There have been conflicting reports regarding somatostatin receptor expression in PPGLs, especially SSTR2 and SSTR3[381,385], and studies have demonstrated mixed responses to treatment with SST analogues[301,302,382-384]. Very few of these explore this relationship based on the underlying genetic mutation. A radiolabelled SST analogue has been shown to be the best way of localising *SDHB* metastatic disease[266]. Therefore, it is possible that differences previously seen in SSTR expression may be due to the specific underlying genetic mutation, and if this were the case this would open up another treatment avenue for patients with aggressive disease.

A TMA was designed to include cores from 55 PPGLs arising from different body sites and to include both benign and malignant tumours. The TMA also included PPGLs from patients with sporadic tumours (tested negative on 10 gene panel) and those with a range of germline mutations (Figure 5.40 & Table 5.7). Malignancy of the sample was clinically defined, based on whether the patient was known to have metastatic disease.

Total no. of patients	55
Benign	45 (81%)
Malignant	11 (19%)
Site of tumour [n (%)]:	
PCC	26 (47.3%)
Abdo PGL	15 (27.3%)
Thorax PGL	6 (10.9%)
Pelvic PGL	5 (9.1%)
HNPGL	3 (5.5%)
Genetics [n (%)]:	
SDHB	17 (30.9%)
SDHD	6 (10.9%)
SDHA	1 (1.8%)
RET	5 (9.1%)
VHL	4 (7.3%)
Sporadic	22 (40%)

Table 5.7: Table showing the clinical details of the PPGLs analysed. *PCC phaeochromocytoma, PGL paraganglioma, Abdo abdominal, HNPGL head & neck paraganglioma, SDH succinate dehydrogenase, VHL von Hippel Lindau, RET rearranged during transfection proto-oncogene (RET).*
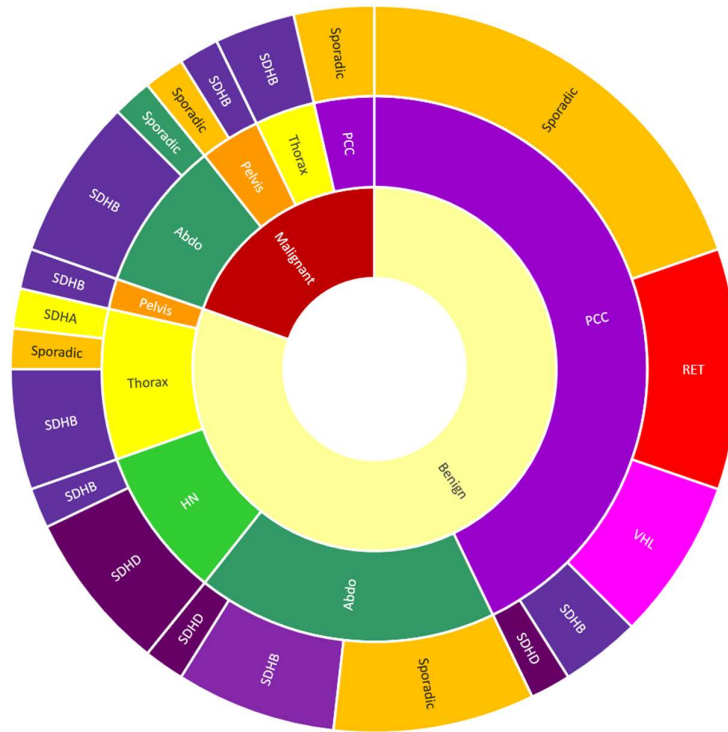
Figure 5.40: Clinical details of the PPGLs included in analysis. *Sunburst pie chart showing the proportion of benign and malignant PPGLs (inner ring), location of theses tumours (middle ring) and underlying genetic diagnosis (outer ring) for each category. PCC phaeochromocytoma, PGL paraganglioma, Abdo abdominal, HNPGL head & neck, SDH succinate dehydrogenase, VHL von Hippel Lindau, RET rearranged during transfection proto-oncogene (RET).*

Eighty percent of PPGLs demonstrated some SSTR2 immunoreactivity. The full spectrum of SSTR2 immunostaining was seen across the PPGLs (Figure 5.41). SSTR5 immunostain was absent in all PPGLs examined (Figure 5.43). Almost all of PPGLs demonstrated some SSTR3 immunoreactivity (97%), although for half of them (53%) this was cytoplasmic staining only (Figure 5.42).
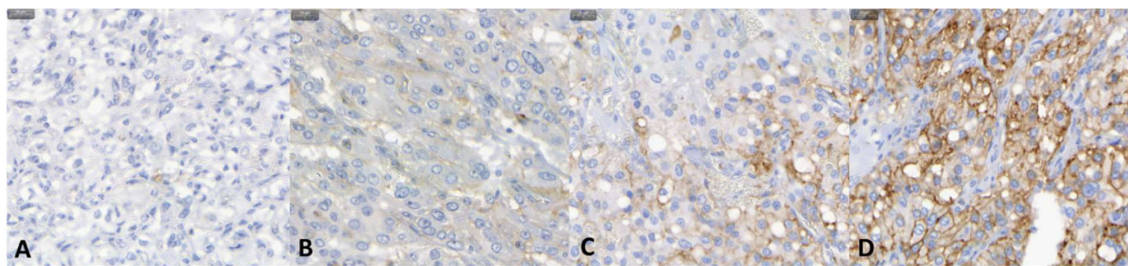
Figure 5.41: SSTR2 immunohistochemistry. *Four cores from selected cases showing the range of different SSTR2 expression in this cohort. A) absence of immunoreactivity (score 0). B) pure cytoplasmic immunoreactivity (score 1). C) membranous reactivity in less than 50% of tumour cells (score 2). D) complete membranous reactivity in greater than 50% of tumour cells (score 3).*
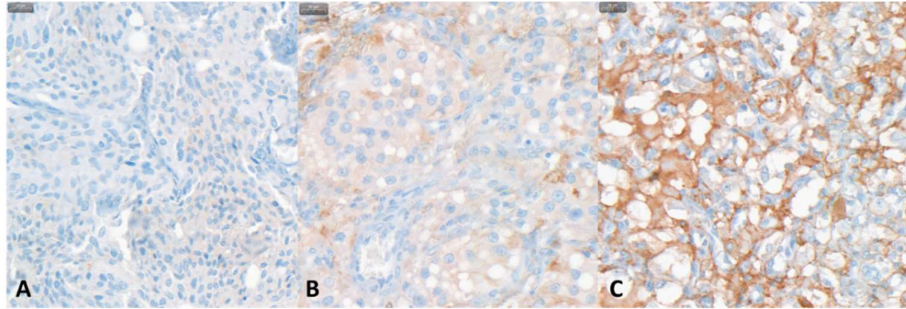
Figure 5.42: SSTR3 immunohistochemistry. *Three cores from selected cases showing the range of different SSTR3 expression in this cohort. A) absence of immunoreactivity (score 0). B) pure cytoplasmic immunoreactivity (score 1). C) membranous reactivity in less than 50% of tumour cells (score 2).*
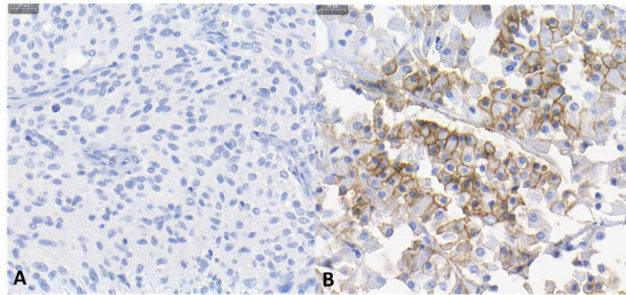
Figure 5.43: SSTR5 immunohistochemistry. *Two cores from selected cases demonstrating the different SSTR5 expression in this cohort. A) absence of immunoreactivity in PPGL tissue (score 0). B) complete membranous staining in greater than 50% of cells in normal pituitary control tissue (score 3).*

There was a significant difference between the SSTR2 scores awarded when the TMA cores were analysed compared to the full slide analysis (p=0.002*, Wilcoxon matched pairs signed rank test). Therefore, it was decided that the immunoreactivity demonstrated in the tumour cores was not representative of the tumours, so full slides were used for analysis for SSTR2 immunostaining. There was no significant difference between the SSTR3 scores awarded on the TMA cores and those of the full slides, therefore cores were used for SSTR3 analysis.

There was a significant difference (p=0.0497) in the SSTR2 score between benign and malignant PPGLs, with malignant tumours all demonstrating high immunoreactivity (scores 2 or 3, complete membranous staining) (Figure 5.44).
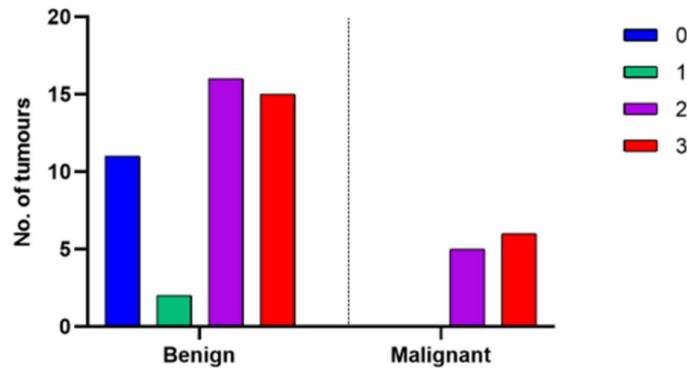
Figure 5.44: SSTR2 scoring for benign and malignant PPGL tumours. *Bar chart showing the number of tumours in each category of SSTR2 scoring for benign and malignant PPGLs. Statistical analysis by Fisher's exact test p=0.0497 when comparing grouped categories of low scores (0/1) with high scores (2/3).*

There was no significant difference between SSTR2 scores between PCCs and PGLs or on location of the tumour.
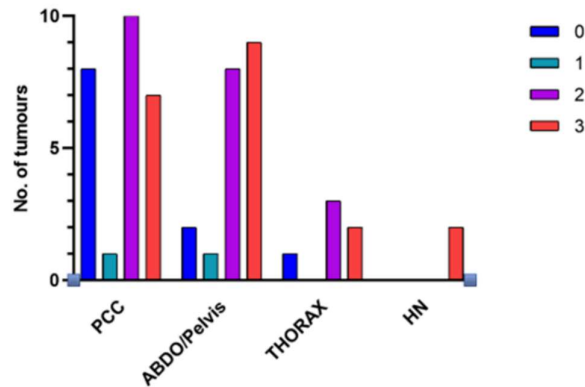
Figure 5.45: SSTR2 score by PPGL location. *Bar chart showing the number of tumours in each category of SSTR2 scoring for each tumour location. Statistical analysis by Chi squared p=0.588. PCC phaeochromocytoma (n=26), Abdo PGL abdominal paraganglioma (n=15), Thorax PGL (n=6), Pelvic PGL (n=5), HNPGL head & neck paraganglioma (n=3).*

There was a significant difference in the SSTR2 scores depending on underlying genetics of the PPGLs (p=0.0093). This significance was maintained when only benign PPGLs were analysed (p=0.009). Tumours with underlying *SDH* mutations had predominately high scores of two or three (only one *SDH* PPGL had absent SSTR2 immunostaining), whereas PPGLs with underlying *VHL* mutations had predominately absent SSTR2 immunostaining. PPGLs with no known underlying genetic mutations (sporadic) demonstrated the full spectrum of SSTR2 scores (0-3). There was no significant association with SSTR2 scoring and aggressiveness of tumour within the *SDHB* group (p=0.99) or the sporadic group (p=0.1206). There were no malignant cases of *SDHD*, *VHL* or *RET* tumours.
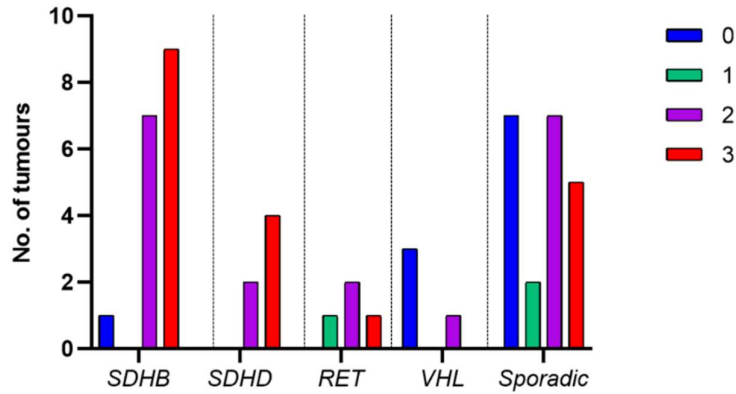
Figure 5.46: SSTR2 scoring for PPGLs categorised by different genetic diagnosis. Bar chart showing the number of tumours in each SSTR2 scoring for each genetic diagnosis of PPGL. Statistical analysis by Chi square test p=0.0451 when all four categories of scoring compared. When comparing grouped categories of low scores (0/1) with high scores (2/3) p=0.0093.

There was a significant difference between the Ki67 scores awarded on the cores from the TMA compared to the pathology report from the original tumour specimen (p=0.0408*), therefore Ki67 scoring from pathology reports were used for analysis as whole sections were used for this scoring. There was no significant correlation between Ki67 score and SSTR2 scores (p=0.4590) or SSTR3 scores (p=0.822).

For SSTR3 immunoreactivity there were no differences based on aggressiveness of tumour (p>0.99), underlying genetics (p=0.37), or tumour location (p=0.65) (data not shown).

In summary, all PPGLs had absent SSTR5 expression and some SSTR3 expression. SSTR2 expression was highest in malignant tumours and *SDH* and *RET* PPGLs, and lowest in *VHL* PCCs. SSTR2 expression did not differ based on tumour location.

5.4   Discussion

Clinically the most important objective is to attempt to identify markers which distinguish the tumours that are at risk of malignant transformation at early stages or ideally at initial diagnosis. If it was possible to know which tumours would remain benign and which become malignant this would relieve pressure on surveillance screening programmes which could then be individually tailored and also introduce the possibility of using adjuvant treatments in the same way they are used for other malignant tumours.

5.4.1   Cytokine profiles

These data suggest that PPGL tumours are more secretory of cytokines and chemokines than non-pathological adrenal medullary chromaffin cells and can generate a local immune response within the TME. The majority of the cytokines/chemokines that were secreted in higher concentrations were pro-inflammatory in nature. All are involved in monocyte (IP10, MCP1), macrophage (MDC, IP10, IFNγ, MCP1) and neutrophil recruitment (IFNγ, IL8) or T-cell (IP10, IL18) and natural killer cell (IP10, IL18) activation. The majority are secreted by macrophages (IL6, IL8, TNFα, MDC) or T-cells (IL18, IFNγ, IL6). Although routine measurement of cytokines in PPGL TME is not currently a viable option for each patient, these data show that PPGLs are immunologically active in contrast to widespread perception[307-309]. This knowledge could potentially be exploited for use of new therapies in these tumours. To my knowledge no other study has investigated local cytokine production in the TME of PPGLs, but the handful of cases that have been reported with systemic increase in cytokines (IL6, IL8, TNFα)[145] include some of the cytokines that were raised at concentrations 10 times higher in the PPGL tumours compared to the non-pathological medulla cells.

Time limitations and working restrictions mean the number of samples processed was small and therefore results need to be interpreted with caution. Unfortunately, use of a metanephrine assay only became available after the first set of primary cultures had been undertaken identifying the potential problem of the cells dying off too quickly in the media containing 1% serum. Metanephrine concentrations and cell density assays showed cultured non-pathological medulla cells die off more quickly than cultured PPGL tumour cells, but both cell types die off quickly when depleted of serum. Due to low sample numbers sub-analysis to see if cytokine profiles differed based on clinical or tumoural factors was not performed.

5.4.2 Infiltrating immune cells in the TME of PPGLs

In keeping with the cytokine data, these data has shown that immune cells do infiltrate the TME of PPGLs, with significantly higher levels than in non-pathological medulla. This immune cell infiltrate is dominated by macrophages, confirming that PPGLs should be considered immunologically active tumours. Similar to previous studies, macrophages were observed to be the abundant immune cell type[387-389], with a relative lymphocyte depletion and very low levels of neutrophils. Lymphocyte depletion may be a catecholamine effect, as they have been reported to suppress T lymphocytes Th1, Th2, cytotoxic and NK cells[390,391] and exert inhibitory effects on T cell proliferation due to chronic stress in mice[392]. Large variations in immune cell infiltration amongst samples were observed as reported in other cohorts[308,387,389].

Surprisingly, non-pathological adrenal medulla taken from tissue adjacent to the PCC contained similar amounts of infiltrating macrophages to the actual tumour tissue. This suggests that the macrophages need to migrate through the non-pathological medulla tissue to reach the tumour, suggesting that there may be specific antigens or receptors in tumour cells that subsequently 'activate' the macrophages. These factors may include the cytokines or chemokines outlined above that are secreted by the tumour cells. Macrophages are recruited by cytokines and chemokines secreted in the TME and subsequently release further cytokines/chemokines to enhance recruitment of more macrophages as well as other immune cells. As shown above, many of the cytokines that were found to be increased in the cultured PPGL cells were cytokines involved in macrophage and monocyte recruitment and activation (MDC, IP10, IFNγ, MCP1 IP10, MCP1). It is described that when exposed to hypoxia they switch on mitogenic and proangiogenic cytokines[318], and this stimulus may occur when macrophages infiltrate the tumoural mass. There was a higher M2:M1 ratio in PPGLs with known pseudohypoxic cluster 1 mutations compared to the kinase-signalling cluster 2 mutations, with the highest levels of M2 macrophages in the TCA-cycle related cluster 1a mutations, compatible with the hypoxic stimulus causing a phenotypic change in the macrophages[318].

Despite *SDHB* PPGLs being associated with a higher malignancy risk and *VHL* and *RET* considered more benign disease, very few differences were observed in immune cell infiltration on sub-analysis of the different underlying mutational status, similar to previous reports[308]. These data may indicate that the underlying genetic fault has little influence on the composition of the TME, although this may have been due to too few samples for the individual groups in these cohorts to reach statistical significance. However, this may also reflect the wide clinical heterogeneity within each genetic group with regards to behaviour of the tumour, as although *SDHB* PPGLs are associated with a higher malignant potential, many remain benign. The only differences observed between the different genetic groups was a lower

density of cytotoxic T lymphocytes in all genetic positive tumours compared to negative tumours and specifically the lowest levels were observed in PPGLs due to *SDHB* mutations. Cytotoxic T cells are usually associated with good clinical outcomes as they have the ability to kill tumour cells, so the fact that the lowest levels were observed in *SDHB* tumours may suggest that there is something about this particular genetic mutation that inhibits the recruitment or action of these cells, allowing these tumours greater chance of proliferation and malignant transformation, due to immune system evasion. Batchu *et al*[389] investigated effects of somatic mutations and found *FRG1B* and *RET* mutations correlated with increasing M2 macrophage infiltration, but germline mutations were unknown in this study. Tamberero *et* al[317] found some suggestions of differences with mutational status at a somatic level of *HRAS* mutation in PGLs associated with highly cytotoxic immunophenotypes and *NF1* mutations in PGLs with poorly cytotoxic immunophenotypes. Another study performed an analysis of TMA cores of 48 PCCs and four PGLs and found the highest density of M2 macrophages occurred in three out of four of their *SDH t*umours[308] and therefore this area requires further investigation.

The question has previously been raised whether tumours arising at different locations in the body had different TME's[312]. Although one small study showed that there was no difference in immune cell infiltration between PCC and PGLs[308], this study used TMA cores and only included four PGLs, therefore this question has not been well addressed. These data showed that although both PCC and PGLs had higher immune infiltration compared to non-pathological medulla tissue, the only observed difference was in the density of T helper lymphocytes, with higher density seen in PCC compared to PGLs. There were no differences in all the other immune cell profiles across the different locations of the tumours. This is consistent with a previous finding[308], and another recently published study that used a machine learning RNA deconvolution algorithm to look at the relative expression of signature immune cell genes in 31 PGLs and 148 PCCs and found no obvious clustering to differentiate between PGLs and PCC using principle component analysis[389].

The higher concentration of immune cells was applicable to both benign and malignant tumours, but only subset analysis of macrophages and lymphocytes demonstrated a difference between the tumour groups. There was a higher concentration of M1 macrophages and CD4 T cells in benign tumours compared to malignant and a higher M2:M1 ratio in malignant tumours. These data are in accordance with the observed results in another study looking at RNAseq data which showed low levels of activated CD4 and CD8 cells in metastatic primary tumours[393]. M1 macrophages promote inflammation, which can lead to tumour rejection[322,386], which may be a mechanism for why these tumours remain benign and do not metastasise. These data suggest that the TME of PPGL tumour cells is dominated by M2 macrophages, whereas non-pathological medulla ECM predominately contains

M1 macrophages. M2 macrophages, also known as tumour-associated macrophages or TAMS, are anti-inflammatory and promote tolerance, allowing the tumour to evade the immune system[322,386]. TAMs are associated with cell proliferation and tumour progression in other solid tumours[324-330], and the higher density of TAMs in PPGLs demonstrated by our data may indicate that this is also true for PPGLs. M2 macrophages are reported to be the most representative immune cell in human malignancies such as breast, bladder and prostate[320,321]. Although the distinction between M1 and M2 polarised macrophages is probably an oversimplification of the true situation, as macrophages are considered highly plastic and adaptable cells[322]. However, this distinction represents the phenotypic extremes of a continuum polarisation spectrum, and are widely used for research purposes[319,325].

There was a higher density of T helper cells and lower CD8:CD4 ratio in tumours compared to non-pathological medulla. This is in agreement with other studies showing a higher CD8 T cell density, which is generally thought to be associated with better prognosis. Gao *et al*[387] showed higher CD8 infiltrate, CD31 and PNMT in PPGLs with 'PCC of the Adrenal gland Scoring System' (PASS) scores <4 and well differentiated tumours (although of note no poorly differentiated tumours were included and only recent cases were studied limiting clinical details and long-term follow up data, so whether these patients subsequently developed metastatic disease is unknown) and they reported a correlation with lymphocyte infiltration and M1 macrophages[387]. Guadagno *et al*[388], however, found no correlation between PASS and 'Grading system for PCC and PGLs' (GAPP) scores. Studies into other cancer types have generally shown higher numbers of tumour-infiltrating lymphocytes (TILs) to be associated with a better prognosis[335,394,395], but overall low levels of lymphocytes were observed in PPGL tumours in this cohort. The small number of studies investigating PPGLs have generally shown lymphocyte depletion. In contrast to these previous studies one study reported that 44% of primary mPPGLs tumours had a high infiltration of TILs[307], although they acknowledge this did not correlate with improved survival or response to ICB therapy, and many tumours had no or minimal TILs. Very little difference in the lymphocyte infiltrates between benign and malignant tumours was observed. In their vast assessment of over 9000 solid tumours, Tamborero *et al*[317], included 178 PPGLs and reported huge variability in immunophenotypes in PPGLs based on their cytotoxic T cell classification with 20% in the complete lymphocyte depletion category and 30-40% in the highly dense category, and therefore these data and other studies are likely to be highly influenced by the heterogeneity of these tumours.

Specifically, with the PPGLs from patients with underlying *SDHB* mutations there was a higher infiltration of overall macrophages, for which M2 macrophages dominated and there were higher Ki67 scores in malignant tumours compared to benign. These histological tumour markers could potentially

be used in addition to clinical factors (tumour size etc) to aid in predicting which tumours have the highest malignancy potential and allow for surveillance to be tailored to the individual's risk.

Gao *et al*[387] reported a negative correlation between tumour size and immune cell infiltrate; however, in these data a trend towards higher concentrations of macrophages and lymphocytes in larger tumours (when small recurrent tumours were removed) and more macrophages (especially TAMs) were observed with increasing Ki67 scores. Surprisingly no correlation was observed between increasing tumour size and Ki67, but it is well known that many large PPGL tumours have very low scores and remain benign, which is why Ki67 index is not as useful a pathological marker for malignancy in PPGLs as it is in other neoplasms. General consensus reports PPGL tumours >40 mm are ones to watch for malignant transformation and when recurrent tumours were removed (19 and 22 mm) from analysis, all malignant tumours in this cohort were >40 mm and had a higher M2 macrophage signature.

Exciting new therapies, for example pembrolizumab, a PD-1 inhibitor, have recently been tested in small phase 2 trials[307]. Eleven patients with metastatic PPGL were included and four had underlying germline mutations (2 *SDHB*, 1 *SDHD*, 1 *PMS2*). Four patients achieved the primary end point of non-progression at 27 weeks, with a clinical benefit rate of 73%, progression free survival of 5.7 months, and median survival of 19 months. One of the *SDHB* patients experienced a substantial reduction in tumour size, but sadly had to stop treatment due to toxicity. It has been reported that higher levels of cytotoxic lymphocytes are associated with a better response to ICB therapy. In our cohort, although this did not reach significance (perhaps due to low sample numbers), there were higher mean levels of CD8:CD4 levels in *SDHB* tumours compared to those with other underlying genetic mutations, although the overall density of lymphocytes were lowest in *SDHB* tumours. This suggests that it may be the balance of the different subsets of lymphocytes that is important rather than the absolute values, and tumours due to *SDHB* mutations may be more responsive to this treatment because of the relative increase in cytotoxic lymphocytes. Although the clinical trial found no clear association between PDL1 expression or TILs in primary tumours and clinical response, the TILs scoring was based on a simplistic categorical scoring system of 0-3 based on density of lymphocytes. Therefore, more advanced scoring systems or use of cell density counts (as used in this study and others[335,387]) may prove that these histological staining methods could provide further insight into which tumours may be more responsive to these new therapies.

5.4.3   Effect of tumoural secretion on PPGL TME immune profile

There was good correlation with plasma and urine metanephrine concentrations, but not 3MT as previously described[23]. A higher proportion of the malignant tumours were non-functional, but this may reflect a bias as non-functional PPGLs tend to remain undetected *in situ* for longer and grow to a larger size which is associated with increased malignant potential. Similarly, Gao *et al* found higher PNMT and CD8 infiltrate in PPGL tumours with a low PASS scores (<4) and well differentiated tumours (based on GAPP scoring)[387]. For those malignant tumours that were functional a higher proportion produced 3MT, with very few producing MN, consistent with conventional wisdom[23]. In keeping with this and the previously described data above, there was a higher M2:M1 ratio in non-functional tumours (more likely to be malignant). Interestingly the recent clinical trial of a PDL1 inhibitor found the longest stability of disease with non-hormonally active tumours[307].

Generally, there were low levels of lymphocytes detected in PPGLs as previously reported[308,317,323]. The highest levels of lymphocytes were found in MN producing PPGLs, with a positive correlation between lymphocyte and neutrophil density and MN concentration, which are generally associated with a benign course of disease, and negative correlation with NA producing tumours. Catecholamines have been reported to suppress lymphocyte action[390-392], but these findings suggest that this may in fact be an effect of norepinephrine rather than epinephrine. These data suggest that hormone production by the tumour may influence the immune cell infiltration into the TME. Epinephrine production may recruit lymphocytes and neutrophils to the PPGL TME and this may trigger a positive immune reaction for tumouricidal and cytotoxic effects thereby inhibiting malignant transformation. In support of this theory, Gao *et al* found a positive correlation between CD8 T cells and plasma epinephrine levels and negative correlation with GAPP score[387]. Conversely, norepinephrine seems to inhibit T cell proliferation and therefore it may be possible to improve responsiveness to immune checkpoint inhibitors if first the effects of norepinephrine could be inhibited. A recent study looking at TILs in adrenocortical carcinoma reported a similar finding with lower levels of TILs in ACCs that secrete higher levels of glucocorticoids associated with a worse prognosis[335].

5.4.4 Patient serum inflammatory markers

All patients undergo blood tests during diagnostic work up and pre-operatively. These are inexpensive and easily obtainable tests. It would be an ideal scenario if a prognostic biomarker obtained from patients' serum could be identified to help stratify patients into malignant risk to allow individualised surveillance to be implemented. Serum inflammatory scores have been used in other endocrine tumours to predict clinical outcome[193,196-200,367-369]. Within small PCC cohorts patients have been previously identified to have higher leukocytes, neutrophils, CRP and NLR and lower lymphocyte levels compared to hypertensive controls[18] or patients with either ACC or adrenal adenomas[68]. These inflammatory markers have been shown to decrease following adrenalectomy[142,145,146,174], demonstrating that PCC can cause a systemic inflammatory response. To my knowledge this has not be investigated within subgroups of patients with PPGLs.

In this cohort higher leukocytes were observed in patients with malignant PPGLs compared to those with benign tumours. Unlike other studies that suggest high NLR and PLR are associated with worse clinical outcomes, in this cohort higher NLR and PLR scores in the benign tumours compared to the malignant ones were observed. This may suggest that in patients with PPGLs, low NLR and PLR scores are associated with worse clinical outcomes; however, these data should be interpreted with caution as the number of samples in the malignant group was small (n=8). Increasing Ki67 scores were associated with increasing NPS scores, which are known to be associated with poor clinical outcomes. LMR scores were negatively associated with tumour macrophage infiltrates and positively associated with tumour neutrophil infiltrate. Low LMR are reported to be associated with a poor clinical outcome, suggesting that higher levels of tumour macrophages and lower levels of neutrophil and lymphocyte infiltrates may be signs of poor clinical outcome.

5.4.5 SSTR expression

Intensity of SSTR2 expression varied between PPGLs dependant on the aggressiveness of the tumour and underlying genetics, so this may be a useful indicator to guide clinical management. Although there was some variation in SSTR3 immunostaining between tumours, no significant associations were identified based on aggressiveness of tumour, location of tumour or underlying genetics; the majority had cytoplasmic staining only. SSTR5 expression was absent in all PPGL tissue and therefore not clinically useful.

These data demonstrated a correlation between SSTR2 expression and aggressiveness of PPGL, with malignant tumours showing higher levels of SSTR2 expression. This result is in keeping with other

reports[217,396]. Whereas benign lesions displayed the full range of SSTR2 expression from absent staining (score 0) to complete membranous staining (score 3), all malignant tumours demonstrated high SSTR2 expression. Therefore, negative SSTR2 staining could be a sign of a benign lesion. This would need to be replicated on a larger sample set to be confirmed. Interestingly, this is contradictory to some studies on NETs that suggest higher SSTR2 expression is associated with a favourable prognosis[397,398]. Studies looking at SSTR expression and prognosis or overall survival are problematic, as it is difficult to adjust for bias of different treatments. One study demonstrated the association was only significant in a subset of patients with small intestinal NETs, and a subset of these had been treated with SST analogues. Within this group the authors conclude that the highest overall survival in the treated patients was in those with the highest SSTR2 expression (presumably due to increased sensitivity to treatment with SST analogue due to higher expression of receptors)[398]. Another study looking at pancreatic NETs concluded that negative SSTR scores was a poor prognostic indicator, but on further evaluation the tumours that scored zero also had a greater mean diameter and higher TMN staging[397].

Malignancy of the samples used in this study was pre-defined by clinical diagnosis of metastatic disease. Ki67 (cell proliferation index) is a molecular marker ascribed to the aggressiveness of tumours, with the higher values being recognised in more aggressive tumours. It was therefore unexpected that there was no significant correlation between Ki67 and SSTR2 score, given that an association was demonstrated based on clinical classification of the tumour as malignant. However, one of the problems with PPGLS is that Ki67 scores vary greatly with some malignant tumours having low scores and therefore because of this variation this small sample size may not have been able to detect an association to a significant level.

SSTR2 expression correlated with genetic status and interestingly there was a significant difference between PCCs due to *RET* and *VHL* mutations; with *RET* PCCs having a high expression of SSTR2 and *VHL* PCCs having mostly absent SSTR2 expression. PGLs caused by both *SDHB* and *SDHD* mutations tended to have higher SSTR2 expression. As the majority of *SDHD* PPGLs included were parasympathetic in origin, this is in keeping with previous reports that ^{68}Ga-DOTATATE (a selective somatostatin analogue ligand) is superior in localising HNPGLs[266,267]. A few studies have investigated SSTR expression in PPGL tumours, with conflicting results[399-401], but few have divided PPGLs based on underlying genetic mutations, which may influence SSTR expression. Only one other study has investigated SSTR expression in *SDH* PPGLs and similarly demonstrated an increased expression of SSTR2 in *SDH*-associated PPGLs[385] compared to non-*SDH* PPGLs. The authors of this study also suggested a difference in expression of SSTR2 between *SDH* and non-*SDH* PPGL metastases (but the

number of samples was small)[385]. This is supported by other observations of stronger SSTR2 immunoreactivity in metastatic lesions[217,396]. A recent review[402] of the uses of somatostatin analogues in imaging and treatment of PPGLs confirms ^{68}Ga-DOTATATE to be a superior radiotracer for imaging PPGLs in *SDH* cohorts and metastatic PGLs, in keeping with the above findings.

In case there was any bias of higher SSTR2 expression in malignant tumours affecting the correlation by genetic status (i.e. more malignant tumours due to *SDHB* compared to the other mutations), the analysis was also performed with malignant PPGLs removed. Significance remained with the majority of *SDHB* and *SDHD* tumours having moderate or complete expression of SSTR2. For sporadic PPGLs SSTR2 expression was more varied, and this may explain the contradictory results previously reported as few previous studies defined genetic status. There was no correlation found here between SSTR expression and location of the PPGL, suggesting genetic cause of the PPGL may be more important to SSTR2 expression than the location. One study identified a significantly better response of metastatic PGL with [90]Yttrium-DOTATATE therapy compared to MIBI, but no differences were observed in PCCs[403].

Within the *SDHB* subgroup there was no association demonstrated based on aggressiveness of tumour. However, when only benign PPGLs were analysed a significant association remained between genetic diagnosis. This suggests that perhaps the underlying genetic mutation is more important in dictating SSTR2 expression than the aggressiveness of the tumour; e.g. *all SDH* PGLs scored high regardless of whether benign or malignant; however, it may be that the sample size was too small to detect significance on subgroup analysis.

[177]Lutetium labelled DOTATATE (Lutathera®) has been approved for use for treatment of gastrointestinal neuroendocrine tumours. These preliminary results suggest that SST analogue therapy targeting SSTR2 receptors may also have a role in treating PPGLs that are not amenable to surgical intervention as well as those that are malignant; especially those due to underlying *SDH* mutations.

Immunostaining of PPGL tumour tissue for SSTR2 may aid in guiding which patients may benefit from treatment with radioisotope-labelled somatostatin analogues. Lanreotide and Octreotide target SST2, newer analogues such as Paserotide and Somatoprim have a broader range of targets across the SST receptor subtypes, so use of SST immunostaining may help in selecting the right treatment as we move towards personalised medicine. PPGL tumours do not appear to express SSTR5.

Since this preliminary work was undertaken a handful of case series and studies have been reported investigating the use of radiolabelled somatostatin analogues in the treatment of PPGLs and several

phase II clinical trials are now underway, although very few studies have investigated the expression of SSTRs in PPGLs. A recent review by Patel *et al*[402] summarises the small studies and case series to date that have utilised radiolabelled somatostatin analogues for treatment of PPGLs. There is a current phase II study at the National Institutes of Health (NCT03206060) using ^{177}Lu-DOTATATE for the treatment of *SDH* versus sporadic PGLs and a clinical trial assessing Lanreotide use in mPPGLs (NCT03946527) is ongoing.

5.5   General conclusions and future work

It has been 20 years since first attempts were made at devising a scoring system for PPGL based on histopathological features. There are two excellent recent reviews of the different scoring systems that have been proposed[195,404] (Appendix 8: Grading and scoring methods for PPGLs). In brief, the phaeochromocytoma of the adrenal gland scoring system (PASS) proposed in 2002[405], contains 12 different histological features and scores of ≥4 are considered malignant or biologically more aggressive; however, there have been controversies over its application due to concerns over reproducibility and it has not been widely adopted. Therefore in 2014, Kimura *et al*[406] subsequently proposed another scoring system 'Grading system for phaeochromocytoma and paraganglioma' (GAPP), which takes into account both histological features including histological patterns, cellularity, necrosis type, capsular/vascular invasion, proliferative index and a single clinical factor (catecholamine type) and categorises PPGLs into well-differentiated, moderately differentiated and poorly differentiated tumours. Although this later scoring system seems to have more reproducibility, it is not widely used clinically, as its prognostic values are not clear. A further modification to this scoring system was proposed in 2017[407] by the addition of SDHB immunohistochemistry, which became known as Modified-GAPP or M-GAPP. The sensitivity of GAPP and M-GAPP are relatively high, but specificity only reaches 50-60%[404]. Therefore, the addition of clinical factors into a scoring system were considered important. An entirely clinical model, ASES (age, size, extra-adrenal location and secretory type), was proposed by Cho *et al*[408] in 2018 with predictive scoring of malignant tumour behaviour to be 0.735 AUC, and high prediction accuracy for non-metastatic PPGL of 97%, but lower sensitivity and specificity for metastasis (61% and 80% respectively)[195]. Finally, the composite pheochromocytoma/paraganglioma prognostic score (COPPs) was proposed by Pierre *et al*[409] in 2019, which combines clinicopathological features (tumour size, central necrosis and vascular invasion) and immunohistochemical findings of S100 (a marker of sustentacular cells, whose absence may indicate a higher malignant potential[410]) and SDHB. They reported a sensitivity of 100% and specificity of 94.7% to predict potential metastasis, but subsequent validation studies are awaited.

Understanding the importance of the TME in PPGL has two important clinical implications. Firstly, if the TME has a role in the pathogenesis of more aggressive tumour phenotypes, then greater understanding of its components may open up potential therapeutic interventions targeting the TME. A more immediate implication would be to help define those PPGLs with a more aggressive potential that may benefit from closer post-operative surveillance. If validated in a larger tumour set, the TME may be an additional factor that could be included in PPGL scoring systems.

5.5.1 Limitations

Limitations with these studies include the small sample sizes, especially for the cytokine study. As these were based on freshly cultured tissue taken straight from the operating theatre I was restricted by availability of tissue. This also meant that it was difficult to include tumours caused by different underlying genetics and specific sites of disease etc as availability of tissue was dictated by surgical lists. This was further hampered by subsequent working restrictions. I was therefore unable to perform sub-analyses to see if cytokine profiles differed based on clinical or tumoural factors, and this is an area of future work.

Ideally these types of studies should be undertaken with the cells grown in serum free media to avoid any contamination of the serum to the cytokine/chemokine concentrations. However, it became quickly apparent that the chromaffin cells (both tumour and normal) would not survive more than a few hours when deprived of serum. Under microscopy examination cells cultured in media containing 1% bovine serum were visible and adherent, albeit in lower density. Unfortunately, analysis of metanephrine concentrations in the supernatant only became available after the first set of primary cultures had been undertaken. This identified the problem of cell death that occurred with using the 1% serum media, and thus complete media (containing 10% bovine serum) was used for the rest of the studies. To limit the contribution of the serum to the cytokine/chemokine concentrations measured samples of cell free serum were also analysed, and the production of cytokines was minimal in the serum alone for the majority of the cytokines tested. As chromaffin cells die off quickly in media depleted of serum, studies that could be undertaken on these cells were limited. A method of single cell suspension cell culture was employed and therefore this is not truly representative of the situation *in vivo* where the structure of the tumour and how the cells communicate with one another may contribute to the cytokine/chemokine response. To validate these results attempts were made to culture sections of tissue tumour cut using a vibrotome machine, unfortunately the PPGL tumour tissue turned out to be too fragile for this approach. Another approach for future studies could be to use spheroid cell cultures.

A larger cohort of samples were analysed to investigate the infiltrating immune cells as tissue was taken from paraffin blocks. A hotspot method of analysis was applied which may not be truly representative of each tumour, although Guadagno *et al*[388] demonstrated no difference between the immune infiltration between the periphery and centre of the tumour. I found wide variation in immune cell infiltration between tumours, even within the same types, which may partly be due to the method used, although previous studies have reported similar large variations. An alternative method of analysis could have been to identify a specific area or areas of each tumour and then use identical areas for analysis for each type of immune cell. Although this method would have worked well for analysing the macrophages which had the highest density in the PPGL tumours, many of the other immune cells were only seen in small densities in single cells or in small clusters and therefore using this method would likely have resulted in many tumours scoring zero when in fact they did contain a small number of these cell types. Due to this limitation the hotspot method was chosen.

These data showed that the adjacent non-pathological medulla taken from the same adrenal gland as a tumour had similar levels of macrophages to the tumour tissue and higher than that of 'normal' medulla taken from an independent non-pathological adrenal medulla. This may reflect that the 'normal' medulla that is adjacent to a PCC tumour is not 'normal' at all, therefore samples obtained from independent non-pathological medulla were also used for comparison.

I was unfortunately unable to acquire reproducible results using immunocytochemistry methods due to a large amount of background autofluorescence and therefore each immune cell was analysed independently rather than using dual markers, which would have been helpful to investigate interactions between the cell types especially when analysing the ratios between the subtypes of macrophages and lymphocytes. I also fully acknowledge that the surface markers (HLA-DR3 and CD163) I have used to distinguish between M1 and M2 macrophages is a simplistic approach, and may not truly represent the complex interactions that exist.

Unfortunately, GAPP and PASS scores were unable to be calculated for the samples and therefore could not compare results directly with those reported in the literature.

Small sample sizes were a limiting factor when assessing systemic inflammatory scores, and SSTR expression in predicting aggressive behaviour, especially when performing sub-analyses, for example the malignant group contained just eight samples. Therefore, these observations need to be interpreted with caution and replicated in a larger cohort.

5.5.2 Future work

The cytokine data presented is preliminary work on a small sample size and therefore needs to be validated in a larger cohort, and potentially using spheroid cell cultures instead of single cell suspensions. The fact that the adjacent non-pathological medulla had similar levels of macrophages to the tumour tissue and higher than that seen in independent non-pathological adrenal medulla may reflect the reality that the adjacent medulla is not truly non-pathological. This raises the possibility that the macrophages need to migrate through the normal medulla tissue to reach the tumour area, suggesting that there may be specific antigens or receptors in tumour cells that subsequently 'activate' the macrophages. These factors may include the cytokines or chemokines discussed in this thesis that are secreted by the tumour cells, but the mechanism underlying this requires further investigation.

Another avenue for future research would be to investigate cytokine profiles of PPGL TMEs to see if they differed based on clinical or tumoural factors; such as underlying genetics or location of tumour. In addition to using fresh tumour samples another approach could be to use a knock-out cell line for example to investigate in more detail if there were any differences between the mutations in the different *SDH* subtypes. It is described that macrophages switch their phenotypic state (e.g. from M1 to M2) when exposed to hypoxia[318] and therefore it would be interesting to investigate further whether there are differences in macrophage numbers and subtypes between the cluster 1 mutations that cause pseudohypoxia and the kinase-signalling cluster 2 mutations.

It was surprising that little difference was identified in immune cell infiltration between tumours caused by the different genetic mutations, especially given that some mutations are associated with much higher rates of metastatic disease. This may be due to the small sample size when the cohort was spilt for sub-analyses and therefore this avenue requires further research with a larger cohort.

Further characterisation of components of the PPGL TME could include investigating the presence of other immune cell types such as natural killer cells, dendritic cells, Th17 lymphocytes and mast cells. As well as the application of other molecular techniques such as dual staining immunocytochemistry, fluorescence-activated cell sorting (FACS) and magnetic beads for immune cell separation.

As part of the work undertaken with the fresh culture tissue, cancer-associated-fibroblasts (CAFs) and fibroblasts grown from the cultured non-pathological medulla cells were also cultivated. Another avenue of further work could be to look into the contribution of fibroblasts which are part of the TME and what cytokine/chemokines they contribute. This potentially also opens up the possibility of being able to use CAFs to test novel drug therapies, which is not possible on the primary cultured chromaffin cells as they do not survive long enough. In a preliminary experiment measuring the metanephrine

levels in the cultured CAFs that had been grown for several weeks (so all chromaffin cells should have died) there were measurable levels. The reason for this is unclear as fibroblasts do not produce catecholamines and therefore raises the possibility that there may have been an immortalised chromaffin cell within the cultured CAFs. Another explanation may be that the dying chromaffin cells released all of their catecholamines and these remained in the supernatant that was frozen and stored.

Chapter 6. Final conclusions

The aim of the thesis was to improve the clinical care of patients with PPGLs with three main strands: to improve compliance and reduce morbidity with pre-operative medical therapy, enable earlier identification of tumours in individuals with a genetic predisposition, and investigate potential directions for novel treatments.

Firstly, ways to improve pre-operative management for all patients with a functional PPGL were investigated. Two main pre-operative areas were addressed (chapter 3): improving patient tolerance of alpha-blockade medication and assessing additional benefits derived from treatment with medical therapy.

Data presented in this thesis suggest that the use of HBPM may be beneficial for outpatient management. By utilizing HBPM and personalised titration of medications through a dedicated clinic these data have shown improved compliance with alpha-blockade medication resulting in higher tolerated doses, lower BP and HR and thus shorter hospital admissions pre-operatively. In addition, the longer duration of treatment with alpha-blockade appears to be an important factor in reducing intra-operative HDI and frequency of post-operative hypotension. If patients are able to tolerate higher doses of alpha- +/- beta-blockade medications in the community they will be safer from the cardiovascular effects of catecholamine excess whilst awaiting their operations. This would also reduce the amount of time patients need to be in hospital pre-operatively, thereby improving patients' quality of life, as well as reducing the burden on NHS resources.

Bioimpedance analysis and measurements of serum inflammatory and immune markers were studied to explore potential additional physiological benefits of alpha-blockade therapy to PPGL patients pre-operatively. These data demonstrated the potential to reverse the inflammatory and catabolic effects of catecholamine excess with pre-operative alpha-blockade therapy. Seven to fourteen days is unlikely to be a long enough duration of treatment for these anabolic benefits to become evident. The presented data would suggest longer durations of treatment can provide extra benefits to patients resulting in them being physiologically more prepared for their operations. This may potentially result in fewer post-operative complications, quicker wound healing times and fewer days in hospital.

As PPGLs can arise in familial as well as sporadic forms, the next focus of this thesis was on aspects of familial PPGLs with regards to post-operative monitoring of patients and surveillance screening of asymptomatic carriers (chapter 4). This chapter concentrated on genetic mutations in the *SDH* genes. At the time this work was undertaken no guidelines existed on the surveillance of asymptomatic

relatives that carried a genetic mutation in an *SDH* gene. Lifelong surveillance has significant implications with regards to resources, time, incidental findings and anxiety to the individuals. The aim of any *SDH* surveillance programme must be to identify disease at an early stage with smaller tumour sizes to limit the chance of malignant transformation. The different *SDH* subunits have different penetrance, clinical phenotypes and behaviours and therefore surveillance programmes need to be adapted for the individual *SDH* subtype. Collated data from the literature as well as cohorts from St. Bartholomew's Hospital are presented in this thesis and a suggested model for surveillance monitoring is proposed based on these data.

Surveillance screening programmes are resource heavy and can cause much unease to individuals that undergo them. In an ideal world tumour markers would exist that could differentiate between PPGLs that are benign and those with malignant potential. Towards this goal the final area that this thesis aimed to investigate were potential avenues to identify novel biomarkers and treatment strategies, through examination of resected PPGL tissue (chapter 5). If it was possible to distinguish between tumours with different clinical behaviours those with aggressive potential could be identified, that may benefit from closer post-operative surveillance. In addition identification of less aggressive tumours would alleviate apprehension for some carriers. Interest in the contribution of the TME has grown in recent years with evidence linking the TME profile with tumour behaviour, however little is known about the TME of PPGLs. Data presented in this thesis demonstrates that PPGLs generate a local immunological response, with PPGL tumour cells being an active source of cytokines. A higher percentage of immune cells were identified in the PPGL TME compared to the TME of the non-pathological medulla cells. The PPGL TME was dominated by macrophages. The majority of the cytokines identified are secreted by macrophages or T-cells and are involved in macrophage, monocyte or neutrophil recruitment. Differences were observed between benign and malignant PPGLs on subset analyses with higher concentrations of M1 macrophages and CD4 T-cells in benign tumours and a higher M2:M1 ratio in malignant PPGLs. Understanding the importance of inflammatory cells in PPGLs has two important clinical implications. Firstly, differences within the TME could potentially be exploited as an aid in predicting tumour behaviour by contributing to scoring systems, and thus identifying patients that require closer post-operative surveillance. Secondly, if components of the TME have a role in the pathogenesis of more aggressive tumour phenotypes, then a greater understanding may lead to potential new targeted therapeutic interventions.

This research has addressed some of the complex clinical issues in caring for patients with PPGLs pre- and post-operatively, and for those with a predisposition to developing PPGLs. Data from this thesis has contributed to the production of a European consensus statement on surveillance screening of

SDH mutation carriers. The preliminary data on the TME components of PPGLs poses promising avenues for future work for predicating tumour behaviour and potential novel therapeutic treatments.

Bibliography

1.   Nozdrachev AD. [The 90th anniversary of the creation by J. Newport Langley of the theory of autonomic nervous system structure (historical essay)]. Fiziol Zh Im I M Sechenova. 1995;81(12):175-84.
2.   Else T. 15 YEARS OF PARAGANGLIOMA: Pheochromocytoma, paraganglioma and genetic syndromes: a historical perspective. Endocr Relat Cancer. 2015;22(4):T147-59.
3.   Pasini B, Stratakis CA. SDH mutations in tumorigenesis and inherited endocrine tumours: lesson from the phaeochromocytoma-paraganglioma syndromes. J Intern Med. 2009;266(1):19-42.
4.   DeLellis R, A. Lloyd, R. V. Heitz, P. U. Eng, C (eds). Tumours of the endocrine organs: IARC, Lyons; 2004.
5.   Bausch B, Schiavi F, Ni Y, Welander J, Patocs A, Ngeow J, et al. Clinical Characterization of the Pheochromocytoma and Paraganglioma Susceptibility Genes SDHA, TMEM127, MAX, and SDHAF2 for Gene-Informed Prevention. JAMA Oncol. 2017;3(9):1204-12.
6.   Neumann HP, Vortmeyer A, Schmidt D, Werner M, Erlic Z, Cascon A, et al. Evidence of MEN-2 in the original description of classic pheochromocytoma. N Engl J Med. 2007;357(13):1311-5.
7.   Lefebvre M, Foulkes WD. Pheochromocytoma and paraganglioma syndromes: genetics and management update. Curr Oncol. 2014;21(1):e8-e17.
8.   Stenstrom G, Svardsudd K. Pheochromocytoma in Sweden 1958-1981. An analysis of the National Cancer Registry Data. Acta Med Scand. 1986;220(3):225-32.
9.   Beard CM, Sheps SG, Kurland LT, Carney JA, Lie JT. Occurrence of pheochromocytoma in Rochester, Minnesota, 1950 through 1979. Mayo Clin Proc. 1983;58(12):802-4.
10.   Ariton M, Juan CS, AvRuskin TW. Pheochromocytoma: clinical observations from a Brooklyn tertiary hospital. Endocr Pract. 2000;6(3):249-52.
11.   Martucci VL, Pacak K. Pheochromocytoma and paraganglioma: diagnosis, genetics, management, and treatment. Curr Probl Cancer. 2014;38(1):7-41.
12.   Lenders JW, Duh QY, Eisenhofer G, Gimenez-Roqueplo AP, Grebe SK, Murad MH, et al. Pheochromocytoma and paraganglioma: an endocrine society clinical practice guideline. J Clin Endocrinol Metab. 2014;99(6):1915-42.
13.   Kirmani S, Young WF. Hereditary Paraganglioma-Pheochromocytoma Syndromes. In: Pagon RA, Adam MP, Ardinger HH, Wallace SE, Amemiya A, Bean LJH, et al., editors. GeneReviews(R). Seattle (WA)2014.
14.   McNeil AR, Blok BH, Koelmeyer TD, Burke MP, Hilton JM. Phaeochromocytomas discovered during coronial autopsies in Sydney, Melbourne and Auckland. Aust N Z J Med. 2000;30(6):648-52.
15.   Platts JK, Drew PJ, Harvey JN. Death from phaeochromocytoma: lessons from a post-mortem survey. J R Coll Physicians Lond. 1995;29(4):299-306.
16.   Lo CY, Lam KY, Wat MS, Lam KS. Adrenal pheochromocytoma remains a frequently overlooked diagnosis. Am J Surg. 2000;179(3):212-5.
17.   Pacak K. Phaeochromocytoma: a catecholamine and oxidative stress disorder. Endocr Regul. 2011;45(2):65-90.
18.   Dutch guideline for detecting hereditary tumors 2010. https://www.stoet.nl.
19.   Eisenhofer G, Goldstein DS, Kopin IJ, Crout JR. Pheochromocytoma: rediscovery as a catecholamine-metabolizing tumor. Endocr Pathol. 2003;14(3):193-212.
20.   Pocock GR, C D. The hormonal regulation of the body. Human Physiology The Basis of Medicine. Oxford: Oxford Medical Publications; 1999. p. 223-5.
21.   Eisenhofer G, Siegert G, Kotzerke J, Bornstein SR, Pacak K. Current progress and future challenges in the biochemical diagnosis and treatment of pheochromocytomas and paragangliomas. Horm Metab Res. 2008;40(5):329-37.

22.   Eisenhofer G, Lenders JW, Timmers H, Mannelli M, Grebe SK, Hofbauer LC, et al. Measurements of plasma methoxytyramine, normetanephrine, and metanephrine as discriminators of different hereditary forms of pheochromocytoma. Clin Chem. 2011;57(3):411-20.

23.   Eisenhofer G, Lenders JW, Siegert G, Bornstein SR, Friberg P, Milosevic D, et al. Plasma methoxytyramine: a novel biomarker of metastatic pheochromocytoma and paraganglioma in relation to established risk factors of tumour size, location and SDHB mutation status. Eur J Cancer. 2012;48(11):1739-49.

24.   Dahia PL. Pheochromocytoma and paraganglioma pathogenesis: learning from genetic heterogeneity. Nat Rev Cancer. 2014;14(2):108-19.

25.   Eisenhofer G, Pacak K, Huynh TT, Qin N, Bratslavsky G, Linehan WM, et al. Catecholamine metabolomic and secretory phenotypes in phaeochromocytoma. Endocr Relat Cancer. 2011;18(1):97-111.

26.   Nolting S, Bechmann N, Taieb D, Beuschlein F, Fassnacht M, Kroiss M, et al. Personalized Management of Pheochromocytoma and Paraganglioma. Endocr Rev. 2022;43(2):199-239.

27.   Fishbein L, Leshchiner I, Walter V, Danilova L, Robertson AG, Johnson AR, et al. Comprehensive Molecular Characterization of Pheochromocytoma and Paraganglioma. Cancer Cell. 2017;31(2):181-93.

28.   Jochmanova I, Pacak K. Genomic Landscape of Pheochromocytoma and Paraganglioma. Trends Cancer. 2018;4(1):6-9.

29.   Castro-Vega LJ, Lepoutre-Lussey C, Gimenez-Roqueplo AP, Favier J. Rethinking pheochromocytomas and paragangliomas from a genomic perspective. Oncogene. 2016;35(9):1080-9.

30.   Benn DE, Robinson BG, Clifton-Bligh RJ. 15 YEARS OF PARAGANGLIOMA: Clinical manifestations of paraganglioma syndromes types 1-5. Endocr Relat Cancer. 2015;22(4):T91-103.

31.   Favier J, Amar L, Gimenez-Roqueplo AP. Paraganglioma and phaeochromocytoma: from genetics to personalized medicine. Nat Rev Endocrinol. 2015;11(2):101-11.

32.   Chase W. Familial and bilateral tumours of the carotid body. . Journal of Pathology and Bacteriology. 1933;36 1-12.

33.   Cawthon RM, O'Connell P, Buchberg AM, Viskochil D, Weiss RB, Culver M, et al. Identification and characterization of transcripts from the neurofibromatosis 1 region: the sequence and genomic structure of EVI2 and mapping of other transcripts. Genomics. 1990;7(4):555-65.

34.   Mulligan LM, Kwok JB, Healey CS, Elsdon MJ, Eng C, Gardner E, et al. Germ-line mutations of the RET proto-oncogene in multiple endocrine neoplasia type 2A. Nature. 1993;363(6428):458-60.

35.   Latif F, Tory K, Gnarra J, Yao M, Duh FM, Orcutt ML, et al. Identification of the von Hippel-Lindau disease tumor suppressor gene. Science. 1993;260(5112):1317-20.

36.   Crossey PA, Richards FM, Foster K, Green JS, Prowse A, Latif F, et al. Identification of intragenic mutations in the von Hippel-Lindau disease tumour suppressor gene and correlation with disease phenotype. Hum Mol Genet. 1994;3(8):1303-8.

37.   Remacha L, Curras-Freixes M, Torres-Ruiz R, Schiavi F, Torres-Perez R, Calsina B, et al. Gain-of-function mutations in DNMT3A in patients with paraganglioma. Genet Med. 2018;20(12):1644-51.

38.   Buffet A, Morin A, Castro-Vega LJ, Habarou F, Lussey-Lepoutre C, Letouze E, et al. Germline Mutations in the Mitochondrial 2-Oxoglutarate/Malate Carrier SLC25A11 Gene Confer a Predisposition to Metastatic Paragangliomas. Cancer Res. 2018;78(8):1914-22.

39.   Remacha L, Pirman D, Mahoney CE, Coloma J, Calsina B, Curras-Freixes M, et al. Recurrent Germline DLST Mutations in Individuals with Multiple Pheochromocytomas and Paragangliomas. Am J Hum Genet. 2019;104(5):1008-10.

40.   Wachtel H, Fishbein L. Genetics of pheochromocytoma and paraganglioma. Curr Opin Endocrinol Diabetes Obes. 2021;28(3):283-90.

41.   Yankovskaya V, Horsefield R, Tornroth S, Luna-Chavez C, Miyoshi H, Leger C, et al. Architecture of succinate dehydrogenase and reactive oxygen species generation. Science. 2003;299(5607):700-4.

42.   Loughrey PB, Roncaroli F, Healy E, Weir P, Basetti M, Casey RT, et al. Succinate dehydrogenase and MYC-associated factor X mutations in pituitary neuroendocrine tumours. Endocr Relat Cancer. 2022;29(10):R157-R72.

43.   Letouze E, Martinelli C, Loriot C, Burnichon N, Abermil N, Ottolenghi C, et al. SDH mutations establish a hypermethylator phenotype in paraganglioma. Cancer Cell. 2013;23(6):739-52.

44.   Gerald D, Berra E, Frapart YM, Chan DA, Giaccia AJ, Mansuy D, et al. JunD reduces tumor angiogenesis by protecting cells from oxidative stress. Cell. 2004;118(6):781-94.

45.   Gimenez-Roqueplo AP, Favier J, Rustin P, Rieubland C, Crespin M, Nau V, et al. Mutations in the SDHB gene are associated with extra-adrenal and/or malignant phaeochromocytomas. Cancer Res. 2003;63(17):5615-21.

46.   Baysal BE, Ferrell RE, Willett-Brozick JE, Lawrence EC, Myssiorek D, Bosch A, et al. Mutations in SDHD, a mitochondrial complex II gene, in hereditary paraganglioma. Science. 2000;287(5454):848-51.

47.   Gimm O, Armanios M, Dziema H, Neumann HP, Eng C. Somatic and occult germ-line mutations in SDHD, a mitochondrial complex II gene, in nonfamilial pheochromocytoma. Cancer Res. 2000;60(24):6822-5.

48.   Niemann S, Muller U. Mutations in SDHC cause autosomal dominant paraganglioma, type 3. Nat Genet. 2000;26(3):268-70.

49.   Astuti D, Latif F, Dallol A, Dahia PL, Douglas F, George E, et al. Gene mutations in the succinate dehydrogenase subunit SDHB cause susceptibility to familial pheochromocytoma and to familial paraganglioma. Am J Hum Genet. 2001;69(1):49-54.

50.   Hao HX, Khalimonchuk O, Schraders M, Dephoure N, Bayley JP, Kunst H, et al. SDH5, a gene required for flavination of succinate dehydrogenase, is mutated in paraganglioma. Science. 2009;325(5944):1139-42.

51.   Burnichon N, Briere JJ, Libe R, Vescovo L, Riviere J, Tissier F, et al. SDHA is a tumor suppressor gene causing paraganglioma. Hum Mol Genet. 2010;19(15):3011-20.

52.   Bayley JP, Devilee P, Taschner PE. The SDH mutation database: an online resource for succinate dehydrogenase sequence variants involved in pheochromocytoma, paraganglioma and mitochondrial complex II deficiency. BMC Med Genet. 2005;6:39.

53.   Benn DE, Gimenez-Roqueplo AP, Reilly JR, Bertherat J, Burgess J, Byth K, et al. Clinical presentation and penetrance of pheochromocytoma/paraganglioma syndromes. J Clin Endocrinol Metab. 2006;91(3):827-36.

54.   Neumann HP, Pawlu C, Peczkowska M, Bausch B, McWhinney SR, Muresan M, et al. Distinct clinical features of paraganglioma syndromes associated with SDHB and SDHD gene mutations. JAMA. 2004;292(8):943-51.

55.   Jochmanova I, Wolf KI, King KS, Nambuba J, Wesley R, Martucci V, et al. SDHB-related pheochromocytoma and paraganglioma penetrance and genotype-phenotype correlations. J Cancer Res Clin Oncol. 2017.

56.   Andrews KA, Ascher DB, Pires DEV, Barnes DR, Vialard L, Casey RT, et al. Tumour risks and genotype-phenotype correlations associated with germline variants in succinate dehydrogenase subunit genes SDHB, SDHC and SDHD. J Med Genet. 2018.

57.   Schiavi F, Milne RL, Anda E, Blay P, Castellano M, Opocher G, et al. Are we overestimating the penetrance of mutations in SDHB? Hum Mutat. 2010;31(6):761-2.

58.   Eijkelenkamp K, Osinga TE, de Jong MM, Sluiter WJ, Dullaart RP, Links TP, et al. Calculating the optimal surveillance for head and neck paraganglioma in SDHB-mutation carriers. Fam Cancer. 2017;16(1):123-30.

59.   Timmers HJ, Kozupa A, Eisenhofer G, Raygada M, Adams KT, Solis D, et al. Clinical presentations, biochemical phenotypes, and genotype-phenotype correlations in patients with succinate dehydrogenase subunit B-associated pheochromocytomas and paragangliomas. J Clin Endocrinol Metab. 2007;92(3):779-86.

60. Amar L, Baudin E, Burnichon N, Peyrard S, Silvera S, Bertherat J, et al. Succinate dehydrogenase B gene mutations predict survival in patients with malignant pheochromocytomas or paragangliomas. J Clin Endocrinol Metab. 2007;92(10):3822-8.

61. Darr R, Lenders JW, Hofbauer LC, Naumann B, Bornstein SR, Eisenhofer G. Pheochromocytoma - update on disease management. Ther Adv Endocrinol Metab. 2012;3(1):11-26.

62. Ayala-Ramirez M, Feng L, Johnson MM, Ejaz S, Habra MA, Rich T, et al. Clinical risk factors for malignancy and overall survival in patients with pheochromocytomas and sympathetic paragangliomas: primary tumor size and primary tumor location as prognostic indicators. J Clin Endocrinol Metab. 2011;96(3):717-25.

63. Jafri M, Whitworth J, Rattenberry E, Vialard L, Kilby G, Kumar AV, et al. Evaluation of SDHB, SDHD and VHL gene susceptibility testing in the assessment of individuals with non-syndromic phaeochromocytoma, paraganglioma and head and neck paraganglioma. Clin Endocrinol (Oxf). 2013;78(6):898-906.

64. Jasperson KW, Kohlmann W, Gammon A, Slack H, Buchmann L, Hunt J, et al. Role of rapid sequence whole-body MRI screening in SDH-associated hereditary paraganglioma families. Fam Cancer. 2014;13(2):257-65.

65. Tufton N, Shapiro L, Srirangalingam U, Richards P, Sahdev A, Kumar AV, et al. Outcomes of annual surveillance imaging in an adult and paediatric cohort of succinate dehydrogenase B mutation carriers. Clin Endocrinol (Oxf). 2017;86(2):286-96.

66. Ricketts CJ, Shuch B, Vocke CD, Metwalli AR, Bratslavsky G, Middelton L, et al. Succinate dehydrogenase kidney cancer: an aggressive example of the Warburg effect in cancer. J Urol. 2012;188(6):2063-71.

67. Ricketts C, Woodward ER, Killick P, Morris MR, Astuti D, Latif F, et al. Germline SDHB mutations and familial renal cell carcinoma. J Natl Cancer Inst. 2008;100(17):1260-2.

68. Gill AJ, Pachter NS, Chou A, Young B, Clarkson A, Tucker KM, et al. Renal tumors associated with germline SDHB mutation show distinctive morphology. Am J Surg Pathol. 2011;35(10):1578-85.

69. Niemeijer ND, Rijken JA, Eijkelenkamp K, van der Horst-Schrivers ANA, Kerstens MN, Tops CM, et al. The Phenotype of SDHB Germline Mutation Carriers; a Nationwide Study. Eur J Endocrinol. 2017.

70. Gill AJ, Hes O, Papathomas T, Sedivcova M, Tan PH, Agaimy A, et al. Succinate dehydrogenase (SDH)-deficient renal carcinoma: a morphologically distinct entity: a clinicopathologic series of 36 tumors from 27 patients. Am J Surg Pathol. 2014;38(12):1588-602.

71. Vanharanta S, Buchta M, McWhinney SR, Virta SK, Peczkowska M, Morrison CD, et al. Early-onset renal cell carcinoma as a novel extraparaganglial component of SDHB-associated heritable paraganglioma. Am J Hum Genet. 2004;74(1):153-9.

72. Kuroda N, Yorita K, Nagasaki M, Harada Y, Ohe C, Jeruc J, et al. Review of succinate dehydrogenase-deficient renal cell carcinoma with focus on clinical and pathobiological aspects. Pol J Pathol. 2016;67(1):3-7.

73. Gill A AM, Smith S, Trpkov K. Succinate dehydrogenase-deficient renal carcinoma. In: Moch H HP, Reuter VE (eds), editor. WHO Classification of Tumors of the Kidney, Bladder and Male Genital tract. Lyon: IARC Press.

74. Srigley JR, Delahunt B, Eble JN, Egevad L, Epstein JI, Grignon D, et al. The International Society of Urological Pathology (ISUP) Vancouver Classification of Renal Neoplasia. Am J Surg Pathol. 2013;37(10):1469-89.

75. Eng C. SDHB--a gene for all tumors? J Natl Cancer Inst. 2008;100(17):1193-5.

76. Casey RT, Warren AY, Martin JE, Challis BG, Rattenberry E, Whitworth J, et al. Clinical and Molecular Features of Renal and Pheochromocytoma/Paraganglioma Tumor Association Syndrome (RAPTAS): Case Series and Literature Review. J Clin Endocrinol Metab. 2017;102(11):4013-22.

77. Denes J, Swords F, Rattenberry E, Stals K, Owens M, Cranston T, et al. Heterogeneous genetic background of the association of pheochromocytoma/paraganglioma and pituitary adenoma: results from a large patient cohort. J Clin Endocrinol Metab. 2015;100(3):E531-41.

78.	O'Toole SM, Denes J, Robledo M, Stratakis CA, Korbonits M. 15 YEARS OF PARAGANGLIOMA: The association of pituitary adenomas and phaeochromocytomas or paragangliomas. Endocr Relat Cancer. 2015;22(4):T105-22.

79.	Taieb D, Kaliski A, Boedeker CC, Martucci V, Fojo T, Adler JR, Jr., et al. Current approaches and recent developments in the management of head and neck paragangliomas. Endocr Rev. 2014;35(5):795-819.

80.	Ricketts CJ, Forman JR, Rattenberry E, Bradshaw N, Lalloo F, Izatt L, et al. Tumor risks and genotype-phenotype-proteotype analysis in 358 patients with germline mutations in SDHB and SDHD. Hum Mutat. 2010;31(1):41-51.

81.	Xekouki P, Szarek E, Bullova P, Giubellino A, Quezado M, Mastroyannis SA, et al. Pituitary adenoma with paraganglioma/pheochromocytoma (3PAs) and succinate dehydrogenase defects in humans and mice. J Clin Endocrinol Metab. 2015;100(5):E710-9.

82.	Papathomas TG, Gaal J, Corssmit EP, Oudijk L, Korpershoek E, Heimdal K, et al. Non-pheochromocytoma (PCC)/paraganglioma (PGL) tumors in patients with succinate dehydrogenase-related PCC-PGL syndromes: a clinicopathological and molecular analysis. Eur J Endocrinol. 2014;170(1):1-12.

83.	Schiavi F, Boedeker CC, Bausch B, Peczkowska M, Gomez CF, Strassburg T, et al. Predictors and prevalence of paraganglioma syndrome associated with mutations of the SDHC gene. JAMA. 2005;294(16):2057-63.

84.	Mannelli M, Castellano M, Schiavi F, Filetti S, Giacche M, Mori L, et al. Clinically guided genetic screening in a large cohort of italian patients with pheochromocytomas and/or functional or nonfunctional paragangliomas. J Clin Endocrinol Metab. 2009;94(5):1541-7.

85.	Peczkowska M, Cascon A, Prejbisz A, Kubaszek A, Cwikla BJ, Furmanek M, et al. Extra-adrenal and adrenal pheochromocytomas associated with a germline SDHC mutation. Nat Clin Pract Endocrinol Metab. 2008;4(2):111-5.

86.	Neumann HP, Erlic Z, Boedeker CC, Rybicki LA, Robledo M, Hermsen M, et al. Clinical predictors for germline mutations in head and neck paraganglioma patients: cost reduction strategy in genetic diagnostic process as fall-out. Cancer Res. 2009;69(8):3650-6.

87.	Baysal BE, Willett-Brozick JE, Filho PA, Lawrence EC, Myers EN, Ferrell RE. An Alu-mediated partial SDHC deletion causes familial and sporadic paraganglioma. J Med Genet. 2004;41(9):703-9.

88.	Erlic Z, Rybicki L, Peczkowska M, Golcher H, Kann PH, Brauckhoff M, et al. Clinical predictors and algorithm for the genetic diagnosis of pheochromocytoma patients. Clin Cancer Res. 2009;15(20):6378-85.

89.	Miederer M, Fottner C, Rossmann H, Helisch A, Papaspyrou K, Bartsch O, et al. High incidence of extraadrenal paraganglioma in families with SDHx syndromes detected by functional imaging with [18F]fluorodihydroxyphenylalanine PET. Eur J Nucl Med Mol Imaging. 2013;40(6):889-96.

90.	Burnichon N, Rohmer V, Amar L, Herman P, Leboulleux S, Darrouzet V, et al. The succinate dehydrogenase genetic testing in a large prospective series of patients with paragangliomas. J Clin Endocrinol Metab. 2009;94(8):2817-27.

91.	Bourdeau I, Grunenwald S, Burnichon N, Khalifa E, Dumas N, Binet MC, et al. A SDHC Founder Mutation Causes Paragangliomas (PGLs) in the French Canadians: New Insights on the SDHC-Related PGL. J Clin Endocrinol Metab. 2016;101(12):4710-8.

92.	Daniel E, Jones R, Bull M, Newell-Price J. Rapid-sequence MRI for long-term surveillance for paraganglioma and phaeochromocytoma in patients with succinate dehydrogenase mutations. Eur J Endocrinol. 2016;175(6):561-70.

93.	Malinoc A, Sullivan M, Wiech T, Schmid KW, Jilg C, Straeter J, et al. Biallelic inactivation of the SDHC gene in renal carcinoma associated with paraganglioma syndrome type 3. Endocr Relat Cancer. 2012;19(3):283-90.

94.	Janeway KA, Kim SY, Lodish M, Nose V, Rustin P, Gaal J, et al. Defects in succinate dehydrogenase in gastrointestinal stromal tumors lacking KIT and PDGFRA mutations. Proc Natl Acad Sci U S A. 2011;108(1):314-8.

95.   Gill AJ, Lipton L, Taylor J, Benn DE, Richardson AL, Frydenberg M, et al. Germline SDHC mutation presenting as recurrent SDH deficient GIST and renal carcinoma. Pathology. 2013;45(7):689-91.

96.   Gill AJ. Succinate dehydrogenase (SDH)-deficient neoplasia. Histopathology. 2018;72(1):106-16.

97.   Bourgeron T, Rustin P, Chretien D, Birch-Machin M, Bourgeois M, Viegas-Pequignot E, et al. Mutation of a nuclear succinate dehydrogenase gene results in mitochondrial respiratory chain deficiency. Nat Genet. 1995;11(2):144-9.

98.   Renkema GH, Wortmann SB, Smeets RJ, Venselaar H, Antoine M, Visser G, et al. SDHA mutations causing a multisystem mitochondrial disease: novel mutations and genetic overlap with hereditary tumors. Eur J Hum Genet. 2015;23(2):202-9.

99.   Newey PJ, Berg JN, Zhou K, Palmer CNA, Thakker RV. Utility of Population-Level DNA Sequence Data in the Diagnosis of Hereditary Endocrine Disease. J Endocr Soc. 2017;1(12):1507-26.

100.   Kunst HP, Rutten MH, de Monnink JP, Hoefsloot LH, Timmers HJ, Marres HA, et al. SDHAF2 (PGL2-SDH5) and hereditary head and neck paraganglioma. Clin Cancer Res. 2011;17(2):247-54.

101.   Bayley JP, Kunst HP, Cascon A, Sampietro ML, Gaal J, Korpershoek E, et al. SDHAF2 mutations in familial and sporadic paraganglioma and phaeochromocytoma. Lancet Oncol. 2010;11(4):366-72.

102.   Richards S, Aziz N, Bale S, Bick D, Das S, Gastier-Foster J, et al. Standards and guidelines for the interpretation of sequence variants: a joint consensus recommendation of the American College of Medical Genetics and Genomics and the Association for Molecular Pathology. Genet Med. 2015;17(5):405-24.

103.   ICRP. The 2007 Recommedndations of the International Commission on Radiological Protection. In: ICRP, editor.: ICRP Publication; 2007. p. 2-4.

104.   Bugada D, Allegri M, Lavand'homme P, De Kock M, Fanelli G. Inflammation-based scores: a new method for patient-targeted strategies and improved perioperative outcome in cancer patients. Biomed Res Int. 2014;2014:142425.

105.   Liang R, Li J, Tang X, Liu Y. The prognostic role of preoperative systemic immune-inflammation index and albumin/globulin ratio in patients with newly diagnosed high-grade glioma. Clin Neurol Neurosurg. 2019;184:105397.

106.   Watt DG, Proctor MJ, Park JH, Horgan PG, McMillan DC. The Neutrophil-Platelet Score (NPS) Predicts Survival in Primary Operable Colorectal Cancer and a Variety of Common Cancers. PLoS One. 2015;10(11):e0142159.

107.   Wang PF, Meng Z, Song HW, Yao K, Duan ZJ, Yu CJ, et al. Preoperative Changes in Hematological Markers and Predictors of Glioma Grade and Survival. Front Pharmacol. 2018;9:886.

108.   Excellence NIfHaC. Hypertension in adults: diagnosis and management. Clinical guideline CG127. NICE; 2011.

109.   Roizen MF, Hunt TK, Beaupre PN, Kremer P, Firmin R, Chang CN, et al. The effect of alpha-adrenergic blockade on cardiac performance and tissue oxygen delivery during excision of pheochromocytoma. Surgery. 1983;94(6):941-5.

110.   Whitelaw BC, Prague JK, Mustafa OG, Schulte KM, Hopkins PA, Gilbert JA, et al. Phaeochromocytoma [corrected] crisis. Clin Endocrinol (Oxf). 2014;80(1):13-22.

111.   Pacak K. Preoperative management of the pheochromocytoma patient. J Clin Endocrinol Metab. 2007;92(11):4069-79.

112.   Buitenwerf E, Boekel MF, van der Velde MI, Voogd MF, Kerstens MN, Wietasch G, et al. The haemodynamic instability score: Development and internal validation of a new rating method of intra-operative haemodynamic instability. Eur J Anaesthesiol. 2019;36(4):290-6.

113.   Manger WM, Gifford RW. Pheochromocytoma. New York: Springer-Verlag; 1977. xxiv, 398 p. p.

114.   Papathomas TG, Oudijk L, Persu A, Gill AJ, van Nederveen F, Tischler AS, et al. SDHB/SDHA immunohistochemistry in pheochromocytomas and paragangliomas: a multicenter interobserver

variation analysis using virtual microscopy: a Multinational Study of the European Network for the Study of Adrenal Tumors (ENS@T). Mod Pathol. 2015;28(6):807-21.

115.   Volante M, Brizzi MP, Faggiano A, La Rosa S, Rapa I, Ferrero A, et al. Somatostatin receptor type 2A immunohistochemistry in neuroendocrine tumors: a proposal of scoring system correlated with somatostatin receptor scintigraphy. Mod Pathol. 2007;20(11):1172-82.

116.   Iacovazzo D, Carlsen E, Lugli F, Chiloiro S, Piacentini S, Bianchi A, et al. Factors predicting pasireotide responsiveness in somatotroph pituitary adenomas resistant to first-generation somatostatin analogues: an immunohistochemical study. Eur J Endocrinol. 2016;174(2):241-50.

117.   Qiagen.   QIAamp   DNA   Mini   Blood   Mini   Handbook   -   EN https://www.qiagen.com/us/resources/resourcedetail?id=62a200d6-faf4-469b-b50f-2b59cf738962&lang=en2016 [5th:[Protocol].

118.   PreAnalytix. PAXgene Blood RNA Kit Handbook 2016 [

119.   Bankhead P, Loughrey MB, Fernandez JA, Dombrowski Y, McArt DG, Dunne PD, et al. QuPath: Open source software for digital pathology image analysis. Scientific Reports. 2017;7.

120.   Lenders JW, Eisenhofer G, Mannelli M, Pacak K. Phaeochromocytoma. Lancet. 2005;366(9486):665-75.

121.   Zhang R, Gupta D, Albert SG. Pheochromocytoma as a reversible cause of cardiomyopathy: Analysis and review of the literature. Int J Cardiol. 2017;249:319-23.

122.   Stolk RF, Bakx C, Mulder J, Timmers HJ, Lenders JW. Is the excess cardiovascular morbidity in pheochromocytoma related to blood pressure or to catecholamines? J Clin Endocrinol Metab. 2013;98(3):1100-6.

123.   Pace NB, M. Phaeochromocytoma. British Journal of Anaesthsia. 2003;3:20-3.

124.   O'Riordan JA. Pheochromocytomas and anesthesia. Int Anesthesiol Clin. 1997;35(4):99-127.

125.   Corssmit EP, Romijn JA. Clinical management of paragangliomas. Eur J Endocrinol. 2014;171(6):R231-43.

126.   Dupin C, Lang P, Dessard-Diana B, Simon JM, Cuenca X, Mazeron JJ, et al. Treatment of head and neck paragangliomas with external beam radiation therapy. Int J Radiat Oncol Biol Phys. 2014;89(2):353-9.

127.   Moore MG, Netterville JL, Mendenhall WM, Isaacson B, Nussenbaum B. Head and Neck Paragangliomas: An Update on Evaluation and Management. Otolaryngol Head Neck Surg. 2016;154(4):597-605.

128.   Niemann U, Hiller W, Behrend M. 25 years experience of the surgical treatment of phaeochromocytoma. Eur J Surg. 2002;168(12):716-9.

129.   Boutros AR, Bravo EL, Zanettin G, Straffon RA. Perioperative management of 63 patients with pheochromocytoma. Cleve Clin J Med. 1990;57(7):613-7.

130.   Weingarten TN, Cata JP, O'Hara JF, Prybilla DJ, Pike TL, Thompson GB, et al. Comparison of two preoperative medical management strategies for laparoscopic resection of pheochromocytoma. Urology. 2010;76(2):508 e6-11.

131.   Roizen MFH, R. W. Koike, M. Eger, I. E. Mulroy, M. F. Frazer, B. . prospective randomized trial of four anesthetic techniques for resection of pheochromocytoma. Anesthesiology. 1982;57(A43).

132.   Roizen MFS, B. D. Hassan, S. Z. Anesthesia for patients with pheochromocytoma. . Anesthesiol Clin North America 1987;5:269-75.

133.   Bruynzeel H, Feelders RA, Groenland TH, van den Meiracker AH, van Eijck CH, Lange JF, et al. Risk Factors for Hemodynamic Instability during Surgery for Pheochromocytoma. J Clin Endocrinol Metab. 2010;95(2):678-85.

134.   Ramakrishna H. Pheochromocytoma resection: Current concepts in anesthetic management. J Anaesthesiol Clin Pharmacol. 2015;31(3):317-23.

135.   Takeda T, Hakozaki K, Yanai Y, Masuda T, Yasumizu Y, Tanaka N, et al. Risk factors for haemodynamic instability and its prolongation during laparoscopic adrenalectomy for pheochromocytoma. Clin Endocrinol (Oxf). 2021;95(5):716-26.

136.   Kiernan CM, Du L, Chen X, Broome JT, Shi C, Peters MF, et al. Predictors of hemodynamic instability during surgery for pheochromocytoma. Ann Surg Oncol. 2014;21(12):3865-71.

137.   Buitenwerf E, Osinga TE, Timmers H, Lenders JWM, Feelders RA, Eekhoff EMW, et al. Efficacy of alpha-Blockers on Hemodynamic Control during Pheochromocytoma Resection: A Randomized Controlled Trial. J Clin Endocrinol Metab. 2020;105(7).

138.   Kong H, Li N, Li XY, Wang DX. The role of pre-operative alpha-blockade in patients with normotensive phaeochromocytoma or paraganglioma: A retrospective cohort study. Eur J Anaesthesiol. 2018;35(11):898-9.

139.   Groeben H, Nottebaum BJ, Alesina PF, Traut A, Neumann HP, Walz MK. Perioperative alpha-receptor blockade in phaeochromocytoma surgery: an observational case series. Br J Anaesth. 2017;118(2):182-9.

140.   Isaacs M, Lee P. Preoperative alpha-blockade in phaeochromocytoma and paraganglioma: is it always necessary? Clin Endocrinol (Oxf). 2017;86(3):309-14.

141.   Bosanska L, Petrak O, Zelinka T, Mraz M, Widimsky J, Jr., Haluzik M. The effect of pheochromocytoma treatment on subclinical inflammation and endocrine function of adipose tissue. Physiol Res. 2009;58(3):319-25.

142.   Petrak O, Haluzikova D, Kavalkova P, Strauch B, Rosa J, Holaj R, et al. Changes in energy metabolism in pheochromocytoma. J Clin Endocrinol Metab. 2013;98(4):1651-8.

143.   An Y, Reimann M, Masjkur J, Langton K, Peitzsch M, Deutschbein T, et al. Adrenomedullary function, obesity and permissive influences of catecholamines on body mass in patients with chromaffin cell tumours. Int J Obes (Lond). 2019;43(2):263-75.

144.   Okamura T, Nakajima Y, Satoh T, Hashimoto K, Sapkota S, Yamada E, et al. Changes in visceral and subcutaneous fat mass in patients with pheochromocytoma. Metabolism. 2015;64(6):706-12.

145.   van der Heijden C, Groh L, Keating ST, Kaffa C, Noz MP, Kersten S, et al. Catecholamines Induce Trained Immunity in Monocytes In Vitro and In Vivo. Circ Res. 2020;127(2):269-83.

146.   Zelinka T, Petrak O, Strauch B, Holaj R, Kvasnicka J, Mazoch J, et al. Elevated inflammation markers in pheochromocytoma compared to other forms of hypertension. Neuroimmunomodulation. 2007;14(1):57-64.

147.   Goldstein RE, O'Neill JA, Jr., Holcomb GW, 3rd, Morgan WM, 3rd, Neblett WW, 3rd, Oates JA, et al. Clinical experience over 48 years with pheochromocytoma. Ann Surg. 1999;229(6):755-64; discussion 64-6.

148.   Brunaud L, Boutami M, Nguyen-Thi PL, Finnerty B, Germain A, Weryha G, et al. Both preoperative alpha and calcium channel blockade impact intraoperative hemodynamic stability similarly in the management of pheochromocytoma. Surgery. 2014;156(6):1410-7; discussion7-8.

149.   Mannelli M. Management and treatment of pheochromocytomas and paragangliomas. Ann N Y Acad Sci. 2006;1073:405-16.

150.   Wolf KI, Santos JRU, Pacak K. Why Take the Risk? We Only Live Once: The Dangers Associated with Neglecting a Pre-Operative Alpha Adrenoceptor Blockade in Pheochromocytoma Patients. Endocr Pract. 2019;25(1):106-8.

151.   Tufton N, Gunganah K, Hussain S, Druce M, Carpenter R, Ashby M, et al. Alpha blockade-not to be underdone. Clin Endocrinol (Oxf). 2016.

152.   Zelinka T, Strauch B, Pecen L, Widimsky J, Jr. Diurnal blood pressure variation in pheochromocytoma, primary aldosteronism and Cushing's syndrome. J Hum Hypertens. 2004;18(2):107-11.

153.   Stergiou GS, Ntineri A. The optimal schedule for self-home blood pressure monitoring. J Hypertens. 2015;33(4):693-7.

154.   Challis BG, Casey RT, Simpson HL, Gurnell M. Is there an optimal preoperative management strategy for phaeochromocytoma/paraganglioma? Clin Endocrinol (Oxf). 2017;86(2):163-7.

155.   Missale C, Nash SR, Robinson SW, Jaber M, Caron MG. Dopamine receptors: from structure to function. Physiol Rev. 1998;78(1):189-225.

156.   Velasco M, Luchsinger A. Dopamine: pharmacologic and therapeutic aspects. Am J Ther. 1998;5(1):37-43.

157.   Russell WJ, Metcalfe IR, Tonkin AL, Frewin DB. The preoperative management of phaeochromocytoma. Anaesth Intensive Care. 1998;26(2):196-200.

158.   Ross EJ, Prichard BN, Kaufman L, Robertson AI, Harries BJ. Preoperative and operative management of patients with phaeochromocytoma. Br Med J. 1967;1(5534):191-8.

159.   Kocak S, Aydintug S, Canakci N. Alpha blockade in preoperative preparation of patients with pheochromocytomas. Int Surg. 2002;87(3):191-4.

160.   van der Zee PA, de Boer A. Pheochromocytoma: a review on preoperative treatment with phenoxybenzamine or doxazosin. Neth J Med. 2014;72(4):190-201.

161.   Maskey P, Shrestha GK, Luitel BR, Gupta DK, Sidarth, Chalise PR, et al. Phaeochromocytoma in Nepal--a single centre experience. Kathmandu Univ Med J (KUMJ). 2012;10(39):52-5.

162.   Fishbein L, Orlowski R, Cohen D. Pheochromocytoma/Paraganglioma: Review of perioperative management of blood pressure and update on genetic mutations associated with pheochromocytoma. J Clin Hypertens (Greenwich). 2013;15(6):428-34.

163.   Lentschener C, Gaujoux S, Baillard C, Dousset B. Inappropriate adrenoreceptor blockade prior to phaeochromocytoma removal is perhaps a 'timely reappraisal'? Clin Endocrinol (Oxf). 2016;85(6):989-90.

164.   Ferreira VM, Marcelino M, Piechnik SK, Marini C, Karamitsos TD, Ntusi NA, et al. Pheochromocytoma Is Characterized by Catecholamine-Mediated Myocarditis, Focal and Diffuse Myocardial Fibrosis, and Myocardial Dysfunction. J Am Coll Cardiol. 2016;67(20):2364-74.

165.   Piccoli A, Rossi B, Pillon L, Bucciante G. A new method for monitoring body fluid variation by bioimpedance analysis: the RXc graph. Kidney Int. 1994;46(2):534-9.

166.   Lee SH, Kwak MK, Ahn SH, Kim H, Cho YY, Suh S, et al. Change of skeletal muscle mass in patients with pheochromocytoma. J Bone Miner Metab. 2019;37(4):694-702.

167.   Spyroglou A, Adolf C, Hahner S, Quinkler M, Ladurner R, Reincke M, et al. Changes in Body Mass Index in Pheochromocytoma Patients Following Adrenalectomy. Horm Metab Res. 2017;49(3):208-13.

168.   Krumeich LN, Cucchiara AJ, Nathanson KL, Kelz RR, Fishbein L, Fraker DL, et al. Correlation Between Plasma Catecholamines, Weight, and Diabetes in Pheochromocytoma and Paraganglioma. J Clin Endocrinol Metab. 2021;106(10):e4028-e38.

169.   McCullagh EP, Engel WJ. Pheochromocytoma with Hypermetabolism: Report of Two Cases. Ann Surg. 1942;116(1):61-75.

170.   Engelman K, Mueller PS, Sjoerdsma A. Elevated Plasma Free Fatty Acid Concentrations in Patients with Pheochromocytoma. Changes with Therapy and Correlations with the Basal Metabolic Rate. N Engl J Med. 1964;270:865-70.

171.   Spergel G, Bleicher SJ, Ertel NH. Carbohydrate and fat metabolism in patients with phaeochromocytoma. N Engl J Med. 1968;278(15):803-9.

172.   Brooks MH, Guha A, Danforth E, Jr., Weinstein JJ, Barry KG. Pheochromocytoma: observations on mechanism of carbohydrate intolerance and abnormalities associated with development of Goldblatt kidney following removal of tumor. Metabolism. 1969;18(6):445-59.

173.   Turnbull DM, Johnston DG, Alberti KG, Hall R. Hormonal and metabolic studies in a patient with a pheochromocytoma. J Clin Endocrinol Metab. 1980;51(4):930-3.

174.   Arikan MGOG, A. Iskan, N, G. Sut, N. Yuksel, I. Arda, E. Can Hematological Parameters Play a Role in the Differential Diagnosis of Adrenal Tumors? Uro. 2021;1:39-44.

175.   Benschop RJ, Rodriguez-Feuerhahn M, Schedlowski M. Catecholamine-induced leukocytosis: early observations, current research, and future directions. Brain Behav Immun. 1996;10(2):77-91.

176.   Kang JM, Lee WJ, Kim WB, Kim TY, Koh JM, Hong SJ, et al. Systemic inflammatory syndrome and hepatic inflammatory cell infiltration caused by an interleukin-6 producing pheochromocytoma. Endocr J. 2005;52(2):193-8.

177.   Carvalho Cunha N, Gomes L, Saraiva J, Paiva I. Interleukin-6 Producing Pheochromocytoma: A Rare Cause of Systemic Inflammatory Response Syndrome. Case Rep Endocrinol. 2019;2019:7906272.
178.   Minetto M, Dovio A, Ventura M, Cappia S, Daffara F, Terzolo M, et al. Interleukin-6 producing pheochromocytoma presenting with acute inflammatory syndrome. J Endocrinol Invest. 2003;26(5):453-7.
179.   Shimizu C, Kubo M, Takano K, Takano A, Kijima H, Saji H, et al. Interleukin-6 (IL-6) producing phaeochromocytoma: direct IL-6 suppression by non-steroidal anti-inflammatory drugs. Clin Endocrinol (Oxf). 2001;54(3):405-10.
180.   Takagi M, Egawa T, Motomura T, Sakuma-Mochizuki J, Nishimoto N, Kasayama S, et al. Interleukin-6 secreting phaeochromocytoma associated with clinical markers of inflammation. Clin Endocrinol (Oxf). 1997;46(4):507-9.
181.   Kuroki M, Suzuki H, Kurota M, Nakane M, Kawamae K. Perioperative management of a patient undergoing resection of interleukin-6 producing pheochromocytoma. JA Clin Rep. 2021;7(1):49.
182.   Goddard AF, James MW, McIntyre AS, Scott BB, British Society of G. Guidelines for the management of iron deficiency anaemia. Gut. 2011;60(10):1309-16.
183.   Youssef A, Hamade A. Pheochromocytoma: A Cause of Anemia. Urol Case Rep. 2017;11:53-4.
184.   Eun CR, Ahn JH, Seo JA, Kim NH. Pheochromocytoma with markedly abnormal liver function tests and severe leukocytosis. Endocrinol Metab (Seoul). 2014;29(1):83-90.
185.   Wang P, Tait SM, Chaudry IH. Sustained elevation of norepinephrine depresses hepatocellular function. Biochim Biophys Acta. 2000;1535(1):36-44.
186.   Moran ME, Rosenberg DJ, Zornow DH. Pheochromocytoma multisystem crisis. Urology. 2006;67(4):846 e19-20.
187.   Wang DP, Kang K, Lin Q, Hai J. Prognostic Significance of Preoperative Systemic Cellular Inflammatory Markers in Gliomas: A Systematic Review and Meta-Analysis. Clin Transl Sci. 2020;13(1):179-88.
188.   Sardesai SH, Mourant AJ, Sivathandon Y, Farrow R, Gibbons DO. Phaeochromocytoma and catecholamine induced cardiomyopathy presenting as heart failure. Br Heart J. 1990;63(4):234-7.
189.   Bernini G, Galetta F, Franzoni F, Bardini M, Taurino C, Moretti A, et al. Normalization of catecholamine production following resection of phaeochromocytoma positively influences carotid vascular remodelling. Eur J Endocrinol. 2008;159(2):137-43.
190.   Ferreira VM, Marcelino M, Piechnik SK, Marini C, Karamitsos TD, Ntusi NAB, et al. Pheochromocytoma Is Characterized by Catecholamine-Mediated Myocarditis, Focal and Diffuse Myocardial Fibrosis, and Myocardial Dysfunction. J Am Coll Cardiol. 2016;67(20):2364-74.
191.   Kassim TA, Clarke DD, Mai VQ, Clyde PW, Mohamed Shakir KM. Catecholamine-induced cardiomyopathy. Endocr Pract. 2008;14(9):1137-49.
192.   Prejbisz A, Lenders JW, Eisenhofer G, Januszewicz A. Cardiovascular manifestations of phaeochromocytoma. J Hypertens. 2011;29(11):2049-60.
193.   Marques P, de Vries F, Dekkers OM, van Furth WR, Korbonits M, Biermasz NR, et al. Pre-operative serum inflammation-based scores in patients with pituitary adenomas. Pituitary. 2021;24(3):334-50.
194.   Lin M, Hu T, Yan L, Xiao D, Zhao H, Yan P. Can Systemic Inflammatory Markers Be Used to Predict the Pathological Grade of Meningioma Before Surgery? World Neurosurg. 2019;127:e677-e84.
195.   Wang Y, Li M, Deng H, Pang Y, Liu L, Guan X. The systems of metastatic potential prediction in pheochromocytoma and paraganglioma. Am J Cancer Res. 2020;10(3):769-80.
196.   Chen M, Zheng SH, Yang M, Chen ZH, Li ST. The diagnostic value of preoperative inflammatory markers in craniopharyngioma: a multicenter cohort study. J Neurooncol. 2018;138(1):113-22.
197.   Luo G, Liu C, Cheng H, Jin K, Guo M, Lu Y, et al. Neutrophil-lymphocyte ratio predicts survival in pancreatic neuroendocrine tumors. Oncol Lett. 2017;13(4):2454-8.
198.   McDermott SM, Saunders ND, Schneider EB, Strosberg D, Onesti J, Dillhoff M, et al. Neutrophil Lymphocyte Ratio and Transarterial Chemoembolization in Neuroendocrine Tumor Metastases. J Surg Res. 2018;232:369-75.

199.   Okui M, Yamamichi T, Asakawa A, Harada M, Saito M, Horio H. Prognostic significance of neutrophil-lymphocyte ratios in large cell neuroendocrine carcinoma. Gen Thorac Cardiovasc Surg. 2017;65(11):633-9.

200.   Salman T, Kazaz SN, Varol U, Oflazoglu U, Unek IT, Kucukzeybek Y, et al. Prognostic Value of the Pretreatment Neutrophil-to-Lymphocyte Ratio and Platelet-to-Lymphocyte Ratio for Patients with Neuroendocrine Tumors: An Izmir Oncology Group Study. Chemotherapy. 2016;61(6):281-6.

201.   Plouin PF, Degoulet P, Tugaye A, Ducrocq MB, Menard J. [Screening for phaeochromocytoma : in which hypertensive patients? A semiological study of 2585 patients, including 11 with phaeochromocytoma (author's transl)]. Nouv Presse Med. 1981;10(11):869-72.

202.   Pourian M, Mostafazadeh DB, Soltani A. Does this patient have pheochromocytoma? A systematic review of clinical signs and symptoms. J Diabetes Metab Disord. 2015;15:11.

203.   Geroula A, Deutschbein T, Langton K, Masjkur J, Pamporaki C, Peitzsch M, et al. Pheochromocytoma and paraganglioma: clinical feature-based disease probability in relation to catecholamine biochemistry and reason for disease suspicion. Eur J Endocrinol. 2019;181(4):409-20.

204.   Black HR, Bursten SL. A clinical scoring system for detection of patients with pheochromocytomas. Yale J Biol Med. 1984;57(3):259-72.

205.   Group NGSiPS, Toledo RA, Burnichon N, Cascon A, Benn DE, Bayley JP, et al. Consensus Statement on next-generation-sequencing-based diagnostic testing of hereditary phaeochromocytomas and paragangliomas. Nat Rev Endocrinol. 2017;13(4):233-47.

206.   Eisenhofer G, Lenders JW, Goldstein DS, Mannelli M, Csako G, Walther MM, et al. Pheochromocytoma catecholamine phenotypes and prediction of tumor size and location by use of plasma free metanephrines. Clin Chem. 2005;51(4):735-44.

207.   Timmers HJ, Pacak K, Huynh TT, Abu-Asab M, Tsokos M, Merino MJ, et al. Biochemically silent abdominal paragangliomas in patients with mutations in the succinate dehydrogenase subunit B gene. J Clin Endocrinol Metab. 2008;93(12):4826-32.

208.   Koch CA, Vortmeyer AO, Zhuang Z, Brouwers FM, Pacak K. New insights into the genetics of familial chromaffin cell tumors. Ann N Y Acad Sci. 2002;970:11-28.

209.   Turkova H, Prodanov T, Maly M, Martucci V, Adams K, Widimsky J, Jr., et al. Characteristics and Outcomes of Metastatic Sdhb and Sporadic Pheochromocytoma/Paraganglioma: An National Institutes of Health Study. Endocr Pract. 2016;22(3):302-14.

210.   Schovanek J, Martucci V, Wesley R, Fojo T, Del Rivero J, Huynh T, et al. The size of the primary tumor and age at initial diagnosis are independent predictors of the metastatic behavior and survival of patients with SDHB-related pheochromocytoma and paraganglioma: a retrospective cohort study. BMC Cancer. 2014;14:523.

211.   Fish JH, Klein-Weigel P, Biebl M, Janecke A, Tauscher T, Fraedrich G. Systematic screening and treatment evaluation of hereditary neck paragangliomas. Head Neck. 2007;29(9):864-73.

212.   Srirangalingam U, Walker L, Khoo B, MacDonald F, Gardner D, Wilkin TJ, et al. Clinical manifestations of familial paraganglioma and phaeochromocytomas in succinate dehydrogenase B (SDH-B) gene mutation carriers. Clin Endocrinol (Oxf). 2008;69(4):587-96.

213.   Neumann HP, Eng C. The approach to the patient with paraganglioma. J Clin Endocrinol Metab. 2009;94(8):2677-83.

214.   Timmers HJ, Chen CC, Carrasquillo JA, Whatley M, Ling A, Eisenhofer G, et al. Staging and functional characterization of pheochromocytoma and paraganglioma by 18F-fluorodeoxyglucose (18F-FDG) positron emission tomography. J Natl Cancer Inst. 2012;104(9):700-8.

215.   Taieb D, Timmers HJ, Hindie E, Guillet BA, Neumann HP, Walz MK, et al. EANM 2012 guidelines for radionuclide imaging of phaeochromocytoma and paraganglioma. Eur J Nucl Med Mol Imaging. 2012;39(12):1977-95.

216.   Gimenez-Roqueplo AP, Caumont-Prim A, Houzard C, Hignette C, Hernigou A, Halimi P, et al. Imaging work-up for screening of paraganglioma and pheochromocytoma in SDHx mutation carriers: a multicenter prospective study from the PGL.EVA Investigators. J Clin Endocrinol Metab. 2013;98(1):E162-73.

217. Janssen I, Blanchet EM, Adams K, Chen CC, Millo CM, Herscovitch P, et al. Superiority of [68Ga]-DOTATATE PET/CT to Other Functional Imaging Modalities in the Localization of SDHB-Associated Metastatic Pheochromocytoma and Paraganglioma. Clin Cancer Res. 2015;21(17):3888-95.

218. Plouin PF, Amar L, Dekkers OM, Fassnacht M, Gimenez-Roqueplo AP, Lenders JW, et al. European Society of Endocrinology Clinical Practice Guideline for long-term follow-up of patients operated on for a phaeochromocytoma or a paraganglioma. Eur J Endocrinol. 2016;174(5):G1-G10.

219. Kornaczewski ER, Pointon OP, Burgess JR. Utility of FDG-PET imaging in screening for succinate dehydrogenase B and D mutation-related lesions. Clin Endocrinol (Oxf). 2016;85(2):172-9.

220. Gill AJ, Benn DE, Chou A, Clarkson A, Muljono A, Meyer-Rochow GY, et al. Immunohistochemistry for SDHB triages genetic testing of SDHB, SDHC, and SDHD in paraganglioma-pheochromocytoma syndromes. Hum Pathol. 2010;41(6):805-14.

221. Santi R, Rapizzi E, Canu L, Ercolino T, Baroni G, Fucci R, et al. Potential Pitfalls of SDH Immunohistochemical Detection in Paragangliomas and Phaeochromocytomas Harbouring Germline SDHx Gene Mutation. Anticancer Res. 2017;37(2):805-12.

222. van Nederveen FH, Gaal J, Favier J, Korpershoek E, Oldenburg RA, de Bruyn EM, et al. An immunohistochemical procedure to detect patients with paraganglioma and phaeochromocytoma with germline SDHB, SDHC, or SDHD gene mutations: a retrospective and prospective analysis. Lancet Oncol. 2009;10(8):764-71.

223. Dahia PL, Ross KN, Wright ME, Hayashida CY, Santagata S, Barontini M, et al. A HIF1alpha regulatory loop links hypoxia and mitochondrial signals in pheochromocytomas. PLoS Genet. 2005;1(1):72-80.

224. Douwes Dekker PB, Hogendoorn PC, Kuipers-Dijkshoorn N, Prins FA, van Duinen SG, Taschner PE, et al. SDHD mutations in head and neck paragangliomas result in destabilization of complex II in the mitochondrial respiratory chain with loss of enzymatic activity and abnormal mitochondrial morphology. J Pathol. 2003;201(3):480-6.

225. Castelblanco E, Santacana M, Valls J, de Cubas A, Cascon A, Robledo M, et al. Usefulness of negative and weak-diffuse pattern of SDHB immunostaining in assessment of SDH mutations in paragangliomas and pheochromocytomas. Endocr Pathol. 2013;24(4):199-205.

226. Evenepoel L, Papathomas TG, Krol N, Korpershoek E, de Krijger RR, Persu A, et al. Toward an improved definition of the genetic and tumor spectrum associated with SDH germ-line mutations. Genet Med. 2015;17(8):610-20.

227. Kopanos C, Tsiolkas V, Kouris A, Chapple CE, Albarca Aguilera M, Meyer R, et al. VarSome: the human genomic variant search engine. Bioinformatics. 2019;35(11):1978-80.

228. van der Tuin K, Mensenkamp AR, Tops CMJ, Corssmit EPM, Dinjens WN, van de Horst-Schrivers AN, et al. Clinical Aspects of SDHA-Related Pheochromocytoma and Paraganglioma: A Nationwide Study. J Clin Endocrinol Metab. 2018;103(2):438-45.

229. Amar L, Pacak K, Steichen O, Akker SA, Aylwin SJB, Baudin E, et al. International consensus on initial screening and follow-up of asymptomatic SDHx mutation carriers. Nat Rev Endocrinol. 2021;17(7):435-44.

230. Korpershoek E, Favier J, Gaal J, Burnichon N, van Gessel B, Oudijk L, et al. SDHA immunohistochemistry detects germline SDHA gene mutations in apparently sporadic paragangliomas and pheochromocytomas. J Clin Endocrinol Metab. 2011;96(9):E1472-6.

231. Casey RT, Ascher DB, Rattenberry E, Izatt L, Andrews KA, Simpson HL, et al. SDHA related tumorigenesis: a new case series and literature review for variant interpretation and pathogenicity. Mol Genet Genomic Med. 2017;5(3):237-50.

232. Casey RT, Ascher DB, Rattenberry E, Izatt L, Andrews KA, Simpson HL, et al. SDHA related tumorigenesis: a new case series and literature review for variant interpretation and pathogenicity. Molecular Genetics & Genomic Medicine. 2017;5(3):237-50.

233. Tufton N, Ghelani R, Srirangalingam U, Kumar AV, Drake WM, Iacovazzo D, et al. SDHA mutated paragangliomas may be at high risk of metastasis. Endocr Relat Cancer. 2017;24(7):L43-L9.

234. Astuti D, Hart-Holden N, Latif F, Lalloo F, Black GC, Lim C, et al. Genetic analysis of mitochondrial complex II subunits SDHD, SDHB and SDHC in paraganglioma and phaeochromocytoma susceptibility. Clin Endocrinol (Oxf). 2003;59(6):728-33.

235. King KS, Prodanov T, Kantorovich V, Fojo T, Hewitt JK, Zacharin M, et al. Metastatic pheochromocytoma/paraganglioma related to primary tumor development in childhood or adolescence: significant link to SDHB mutations. J Clin Oncol. 2011;29(31):4137-42.

236. Solis DC, Burnichon N, Timmers HJ, Raygada MJ, Kozupa A, Merino MJ, et al. Penetrance and clinical consequences of a gross SDHB deletion in a large family. Clin Genet. 2009;75(4):354-63.

237. Rijken JA, Niemeijer ND, Corssmit EP, Jonker MA, Leemans CR, Menko FH, et al. Low penetrance of paraganglioma and pheochromocytoma in an extended kindred with a germline SDHB exon 3 deletion. Clin Genet. 2016;89(1):128-32.

238. Cascon A, Ruiz-Llorente S, Cebrian A, Telleria D, Rivero JC, Diez JJ, et al. Identification of novel SDHD mutations in patients with phaeochromocytoma and/or paraganglioma. Eur J Hum Genet. 2002;10(8):457-61.

239. Astuti D, Douglas F, Lennard TW, Aligianis IA, Woodward ER, Evans DG, et al. Germline SDHD mutation in familial phaeochromocytoma. Lancet. 2001;357(9263):1181-2.

240. Neumann HP, Bausch B, McWhinney SR, Bender BU, Gimm O, Franke G, et al. Germ-line mutations in nonsyndromic pheochromocytoma. N Engl J Med. 2002;346(19):1459-66.

241. Dannenberg H, van Nederveen FH, Abbou M, Verhofstad AA, Komminoth P, de Krijger RR, et al. Clinical characteristics of pheochromocytoma patients with germline mutations in SDHD. J Clin Oncol. 2005;23(9):1894-901.

242. Simi L, Sestini R, Ferruzzi P, Gagliano MS, Gensini F, Mascalchi M, et al. Phenotype variability of neural crest derived tumours in six Italian families segregating the same founder SDHD mutation Q109X. J Med Genet. 2005;42(8):e52.

243. Heesterman BL, Bayley JP, Tops CM, Hes FJ, van Brussel BT, Corssmit EP, et al. High prevalence of occult paragangliomas in asymptomatic carriers of SDHD and SDHB gene mutations. Eur J Hum Genet. 2013;21(4):469-70.

244. Havekes B, Corssmit EP, Jansen JC, van der Mey AG, Vriends AH, Romijn JA. Malignant paragangliomas associated with mutations in the succinate dehydrogenase D gene. J Clin Endocrinol Metab. 2007;92(4):1245-8.

245. Timmers HJ, Pacak K, Bertherat J, Lenders JW, Duet M, Eisenhofer G, et al. Mutations associated with succinate dehydrogenase D-related malignant paragangliomas. Clin Endocrinol (Oxf). 2008;68(4):561-6.

246. Daniels D, Guez D, Last D, Hoffmann C, Nass D, Talianski A, et al. Early Biomarkers from Conventional and Delayed-Contrast MRI to Predict the Response to Bevacizumab in Recurrent High-Grade Gliomas. AJNR Am J Neuroradiol. 2016.

247. Tufton N, Ghelani R, Srirangalingam U, Kumar VKA, Drake W, Iacovazzo D, et al. SDHA mutated paragangliomas may be at high risk of metastasis. Endocr Relat Cancer. 2017.

248. Welander J, Garvin S, Bohnmark R, Isaksson L, Wiseman RW, Soderkvist P, et al. Germline SDHA mutation detected by next-generation sequencing in a young index patient with large paraganglioma. J Clin Endocrinol Metab. 2013;98(8):E1379-80.

249. Dwight T, Mann K, Benn DE, Robinson BG, McKelvie P, Gill AJ, et al. Familial SDHA mutation associated with pituitary adenoma and pheochromocytoma/paraganglioma. J Clin Endocrinol Metab. 2013;98(6):E1103-8.

250. von Dobschuetz E, Leijon H, Schalin-Jantti C, Schiavi F, Brauckhoff M, Peczkowska M, et al. A registry-based study of thyroid paraganglioma: histological and genetic characteristics. Endocr Relat Cancer. 2015;22(2):191-204.

251. Qin Y, Yao L, King EE, Buddavarapu K, Lenci RE, Chocron ES, et al. Germline mutations in TMEM127 confer susceptibility to pheochromocytoma. Nat Genet. 2010;42(3):229-33.

252.	Abermil N, Guillaud-Bataille M, Burnichon N, Venisse A, Manivet P, Guignat L, et al. TMEM127 screening in a large cohort of patients with pheochromocytoma and/or paraganglioma. J Clin Endocrinol Metab. 2012;97(5):E805-9.
253.	van Hulsteijn LT, Dekkers OM, Hes FJ, Smit JW, Corssmit EP. Risk of malignant paraganglioma in SDHB-mutation and SDHD-mutation carriers: a systematic review and meta-analysis. J Med Genet. 2012;49(12):768-76.
254.	Srirangalingam U, Banerjee A, Patki P, Peters J, George E, Chew SL, et al. Succinate Dehydrogenase B (SDHB)-Associated Bladder Paragangliomas. Clin Genitourin Cancer. 2017;15(1):e131-e6.
255.	Martucci VL, Lorenzo ZG, Weintraub M, del Rivero J, Ling A, Merino M, et al. Association of urinary bladder paragangliomas with germline mutations in the SDHB and VHL genes. Urol Oncol. 2015;33(4):167 e13-20.
256.	Casey RT, Challis BG, Marker A, Pitfield D, Cheow HK, Shaw A, et al. A case of a metastatic SDHA mutated paraganglioma re-presenting twenty-three years after initial surgery. Endocr Relat Cancer. 2017;24(8):L69-L71.
257.	Maniam P, Zhou K, Lonergan M, Berg JN, Goudie DR, Newey PJ. Pathogenicity and Penetrance of Germline SDHA Variants in Pheochromocytoma and Paraganglioma (PPGL). J Endocr Soc. 2018;2(7):806-16.
258.	Miettinen M, Killian JK, Wang ZF, Lasota J, Lau C, Jones L, et al. Immunohistochemical loss of succinate dehydrogenase subunit A (SDHA) in gastrointestinal stromal tumors (GISTs) signals SDHA germline mutation. Am J Surg Pathol. 2013;37(2):234-40.
259.	Maurea S, Cuocolo A, Reynolds JC, Neumann RD, Salvatore M. Diagnostic imaging in patients with paragangliomas. Computed tomography, magnetic resonance and MIBG scintigraphy comparison. Q J Nucl Med. 1996;40(4):365-71.
260.	Ilias I, Pacak K. Current approaches and recommended algorithm for the diagnostic localization of pheochromocytoma. J Clin Endocrinol Metab. 2004;89(2):479-91.
261.	Castinetti F, Kroiss A, Kumar R, Pacak K, Taieb D. 15 YEARS OF PARAGANGLIOMA: Imaging and imaging-based treatment of pheochromocytoma and paraganglioma. Endocr Relat Cancer. 2015;22(4):T135-45.
262.	Taieb D, Neumann H, Rubello D, Al-Nahhas A, Guillet B, Hindie E. Modern nuclear imaging for paragangliomas: beyond SPECT. J Nucl Med. 2012;53(2):264-74.
263.	Timmers HJ, Chen CC, Carrasquillo JA, Whatley M, Ling A, Havekes B, et al. Comparison of 18F-fluoro-L-DOPA, 18F-fluoro-deoxyglucose, and 18F-fluorodopamine PET and 123I-MIBG scintigraphy in the localization of pheochromocytoma and paraganglioma. J Clin Endocrinol Metab. 2009;94(12):4757-67.
264.	Timmers HJ, Kozupa A, Chen CC, Carrasquillo JA, Ling A, Eisenhofer G, et al. Superiority of fluorodeoxyglucose positron emission tomography to other functional imaging techniques in the evaluation of metastatic SDHB-associated pheochromocytoma and paraganglioma. J Clin Oncol. 2007;25(16):2262-9.
265.	Tufton N, Sahdev A, Akker SA. Radiological Surveillance Screening in Asymptomatic Succinate Dehydrogenase Mutation Carriers. J Endocr Soc. 2017;1(7):897-907.
266.	Janssen I, Chen CC, Taieb D, Patronas NJ, Millo CM, Adams KT, et al. 68Ga-DOTATATE PET/CT in the Localization of Head and Neck Paragangliomas Compared with Other Functional Imaging Modalities and CT/MRI. J Nucl Med. 2016;57(2):186-91.
267.	Archier A, Varoquaux A, Garrigue P, Montava M, Guerin C, Gabriel S, et al. Prospective comparison of (68)Ga-DOTATATE and (18)F-FDOPA PET/CT in patients with various pheochromocytomas and paragangliomas with emphasis on sporadic cases. Eur J Nucl Med Mol Imaging. 2016;43(7):1248-57.
268.	Gravel G, Niccoli P, Rohmer V, Moulin G, Borson-Chazot F, Rousset P, et al. The value of a rapid contrast-enhanced angio-MRI protocol in the detection of head and neck paragangliomas in SDHx

mutations carriers: a retrospective study on behalf of the PGL.EVA investigators. Eur Radiol. 2016;26(6):1696-704.

269.   Fonte JS, Robles JF, Chen CC, Reynolds J, Whatley M, Ling A, et al. False-negative (1)(2)(3)I-MIBG SPECT is most commonly found in SDHB-related pheochromocytoma or paraganglioma with high frequency to develop metastatic disease. Endocr Relat Cancer. 2012;19(1):83-93.

270.   Wall BF, Haylockm R. Jansen, J. T. M. Hillier, M. C. Hart, D and Shrimpton, P. C. HPA-CRCE-028. Radiation Risks from Medical X-ray Examinations as a Function of the Age and Sex of the Patient. . In: Agency HP, editor. 2011. p. 6-12.

271.   Brenner DJ, Elliston CD. Estimated radiation risks potentially associated with full-body CT screening. Radiology. 2004;232(3):735-8.

272.   Huang B, Law MW, Khong PL. Whole-body PET/CT scanning: estimation of radiation dose and cancer risk. Radiology. 2009;251(1):166-74.

273.   Imamura H, Muroya K, Tanaka E, Konomoto T, Moritake H, Sato T, et al. Sporadic paraganglioma caused by de novo SDHB mutations in a 6-year-old girl. Eur J Pediatr. 2016;175(1):137-41.

274.   Bayley JP, Bausch B, Rijken JA, van Hulsteijn LT, Jansen JC, Ascher D, et al. Variant type is associated with disease characteristics in SDHB, SDHC and SDHD-linked phaeochromocytoma-paraganglioma. J Med Genet. 2020;57(2):96-103.

275.   Bayley JP, Devilee P. Hypothesis: Why Different Types of SDH Gene Variants Cause Divergent Tumor Phenotypes. Genes (Basel). 2022;13(6).

276.   Job S, Draskovic I, Burnichon N, Buffet A, Cros J, Lepine C, et al. Telomerase Activation and ATRX Mutations Are Independent Risk Factors for Metastatic Pheochromocytoma and Paraganglioma. Clin Cancer Res. 2019;25(2):760-70.

277.   Williams ST, Chatzikyriakou P, Carroll PV, McGowan BM, Velusamy A, White G, et al. SDHC phaeochromocytoma and paraganglioma: A UK-wide case series. Clin Endocrinol (Oxf). 2022;96(4):499-512.

278.   MacFarlane J, Seong KC, Bisambar C, Madhu B, Allinson K, Marker A, et al. A review of the tumour spectrum of germline succinate dehydrogenase gene mutations: Beyond phaeochromocytoma and paraganglioma. Clin Endocrinol (Oxf). 2020;93(5):528-38.

279.   Lloyd RVOR KG, Rosai J. WHO classification of tumours: pathology
and genetics of tumours of endocrine organs. 2017.

280.   Tufton N, Shapiro L, Sahdev A, Kumar AV, Martin L, Drake WM, et al. An analysis of surveillance screening for SDHB-related disease in childhood and adolescence. Endocr Connect. 2019;8(3):162-72.

281.   Wong MY, Andrews KA, Challis BG, Park SM, Acerini CL, Maher ER, et al. Clinical Practice Guidance: Surveillance for phaeochromocytoma and paraganglioma in paediatric succinate dehydrogenase gene mutation carriers. Clin Endocrinol (Oxf). 2019;90(4):499-505.

282.   Burnichon N, Mazzella JM, Drui D, Amar L, Bertherat J, Coupier I, et al. Risk assessment of maternally inherited SDHD paraganglioma and phaeochromocytoma. J Med Genet. 2017;54(2):125-33.

283.   Peitzsch M, Mangelis A, Eisenhofer G, Huebner A. Age-specific pediatric reference intervals for plasma free normetanephrine, metanephrine, 3-methoxytyramine and 3-O-methyldopa: Particular importance for early infancy. Clin Chim Acta. 2019;494:100-5.

284.   Langton K, Tufton N, Akker S, Deinum J, Eisenhofer G, Timmers H, et al. Pregnancy and phaeochromocytoma/paraganglioma: clinical clues affecting diagnosis and outcome - a systematic review. BJOG. 2021;128(8):1264-72.

285.   Bancos I, Atkinson E, Eng C, Young WF, Jr., Neumann HPH, International P, et al. Maternal and fetal outcomes in phaeochromocytoma and pregnancy: a multicentre retrospective cohort study and systematic review of literature. Lancet Diabetes Endocrinol. 2021;9(1):13-21.

286.   Winzeler B, Tufton N, E SL, Challis BG, Park SM, Izatt L, et al. Investigating the role of somatic sequencing platforms for phaeochromocytoma and paraganglioma in a large UK cohort. Clin Endocrinol (Oxf). 2021.

287.   Udager AM, Magers MJ, Goerke DM, Vinco ML, Siddiqui J, Cao X, et al. The utility of SDHB and FH immunohistochemistry in patients evaluated for hereditary paraganglioma-pheochromocytoma syndromes. Hum Pathol. 2018;71:47-54.

288.   Yao L, Schiavi F, Cascon A, Qin Y, Inglada-Perez L, King EE, et al. Spectrum and prevalence of FP/TMEM127 gene mutations in pheochromocytomas and paragangliomas. JAMA. 2010;304(23):2611-9.

289.   Neumann HP, Sullivan M, Winter A, Malinoc A, Hoffmann MM, Boedeker CC, et al. Germline mutations of the TMEM127 gene in patients with paraganglioma of head and neck and extraadrenal abdominal sites. J Clin Endocrinol Metab. 2011;96(8):E1279-82.

290.   Bausch B, Schiavi F, Ni Y, Welander J, Patocs A, Ngeow J, et al. Clinical Characterization of the Pheochromocytoma and Paraganglioma Susceptibility Genes SDHA, TMEM127, MAX, and SDHAF2 for Gene-Informed Prevention. JAMA Oncol. 2017.

291.   Toledo SP, Lourenco DM, Jr., Sekiya T, Lucon AM, Baena ME, Castro CC, et al. Penetrance and clinical features of pheochromocytoma in a six-generation family carrying a germline TMEM127 mutation. J Clin Endocrinol Metab. 2015;100(2):E308-18.

292.   Maher M, Roncaroli F, Mendoza N, Meeran K, Canham N, Kosicka-Slawinska M, et al. A patient with a germline SDHB mutation presenting with an isolated pituitary macroprolactinoma. Endocrinol Diabetes Metab Case Rep. 2018;2018.

293.   Pollard PJ, Briere JJ, Alam NA, Barwell J, Barclay E, Wortham NC, et al. Accumulation of Krebs cycle intermediates and over-expression of HIF1alpha in tumours which result from germline FH and SDH mutations. Hum Mol Genet. 2005;14(15):2231-9.

294.   Lam AK. Update on Adrenal Tumours in 2017 World Health Organization (WHO) of Endocrine Tumours. Endocr Pathol. 2017;28(3):213-27.

295.   Jimenez C, Rohren E, Habra MA, Rich T, Jimenez P, Ayala-Ramirez M, et al. Current and future treatments for malignant pheochromocytoma and sympathetic paraganglioma. Curr Oncol Rep. 2013;15(4):356-71.

296.   Niemeijer ND, Alblas G, van Hulsteijn LT, Dekkers OM, Corssmit EP. Chemotherapy with cyclophosphamide, vincristine and dacarbazine for malignant paraganglioma and pheochromocytoma: systematic review and meta-analysis. Clin Endocrinol (Oxf). 2014;81(5):642-51.

297.   Pryma DA, Chin BB, Noto RB, Dillon JS, Perkins S, Solnes L, et al. Efficacy and Safety of High-Specific-Activity (131)I-MIBG Therapy in Patients with Advanced Pheochromocytoma or Paraganglioma. J Nucl Med. 2019;60(5):623-30.

298.   Jimenez P, Tatsui C, Jessop A, Thosani S, Jimenez C. Treatment for Malignant Pheochromocytomas and Paragangliomas: 5 Years of Progress. Curr Oncol Rep. 2017;19(12):83.

299.   Kulke MH, Stuart K, Enzinger PC, Ryan DP, Clark JW, Muzikansky A, et al. Phase II study of temozolomide and thalidomide in patients with metastatic neuroendocrine tumors. J Clin Oncol. 2006;24(3):401-6.

300.   Tong A, Li M, Cui Y, Ma X, Wang H, Li Y. Temozolomide Is a Potential Therapeutic Tool for Patients With Metastatic Pheochromocytoma/Paraganglioma-Case Report and Review of the Literature. Front Endocrinol (Lausanne). 2020;11:61.

301.   Forrer F, Riedweg I, Maecke HR, Mueller-Brand J. Radiolabeled DOTATOC in patients with advanced paraganglioma and pheochromocytoma. Q J Nucl Med Mol Imaging. 2008;52(4):334-40.

302.   van Essen M, Krenning EP, Kooij PP, Bakker WH, Feelders RA, de Herder WW, et al. Effects of therapy with [177Lu-DOTA0, Tyr3]octreotate in patients with paraganglioma, meningioma, small cell lung carcinoma, and melanoma. J Nucl Med. 2006;47(10):1599-606.

303.   Hadoux J, Terroir M, Leboulleux S, Deschamps F, Al Ghuzlan A, Hescot S, et al. Interferon-alpha Treatment for Disease Control in Metastatic Pheochromocytoma/Paraganglioma Patients. Horm Cancer. 2017;8(5-6):330-7.

304.   Kirkwood J. Cancer immunotherapy: the interferon-alpha experience. Semin Oncol. 2002;29(3 Suppl 7):18-26.

305.	La-Beck NM, Jean GW, Huynh C, Alzghari SK, Lowe DB. Immune Checkpoint Inhibitors: New Insights and Current Place in Cancer Therapy. Pharmacotherapy. 2015;35(10):963-76.

306.	Chouaib S, Noman MZ, Kosmatopoulos K, Curran MA. Hypoxic stress: obstacles and opportunities for innovative immunotherapy of cancer. Oncogene. 2017;36(4):439-45.

307.	Jimenez C, Subbiah V, Stephen B, Ma J, Milton D, Xu M, et al. Phase II Clinical Trial of Pembrolizumab in Patients with Progressive Metastatic Pheochromocytomas and Paragangliomas. Cancers (Basel). 2020;12(8).

308.	Farhat NA, Powers JF, Shepard-Barry A, Dahia P, Pacak K, Tischler AS. A Previously Unrecognized Monocytic Component of Pheochromocytoma and Paraganglioma. Endocr Pathol. 2019;30(2):90-5.

309.	Spranger S, Luke JJ, Bao R, Zha Y, Hernandez KM, Li Y, et al. Density of immunogenic antigens does not explain the presence or absence of the T-cell-inflamed tumor microenvironment in melanoma. Proc Natl Acad Sci U S A. 2016;113(48):E7759-E68.

310.	Barnes MA, Carson MJ, Nair MG. Non-traditional cytokines: How catecholamines and adipokines influence macrophages in immunity, metabolism and the central nervous system. Cytokine. 2015;72(2):210-9.

311.	Stolk RF, van der Poll T, Angus DC, van der Hoeven JG, Pickkers P, Kox M. Potentially Inadvertent Immunomodulation: Norepinephrine Use in Sepsis. Am J Respir Crit Care Med. 2016;194(5):550-8.

312.	Balkwill FR, Capasso M, Hagemann T. The tumor microenvironment at a glance. J Cell Sci. 2012;125(Pt 23):5591-6.

313.	Wang M, Zhao J, Zhang L, Wei F, Lian Y, Wu Y, et al. Role of tumor microenvironment in tumorigenesis. J Cancer. 2017;8(5):761-73.

314.	Cuny T, de Herder W, Barlier A, Hofland LJ. Role of the tumor microenvironment in digestive neuroendocrine tumors. Endocr Relat Cancer. 2018;25(11):R519-R44.

315.	Hanahan D, Weinberg RA. Hallmarks of cancer: the next generation. Cell. 2011;144(5):646-74.

316.	Hendry S, Salgado R, Gevaert T, Russell PA, John T, Thapa B, et al. Assessing Tumor-infiltrating Lymphocytes in Solid Tumors: A Practical Review for Pathologists and Proposal for a Standardized Method From the International Immunooncology Biomarkers Working Group: Part 1: Assessing the Host Immune Response, TILs in Invasive Breast Carcinoma and Ductal Carcinoma In Situ, Metastatic Tumor Deposits and Areas for Further Research. Adv Anat Pathol. 2017;24(5):235-51.

317.	Tamborero D, Rubio-Perez C, Muinos F, Sabarinathan R, Piulats JM, Muntasell A, et al. A Pan-cancer Landscape of Interactions between Solid Tumors and Infiltrating Immune Cell Populations. Clin Cancer Res. 2018;24(15):3717-28.

318.	Murdoch C, Giannoudis A, Lewis CE. Mechanisms regulating the recruitment of macrophages into hypoxic areas of tumors and other ischemic tissues. Blood. 2004;104(8):2224-34.

319.	Mantovani A, Sozzani S, Locati M, Allavena P, Sica A. Macrophage polarization: tumor-associated macrophages as a paradigm for polarized M2 mononuclear phagocytes. Trends Immunol. 2002;23(11):549-55.

320.	Mantovani A, Marchesi F, Malesci A, Laghi L, Allavena P. Tumour-associated macrophages as treatment targets in oncology. Nat Rev Clin Oncol. 2017;14(7):399-416.

321.	Ruffell B, Coussens LM. Macrophages and therapeutic resistance in cancer. Cancer Cell. 2015;27(4):462-72.

322.	Viola A, Munari F, Sanchez-Rodriguez R, Scolaro T, Castegna A. The Metabolic Signature of Macrophage Responses. Front Immunol. 2019;10:1462.

323.	Thorsson V, Gibbs DL, Brown SD, Wolf D, Bortone DS, Ou Yang TH, et al. The Immune Landscape of Cancer. Immunity. 2018;48(4):812-30 e14.

324.	Carron EC, Homra S, Rosenberg J, Coffelt SB, Kittrell F, Zhang Y, et al. Macrophages promote the progression of premalignant mammary lesions to invasive cancer. Oncotarget. 2017;8(31):50731-46.

325.   Hao NB, Lu MH, Fan YH, Cao YL, Zhang ZR, Yang SM. Macrophages in tumor microenvironments and the progression of tumors. Clin Dev Immunol. 2012;2012:948098.

326.   Maolake A, Izumi K, Shigehara K, Natsagdorj A, Iwamoto H, Kadomoto S, et al. Tumor-associated macrophages promote prostate cancer migration through activation of the CCL22-CCR4 axis. Oncotarget. 2017;8(6):9739-51.

327.   Lan C, Huang X, Lin S, Huang H, Cai Q, Wan T, et al. Expression of M2-polarized macrophages is associated with poor prognosis for advanced epithelial ovarian cancer. Technol Cancer Res Treat. 2013;12(3):259-67.

328.   Fang W, Ye L, Shen L, Cai J, Huang F, Wei Q, et al. Tumor-associated macrophages promote the metastatic potential of thyroid papillary cancer by releasing CXCL8. Carcinogenesis. 2014;35(8):1780-7.

329.   Ryder M, Ghossein RA, Ricarte-Filho JC, Knauf JA, Fagin JA. Increased density of tumor-associated macrophages is associated with decreased survival in advanced thyroid cancer. Endocr Relat Cancer. 2008;15(4):1069-74.

330.   Wei IH, Harmon CM, Arcerito M, Cheng DF, Minter RM, Simeone DM. Tumor-associated macrophages are a useful biomarker to predict recurrence after surgical resection of nonfunctional pancreatic neuroendocrine tumors. Ann Surg. 2014;260(6):1088-94.

331.   Fridman WH, Pages F, Sautes-Fridman C, Galon J. The immune contexture in human tumours: impact on clinical outcome. Nat Rev Cancer. 2012;12(4):298-306.

332.   Blessin NC, Spriestersbach P, Li W, Mandelkow T, Dum D, Simon R, et al. Prevalence of CD8(+) cytotoxic lymphocytes in human neoplasms. Cell Oncol (Dordr). 2020;43(3):421-30.

333.   Fridman WH. The immune microenvironment as a guide for cancer therapies. Oncoimmunology. 2012;1(3):261-2.

334.   Campbell DJ, Koch MA. Phenotypical and functional specialization of FOXP3+ regulatory T cells. Nat Rev Immunol. 2011;11(2):119-30.

335.   Landwehr LS, Altieri B, Schreiner J, Sbiera I, Weigand I, Kroiss M, et al. Interplay between glucocorticoids and tumor-infiltrating lymphocytes on the prognosis of adrenocortical carcinoma. J Immunother Cancer. 2020;8(1).

336.   Waugh DJ, Wilson C. The interleukin-8 pathway in cancer. Clin Cancer Res. 2008;14(21):6735-41.

337.   De Larco JE, Wuertz BR, Furcht LT. The potential role of neutrophils in promoting the metastatic phenotype of tumors releasing interleukin-8. Clin Cancer Res. 2004;10(15):4895-900.

338.   Mantovani A, Savino B, Locati M, Zammataro L, Allavena P, Bonecchi R. The chemokine system in cancer biology and therapy. Cytokine Growth Factor Rev. 2010;21(1):27-39.

339.   Yapa S, Mulla O, Green V, England J, Greenman J. The Role of Chemokines in Thyroid Carcinoma. Thyroid. 2017;27(11):1347-59.

340.   Balkwill F, Coussens LM. Cancer: an inflammatory link. Nature. 2004;431(7007):405-6.

341.   Brabek J, Mierke CT, Rosel D, Vesely P, Fabry B. The role of the tissue microenvironment in the regulation of cancer cell motility and invasion. Cell Commun Signal. 2010;8:22.

342.   Douglas SA, Sreenivasan D, Carman FH, Bunn SJ. Cytokine interactions with adrenal medullary chromaffin cells. Cell Mol Neurobiol. 2010;30(8):1467-75.

343.   Path G, Bornstein SR, Ehrhart-Bornstein M, Scherbaum WA. Interleukin-6 and the interleukin-6 receptor in the human adrenal gland: expression and effects on steroidogenesis. J Clin Endocrinol Metab. 1997;82(7):2343-9.

344.   Bornstein SR, Ehrhart-Bornstein M, Gonzalez-Hernandez J, Schroder S, Scherbaum WA. Expression of interleukin-1 in human pheochromocytoma. J Endocrinol Invest. 1996;19(10):693-8.

345.   Tannahill GM, Curtis AM, Adamik J, Palsson-McDermott EM, McGettrick AF, Goel G, et al. Succinate is an inflammatory signal that induces IL-1beta through HIF-1alpha. Nature. 2013;496(7444):238-42.

346.   Li Y, Wang L, Pappan L, Galliher-Beckley A, Shi J. IL-1beta promotes stemness and invasiveness of colon cancer cells through Zeb1 activation. Mol Cancer. 2012;11:87.

347.   Lee CH, Chang JS, Syu SH, Wong TS, Chan JY, Tang YC, et al. IL-1beta promotes malignant transformation and tumor aggressiveness in oral cancer. J Cell Physiol. 2015;230(4):875-84.

348.   Nilsson O, Wangberg B, Kolby L, Schultz GS, Ahlman H. Expression of transforming growth factor alpha and its receptor in human neuroendocrine tumours. Int J Cancer. 1995;60(5):645-51.

349.   Ciacciarelli M, Bellini D, Laghi A, Polidoro A, Pacelli A, Bottaccioli AG, et al. IL-6-Producing, Noncatecholamines Secreting Pheochromocytoma Presenting as Fever of Unknown Origin. Case Rep Med. 2016;2016:3489046.

350.   Nagaishi R, Akehi Y, Ashida K, Higuchi-Tubouchi K, Yokoyama H, Nojiri T, et al. Acute inflammatory syndrome and intrahepatic cholestasis caused by an interleukin-6-producing pheochromocytoma with pregnancy. Fukuoka Igaku Zasshi. 2010;101(1):10-8.

351.   Saba Radhi M, Kenneth Nugent, MD, and Raed Alalawi, MD. Pheochromocytoma Presenting as Systemic Inflammatory Response Syndrome and Lactic Acidosis. ICU Director. 2010;1(5).

352.   Yarman S, Soyluk O, Altunoglu E, Tanakol R. Interleukin-6-producing pheochromocytoma presenting with fever of unknown origin. Clinics (Sao Paulo). 2011;66(10):1843-5.

353.   Salahuddin A, Rohr-Kirchgraber T, Shekar R, West B, Loewenstein J. Interleukin-6 in the fever and multiorgan crisis of pheochromocytoma. Scand J Infect Dis. 1997;29(6):640-2.

354.   Suzuki K, Miyashita A, Inoue Y, Iki S, Enomoto H, Takahashi Y, et al. Interleukin-6-producing pheochromocytoma. Acta Haematol. 1991;85(4):217-9.

355.   Meijs AC, Snel M, Corssmit EPM. Pheochromocytoma/paraganglioma crisis: case series from a tertiary referral center for pheochromocytomas and paragangliomas. Hormones (Athens). 2021;20(2):395-403.

356.   Tong AL, Zeng ZP, Li HZ, Yang D, Lu L, Li M. Expression and effect of transforming growth factor-alpha and tumor necrosis factor-alpha in human pheochromocytoma. Ann N Y Acad Sci. 2006;1073:277-83.

357.   Kanauchi H, Mimura Y, Hiki N, Kaminishi M. Catecholamine and cytokine response to laparoscopic adrenalectomy in patients with pheochromocytoma. Biomed Pharmacother. 2000;54 Suppl 1:191s-3s.

358.   Kontogeorgos G, Scheithauer BW, Kovacs K, Horvath E, Melmed S. Growth factors and cytokines in paragangliomas and pheochromocytomas, with special reference to sustentacular cells. Endocr Pathol. 2002;13(3):197-206.

359.   Zhou J, Qi ST, Chen LG, Huang CR, You J, Zhang C, et al. [Expression pattern of inflammatory cytokines at various inflammatory levels of adamantinomatous craniopharyngioma]. Zhonghua Yi Xue Za Zhi. 2013;93(31):2499-501.

360.   Nie J, Huang GL, Deng SZ, Bao Y, Liu YW, Feng ZP, et al. The purine receptor P2X7R regulates the release of pro-inflammatory cytokines in human craniopharyngioma. Endocr Relat Cancer. 2017;24(6):287-96.

361.   Rapizzi E, Fucci R, Giannoni E, Canu L, Richter S, Cirri P, et al. Role of microenvironment on neuroblastoma SK-N-AS SDHB-silenced cell metabolism and function. Endocr Relat Cancer. 2015;22(3):409-17.

362.   D'Antongiovanni V, Martinelli S, Richter S, Canu L, Guasti D, Mello T, et al. The microenvironment induces collective migration in SDHB-silenced mouse pheochromocytoma spheroids. Endocr Relat Cancer. 2017;24(10):555-64.

363.   Brohee D, Vanhaeverbeek M, Kennes B, Neve P. Leukocyte and lymphocyte subsets after a short pharmacological stress by intravenous epinephrine and hydrocortisone in healthy humans. Int J Neurosci. 1990;53(2-4):53-62.

364.   Brenner I, Shek PN, Zamecnik J, Shephard RJ. Stress hormones and the immunological responses to heat and exercise. Int J Sports Med. 1998;19(2):130-43.

365.   Sevastos N, Theodossiades G, Malaktari S, Archimandritis AJ. Persistent neutrophilia as a preceding symptom of pheochromocytoma. J Clin Endocrinol Metab. 2005;90(4):2472; author reply - 3.

366.   Ahmad J, Grimes N, Farid S, Morris-Stiff G. Inflammatory response related scoring systems in assessing the prognosis of patients with pancreatic ductal adenocarcinoma: a systematic review. Hepatobiliary Pancreat Dis Int. 2014;13(5):474-81.

367.   Liu CL, Lee JJ, Liu TP, Chang YC, Hsu YC, Cheng SP. Blood neutrophil-to-lymphocyte ratio correlates with tumor size in patients with differentiated thyroid cancer. J Surg Oncol. 2013;107(5):493-7.

368.   Ozmen S, Timur O, Calik I, Altinkaynak K, Simsek E, Gozcu H, et al. Neutrophil-lymphocyte ratio (NLR) and platelet-lymphocyte ratio (PLR) may be superior to C-reactive protein (CRP) for predicting the occurrence of differentiated thyroid cancer. Endocr Regul. 2017;51(3):131-6.

369.   Zhang J, He M, Liu Z, Song Y, Wang Y, Liang R, et al. Impact of neutrophil-lymphocyte ratio on long-term outcome in patients with craniopharyngioma. Medicine (Baltimore). 2018;97(37):e12375.

370.   Chang X, Zhang F, Liu T, Wang W, Guo H. Neutrophil-to-lymphocyte ratio as an independent predictor for survival in patients with localized clear cell renal cell carcinoma after radiofrequency ablation: a propensity score matching analysis. Int Urol Nephrol. 2017;49(6):967-74.

371.   Tang H, Lu W, Li B, Li C, Xu Y, Dong J. Prognostic significance of neutrophil-to-lymphocyte ratio in biliary tract cancers: a systematic review and meta-analysis. Oncotarget. 2017;8(22):36857-68.

372.   Bhatti I, Peacock O, Lloyd G, Larvin M, Hall RI. Preoperative hematologic markers as independent predictors of prognosis in resected pancreatic ductal adenocarcinoma: neutrophil-lymphocyte versus platelet-lymphocyte ratio. Am J Surg. 2010;200(2):197-203.

373.   Chan JC, Chan DL, Diakos CI, Engel A, Pavlakis N, Gill A, et al. The Lymphocyte-to-Monocyte Ratio is a Superior Predictor of Overall Survival in Comparison to Established Biomarkers of Resectable Colorectal Cancer. Ann Surg. 2017;265(3):539-46.

374.   Yang T, Zhu J, Zhao L, Mai K, Ye J, Huang S, et al. Lymphocyte to monocyte ratio and neutrophil to lymphocyte ratio are superior inflammation-based predictors of recurrence in patients with hepatocellular carcinoma after hepatic resection. J Surg Oncol. 2017;115(6):718-28.

375.   McMillan DC. Systemic inflammation, nutritional status and survival in patients with cancer. Curr Opin Clin Nutr Metab Care. 2009;12(3):223-6.

376.   Caplin ME, Pavel M, Cwikla JB, Phan AT, Raderer M, Sedlackova E, et al. Lanreotide in metastatic enteropancreatic neuroendocrine tumors. N Engl J Med. 2014;371(3):224-33.

377.   Rinke A, Muller HH, Schade-Brittinger C, Klose KJ, Barth P, Wied M, et al. Placebo-controlled, double-blind, prospective, randomized study on the effect of octreotide LAR in the control of tumor growth in patients with metastatic neuroendocrine midgut tumors: a report from the PROMID Study Group. J Clin Oncol. 2009;27(28):4656-63.

378.   Modlin IM, Pavel M, Kidd M, Gustafsson BI. Review article: somatostatin analogues in the treatment of gastroenteropancreatic neuroendocrine (carcinoid) tumours. Aliment Pharmacol Ther. 2010;31(2):169-88.

379.   Eriksson B, Oberg K. Summing up 15 years of somatostatin analog therapy in neuroendocrine tumors: future outlook. Ann Oncol. 1999;10 Suppl 2:S31-8.

380.   Costa F, Gumz B. Octreotide - A Review of its Use in Treating Neuroendocrine Tumours. Eur Endocrinol. 2014;10(1):70-4.

381.   Reubi JC, Waser B, Khosla S, Kvols L, Goellner JR, Krenning E, et al. In vitro and in vivo detection of somatostatin receptors in pheochromocytomas and paragangliomas. J Clin Endocrinol Metab. 1992;74(5):1082-9.

382.   Tenenbaum F, Schlumberger M, Lumbroso J, Parmentier C. Beneficial effects of octreotide in a patient with a metastatic paraganglioma. Eur J Cancer. 1996;32A(4):737.

383.   Tonyukuk V, Emral R, Temizkan S, Sertcelik A, Erden I, Corapcioglu D. Case report: patient with multiple paragangliomas treated with long acting somatostatin analogue. Endocr J. 2003;50(5):507-13.

384.   Plouin PF, Bertherat J, Chatellier G, Billaud E, Azizi M, Grouzmann E, et al. Short-term effects of octreotide on blood pressure and plasma catecholamines and neuropeptide Y levels in patients with phaeochromocytoma: a placebo-controlled trial. Clin Endocrinol (Oxf). 1995;42(3):289-94.

385.	Elston MS, Meyer-Rochow GY, Conaglen HM, Clarkson A, Clifton-Bligh RJ, Conaglen JV, et al. Increased SSTR2A and SSTR3 expression in succinate dehydrogenase-deficient pheochromocytomas and paragangliomas. Hum Pathol. 2015;46(3):390-6.

386.	Liu Y, Xu R, Gu H, Zhang E, Qu J, Cao W, et al. Metabolic reprogrammeming in macrophage responses. Biomark Res. 2021;9(1):1.

387.	Gao X, Yamazaki Y, Pecori A, Tezuka Y, Ono Y, Omata K, et al. Histopathological Analysis of Tumor Microenvironment and Angiogenesis in Pheochromocytoma. Front Endocrinol (Lausanne). 2020;11:587779.

388.	Guadagno E, Russo D, Pignatiello S, Del Basso De Caro M. Inflammation in the neoplasms of the adrenal gland: Is there a prognostic role? An immunohistochemical study. Pathol Res Pract. 2020;216(9):153070.

389.	Batchu S. Age-related differences of immune infiltrates in pheochromocytomas and paragangliomas. J Endocrinol Invest. 2021;44(7):1543-6.

390.	Madden KS, Sanders VM, Felten DL. Catecholamine influences and sympathetic neural modulation of immune responsiveness. Annu Rev Pharmacol Toxicol. 1995;35:417-48.

391.	Nasi G, Ahmed T, Rasini E, Fenoglio D, Marino F, Filaci G, et al. Dopamine inhibits human CD8+ Treg function through D1-like dopaminergic receptors. J Neuroimmunol. 2019;332:233-41.

392.	Edgar VA, Silberman DM, Cremaschi GA, Zieher LM, Genaro AM. Altered lymphocyte catecholamine reactivity in mice subjected to chronic mild stress. Biochem Pharmacol. 2003;65(1):15-23.

393.	Calsina B, Pineiro-Yanez E, Martinez-Montes AM, Caleiras E, Fernandez-Sanroman A, Monteagudo M, et al. Genomic and immune landscape Of metastatic pheochromocytoma and paraganglioma. Nat Commun. 2023;14(1):1122.

394.	Zhang L, Conejo-Garcia JR, Katsaros D, Gimotty PA, Massobrio M, Regnani G, et al. Intratumoral T cells, recurrence, and survival in epithelial ovarian cancer. N Engl J Med. 2003;348(3):203-13.

395.	Zhu L, Narloch JL, Onkar S, Joy M, Broadwater G, Luedke C, et al. Metastatic breast cancers have reduced immune cell recruitment but harbor increased macrophages relative to their matched primary tumors. J Immunother Cancer. 2019;7(1):265.

396.	Kimura N, Pilichowska M, Date F, Kimura I, Schindler M. Immunohistochemical expression of somatostatin type 2A receptor in neuroendocrine tumors. Clin Cancer Res. 1999;5(11):3483-7.

397.	Okuwaki K, Kida M, Mikami T, Yamauchi H, Imaizumi H, Miyazawa S, et al. Clinicopathologic characteristics of pancreatic neuroendocrine tumors and relation of somatostatin receptor type 2A to outcomes. Cancer. 2013;119(23):4094-102.

398.	Qian ZR, Li T, Ter-Minassian M, Yang J, Chan JA, Brais LK, et al. Association Between Somatostatin Receptor Expression and Clinical Outcomes in Neuroendocrine Tumors. Pancreas. 2016;45(10):1386-93.

399.	Fischer T, Doll C, Jacobs S, Kolodziej A, Stumm R, Schulz S. Reassessment of sst2 somatostatin receptor expression in human normal and neoplastic tissues using the novel rabbit monoclonal antibody UMB-1. J Clin Endocrinol Metab. 2008;93(11):4519-24.

400.	Unger N, Serdiuk I, Sheu SY, Walz MK, Schulz S, Saeger W, et al. Immunohistochemical localization of somatostatin receptor subtypes in benign and malignant adrenal tumours. Clin Endocrinol (Oxf). 2008;68(6):850-7.

401.	Saveanu A, Muresan M, De Micco C, Taieb D, Germanetti AL, Sebag F, et al. Expression of somatostatin receptors, dopamine D(2) receptors, noradrenaline transporters, and vesicular monoamine transporters in 52 pheochromocytomas and paragangliomas. Endocr Relat Cancer. 2011;18(2):287-300.

402.	Patel M, Tena I, Jha A, Taieb D, Pacak K. Somatostatin Receptors and Analogs in Pheochromocytoma and Paraganglioma: Old Players in a New Precision Medicine World. Front Endocrinol (Lausanne). 2021;12:625312.

403. Nastos K, Cheung VTF, Toumpanakis C, Navalkissoor S, Quigley AM, Caplin M, et al. Peptide Receptor Radionuclide Treatment and (131)I-MIBG in the management of patients with metastatic/progressive phaeochromocytomas and paragangliomas. J Surg Oncol. 2017;115(4):425-34.

404. Yamazaki Y, Gao X, Pecori A, Nakamura Y, Tezuka Y, Omata K, et al. Recent Advances in Histopathological and Molecular Diagnosis in Pheochromocytoma and Paraganglioma: Challenges for Predicting Metastasis in Individual Patients. Front Endocrinol (Lausanne). 2020;11:587769.

405. Thompson LD. Pheochromocytoma of the Adrenal gland Scaled Score (PASS) to separate benign from malignant neoplasms: a clinicopathologic and immunophenotypic study of 100 cases. Am J Surg Pathol. 2002;26(5):551-66.

406. Kimura N, Takekoshi K, Naruse M. Risk Stratification on Pheochromocytoma and Paraganglioma from Laboratory and Clinical Medicine. J Clin Med. 2018;7(9).

407. Koh JM, Ahn SH, Kim H, Kim BJ, Sung TY, Kim YH, et al. Validation of pathological grading systems for predicting metastatic potential in pheochromocytoma and paraganglioma. PLoS One. 2017;12(11):e0187398.

408. Cho YY, Kwak MK, Lee SE, Ahn SH, Kim H, Suh S, et al. A clinical prediction model to estimate the metastatic potential of pheochromocytoma/paraganglioma: ASES score. Surgery. 2018;164(3):511-7.

409. Pierre C, Agopiantz M, Brunaud L, Battaglia-Hsu SF, Max A, Pouget C, et al. COPPS, a composite score integrating pathological features, PS100 and SDHB losses, predicts the risk of metastasis and progression-free survival in pheochromocytomas/paragangliomas. Virchows Arch. 2019;474(6):721-34.

410. Unger P, Hoffman K, Pertsemlidis D, Thung S, Wolfe D, Kaneko M. S100 protein-positive sustentacular cells in malignant and locally aggressive adrenal pheochromocytomas. Arch Pathol Lab Med. 1991;115(5):484-7.

411. Srirangalingam U, Khoo B, Walker L, MacDonald F, Skelly RH, George E, et al. Contrasting clinical manifestations of SDHB and VHL associated chromaffin tumours. Endocr Relat Cancer. 2009;16(2):515-25.

412. Lawrence JK, Maher ER, Sheaves R, Grossman AB. Familial paraganglioma: a novel presentation of a case and response to therapy with radiolabelled MIBG. Hormones (Athens). 2004;3(2):127-31.

Appendices

Appendix 1: Questionnaire to assess PPGL symptoms. *Adapted from Manger et al, 1977[113]*

Patient Name ……..   **Hospital No………………..**

Please circle the relevant symptoms that you experienced before diagnosis of your phaeochromocytoma / paraganglioma and add other comments
If symptoms are not relevant to you, please proceed to next question

1.	**Headache:**		Yes	No		

	a.	Character :	Throbbing	Dull Ache	Burning pain	Pressure feeling
	b.	Region:	Front	Back	On the side	All over

2.	**Excessive Sweating:**	Yes	No		

	a.	Generalised	or	Localised to a specific region? If so where? ………………

3.	a.	**Heart racing**	Yes	No
	a.	**Heart Slowing down**	Yes	No
	b.	**Pounding in chest**	Yes	No
	c.	Other …………………………..		

4.	**Anxiety +/- Nervousness:**	Yes	No

5.	**Constipation**:	Yes	No

6.	**Diarrhoea:**	Yes	No

7.	**Flushing**:	Yes	No

8.	**Tremor** (shaking):	Yes	No

9.	**Pain**	a. Chest	Yes	No
		b. Abdominal (stomach)	Yes	No
		c. Back	Yes	No

10.	**Nausea +/- vomiting**:		Yes	No
	a.	Symptoms relieved following vomiting	Yes	No

11.	**Weakness +/- Fatigue** (tiredness):	Yes	No		
		Mild	Moderate	Severe	

12.	**Weight Loss:**	Yes	No
	How much?		
	Over how long? …………….		

13.	**Dizziness +/- faintness**:	Yes	No
	a. Occurred on standing from lying position (postural)?	Yes	No

14.	**Dyspnoea (difficulty breathing):**	Yes	No

15.	**Visual Disturbance:**		Yes	No
	a. Type:	Pain behind eyes	Visual floaters	blurred vision loss of vision
	b. Were the symptoms associated with headaches:	Yes	No

16.	**Abnormal sensation in arms or legs**		Yes	No	
	a. Type:	Pins and needles	Pain	Cramps	other………
	b. Site:	both hands both feet	one hand	one foot	individual fingers / toes

17. **Seizure/ fit:**		Yes	No
		Generalised fit	Abnormal movement of one limb
	or face		

18. **"Impending sense of doom"**	Yes	No

19. **Please describe any other symptoms not mentioned above:**……………………………………………………

Where there any precipitants to your symptoms ?……………………………………………………………
………
………

How long did you have symptoms before you sought medical help?
……………………………………………………………………
………
……………………………………………….

How long did you have symptoms before you were diagnosed with phaeochromocytoma?
………………………………………………….
………
……………………………………………………

For each symptom you experienced (please circle appropriate response):

Symptom 1:……………………………………   **How long have you had this symptom?** ……………………

   a.   Were the symptoms: Persistent (present all the time and constant)
                                  Paroxysms /intermittent (on and off)

   b.   If intermittent how often did they occur?

                           - Daily   0-5x   5-10x   >10x
                           - Weekly   1x   2-3x   >3x
                           - Monthly

   c.   Duration of symptoms: - less than 1 minute
                                     - 1-10 minutes
                                     - 11 – 60 mins
                                     - more than 1 hour but less than 24 hours
                                     - more than 24 hours but less than a week
                                     - Daily at set times ………………………….

Symptom 2:……………………………………   **How long have you had this symptom?** ……………………

   a.   Were the symptoms: Persistent (present all the time and constant)
                                  Paroxysms /intermittent (on and off)

   b.   If intermittent how often did they occur?

                           - Daily   0-5x   5-10x   >10x
                           - Weekly   1x   2-3x   >3x
                           - Monthly

   c.   Duration of symptoms: - less than 1 minute
                                     - 1-10 minutes
                                     - 11 – 60 mins
                                     - more than 1 hour but less than 24 hours
                                     - more than 24 hours but less than a week
                                     - Daily at set times ………………………….

Symptom 3:……………………………………   **How long have you had this symptom?** ……………………

   a.   Were the symptoms: Persistent (present all the time and constant)
                                  Paroxysms /intermittent (on and off)

   b.   If intermittent how often did they occur?

                           - Daily   0-5x   5-10x   >10x

- Weekly   1x   2-3x   >3x
                                            - Monthly

    c.   Duration of symptoms: - less than 1 minute
                                            - 1-10 minutes
                                            - 11 – 60 mins
                                            - more than 1 hour but less than 24 hours
                                            - more than 24 hours but less than a week
                                            - Daily at set times ………………………….

Symptom 4:…………………………………………   **How long have you had this symptom? ……………………**

    c.   Were the symptoms: Persistent (present all the time and constant)
                                            Paroxysms /intermittent (on and off)

    d.   If intermittent how often did they occur?

                                            - Daily   0-5x   5-10x   >10x
                                            - Weekly   1x   2-3x   >3x
                                            - Monthly

    c.   Duration of symptoms: - less than 1 minute
                                            - 1-10 minutes
                                            - 11 – 60 mins
                                            - more than 1 hour but less than 24 hours
                                            - more than 24 hours but less than a week
                                            - Daily at set times ………………………….

Symptom 5:…………………………………………   **How long have you had this symptom? ……………………**

    c.   Were the symptoms: Persistent (present all the time and constant)
                                            Paroxysms /intermittent (on and off)

    d.   If intermittent how often did they occur?

                                            - Daily   0-5x   5-10x   >10x
                                            - Weekly   1x   2-3x   >3x
                                            - Monthly

    c.   Duration of symptoms: - less than 1 minute
                                            - 1-10 minutes
                                            - 11 – 60 mins
                                            - more than 1 hour but less than 24 hours
                                            - more than 24 hours but less than a week
                                            - Daily at set times ………………………….

Symptom 6:…………………………………………   **How long have you had this symptom? ……………………**

    c.   Were the symptoms: Persistent (present all the time and constant)
                                            Paroxysms /intermittent (on and off)

    d.   If intermittent how often did they occur?

                                            - Daily   0-5x   5-10x   >10x
                                            - Weekly   1x   2-3x   >3x
                                            - Monthly

    c.   Duration of symptoms: - less than 1 minute
                                            - 1-10 minutes
                                            - 11 – 60 mins
                                            - more than 1 hour but less than 24 hours
                                            - more than 24 hours but less than a week
                                            - Daily at set times ………………………….

Appendix 2: Equations used in regression analysis for analysis of symptoms

Equations 1A and 1B:

$$\ln\left(\frac{P}{1-P}\right) = a + b_1 x_1 + b_2 x_2 + b_3 x_3 + \ldots + b_{22} x_{22}$$

$$P = \frac{e^{(a + b_1 x_1 + b_2 x_2 + b_3 x_3 + \ldots + b_{22} x_{22})}}{1 + e^{(a + b_1 x_1 + b_2 x_2 + b_3 x_3 + \ldots + b_{22} x_{22})}}$$

Where P = the probability of a participant having a PPGL, a = intercept, b_n = coefficient of variable x_n, x_n = symptom variable (0 for symptom absence and 1 for symptom presence)

Equation 2:

$$AIC = 2k - 2 \times \ln(L)$$

Where AIC = akaike information criterion, k = the number of parameters in the model and L = the maximum value of the likelihood function for the model

Equation 3:

$$\ln\left(\frac{P}{1-P}\right) = (1.1801 \times Sweating) + (1.0163 \times Anxiety) - (1.8489 \times PainChest)$$
$$+ (2.9783 \times PainAbdomen) + (1.7472 \times WeightLoss) + (1.3829 \times VisDisturb)$$
$$- (1.0069 \times Headache) - 0.9005$$

Appendix 3: *SDHB* cohort at St. Bartholomew's Hospital

The table is grouped by kindred, showing genetic mutation, diagnosis and clinical outcome. Index case is stated for each kindred, or an explanation is provided for the referral to our surveillance programme if the index patient is not under follow-up at our institution.

Kindred	Patient No.		Type of Mutation	Diagnosis	Outcome
1	1 [a]	Index		PCC	Surgical resection + no further disease
	2		Splice Exon 1	No tumour	Active FU
	3			No tumour	Active FU
	4 [b]			No tumour	Active FU
	5			No tumour	Active FU
	6 [b]			No tumour	Active FU
2	7			No tumour	Active FU
	8	Index case diagnosed/ treated elsewhere in UK	Splice Exon 1	No tumour	Active FU
	9			Possible Abdo PGL	Under active surveillance
	10			No tumour	Active FU
3	11	Index case diagnosed/ treated elsewhere in UK	splice exon 1	No tumour	Active FU
4	12	Index	missense exon 6	Abdo PGL	Surgical resection + no further disease
	13			No tumour	Active FU
5	14	Index		Pelvic PGL	Surgical resection + no further disease
	15	Index	Frameshift exon 4	Abdo PGL	Surgical resection + no further disease
	16			No tumour	Active FU
	17			No tumour	Active FU
	18			No tumour	Active FU
6	19[a]	Index		Metastatic Abdo PGL	Deceased
	20[b]		Frameshift exon 4	No tumour	Active FU
	21[a]			Bladder PGL	Surgical resection + no further disease
	22				Awaiting first screening
	23[b]			No tumour	Active FU
	24[b]			No tumour	Active FU
	25[b]			No tumour	Active FU
	26				Awaiting first surveillance imaging
7	27[a]	Index		Thoracic PGL	Surgical resection + no further disease
	28[a]			Metastatic Abdo PGL	Surgical resection. Deceased
	29				Awaiting first surveillance imaging
	30[b]		Nonsense exon 2	No tumour	Active FU
	31[a]			Thoracic PGL	Surgical resection + no further disease
	32			Probable Abdo PGL	Under active surveillance
	33				Awaiting first surveillance imaging

Kindred	Patient No.		Type of Mutation	Diagnosis	Outcome
8	34	Index case diagnosed/ treated elsewhere in UK	Nonsense exon 2	No tumour	Active FU
	35			GIST	Surgical resection
9	36	Index		Abdo PGL	Surgical resection + no further disease
	37			No tumour	Active FU
	38			No tumour	Active FU
	39		Deletion Exon 1	RCC	Under active surveillance
	40			No tumour	Active FU
	41			No tumour	Active FU
	42			No tumour	Active FU
	43			No tumour	Active FU
10	44	Index	Deletion Exon 1	Thoracic PGL 3 x HNPGL Thoracic PGL	surgical resection + chemotherapy + MIBG
	45			Abdo PGL	Awaiting surgical resection
11	46	Index case diagnosed/ treated elsewhere in UK	Deletion Exon 1	No tumour	Active FU
	47			No tumour	Active FU
12	48	Index	Deletion Exon 1	Abdo PGL	Surgical resection + no further disease
13	49[a]	Index	Nonsense Exon 2	Multiple Abdo PGL Metastatic RCC	Deceased
	50[b]			TCC / RCC	Surgical resection
	51[b]			No tumour	Active FU
14	52a	Index	Missense Exon 2	Multiple Abdo PGL Thoracic PGL Metastatic disease	Deceased
	53			TCC	Active FU
	54			No tumour	Active FU
15	55	Index case diagnosed/ treated elsewhere in UK	missense exon 2	No tumour	Active FU
16	56	Posthumous genetic diagnosis for mother	Missense Exon 2	Abdo PGL	Awaiting surgical resection
17	57	Index	Missense exon 2	HNPGL	Surgical resection + no further disease
	58			No tumour	Active FU
18	59	Index	Missense exon 2	Metastatic PCC	Surgical resection, RFA liver, Temozolamide, Cyber knife
	60			Thoracic PGL	Surgical resection + no further disease
	61			RCC	Under active surveillance
	62			No tumour	Active FU
	63			No tumour	Active FU
	64			No tumour	Active FU
19	65	Index	Missense Exon 2	Bladder PGL (locally invasive) + PCC	Surgical resection
	66			No tumour	Active FU
20	67	Index	Missense Exon 4	HNPGL Malignant Abdo PGL	Surgical resection and radiotherapy. Now stable residual disease
	68			Abdo PGL	PGL under active surveillance. Not operated on due to patient age, co-morbidities. Patient asymptomatic
	69			Malignant Abdo PGL	Surgical resection + no further disease

Kindred	Patient No.	Type of Mutation	Diagnosis	Outcome
	70			Awaiting first surveillance imaging
21	71	Index case diagnosed/ treated in Canada	Missense Exon 6	Thoracic PGL	Surgical resection + no further disease
	72[a]			Thoracic PGL	MIBG
22	73[c]	Index	Missense Exon 6	Metastatic multifocal bladder PGL	MIBG treatment
23	74	Index	Frame shift Exon 7	HNPGL (locally invasive)	Surgical resection with residual disease
	75			RCC (predates genetic diagnosis & screening)	Surgical resection
24	76[a]	Index	Missense Exon 4	Metastatic bladder PGL	Deceased
	77[b]			No tumour	Active FU
25	78	Index case diagnosed/ treated elsewhere in UK	Missense Exon 6	No tumour	Active FU
26	79	Index case diagnosed/ treated elsewhere in UK	Missense Exon 4	No tumour	Active FU
27	80	Index	Missense Exon 4	Metastatic Abdo PGL	Surgical resection. Now deceased
28	81[a]	Index	Splice intron 4	PCC	Surgical resection + no further disease
29	82[a]	Index	Splice intron 4	PCC	Surgical resection + no further disease
30	83	Index	Nonsense Exon 2	Metastatic Thoracic PGL	MIBG therapy
31	84[a]	Index	Missense Exon 5	2 x HNPGL PCC Abdo PGL	Deceased
32	85	Index	Nonsense Exon 3	Abdo and Pelvic PGL PTC	Surgical resection
	86			No tumour	Active FU
33	87[a]	Index	Nonsense Exon 3	PCC	Surgical resection + no further disease
34	88	Index	Splice intron 6	Abdo PGL	Surgical resection + no further disease
35	89	Index	Splice Exon 4	HNPGL (locally invasive)	Surgical resection + no further disease
	90			No tumour	Active FU
	91			No tumour	Active FU
36	92	Index case diagnosed/ treated elsewhere in UK	Deletion of entire SDHB gene	HNPGL	Awaiting radiotherapy

SDHB Succinate Dehydrogenase subunit B mutation; Index patient that presented with symptomatic disease; PGL Paraganglioma; Abdo Abdomen; HNPGL Head & neck paraganglioma; RCC Renal cell carcinoma; GIST Gastrointestinal stromal tumour; PTC Papillary thyroid carcinoma; TCC Transitional cell carcinoma of the bladder; FU follow-up

[a] Clinical cases described in detail in previous papers reference[212,411]

[b] Clinical cases described in detail in previous papers reference[212]

[c] Clinical cases described in detail in previous papers reference[212,234,411,412]

Appendix 4: *SDHB* Index cases with multiple tumours and/or malignant disease

Table shows the details of each SDHB index case that presented with, or subsequently developed multiple tumours or malignant disease (defined as local tumour invasion into surrounding structures or disseminated metastatic disease).Year of original diagnosis is provided in brackets. Time to the development of further tumours is shown in column 7 and column 8 details the number of years the patient had been in the surveillance programme. Some of the earlier cases were discharged after initial successful resection of the primary tumour and only joined the surveillance programme after re-presenting with subsequent disease. The final column details the management and outcome for each patient.

Patient No.	*SDHB* Mutation	Age at diagnosis + Gender	Family History	Disease	tumour size (mm) - first lesion	Time to further disease	years into surveillance imaging*	Residual disease or recurrence at original site	Malignant disease+	Plasma / urine metanephrines/ catecholamines	Outcome
44	Deletion whole exon 1	18 M	2 family members with tumours within kindred	Thoracic PGL (1975)	140						Surgical resection + chemotherapy + MIBG
				3 x HNPGL		7	0*				
				Thoracic PGL		17				Negative	
84 [a]	Missense exon 5	40 M	nil - single index case	Left carotid body PGL (HNPGL) (1975)						Positive Norepinephrine	Surgical resection. Died of CVA 20 yrs after diagnosis
				PCC + abdo PGL		0.6	0*				
				right carotid body PGL		1					
67	Missense exon 4	42 M	3 family members with tumours within kindred	Jugular foramen + Abdo PGLs (2008)				Y	Y	Negative	Surgical resection and radiotherapy. Now stable residual disease
65	Missense exon 2	68 F	nil	Bladder PGL (2014)	51					Positive Normetanephrine	surgical resection
				PCC	25	0					

Patient No.	SDHB Mutation	Age at diagnosis + Gender	Family History	Disease	tumour size (mm) - first lesion	Time to further disease	years into surveillance imaging*	Residual disease or recurrence at original site	Malignant disease+	Plasma / urine metanephrines/ catecholamines	Outcome
19 [a]	Frameshift exon 4	29 F	2 family members with tumours within kindred. Mother had PGL died aged 38 (not in cohort)	Abdo PGL (1985)					Y		Surgical resection of primary. Died intra-operatively during resection of second PGL 10 years after initial diagnosis
				Abdo PGL Bone metastasis		10 10	0*				
73 [b]	Nonsense exon 2	24 M	mother died of carotid body tumour (not in cohort)	multifocal bladder (1997)				Y	Y	Positive	MIBG treatment. Some residual bladder lesions remain
				Metastatic disease (neck, bone, thorax)		4	4				
59	Missense exon 2	50 F	3 family members with tumours within kindred	PCC + bone metastasis at diagnosis (2008)					Y	positive 3-methoxytyramine. Negative urinary metanephrines	Surgical resection, RFA liver, Temozolamide, Cyber knife
80	Missense exon 4	44 M	nil known	Abdo PGL (2009)	70				Y	Positive normetanephrine & 3-methoxytyramine	Metastatic disease on first surveillance screening. Committed suicide
				Metastatic disease		5	0*				
76 [a]	Missense exon 5	47 M	nil known	Bladder + Pelvic PGL (2001)	multifocal			Y	Y	positive norepinephrine and epinephrine	Died 6 years after diagnosis of disease burden
				Metastatic disease		3.6	3.6				
83	Nonsense exon 2	33 M	nil known	Thoracic PGL (2012)	92				Y	negative	MIBG therapy
				Metastatic disease		3	3				

Patient No.	SDHB Mutation	Age at diagnosis + Gender	Family History	Disease	tumour size (mm) - first lesion	Time to further disease	years into surveillance imaging*	Residual disease or recurrence at original site	Malignant disease+	Plasma / urine metanephrines/ catecholamines	Outcome
85	Nonsense exon 3	43 M	nil known	2 x Abdo PGL Papillary thyroid carcinoma	360 320	0.2				negative	Surgical resection
52 [a]	Missense exon 2	10 F	Mother had PGL died aged 38yrs. Father has TCC	Abdo PGL (1982)				Y	Y		Died of disease burden 31 years after diagnosis
				5 x Abdo PGL + PCC		1.5	1.5				
				Thoracic PGL		2.5					
				Abdo PGL		2.6					
				Abdo PGL		7.5					
				Metastatic disease		25				Positive norepinephrine	
49 [a]	Nonsense exon 2	10 F	2 family members with tumours within kindred	Abdo PGL (1988)	350			Y	Y	Negative	Died of disease burden 25 years after diagnosis
				RCC		16.5	8				
				Recurrent Abdo PGL		17	9				
				Metastasis from RCC		17.5	9				

*Identified on first imaging when joined surveillance programme

+Malignant disease = tumour invasion into surrounding structures or metastatic disease

[a] Clinical details of cases previously described in articles referenced [212,411]

[b] Clinical details of case previously described in article referenced [212,234,411,412]

Appendix 5: Demographic details of *SDHA* cohort

Table outlining the demographic details of each patient with an underlying SDHA mutation showing the mutation type, specific tumour details, treatment given and other clinical information.

Pt. No.	*SDHA* Mutation	Age at diagnosis / starting screening (years) & gender	Diagnosis	Years of original diagnosis	Size (mm)	Treatment	Biochemistry	Other clinical information	PMH, FH
1 Index		36F	Intrathyroid PGL			Open surgical resection and radiotherapy 60Gy 30#	Not tested pre-operatively	initially thought to be chemodectoma of thyroid	
	c.91C>T exon 2	50	Right breast DCIS	14	100	B/L mastectomies and right axillary clearance	Negative	BRCA1/2 negative	
		52	DCIS right axilla	16	16	25/3/2014 – redo axillary clearance and Radiotherapy 50Gy in 25#	Negative		
2 Carrier		22F	No tumours				Negative		
3 Index		28F	neck mass biopsied MI					biopsied and told indeterminate lesion Troponin positive	MI, depression, IBS
		47	Mediastinal PGL		56	MIBG and open surgical resection	Urine NMA 15607nmol/day Urine 3MT 17169nmol/day	Trop -ve, had angio – unobstructed Biopsy showed brown fat only	
	c.1338del A exon 10	47	Right Carotid body tumour		35	Embolisation, followed by open surgical resection	Urine NMA 1159nmol/day Urine 3MT 6837nmol/day	Urine NMA normalised following resection of mediastinal lesion	
4 Carrier		21F	No tumour				Negative		
5 Carrier		20F	No tumour				Negative		
6 Carrier		25M	No tumour				Negative		

7 Index	c.1753C>T exon 7	34F	Mediastinal PGL			Open surgical resection		Initially diagnosed as NHL – underwent 6 months chemo. Left vocal cord palsy after 1st operation	
		PHPT	30	15	Open surgical resection		Negative	SDH immunostain positive	Strong FH of breast carcinoma
8 Index	c.923G>T exon 8	46M	Left paraadrenal PGL	1993	50	Open surgical resection	Positive		1 son awaiting genetic testing – no tumours
		47	Recurrence aorto iliac junction	1	70	Open surgical resection		Urethral stricture requiring nephrectomy	
		55	PGL above bifurcation between IVC & aorta	8	15	All 4 open surgical resection	Urine NA 4080nmol/day Plasma NA 41.9nmol/L		
		55	Left retro aortic PGL	8	20				
		55	Left para-aortic region above diaphragm	8	12				
		55	Retrocaval PGL	8.5	34		Plasma NA >70nmol/L Plasma AD 3.04nmol/L		
		58	Left retrocrural region	11	24		Negative		
		59	Increase in size of above PGL	12	30	Open surgical resection	Urine NA 880nmol/day Urine AD negative		
		63	Lesion in left adrenal bed	16	14		Urine NA 1309nmol/day	MIBG negative	
		63	L4 metastatic deposit	16	16	EBRT 50Gy 25# over 35days			
		64	L4 deposit increase in size	17	30	Cyber knife 14Gy 1#		Progressive spine lesion	

Patient	Mutation	Age/Sex	Tumour	Size 1	Size 2	Treatment	Biochemistry	Imaging / comments	Family history
9 Index	c.91C>T exon 2	18F	Right PCC			Open surgical resection + nephrectomy			Perforated peptic ulcer, aged 14 years; Chronic autoimmune hepatitis, aged 21 years; Steroid induced Diabetes mellitus
		54	Recurrent right PCC in surgical bed	36			Urine NA 1030nmol/day; Urine/plasma AD negative; Plasma NMN 1.57nmol/L		Grandmother – breast carcinoma; Father – hypertensive stroke
			Metastatic disease to sacrum, T10 + para-aortic LN	36	24 (LN)	Octreotide LAR monthly			
		55	Left adrenal nodule	37	14	Laparoscopic adrenalectomy and LN clearance	Plasma NMN 2.31nmol/L	MIBG avid	
			Paracaval LN	37	15				
10 Carrier		29F	No tumour				Negative		
11 Index	c.91 C>T exon 2	68M	Retroperitoneal (aortic bifurcation) PGL		110	Open surgical resection and pre-operative embolisation	Negative	Metastatic potential (vascular invasion)	Prostate carcinoma; Sister has breast carcinoma; Mother – bladder carcinoma; Daughter – macroprolactinoma; 3 children awaiting genetic testing – no tumours
		73	Macroprolactinoma	5	13	Cabergoline		Tumour reduction demonstrated on MRI after 6 months treatment	

PGL paraganglioma; PCC phaeochromocytoma; LN lymph nodes; NA norepinephrine [reference range urine <814nmol/day, plasma <5.67nmol/L], AD epinephrine [urine <144nmol/day , plasma <4nmol/L]; 3MT 3-methoxytyramine [urine <2500nmol/day]; NMN normetanephrine [urine <4440nmol/day , plasma <1180pmol/L]; MN metanephrine [urine <2000nmol/day, plasma <5.10pmol/L]; NHL non Hodgkins lymphoma; PHPT primary hyperparathyroidism

Appendix 6: Summary of current and historical surveillance recommendations in chronological order.

Table showing surveillance recommendations for *SDH* mutation carriers published in the literature, summarising recommended imaging modalities and frequencies to use, for both cross-sectional and functional imaging, and suggested ages to commence surveillance screening.

Reference	Year	Clinical review and biochemical tests	Anatomical imaging	Functional imaging	Recommended age to commence surveillance
Benn et al[53]	2006	Annual	CT/MRI neck and TAP every 2 years	Consider ^{18}F-DOPA-PET	Commence at age 10 years or at least 10 years before onset of disease in each specific family
Fish et al[211]	2007	Annual	SDHD: Annual HN USS	Baseline scintigraphy	
Timmers et al[59]	2007			^{18}F-FDG PET for staging and monitoring of *SDHB* metastatic disease	
Srirangalingam et al[212]	2008	Annual	MRI of neck and TAP annually		Commence age 5 years
Neumann et al[86]	2009	Annual	Serial MRI skull base to pelvis (frequency not stated)	Consider 123I-MIBG and ^{18}F-DOPA-PET	
Timmers et al[214]	2011		CT or MRI	^{18}F-FDG PET as first line functional imaging and for use in follow up of metastatic PPGL	
European Association of Nuclear medicine guidelines[215]	2012			Choice of nuclear imaging depends on genetic diagnosis and tumour site	
Gimenez-Roqueplo et al[216]	2013		First screen with MRI HN + CT TAP (frequency for follow up surveillance imaging not stated)	First screen with somatostatin receptor scintigraphy (^{111}In-diethylene triamine pentacetic acid-pentetreotide scintigraphy)	
Miederer et al[89]	2013			^{18}F-FDOPA PET/CT at baseline and every 2-5 years	

Reference	Year	Clinical review and biochemical tests	Anatomical imaging	Functional imaging	Recommended age to commence surveillance
Kirmani and Young[13]	2014	Annual	SDHD/SDHC: CT/MRI of HN every 2 years and MRI TAP every 4 years SDHB: CT/MRI CAP every 2 years	^{123}I-MIBG every 4 years	Commence at age 10 years or at least 10 years before onset of disease in each specific family
Taieb et al[79]	2014	Annual	MRI HN every 3 years	Consider PET on individual case basis	
Endocrine society clinical practice guideline[12]	2014	Annual	Periodic MRI (frequency not stated)	Reserved for further characterisation of detected tumours	
Jasperson et al[64]	2014	Annual	Rapid sequence whole body MRI, frequency not stated		
Favier et al[31]	2015	Annual	Initial CT/MRI HN and TAP, and if negative 2-3 yearly whole body MRI	First screen: ^{111}In-pentetreotide scintigraphy or ^{18}F-FDG-PET/CT	
Janssen et al[217]	2015			^{68}Ga-Dodecanetetraacetic acid-Octreotate (DOTATATE) PET/CT	
Tufton et al[65]	2016	Annual	MRI Abdomen annually. MRI HN, thorax, pelvis every 2 years		Commence at 5 years
European society clinical practice guideline[218]	2016	Annual	MRI TAP every 1-2 years for follow up of resected biochemically silent tumours		
Kornaczewski et al[219]	2016		CT whole body every 5 years	^{18}F-FDG PET/CT every 5 years	
Daniel et al[92]	2016	Annual	MRI neck and TAP 2 yearly		
Eijkelenkamp et al[58]	2017	Annual	MRI TAP every 2 years. MRI HN every 3 years		27 years for HNPGL, unable to calculate optimal age for sPGL
Dutch clinical guideline[18]	2017	Annual	*SDHD, SDHAF2*(paternal origin)*, SDHA, SDHC:* MRI HN every 3 years, MRI body if indicated *SDHB:* MRI HN every 3 years, MRI abdomen and thorax minimum every 3 years (sooner if clinically indicated)		*SDHD, AF2, SDHA, SDHC:* Commence at 18 years (consider from 5-10 for earliest manifestation in the family) *SDHB:* Commence at age 10 years

Reference	Year	Clinical review and biochemical tests	Anatomical imaging	Functional imaging	Recommended age to commence surveillance
Niemeijer et al[69]	2017		HN MRI 3 years + MRI/CT body 2years	MIBI +/- PET if metanephrine +ve	

na not applicable; MRI Magnetic resonance imaging; CT Computed tomography; MIBG Metaiodobenzylguanidine scan; PET Positron emission tomography; TAP thoracic abdominal and pelvis; HN head and neck; ^{18}F-FDG 2-deoxy-2-[fluorine-18]fluoro-D-glucose; ^{18}F-DOPA [fluorine-18]- dihydroxyphenylalanine

Appendix 7: Radiation of different imaging modalities Tables show the mean radiation dose delivered by different imaging modalities and the relative risk per sievert radiation exposure to different age groups. Naturally occurring 'background' radiation per year is ~3mSv. A ten hour flight exposes an individual to 0.05mSv. UK legal limit that a classified person who works with radiation maybe exposed to is 20mSv per year (Ionising radiations regulations 1999). Data from Health Protection Agency.

Type of imaging	Mean dose of radiation used
CXR	0.1mSv
CT abdomen	5 mSv
CT TAP	10 mSv
^{123}I MIBG	5 mSv
^{68}Ga PETCT	5-9 mSv
FDG PET	13-32 mSv

Population age (years)	RR per exposure (per Sv)
0 - 9	7.8 – 20 %
30 - 39	2.8 – 9.2 %
60 - 69	0.8 – 6.8 %

Appendix 8: Grading and scoring methods for PPGLs

Name	PASS	GAPP	M-GAPP	ASES	COPPs
Full name	Phaeo of the adrenal gland scoring system	Grading system for PPGL	Modified- GAPP	PPGL clinical model	Composite PPGL prognostic score
Authors	Thompson *et al*	Kimura *et al*	Koh *et al*	Cho *et al*	Piere *et al*
Year	2002	2014	2017	2018	2019
Criteria	Vascular invasion = 1	Histology: Zellballen = 0 Large irregular cell nests = 1 Pseudorosette = 1	Histology: Zellballen = 0 Large irregular cell nests = 1 Comedo-necrosis = 2	Age ≤35 years = 1	Size >7cm = 1
	Capsular invasion = 1	Cellularity: Low = 0 Mod = 1 High = 2	Invasion = 1	Size ≥6cm = 1	Central necrosis = 5
	periadrenal adipose tissue = 2	Comedo necrosis: Absent = 0 Present = 2	Ki67 >1 = 1	Extra-adrenal = 1	Vascular invasion = 1
	large nests or diffuse growth = 2	Invasion = 1	Catecholamines: NF or A = 0 NA = 1	NA secreting = 1	S100 IHC = 2 (sustentacular cells)
	focal or confluent necrosis = 2	Ki67 < = 0 0-1% = 1 >3% = 2	SDHB IHC absence = 1		SDHB IHC = 1
	high cellularity = 2	Catecholamines: A = 0 NA = 1 NF = 0			

	tumour cell spindling = 2				
	cellular monotony = 2				
	increased mitotic figures >3/10 HPF= 2				
	atypical mitotic figures = 2				
	profound nuclear pleomorphism =1				
	hyperchromasia = 1				
Total score	20	10	7	4	10
Increased malignant potential	≥4	WD = 0-2 (3.6%) MD = 3-6 (60%) PD = 7-10 (88%)	≥3	≥2	≥3